

Task 17 PV and Transport

SPVPS

# State-of-the-Art and Expected Benefits of PV-Powered Vehicles 2021



## What is IEA PVPS TCP?

The International Energy Agency (IEA), founded in 1974, is an autonomous body within the framework of the Organization for Economic Cooperation and Development (OECD). The Technology Collaboration Programme (TCP) was created with a belief that the future of energy security and sustainability starts with global collaboration. The programme is made up of 6 000 experts across government, academia, and industry dedicated to advancing common research and the application of specific energy technologies.

The IEA Photovoltaic Power Systems Programme (IEA PVPS) is one of the TCP's within the IEA and was established in 1993. The mission of the programme is to “enhance the international collaborative efforts which facilitate the role of photovoltaic solar energy as a cornerstone in the transition to sustainable energy systems.” In order to achieve this, the Programme's participants have undertaken a variety of joint research projects in PV power systems applications. The overall programme is headed by an Executive Committee, comprised of one delegate from each country or organisation member, which designates distinct ‘Tasks,’ that may be research projects or activity areas.

The IEA PVPS participants are Australia, Austria, Belgium, Canada, Chile, China, Denmark, Finland, France, Germany, Israel, Italy, Japan, Korea, Malaysia, Mexico, Morocco, the Netherlands, Norway, Portugal, South Africa, Spain, Sweden, Switzerland, Thailand, Turkey, and the United States of America. The European Commission, Solar Power Europe, the Smart Electric Power Alliance (SEPA), the Solar Energy Industries Association and the Copper Alliance are also members.

Visit us at: [www.iea-pvps.org](http://www.iea-pvps.org)

## What is IEA PVPS Task 17?

The objective of Task 17 of the IEA Photovoltaic Power Systems Programme is to deploy PV in the transport, which will contribute to reducing CO<sub>2</sub> emissions of the transport and enhancing PV market expansions. The results contribute to clarifying the potential of utilization of PV in transport and to proposal on how to proceed toward realising the concepts.

Task 17's scope includes PV-powered vehicles such as PLDVs (passenger light duty vehicles), LCVs (light commercial vehicles), HDVs (heavy duty vehicles) and other vehicles, as well as PV applications for electric systems and infrastructures, such as charging infrastructure with PV, battery and other power management systems.

### Authors

- **Main Content:** K. Araki (Japan), A.J. Carr (the Netherlands), F. Chabuel (France), B. Commault (France), R. Derks (the Netherlands), K. Ding (Germany), T. Duigou (France), N.J. Ekins-Daukes (Australia), J. Gaume (France), T. Hirota (Japan), O. Kanz (Germany), K. Komoto (Japan), B.K. Newman (the Netherlands), R. Peibst (Germany), A. Reinders (the Netherlands), E. Roman Medina (Spain), M. Sechilariu (France), L. Serra (France), A. Sierra (the Netherlands), A. Valverde (Spain), D. Zurfluh (Switzerland)
- **Editors:** Keiichi Komoto, Toshio Hirota (Task17 Operating Agent)

### DISCLAIMER

The IEA PVPS TCP is organised under the auspices of the International Energy Agency (IEA) but is functionally and legally autonomous. Views, findings and publications of the IEA PVPS TCP do not necessarily represent the views or policies of the IEA Secretariat or its individual member countries.

### COVER PICTURE

New Energy and Industrial Technology Development Organization

ISBN 978-3-907281-15-4: State-of-the-Art and Expected Benefits of PV-Powered Vehicles

INTERNATIONAL ENERGY AGENCY  
PHOTOVOLTAIC POWER SYSTEMS PROGRAMME

**IEA PVPS  
Task 17  
PV and Transport**

**State-of-the-Art and Expected Benefits of  
PV-Powered Vehicles**

Report IEA-PVPS T17-01:2021  
April 2021

ISBN 978-3-907281-15-4



## TABLE OF CONTENTS

---

Table of contents.....	2
Acknowledgments.....	3
List of abbreviations.....	4
Executive summary.....	5
1. Recent trends in PV-powered vehicles.....	13
1.1 Overview and state of the art of PV-powered vehicles.....	13
1.2 Overview and perspectives of the PV technologies for PV-powered vehicles.....	30
1.3 Summary.....	40
2. Expected benefits of PV-powered vehicles.....	41
2.1 Case study on PV-powered passenger vehicles in Japan: Expected CO <sub>2</sub> reduction and charging frequency.....	42
2.2 Case study on PV-powered passenger vehicles in the Netherlands: Reduction of charging, cost and CO <sub>2</sub> emissions.....	55
2.3 Case study on PV-powered light commercial vehicles in Germany: Energy balance and expected CO <sub>2</sub> reduction.....	73
2.4 Case study on PV-powered reefer trucks in Spain: Economic feasibility assessment.....	85
2.5 Case study on PV-powered truck trailers in the Netherlands: PV electricity production on trailers.....	93
2.6 Summary.....	96
3. Vehicle solar irradiance measurements.....	98
3.1 Solar irradiance measurements in the Netherlands and Germany.....	99
3.2 Solar irradiance measurements in Japan.....	101
3.3 Solar irradiance measurements in Switzerland.....	114
3.4 Solar irradiance measurements in Australia.....	123
3.5 Summary.....	126
4. Next steps for realising PV-powered vehicles.....	127
4.1 Potential benefits of PV-powered vehicles.....	127
4.2 Preliminary discussions for standardisation of solar irradiation and module design.....	137
4.3 PV-powered vehicles in stationary mode and combination with possible infrastructures.....	145
4.4 Conclusions and the way forward.....	154



## ACKNOWLEDGMENTS

---

This report received valuable contributions from several IEA PVPS Task 17 members and other international experts. Many thanks to all of them.

The French contribution is funded by the Agency for ecological transition (ADEME) under grant number 1905C0043 (PV2E-Mobility).

The contribution from the Netherlands is supported by the Ministry of Economic Affairs, the Netherlands Enterprise Agency (RVO) and Top Sector Urban Energy (TKI) under the grant TEUE18019.

The German contribution is funded by the German Ministry for Economic Affairs and Energy under grant number 0324275 (Street).

The Spanish contribution was supported by PRIMAFRIO Group Company, providing valuable information and contributing to the chapter edition and revision (A. Valverde, F. Pérez).

The contribution by Switzerland is financially supported by the Swiss Commission for Technology and Innovation (CTI - SCCER program) and the Berner Fachhochschule BFH.

The contribution by Japan is supported by the New Energy and Industrial Technology Development Organization (NEDO) under the Ministry of Economy, Trade, and Industry (METI), Japan. The modelling of VIPV has been discussed in the international web meetings for the standardisation of vehicle's roof PV since December 2017, and a part of activities are supported by the Japan Electrical Manufacturers' Association (JEMA).



## LIST OF ABBREVIATIONS

---

Aux	Auxiliaries
BES	Battery Energy Storage System
CIGS	Copper Indium Gallium Selenide
CPV	Concentrator Photovoltaics
EMS	Energy Management System
EV	Electric Vehicle
HIT	Heterojunction with Intrinsic Thin-layer
IBC	Interdigitated Back Contact
IEC	International Electrotechnical Commission
INES	Institut National de l'Énergie Solaire
MPPT	Maximum Power Point Tracking
Prop	Propulsion
PV	Photovoltaic
R&D	Research and Development
SOC	State-Of-Charge
STC	Standard Test Conditions
SWOT	Strengths, Weaknesses, Opportunities, and Threats
UAV	Unmanned Aerial Vehicle
V2G	Vehicle-to-Grid
V2H	Vehicle-to-Home
V2V	Vehicle-to-Vehicle
V2X	Vehicle-to-Everything
VIPV	Vehicle Integrated Photovoltaics



## EXECUTIVE SUMMARY

---

The market for PV systems has been rapidly expanding with significant penetration in grid-connected markets in an increasing number of countries, connected to both the distributed as well as the central transmission network. This strong PV market expansion has been contributing to savings in fossil fuel consumption and mitigating environmental impacts in residential, commercial, industrial and power sectors. In contrast, the PV market in the transport sector is still small. However, there is a huge potential.

In the transport sector, battery and plug-in hybrid electric vehicles are being adopted globally as a solution to mitigate CO<sub>2</sub> emissions. In line with this, vehicle emissions targets have been proposed and adopted by many countries and policy bodies around the world with goals for the adoption and use of electric vehicles in the near future. With widespread electrification of transportation, PV generated electricity and other renewable energy sources are needed to leverage the EV adoption into even more significant CO<sub>2</sub> emissions reductions. The distributed nature of PV electricity generation offers new opportunities for charging battery electric vehicles.

Options for low-carbon charging of electric vehicles include charging from the existing grid network with PV or other sustainable electricity sources, charging from a dedicated charge point with local PV electricity generation, or directly and independently with on-board PV (PV-powered vehicle).

In order to contribute to reducing the CO<sub>2</sub> emissions of the transport sector and to enhance PV market expansions, IEA PVPS Task 17 is aiming to clarify the potential of the utilization of PV in transport and to propose how to proceed towards realising the concepts. Task 17's scope includes various PV-powered vehicles such as passenger vehicles, light commercial vehicles, heavy duty vehicles and other vehicles, as well as PV applications for electric systems and infrastructures, such as charging infrastructure with PV, battery and other power management systems.

Among these options, this report has focused on PV-powered vehicles, with on-board integrated PV systems, that can run anywhere without or with less dependency on grid electricity. These vehicles offer more than just low emissions transport but also options of convenience and autonomy. The market introduction of PV-powered vehicles can be important for the uptake of electric transport and create opportunities for other PV applications in the transport sector, as well.

This report is the first technical report of Task 17, as an interim report, and presents on the recent trends in PV-powered vehicles including PV technologies, expected benefits of PV-powered vehicles, estimates of solar irradiance on vehicles, and next steps for realising PV-powered vehicles in the market.

### **A. Recent trends in PV-powered vehicles**

In recent years, multiple projects, consortia and companies have been aiming at delivering PV-powered vehicles, especially passenger vehicles. Considering the direct usage of PV electricity for vehicles, the available area for PV modules is limited. However, even in a limited area PV will be able to supply electricity to the battery of the vehicle.

As pioneer manufacturers of PV-powered vehicles in Europe, Sono Motors and Lightyear are developing PV-powered passenger vehicles equipped with crystalline Si solar cells, and their vehicles will be likely coming to the market (see Figs. A-1 and A-2). "Sion", by Sono Motors, has lightweight PV modules at least 20% lighter than comparable metal body parts, which can generate 1 208 Wp. Sono Motors estimates a range of 5 800 km/year using only solar energy and up to 34 km/day (in Munich). "Lightyear One", by Lightyear, has been designed to be very light, with high performance materials. PV modules on 5 m<sup>2</sup> and 215 Wp/m<sup>2</sup> may provide up to 70 km/day. Additionally, CEA-INES developed a prototype vehicle equipped with 1,3 m<sup>2</sup> crystalline Si PV modules.

In Japan, two major car manufacturers, Toyota Motor Corporation (Toyota) and Nissan Motor Corporation (Nissan), engineered prototypes of PV-powered passenger vehicles using high-efficiency III-V multijunction solar cells,



supported by NEDO, and started testing. PV capacity of Toyota's PV-powered vehicle, Prius-HEV, is 860 Wp and that of Nissan's PV-powered vehicle, e-NV200, is 1 150 Wp (see Figs. A-3 and A-4). It is noted that both vehicles are commercial passenger vehicles implying that the III-V multijunction solar cells are capable of being mounted on normal passenger vehicles without sacrificing elegant body shapes.



**Fig. A-1 Sion from Sono Motors**  
(<https://sonomotors.com/en/sion/>)



**Fig. A-2 Lightyear One**  
(<https://lightyear.one/lightyear-one>)



**Fig. A-3 PV-powered Prius-HEV (Toyota)**  
([https://www.nedo.go.jp/news/press/AA5\\_101150.html](https://www.nedo.go.jp/news/press/AA5_101150.html))



**Fig. A-4 PV-powered e-NV200 (Nissan)**  
([https://www.nedo.go.jp/news/press/AA5\\_101326.html](https://www.nedo.go.jp/news/press/AA5_101326.html))

Silicon-based cells are the most common technology for PV-powered vehicles. The modules using silicon-based cells show the best compromise between performances and price with an acceptable level of reliability. The weak point is their lack of flexibility in two-directional bending. III-V multijunction solar cells have also been applied to PV-powered vehicles due to higher power conversion efficiency. The disadvantages are higher price and spectrum mismatching loss compared with crystalline Si solar cells. For reducing such disadvantages, a four-terminal III-V on Si multijunction solar cells has also been demonstrated. Other thin-film solar cells, such as amorphous silicon and chalcogenide, compare unfavourably in efficiency to other photovoltaic technologies. However, they represent the most efficient of the thin-film materials that can be deposited onto glass or metal foil, providing the potential to fabricate curved PV active vehicle body parts directly and perhaps more cheaply. Perovskite cells have the potential of combining high efficiency, low-cost and flexibility, but this technology is not currently manufactured at large scale due to a lack of reliability/durability and, at present, lower efficiency than c-Si based PV at large scale.

From the viewpoint of PV module assembly, there are additional module costs associated with reliable encapsulation of photovoltaic solar cells in curved vehicle body parts. Compared to conventional flat-plate PV modules, these vehicle parts will be manufactured in relatively small volumes for each vehicle design. Curved, flexible and lightweight module technologies with low cost and high reliability are required. The modules will also be subject to vibrational environments that are much more challenging than for standard terrestrial PV modules. The aesthetic appeal of a vehicle will be an important factor in any consumer purchase, so the modules must not only be efficient but also coloured. With well-engineered optical coatings, it is possible to deliver colour with relatively little efficiency loss.



## **B. Expected benefits of PV-powered vehicles**

To a certain extent, PV-powered vehicles replace grid or charging station electricity with on-board PV generated electricity. This offers benefits for users in terms of reduction of CO<sub>2</sub> emissions during driving (in most countries), cost savings, and reduction in the frequency of grid charging, as well as less quantifiable benefits in terms of autonomy and independence. In order to foresee the expected benefits, case studies are included in this report. Modelling and case studies confirm that all PV-powered vehicles will realise the benefits listed above to various levels.

### **Case studies on PV-powered passenger vehicles**

A case study in Japan found that a PV-powered vehicle could produce approximately 220 kg CO<sub>2</sub>-eq/year emission reduction in comparison to the same electric vehicle without PV, especially for longer driving distances. However, for shorter driving distances a 1 kW PV system can result in excess PV generation. In order to increase the environmental benefits of PV-powered vehicles, it is necessary to ensure high utilisation of PV electricity. Thereby, many aspects of the PV-powered vehicle need to be considered and optimised; the PV capacity (considering the effective solar irradiation), the vehicle efficiency, and the vehicle battery, including its capacity, efficiency and operating conditions. The Japanese case study also showed that a PV-powered vehicle will have a decreased charging frequency and that in some cases with a shorter driving distance, the PV-powered vehicle will be free from grid electricity charging. This benefit will make the vehicle attractive, even if the expected environmental benefits will only be small.

A case study in the Netherlands showed that even with a relatively low solar irradiation, PV-powered vehicles could make a significant impact on the electricity consumption of electric vehicles. As PV and EVs become more efficient, the impact can increase. It was also shown that driver behaviour, in the form of charging strategies and driving profiles, can have a measurable effect on the benefits of PV-powered vehicles. This may lead to a 60% reduction in charging frequency, which can increase the autonomy and a feeling of security for the EV driver. While CO<sub>2</sub> emissions reduction will depend on the carbon intensity of the local grid, current values for the Netherlands indicate that there can be an effective CO<sub>2</sub> reduction of about 200 kg CO<sub>2</sub>-eq/year. Finally, cost savings of up to 164 EUR/year are shown, but are likely to be much higher when commercial EV charging rates would be taken into account, which are currently significantly higher than household electricity prices. It is noted that in order to have the most impact on cost savings and CO<sub>2</sub> emissions, the energy generated by the PV should be utilised to the maximum.

Realising benefits of PV-powered vehicles depends on variables such as driving patterns, available solar irradiance on the vehicle, vehicle efficiency, battery size, PV capacity installed and the utilization of the PV resource. Based on the case studies in Japan and the Netherlands, the expected benefits of PV-powered passenger vehicles in all IEA PVPS Task 17 member countries have been estimated (see D).

### **Case studies on PV-powered commercial vehicles and trucks**

A case study in Germany focused on PV-powered light commercial vehicles. Based on the solar irradiance measurements on specific test routes, it was found that a side-to-roof ratio is about 40% on average. Also, it was estimated that a total energy yield from 1 170 kWh/a (Hamburg, Germany) to 2 210 kWh/a (Rome, Italy) for the modules mounted on the roof and side (2 180 W<sub>p</sub> in total). In parallel, a life cycle assessment (LCA) of PV components, assuming production in China and integration in Germany, found that PV-powered vehicles can improve the carbon footprint for the case, based on an average shading factor of 30% and eight years of operation time. The emissions factor of 1 kWh of on-board generated PV electricity is calculated at 0,357 kg CO<sub>2</sub>-eq/kWh, and the average grid emissions for the operation time are expected to be 0,435 kg CO<sub>2</sub>-eq/kWh. The lower shading factor and the longer operation time are important for realising the environmental benefits.

A case study in Spain discussed the economic feasibility of PV-powered reefer trucks, by integrating PV modules on the roof of refrigerated trucks. ICE engine trucks consume diesel fuel, and the fuel consumption varies with the temperature of refrigeration, ambient temperature, the mass of the pay-load, and the costs of diesel (there are different costs for diesel depending on the fuel being used for driving or for refrigeration). The economic feasibility of PV depends of the use given to the produced PV electricity on-board, and how to substitute fuel and freight load, in addition to the cost and performance of PV. As an example, if the same diesel is used both for motion and



refrigeration (0,75 EUR/l), considering that 75% of the time the trucks travel with full load, the best payback time is estimated to be 3,62 years, which seems reasonable from an investment point of view. Based on these conclusions, preliminary concepts for PV-powered heavy-duty vehicles, especially trucks have been indicated.

A case study on PV-powered truck trailers in the Netherlands estimated the PV electricity production on the roof and on the sides of semi-trailers. The vertical installation represents two vertically oriented PV systems attached to the sides of a semi-trailer, and the horizontal installation represents just one roof-based PV system with a similar size as one of the two vertically oriented PV systems. The preliminary studies indicated that the effectiveness of vertical solar panels on trailers, is about 50% of that of roof-based panels. This is highly dependent on the latitude, the route the truck-trailer drives, the locations the truck visits, the surroundings of those locations, the changeability of the weather and the date/time. It will be essential to develop tools and methods to forecast the possible power and energy production during a journey ahead of the actual trip itself.

These case studies have given valuable insights upon which in-depth studies of integrated PV systems for trucks and trailers can build upon. Taking into account the possible use of PV electricity for auxiliary demand, PV integration in trucks and trailers seem close to realisation and will be coming to the market.



**Fig. B-1 PV-powered light commercial vehicle**  
(Photo: Institute for Solar Energy Research Hamelin)



**Fig. B-2 PV truck trailer**  
(Photo: IM Efficiency)

### C. Solar irradiance for PV-powered vehicles

In order to promote development and adoption of PV-powered vehicles, it is necessary to understand the effects of the dynamic environment of the vehicle for optimal design of on-board PV systems. The amount of PV electricity generated on-board depends on factors such as available solar irradiance and temperature. The solar irradiance falling on a PV-powered vehicle depends on the specific location and direction during parking and driving. Additionally, the solar irradiance during use is always changing; due to the surrounding environment of the route (buildings, structures or foliage may cause shade or reflect light on the vehicle). Several different methodologies have been developed for measuring the real irradiance falling on vehicles in some organization by: TNO in the Netherlands, ISFH in Germany, the University of Miyazaki in Japan, Bern University of Applied Sciences in Switzerland and UNSW in Australia (see Table C-1).

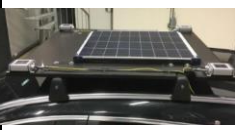
Although there has not yet been enough data collected to make generalisations on the characteristics of the solar irradiance, each approach led to results and from these, a few tendencies and directions were found.

A preliminary study in Japan, which was conducted at limited locations (Miyazaki city and Sapporo city) and periods of time, resulted in the following observations: shades of buildings, trees, power poles, and the like, cause a drop in solar irradiance in affected locations and sections of the car; larger shades like that of a building may cover an entire surface, such as the vehicle's roof, or may only partially shade the surface; due to reflections from buildings, the solar irradiance on a vehicle in some locations and sections may exceed the insolation on a roof or rooftop of a building; fluctuations in solar irradiance due to shades and reflections often occur with very short cycles (less than 0,1 seconds). Fluctuations in solar irradiance on vehicle's roof were observed by measurements in the Netherlands and Germany, as well. Although too few data are available to make generalisations on the characteristics of the solar irradiance on vehicles, it can be stated with some level of confidence that the ratio of solar irradiance on the vehicle's roof during driving relative to GHI may range from 50% to 90%, e.g. from high-rise



sections to urban and open-air sections. A ratio of roof-to-side measured in Miyazaki was from 30% to 50%, 40% on average, which is relatively close to the measured ratio in Germany.

**Table C-1 Solar irradiance measurement by some organisations**

TNO, Netherlands	ISFH, Germany	Univ. of Miyazaki, Japan	Bern University of Applied Sciences, Switzerland	UNSW, Australia
Four horizontal pyranometers and PV module on roof rack	10 kHz irradiance measurements	Five direction pyranometers on roof rack	Five reference cells on two types of vehicles	Low-cost, autonomous irradiance sensor installed on a large number of vehicles
	 Pyranometer SP Lite 2 from Kipp&Zonen with readout time < 500ns	 Irradiance $Irr_{s_{1-5}}$		
High fidelity irradiance measurements on horizontal plane. Partial and dynamic shading quantified	High fidelity irradiance measurements with high temporal accuracy	High fidelity irradiance measurements in all directions.	High fidelity irradiance measurements in all directions.	Crowdsourced irradiance and driving data under 'real-world' conditions, including parking behaviour

Measurements in Burgdorf, Switzerland found that a vehicle's roof gets around 70% of the irradiance that a flat area of the same extent would receive. This value needs to be confirmed in the months to come as it appears to differ with the position of the sun throughout the year. Also, in this case, the vehicle has very good sun exposure during the whole day. In the case of another vehicle, which is parked in the shade most of the time, the ratio was around 21%. This result shows that where the car is parked will greatly influence the electricity generation of PV on vehicles.

In Australia, two initial vehicle irradiance surveys have been carried out. In the case of a long road trip from Sydney to Canberra, a total of 5,4 kWh/m<sup>2</sup> was estimated to fall on the vehicle during the journey that is estimated to add 30 km of solar range to the vehicle. Long term monitoring of a passenger vehicle during the autumn and winter in Melbourne (and during a period of restricted mobility due to the COVID-19 pandemic) showed that the vehicle was parked 97% of the time and that 80% of the irradiance falling on a passenger vehicle took place while the vehicle was stationary.

In addition to the impact of environmental shading, it was found that at higher latitudes (where there is a relative decrease of the sun's height), the inherent curvature of on-board PV had a negative impact on electricity generation. However, the model-based study in Japan found that both the curve-correction factor and effective solar resource to the vehicle's roof, normalized to GHI, do not show a strong correlation to latitude. They are unlike other typical solar resource parameters, more affected by local meteorological conditions. Also, both the curve-correction factor and the effective solar resource relative to GHI, are strongly influenced by the specific distribution of shading objects.

More irradiance measurements are needed in order to more accurately quantify the possible energy yields and driving distances on solar power throughout the year in specific locations and on specific driving routes. Additionally, once a large data set is acquired, the measured values need to be normalized to standard irradiance levels measured in the past decades in order to eliminate statistical deviances.

Data on solar irradiance acquired by a vehicle is a first step toward the use of PV in automobiles and will provide vital information for evaluating the significance and effect, as well as optimal design, of on-board PV systems.



#### D. Next steps for realising PV-powered vehicles

This report presents an overview of recent trends of PV-powered vehicles in the world, and discussed expected benefits of PV-powered vehicles and measurements of solar irradiance on vehicles. Although more and more PV-powered vehicle projects are being started, further actions will be necessary to realise practical deployment of PV-powered vehicles. As next steps for realising PV-powered vehicles, potential benefits of PV-powered passenger vehicles, and issues for realising PV-powered vehicles, standardisation of solar irradiance and module design, and combination with PV-powered infrastructures have been explored.

#### Potential benefits of PV-powered vehicles in IEA PVPS Task 17 member countries

Based on the case studies on PV-powered passenger vehicles described in B, expected benefits of PV-powered passenger vehicles in IEA PVPS Task 17 member countries were estimated (see Fig. D-1).



**Fig. D-1 Comparison of CO<sub>2</sub> emissions for each location with and without PV**

(The locations with the lowest local grid carbon intensity, Bern and Paris, both have no CO<sub>2</sub> benefit from the 800 Wp PV on the long-range vehicle for the simple 15 km commute driving profile.)

In most cases, CO<sub>2</sub> emissions are reduced during the operation of the vehicle by the on-board PV. However, in some cases, e.g. in countries with very clean grid energy, the embedded CO<sub>2</sub> based on the manufacturing of PV modules might lead to slightly higher lifetime emissions. In order to increase the CO<sub>2</sub> reduction achieved for all PV-powered vehicles, PV modules with lower embedded emissions are needed, in addition to higher efficiencies and/or longer PV component lifetimes. Well-integrated PV technologies such as curved, flexible and lightweight PV modules, in addition to higher efficiency PV technologies, will contribute to increased PV electricity generation.

These studies also find that maximizing PV utilisation is important in order to realise the maximum benefits of PV. The value of the PV utilisation ratio where the CO<sub>2</sub> emissions from PV electricity are equal to the CO<sub>2</sub> emissions from the grid corresponds to a crossover point where the PV powered vehicle goes from producing an increase in CO<sub>2</sub> emissions to providing a decrease or an environmental benefit. This point is equal to the ratio of 'CO<sub>2</sub> emission by PV electricity with 100% utilisation ratio' to 'CO<sub>2</sub> emission by grid' (see Fig. D-2).

This cross-over, or minimum PV utilisation ratio, has been calculated for each of the Task 17 countries' locations (see Fig. D-3). The minimum utilisation ratio required varies between locations. The higher the grid carbon intensity and PV generated electricity, the lower the required utilisation ratio. In most locations, the minimum PV utilisation ratio is less than 30%. When the grid carbon intensity is very low, as in Paris and Bern (not shown), the minimum utilisation ratio is above 100% indicative of the higher CO<sub>2</sub> emissions of the PV modules resulting in an increase in CO<sub>2</sub> emissions with PV on-board with current state-of-the-art technology. Research and development to lower embedded emissions of PV modules, as well as increasing efficiency and improved reliability of PV components is needed to increase the environmental impact on on-board PV, in terms of CO<sub>2</sub> emissions. These results do not currently consider the potential for trading battery capacity for on-board PV and the accompanying impact on lifetime CO<sub>2</sub> emissions.

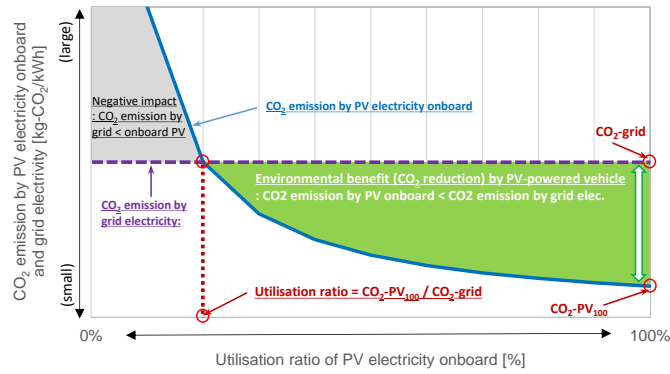


**Fig. D-2 Image of relations between CO<sub>2</sub> emissions of PV/grid electricity, utilisation ratio of PV electricity, and CO<sub>2</sub> reduction by PV-powered vehicle**

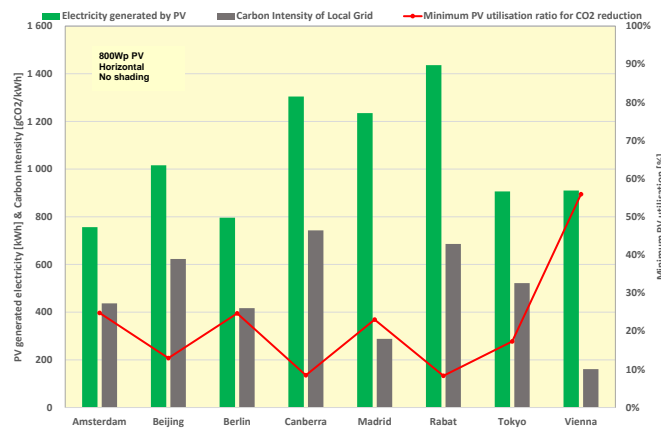


**Fig. D-3 PV generated electricity and carbon intensity of the local grid (left axis) and the minimum utilisation ratio of PV electricity to begin achieving a CO<sub>2</sub> reduction (right axis)**  
(Bern, Switzerland and Paris, France are omitted as they will not have a CO<sub>2</sub> reduction for the given example.)

Driving patterns and solar irradiance vary by region, country, and driver. In order to increase the level of utilised PV electricity, optimised design of PV-powered vehicles with respect to PV capacity considering effective solar irradiation and vehicle efficiency, battery capacity and efficiency and the operating condition is required. On the other hand, increasing the utilisation ratio of PV electricity also avoids surplus PV electricity. One of the most promising approaches will be to provide PV electricity to surroundings when the PV-powered vehicle is parked, i.e. V2X. Another approach to maximise PV utilisation is managing the battery's state-of-charge (SOC) to ensure that enough capacity is available for storing on-board PV electricity. When reserved capacity for PV electricity is well-managed, demand for grid electricity is reduced and less PV electricity generated on-board will go to waste.

### Issues for realising PV-powered vehicles

PV modules integrated into vehicles are a part of a PV system, and as well, part of the components of vehicles. The product will be tested and rated by two standards. For example, the performance of the PV module will need to be verified as a PV system with necessary corrections by the different usage such as moving, frequent shading, etc. At the same time, it is to be tested as an exterior component of vehicles, such as different types of glass. And it is also to be tested as a vehicle's electrical component.

The standard PV modules are installed in such a way to avoid shades on the installation. However, PV modules on the vehicle's roof are not oriented to optimise for the utilization of solar energy. The driver's parking preferences may often lead to shade being cast on the PV. The relative orientation of the PV on the vehicle to the sun's position



is not fixed but frequently changes by driving. The PV on the vehicle's body and the vehicle's roof is curved. It is often shaded by its own surfaces. Therefore, the methodology for performance analysis needs to be reconstructed.

For the moment, there is no published standard as well as no records of publications of official activities for the international standardisation. In order to establish standards for solar irradiation and module design for PV-powered vehicles, rating tests, design qualification, power modelling and energy prediction will need to be addressed. The following vehicle-specific issues will need to be considered: greater chance of shading by objects around the vehicle (trees and buildings), curved surface, varying orientation angles, and mismatching loss by partial shading. As discussions for standardisation will be done by another body like the IEC, technical requirements for PV installation into a vehicle's body will be discussed more in Task 17's next steps.

As another issue, in order to effectively use the PV electricity generated on-board, the potential of PV applications for electric systems and infrastructures will need to be addressed. The combination of PV-powered vehicles and charging infrastructures takes advantage of PV-powered vehicles: PV production impact in stationary mode, requirements regarding the charging infrastructures, and PV benefits when services such as vehicle-to-grid/home/vehicle are available at charging terminals.

Regarding the PV-powered charging infrastructure with a PV vehicle parking shade, the PV-powered vehicles may present maximum PV benefits while parked outside the shade of the station; therefore, an additional study related to the station design is required. Although it will not change the V2X design and technology, the PV electricity produced and stored by PV-powered vehicles can be used as an additional flow of electricity for all the V2X services. However, the real "additional value" earned from vehicles powered by PV is the PV electricity real-time production during the time the vehicle is parked, on public parking or at home. In addition, regarding V2H, if at home the vehicle owner does not have a PV installation, the PV benefits provided by the vehicle could be increased.

These issues will be analysed in Task 17's next steps, which includes the following objectives: requirements, barriers, and solutions for PV-powered infrastructure charging stations, feasibility conditions, and V2X services offered by the PV-powered charging stations.

### **The way forward**

PV-powered vehicles may offer significant benefits to drivers and may offer an important contribution to the energy transition. Their market introduction will require technical optimisation of the PV but also of vehicles and vehicle use. Short driving range commuter vehicles, ultra-light weight vehicles, and high efficiency EVs are the most realistic concepts to apply PV power for smaller passenger vehicles. As a concept of bridge technology to PV-powered vehicles, it will be possible to consider PV-equipped vehicles for auxiliary components such as air conditioning systems, refrigerators and heating systems. This can already be seen in some passenger vehicles. For heavier commercial vehicles such as truck trailers, other goods delivery vehicles, and buses, on-board PV can make significant contributions to these auxiliary systems and the electric conversion of these systems. Taking into account the area available for PV and the possible use of PV electricity for auxiliary demand, PV-powered refrigerated truck trailers and buses are close to market introduction.

The questions of how to directly use and manage PV electricity for different types of vehicles, driving profiles, and locations with different solar irradiance, and how to integrate PV components on-board with keeping mechanical and physical reliability and safety including standardisation will be important for all kinds of PV-powered vehicles.

In order to effectively use the PV electricity generated on-board, an integral approach with PV applications for electric systems and infrastructures will be important. This may also contribute to reducing the impact of widespread PV generation and EV charging on the stability of the grid.

Currently, the PV market in the transport sector is still small. However, the potential impact is large and the electrified transport market will be a key driving force for the further development of PV in the coming years. PV-powered vehicles have the potential to further decrease the CO<sub>2</sub> emissions impact of electrified transport (particularly in the short term) and accelerate the adoption of electric vehicles overall due to decreased dependence on the grid. In order to utilise the potential and to realise PV-powered vehicles, expected benefits should be further validated and evaluated from viewpoints of not only energy, the environment, and from the perspective of users, but also the related industries, and shared with stakeholders such as automotive companies and relevant policy organisations.



# 1. RECENT TRENDS IN PV-POWERED VEHICLES

Battery and plug-in hybrid electric vehicles are being adopted globally as a solution to mitigate CO<sub>2</sub> emissions in the transport sector. In line with this, vehicle emission targets have been proposed and adopted by many countries and policy bodies around the world with goals on the adoption and use of electric vehicles in the near future. With widespread electrification of transportation, PV generated electricity and other renewable energy sources are needed to leverage EV adoption into even more significant CO<sub>2</sub> emission reductions. Exploitation of the distributed nature of PV products in parallel to battery electric vehicles offers a new opportunity in terms of mobile energy generation.

Options for low-carbon charging of electric vehicles include charging from the existing grid network with PV or other sustainable electricity sources, charging from a dedicated charge point with local PV electricity generation, or directly and independently with on-board PV (PV-powered vehicle). Among these options, this report has focused on PV-powered vehicles that can run anywhere without or with less fossil energy.

Considering the direct usage of PV electricity for vehicles generated on-board, e.g. PV-powered vehicles, the available area for PV modules is limited. However, the efficiency of PV cells/modules has been increasing and such PV modules will be able to work for the electricity supply for the vehicle even in a limited area. When larger surfaces are available for PV modules, even conventional PV modules will be able to supply electricity for the vehicle.

This chapter presents an overview of recent trends regarding PV-powered vehicles and relevant PV technologies.

## 1.1 Overview and state of the art of PV-powered vehicles

### 1.1.1 Overview of the commercial offers and R&D projects

In recent years, multiple projects, consortia and companies (both existing and start-ups) have been aimed at delivering PV-powered vehicles. Commercial offers and R&D projects of on-board PV exist on different types of vehicles such as passenger vehicles, camper vans, trains, trucks, boats, planes or spatial vehicles. Examples of such vehicles (proof of concept, prototype or commercial vehicles) are presented below (passenger vehicles on Figs. 1.1-1, 1.1-2 and 1.1-3; camper van on Fig. 1.1-4; train on Fig. 1.1-5; trucks on Figs. 1.1-6, 1.1-7 and 1.1-8; boat on Fig. 1.1-9, drone on Fig. 1.1-10; planes on Figs. 1.1-11 and 1.1-12 and spatial vehicle on Fig. 1.1-13).



Fig. 1.1-1 A passenger vehicle proof of concept - Lightyear one [1]



Fig. 1.1-2 A passenger vehicle prototype - Sion from Sonomotors [2]



Fig. 1.1-3 A commercial passenger vehicle - Prius IV from Toyota [3]



Fig. 1.1-4 A camper van prototype: E-home from Dethleffs [4]



Fig. 1.1-5 A train proof of concept - "TER rayon vert" [5]



Fig. 1.1-6 A coach proof of concept - Starter from Fact Concept Vehicle [6]



Fig. 1.1-7 A truck prototype - Optifuel Lab 2 from Renault Truck [7]



Fig. 1.1-8 A kit for commercial refrigerated trucks - S-Series from TSSC [8]



Fig. 1.1-9 A boat proof of concept - Tûranor form PlanetSolar [9]



Fig. 1.1-10 A drone prototype from Atlantik Solar [10]



Fig. 1.1-11 A plane proof of concept - Solar Impulse [11]



Fig. 1.1-12 A plane prototype – Eraole [12]



Fig. 1.1-13 A spatial vehicle prototype: Stratobus [13]

A list of commercial offers and R&D projects of VIPV is presented in Table 1.1-A, at the end of this section. Although this list is non-exhaustive, the table gathers information such as manufacturer, model, PV surface or power, cell technology or module efficiency.

Among projects listed in Table 1.1-A, a majority are passenger vehicle based (Fig. 1.1-14). These are mainly prototypes vehicles with on-board PV except for passenger vehicles with a significant part of commercial offers (Fig. 1.1-15).

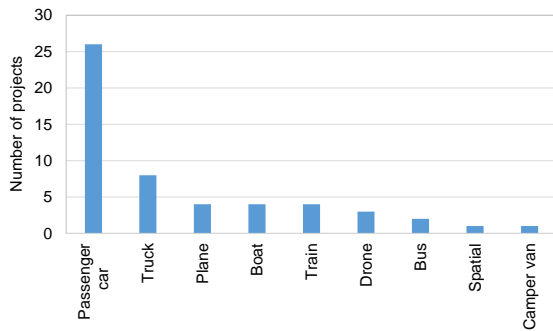


Fig. 1.1-14 Number of projects for the different types of vehicles

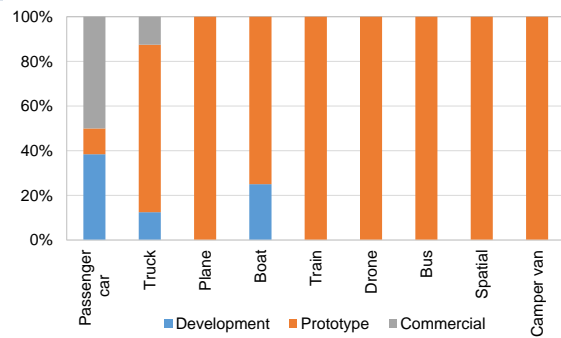


Fig. 1.1-15 Development stage of vehicles per types

In the data collected, the PV surface for each type of vehicle is very different (Fig. 1.1-16). The on board PV surface is from 2,9 m<sup>2</sup> on passenger vehicles up to thousands of square meters on boats. It is easily to understand that as more surface is available, the more PV may be integrated. From the data gathered, the number of passenger vehicle based integrated PV projects is increasing over time (Fig. 1.1-17).

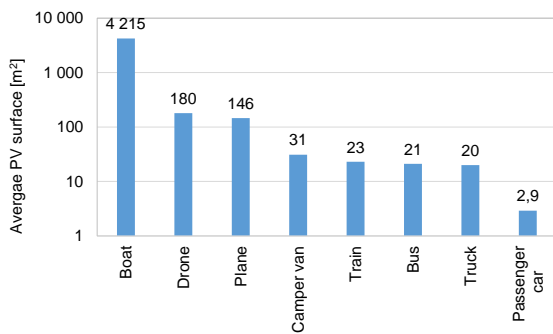


Fig. 1.1-16 Average PV surface (m<sup>2</sup>) for each type of vehicle

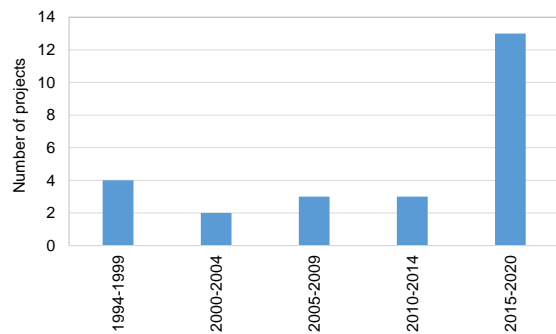


Fig. 1.1-17 Trends in the number of passenger vehicle based integrated PV projects

Camper vans and buses often have a PV module around 100 Wp to keep a lead battery full for auxiliaries' use or to start the vehicle. On buses, trains, and trucks, PV is used for powering auxiliaries; certainly the justification for this use limited to auxiliaries is linked to the voltage values of the PV module and the ease of electrical connection. Several kWp of PV modules may be integrated on such vehicles with a PV surface found between 20-23 m<sup>2</sup>. No commercial offers were found except a PV kit to install. The bigger integrated surfaces are found on boats, drones and planes. Also, spatial vehicles may have the biggest surfaces. The energy is used for propulsion and/or auxiliaries but no commercial offers exist at the moment.

The range extension offered by PV modules integrated on a vehicle will strongly depend on the actual PV production, as well as on the vehicle's efficiency, i.e. the vehicle weight, drag coefficient, etc. (Fig. 1.1-18).

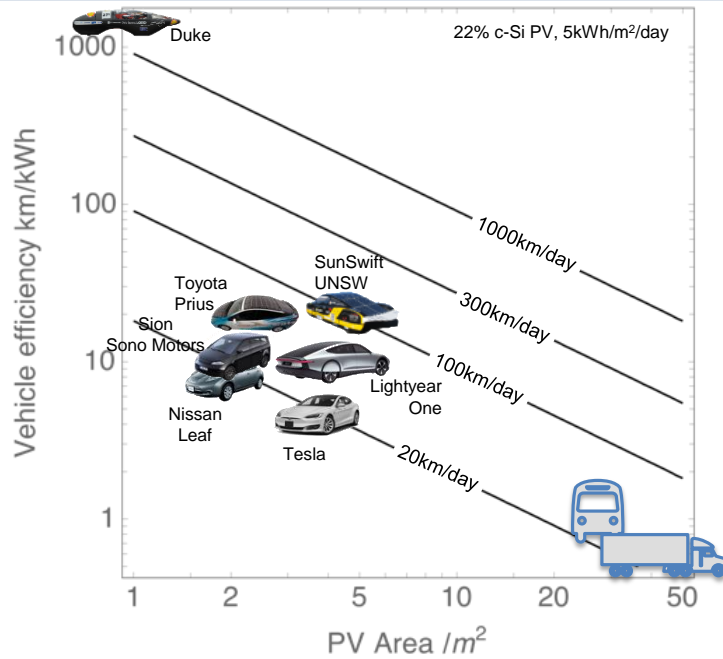


Fig. 1.1-18 Solar range depending of the vehicle efficiency and PV area integrated (log/log scale)

## 1.1.2 PV-powered passenger vehicles fully covered by solar cells

### 1.1.2.1 Vehicles powered by crystalline silicon solar cells

As pioneer manufacturers of PV-powered vehicles, SonoMotors and Lightyear are developing PV-powered passenger vehicles equipped with crystalline solar cells, and their vehicles will be likely coming to the market. Also, the French research institute CEA-INES has developed a prototype of PV-powered vehicles for demonstration.

#### SonoMotors: Sion

“Sion” is a PV-powered vehicle, designed and marketed by SonoMotors; see Fig. 1.1-19. At peak performance, the integrated PV modules with 21% efficiency can generate 1,208 kWp [2]. SonoMotors estimates up to 5 800 km/year using only solar energy and up to 34 km/day (in Munich). Solar body panels are lightweight (4-8 kg/m<sup>2</sup>): at least 20% lighter than comparable metal body parts. The production of the Sion from SonoMotors will be produced in a former Saab plant in Sweden.



Fig. 1.1-19 Sion by SonoMotors (<https://sonomotors.com/en/sion/>)



**Lightyear: Lightyear One**

“Lightyear One” is a PV-powered passenger vehicle, designed by Lightyear; as shown in Fig. 1.1-20 [14]. This vehicle has been designed to be very light, with high performance materials. PV modules on 5 m<sup>2</sup> and 215 Wp/m<sup>2</sup> may provide up to 70 km/day. At peak performance, the integrated PV modules can generate 1,075 kWp [14].



**Fig. 1.1-20 Lightyear One [56]**

Considering basic assumptions such as a location for which the yearly average solar irradiation is moderate, e.g. Compiègne in France, the PV modules slope angle 0°, and initial system loss 14%, Fig. 1.1-21 presents the expected monthly PV array production of Lightyear One.

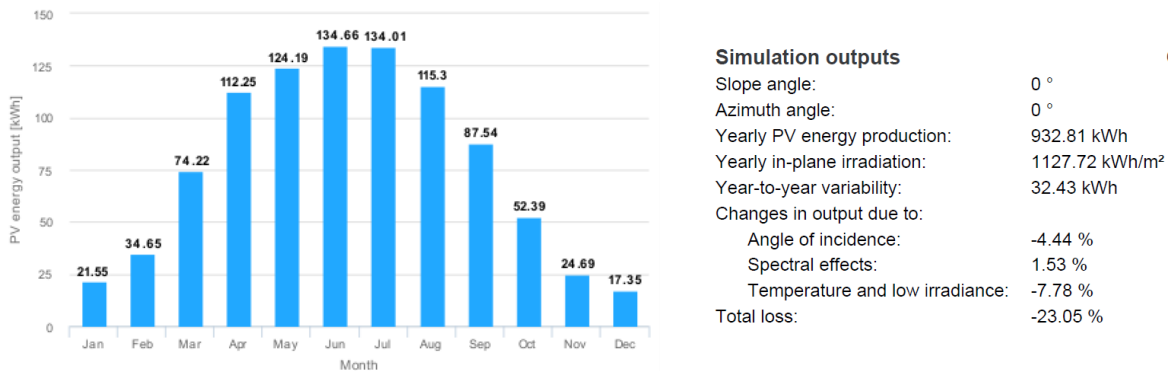


**Fig. 1.1-21 Expected monthly PV energy output from PV array of Lightyear One (PVGIS 2020)**

Based on the data shown in Fig. 1.1-22, the expected PV electricity production by on-board PV (1,075 kWp) is estimated at 932,81 kWh/year. The expected PV production for the least productive month, as well as for the most productive month, is summarized in Table 1.1-1. Considering an eco-drive mode, i.e. 10 kWh/100km, this PV-powered vehicle obtains an additional daily autonomy from 5,6 km to 44,88 km while for normal urban drive, i.e. 15kWh/100km, the additional daily autonomy is from 3,73 to 29,92 km. For dwell time parking with vehicle-to-grid/home/vehicle services, the obtained energy represents an additional one where the impact is variable, from low to high, depending on the energy use (grid, home, and vehicle).

**Table 1.1-1 Expected PV production of Lightyear One for moderately sunny area**

December average PV energy		June average PV energy	
Monthly	Daily	Monthly	Daily
17,35 kWh	0,560 kWh	134,66 kWh	4,488 kWh



### CEA-INES: CZEN vehicle

“CZEN” is a PV-powered vehicle developed by CEA-INES; as shown in Fig. 1.1-22. A static estimation of the collected and produced energy by the CZEN’s PV system is shown in Table 1.1-2.



Fig. 1.1-22 PV modules integration on CZEN vehicle

Table 1.1-2 A static estimation of the collected and produced energy by CZEN’s PV system

Average irradiance at Le Bourget du Lac in a horizontal position representative of a vehicle’s roof	1 350 kWh/m <sup>2</sup>
PV module surface area	1,3 m <sup>2</sup>
PV module efficiency	16%
Energy produced by the PV modules in STC	280,8 kWh
Temperature-related losses (-0,42%/°C), operation at 60 °C (measured in August 2019)	43,3 kWh
Losses linked to the difference in orientation of the 1,3 m <sup>2</sup>	-10%, i.e. 28,1 kWh
Other electrical losses (MPPT, wiring, etc.)	-5% or 14 kWh
Total energy produced	200 kWh
Electricity consumption of CZEN	100 Wh/km (based on actual observations)

Based on these data shown in Table 1.1-2, the number of km produced by solar energy is estimated at 2 000 km/year, i.e. an average of 5-6 km/day at Le Bourget-Du-Lac. Such assessment corresponds to an annual average, the gain in kilometers is closer to 10 km in summer and 0-1 km in winter. The hood contributes to a production ratio of 38%, the front roof to 37% and the rear roof to 25%.

In order to verify these calculations, the vehicle was exposed in a static position for five consecutive days in August 2019, in a south-facing position on the INES site. Therefore, the conditions were optimal: sunny weather and little shade.

As shown in Fig. 1.1-23, the weather on these five days was relatively sunny with a maximum irradiance of more than 950 W/m<sup>2</sup>. The instantaneous power of the PV modules reaches a maximum of about 150 Wp during maximum sunshine. The deviation from the power of 206,5 Wp measured in STC is mainly explained by:

- Orientation: in STC measurement, the PV modules are at normal incidence and receive a flux of 1 000 W/m<sup>2</sup>. In real conditions, the three PV modules are exposed at different angles to the sun and additionally receive a lower maximum irradiance.
- The temperature: STC measurements were performed at 25°C whereas in real conditions, the PV module reaches the temperature of 50-60 °C in August. The theoretical power of the cells decreases by 0,42%/°C, i.e. a loss of 30 Wp between 25 and 60 °C.

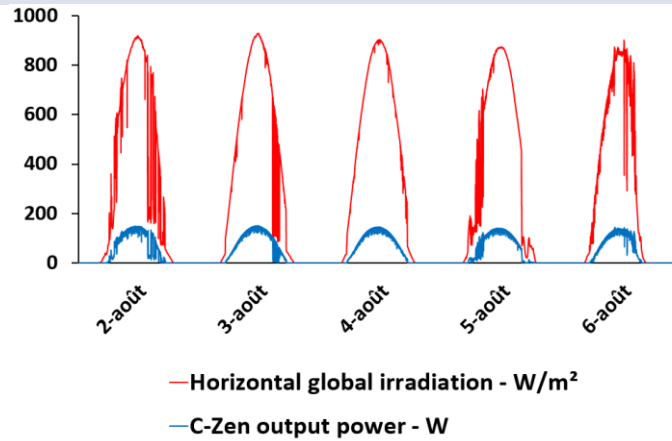


**Fig. 1.1-23 Comparison of the power supplied by the CZEN and the solar irradiance received at the INES site between 2 and 6 August 2019**

From these data, it is possible to calculate the global energy received by the CZEN, the energy produced by the PV modules and the daily gain per kilometer obtained, thanks to the 1,3 m<sup>2</sup> of on-board panels, on an assumption of CZEN consumption of 100 Wh/km.

Fig. 1.1-24 shows that the CZEN's solar autonomy can reach 10 km/day in summer when the weather is favorable, for an installed surface of 1,3 m<sup>2</sup> (206 Wp STC). These results are in agreement with the estimations made previously.

The annual mileage gain on this prototype can thus be estimated at 1 600-2 000 km at the Le Bourget du Lac location.

With a higher module efficiency (20 %) and a larger surface area (> 5 m<sup>2</sup>), the VIPV could contribute to bring more than 10 000 km of autonomy per year, which justifies the real benefits of PV integration on vehicles. This also depends on the size of the battery and if it is drained enough to receive the charge.

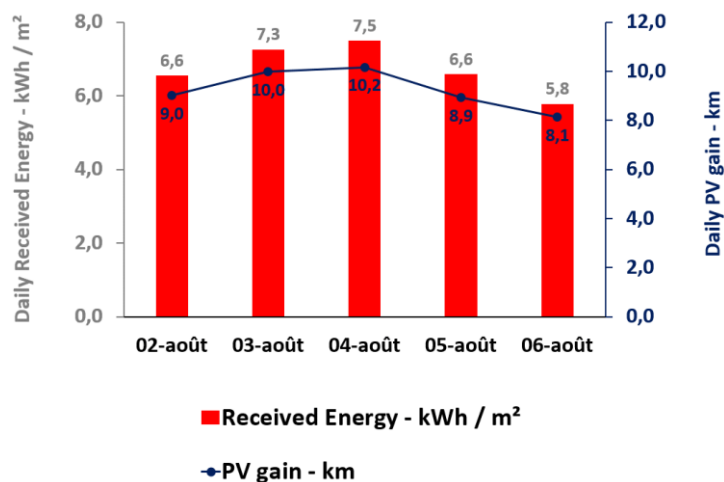


**Fig. 1.1-24 Energy received by the CZEN and equivalent gain in kilometers per day obtained thanks to the on-board PV panels (INES site between 2 and 6 August 2019; hypothesis of CZEN consumption of 100 Wh/km).**



### 1.1.2.2 Vehicles powered by III-V multijunction solar cells

Besides the mainstream of the PV-powered vehicles powered by crystalline Si solar cells, III-V multijunction solar cells are considered to be applied to PV-powered vehicles due to higher power conversion efficiency (typically over 30% of efficiency). The motivation of this challenging solar cell technology to PV-powered vehicles is summarized as follows [15];

1. The best place for the vehicle-integrated PV is the roof of the vehicle, rather than engine hood, rear-window, and vehicle-sides (door and side windows). The real estate of the best residence is limited so that higher power-conversion efficiency is demanded.
2. The typical vehicle-body is three-dimensionally curved. Solar cells are fragile, and they may be able to cover the developable curved surface (cylindrical surface), but it is challenging to cover the entire three-dimensional curved surface. A compromised solution may be searching for vehicles with a less 3D curved area. However, if envisioning the majority of vehicles being equipped by solar panels, it may be necessary to compromise the limitation of the residential area of solar panels. Then, the preferable residential area will be limited, and higher power-conversion efficiency will be desired.
3. The body color is crucial to vehicle sales. It is important to note the fact that roughly 40 000 automobile colors are already used today, and about 1 000 colors are added to the list each year [15-16]. Adding the automobile color to PV with reproduced vivid colours has been developed rapidly and successfully, along with the acceptable power-generation loss [17-19]. Even though the vivid coloring technology for vehicle-integrated PV has progressed, it is certain that some portion of the solar energy will be lost. Higher power-conversion efficiency is demanded as the margin.
4. The curved surface of the PV panel mounted on the curved surface loses output power [15, 20-21]. For a wider variety of the curved shape leading to attractive vehicles, higher power-conversion efficiency is demanded as the margin.

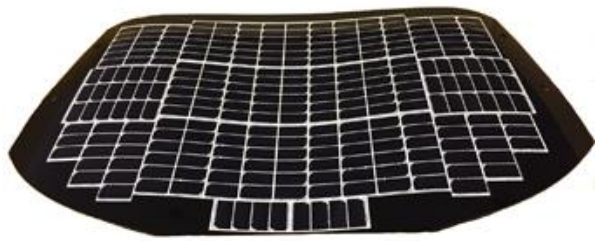
However, the III-V multijunction solar cells have several disadvantages in the application of the vehicle-integrated PV, listed as follows;

1. Higher price than crystalline Si solar cells. This is the main reason why III-V multijunction solar cells are commercially used for space PV, UAV (Unmanned Aerial Vehicle), and CPV (Concentrator Photovoltaics).
2. Sensitivity to spectrum variation and the performance ratio is smaller by the spectrum mismatching loss [22]. However, the amount of the spectrum mismatching loss can be quantitatively counted, and it is also possible to expect the amount of the margin of the power-conversion efficiency [22]. For an ideal configuration (perfect radiative coupling and recycling the recombination radiation due to mismatching loss), the expected maximum annual average efficiency despite the spectrum variation will be 50% [23].
3. For reducing the price and relaxing the spectrum mismatching loss, a four-terminal III-V on Si multijunction solar cells will be a good candidate [24]. However, complicated interconnection will be another disadvantage for vehicle-integrated PV.
4. III-V multijunction solar cells are weak to reverse-bias conditions, and each solar cell has to be protected by a bypass diode, leading to additional protection devices and more complicated interconnections.

Regardless of the above-mentioned disadvantages, the possibility of loading sufficient capacity of PV to normal passenger vehicles will be attractive to car manufacturers. Two major car manufacturers in Japan, Toyota Motor Corporation and Nissan Motor Corporation, engineered prototypes of PV-powered vehicles using III-V multijunction solar cells, supported by NEDO (New Energy and Industrial Technology Development Organization), and started testing [25-26]. The pictures of prototyped PV-powered vehicles are shown in Fig. 1.1-25 and Fig. 1.1-26. The specification of vehicles, PV, and battery, is summarized in Table 1.1-3. It is important to note that both vehicles are commercial passenger vehicles implying that the high-efficiency III-V multijunction solar cells are capable of being mounted on normal passenger vehicles without sacrificing elegant body shapes.



(a)



(b)

Fig. 1.1-25 Prototyped PV-powered vehicle using III-V multijunction solar cells on Toyota Prius; (a) Overall view; (b) PV panel mounted on the back-door [25].



(a)



(b)

Fig. 1.1-26 Prototyped PV-powered vehicle using III-V multijunction solar cells on Nissan e-NV200; (a) Overall view; (b) PV panel mounted on the hood [26].

Table 1.1-3 Summary of the specification of the prototyped PV-powered vehicles using III-V multijunction solar cells [25-26]

	Toyota Prius	Nissan e-NV200
PV capacity*	860 W	1 150 W
PV cell efficiency	> 34 %	
Battery capacity	8,8 kWh	40 kWh

\* The solar cell's total amount of rated power (not tested in the curved conditions nor after module fabrication)



Table 1.1-A Non-exhaustive list of commercial offers and R&amp;D projects of VIPV

Manufacturer	Model/Project	Type	Stage	Year	Vehicle weight (t)	PV surface (m <sup>2</sup> )	PV Power (kWc)	Cell technology	Cell efficiency	Module efficiency	PV use	References
Eco Ship		Boat	Development	2020		12 000	750				Aux.	[27]
Planet Solar	Tûranor	Boat	Prototype	2010	89	516,0	93,5	Standard		18,1 %	Prop. + Aux.	[9]
Energy Observer	Energy Observer	Boat	Prototype	2017	28	130,0	21	Si		16,2 %	Prop. + Aux.	[28]
SoelCat	Catamaran 12	Boat	Prototype	2017	6		8,6				Prop. + Aux.	[29]
Fast Concept Vehicle	Starter	Bus	Prototype			20,5	3,4	Si mono IBC	21,8 %	16,6 %	Aux.	[6]
Dethleffs	E.home	Camper Van	Prototype	2017	5,6	31,0	3	Si mono		9,7 %	Prop. + Aux.	[4][30]
Hyundai	Sonata Hybrid	Passenger vehicle	Commercial	2020		1,3	0,204	Si mono	22,8 %	15,7 %	Prop. + Aux.	[31][32]
Skoda	Superb	Passenger vehicle	Commercial	2000				4*7 cells			Aux.	[33]
Gaia	Wiseman	Passenger vehicle	Commercial		0,8		0,23	Sunpower				[34]
Audi	A8, A6, A4	Passenger vehicle	Commercial	1994			0,04				Aux.	[33]
Volkswagen	Touareg, Phaeton, Passat	Passenger vehicle	Commercial	1994			0,04				Aux.	[33]
Mercedes	E class, Maybach	Passenger vehicle	Commercial	1994			0,04				Aux.	[33]
Nissan	Leaf - SL model	Passenger vehicle	Commercial	2014							Aux.	[35]
Toyota	Toyota - Prius IV	Passenger vehicle	Commercial	2017	1,5	0,9	0,18	HIT		20,0 %	Prop.	[3]
Karma	Karma - Revero	Passenger vehicle	Commercial	2017	2,5		0,2				Prop.	[33]
Karma	Fisker	Passenger vehicle	Commercial	2011			0,12	80 cells - Si mono				[33]
Hyundai/Kia		Passenger vehicle	Development	2018								[36][37]
Tesla	CyberTruck	Passenger vehicle	Development	2019							Prop.	[37]



Manufacturer	Model/Project	Type	Stage	Year	Vehicle weight (t)	PV surface (m <sup>2</sup> )	PV Power (kWc)	Cell technology	Cell efficiency	Module efficiency	PV use	References
Fiat	Phylla	Passenger vehicle	Development	2008	0,75		0,34				Prop.	[39][40]
Toyota	Prius Prime	Passenger vehicle	Prototype	2019			0,86	Triple junction cells	34,0 %		Prop.	[41]
Gazelle Tech	Gazelle	Passenger vehicle	Prototype	2020	0,68	4,0		9 ASCA modules			Prop.	[42][43]
SonoMotors	Sono Motors - Sion	Passenger vehicle	Prototype	2018	1,4	7,5	1,2	Si mono IBC	24,0 %	16,0 %	Prop.	[2]
Hanergy	Hanergy - Solar R, O, L and A	Passenger vehicle	Prototype	2019	2	3,5 – 7,5	1 - 2	GaAs, III-V flexible	29,0 %		Prop.	[44][45]
Ford	C-Max	Passenger vehicle	Prototype	2014		1,5	0,3	<sup>3</sup> (7*4) SunPower cells		20,0 %	Prop.	[46]
Bochum Univ.	Solar racers	Passenger vehicle	Prototype	2004-2017	0,25-0,36		1,2	Sunpower cells			Prop.	[47]
UNSW	Sunswift solar racers	Passenger vehicle	Prototype	1994-2017	0,17 -0,43	4,0 – 7,9	0,8 – 1,8	Si mono IBC	18 – 23 %		Prop.	[48]
Audi	e-tron quattro	Passenger vehicle	Prototype	2015		2,5	0,4					[33]
Venturi	Eclectic	Passenger vehicle	Prototype	2006	0,35	2,5					Prop.	[49]
Lightyear	One	Passenger vehicle	Prototype	2019	2	5,0					Prop.	[1]
Volkswagen	Tiguan GTE	Passenger vehicle	Prototype	2015		2,1	0,11					[50]
ISRO		Passenger vehicle	Prototype	2017							Prop.	[51]
Peugeot	BB1	Passenger vehicle	Prototype	2009					16,0 %		Aux.	[52]
Atlantik Solar		Drone	Prototype	2017				Si mono IBC	23,0 %	21,0 %	Prop.	[10]
NASA	Helios	Drone	Prototype	2001-2003	0,8	180,0	35			19,4 %	Prop. + Aux.	[53]
Airbus DS	Zephyr	Drone	Prototype	2008	0,05			Si bifacial			Prop. + Aux.	[54]
Solar Stratos	Solar Stratos	Plane	Prototype	2014	0,45	22,0			22,0 %		Prop. + Aux.	[55]



Manufacturer	Model/Project	Type	Stage	Year	Vehicle weight (t)	PV surface (m <sup>2</sup> )	PV Power (kWc)	Cell technology	Cell efficiency	Module efficiency	PV use	References
Océan Vital	Eraole	Plane	Prototype	2015	0,75		5,5	Si mono IBC	24,0 %		Prop. + Aux.	[12][56]
	Solar Ship	Plane	Prototype	2014							Prop.	[57]
Solar Impulse	Solar Impulse	Plane	Prototype	2004	2,3	270,0		Si mono IBC	22,6 %		Prop. + Aux.	[11]
Stratobus	Stratobus	Spatial	Prototype	2018				Si mono IBC	24,0 %		Prop. + Aux.	[13]
FlixBus		Bus	Prototype	2020				CIGS		17 %		[58]
India		Train	Prototype	2017				Si			Aux.	[59]
SNCF	TER	Train	Prototype	2010		23,0	3,1	Si mono IBC	21,0 %	13,5 %	Aux.	[5]
JETTY TRAIN		Train	Prototype	2017								[60]
Byron Bay		Train	Prototype				6,5	Si			Prop.	[61]
TSSC	TSSC	Truck	Commercial			6,4	1,2	Si			Aux.	[8]
IM Efficiency	SolarOnTop	Truck	Prototype	2019								[62]
Volvo	SuperTruck Cab	Truck	Prototype	2014			0,27				Aux.	[33][63]
Renault Truck	Optifuel Lab 2	Truck	Prototype	2014		31,1	4,6	Si mono IBC	22,0 %		Aux.	[7]
Renault Volvo Truck		Truck	Development					CIGS			Aux.	[64]
Navistar	Catalyst	Truck	Prototype	2017		22,4	3,64	Si poly		16,3 %	Aux.	[65][66]
Daimler FreightLiner	SuperTurk	Truck	Prototype	2015							Aux.	[67]
Mitsubishi and Nippon	i Cool Solar	Truck	Prototype	2010			0,9	Organic	4,0 %		Aux.	[68]



## [References]

- [1] Le solaire, une énergie d'avenir. <https://www.fr.sunpower.com/fr/etudes-de-cas/le-solaire-une-energie-davenir>.
- [2] Sion Electric Car – Sono Motors. <https://sonomotors.com/en/sion/>.
- [3] Toyota Prius Hybride Rechargeable | Découvrez la brochure. <https://www.toyota.fr/new-cars/prius-plugin/brochure>.
- [4] Clément. DETHLEFFS lève le voile sur l'E-home, un concept 100% électrique. *Campingcarlesite* <https://www.campingcarlesite.com/camping-car-neuf/2320-dethleffs-leve-le-voile-sur-l-e-home-un-concept-100-electrique/> (2017).
- [5] La SNCF teste des trains économes en énergie. *La Tribune* <https://www.latribune.fr/green-business/l-actualite/1065743/la-sncf-teste-des-trains-economes-en-energie.html>.
- [6] Starter hybride solaire : brillant avenir en Vendée ! <https://www.fccbus.fr/actualites.php?news=21>.
- [7] Renault Trucks Corporate - Les communiqués : Optifuel Lab 2: l'excellence énergétique de Renault Trucks. <https://corporate.renault-trucks.com/fr/les-communiques/optifuel-lab-2-l-excellence-energetique-de-renault-trucks.html>.
- [8] Solar Powered Trucks. *TSSC - Technical Supplies and Services Co LLC* <https://tsscgroup.com/products-and-services/truck-bodies-semi-trailers/solar-powered-trucks/>.
- [9] PERRIER, V. Un bateau photovoltaïque. *Conseil Solaire* <http://conseilsolaire.online/bateau-photovoltaïque> (2018).
- [10] atlantiksolar. *atlantiksolar* <http://www.atlantiksolar.ethz.ch/>.
- [11] Solar Impulse Foundation: 1000 profitable solutions for the environment. <https://solarimpulse.com/>.
- [12] Eraole : l'avion hybride de demain. *Sciences et Avenir* [https://www.sciencesetavenir.fr/high-tech/transports/eraole-l-avion-hybride-de-demain\\_111543](https://www.sciencesetavenir.fr/high-tech/transports/eraole-l-avion-hybride-de-demain_111543).
- [13] Space Q&A : Stratobus | Drupal. <https://www.thalesgroup.com/fr/worldwide/espace/magazine/space-qa-stratobus>.
- [14] <https://lightyear.one/lightyear-one>
- [15] Araki, K.; Ji, L.; Kelly, G.; Yamaguchi, M. To Do List for Research and Development and International Standardization to Achieve the Goal of Running a Majority of Electric Vehicles on Solar Energy. *Coatings*, 8, 251, 2018.
- [16] Cerón, I.; Caamaño-Martín, E.; Neila, F.J. 'State-of-the-art' of building integrated photovoltaic products. *Renew. Energy*, 58, 127–133. 2013.
- [17] Masuda, T.; Kudo, Y.; Banerjee, D. Visually Attractive and High-Power-Retention Solar Modules by Coloring with Automotive Paints. *Coatings* 8, 282. 2018.
- [18] Kudo, Y.; Sato, A.; Kimura, K.; Iwamoto, S.; Ohba, H.; Sakabe, M.; Shirai, Y. Solar module laminated constitution for automobiles. In Proceedings of the SAE 2016 World Congress and Exhibition, Detroit, MI, USA, 12–14 April 2016.
- [19] Masuda, T.; Hirai, S.; Inoue, M.; Chantana, J.; Kudo, Y.; Minemoto, T. Colorful, flexible, and light-weight Cu(In,Ga)Se<sub>2</sub> solar cell by lift-off process with automotive painting. *IEEE J. Photovolt.* 2018.



- [20] Araki, K.; Ota, Y.; Yamaguchi, M. Measurement and Modeling of 3D Solar Irradiance for Vehicle-Integrated Photovoltaic. *Appl. Sci.* 10, 872 2020.
- [21] Ota, Y.; Masuda, T.; Araki, K.; Yamaguchi, M. Curve-Correction Factor for Characterization of the Output of a Three-Dimensional Curved Photovoltaic Module on a Car Roof. *Coatings*, 8, 432, 2018.
- [22] Tawa, H.; Saiki, H.; Ota, Y.; Araki, K.; Takamoto, T.; Nishioka, K. Accurate Output Forecasting Method for Various Photovoltaic Modules Considering Incident Angle and Spectral Change Owing to Atmospheric Parameters and Cloud Conditions. *Appl. Sci.* 10, 703, 2020.
- [23] Araki, K.; Ota, Y.; Saiki, H.; Tawa, H.; Nishioka, K.; Yamaguchi, M. Super-Multi-Junction Solar Cells— Device Configuration with the Potential for More Than 50% Annual Energy Conversion Efficiency (Non-Concentration). *Appl. Sci.*, 9, 4598, 2019.
- [24] Araki, K.; Tawa, H.; Saiki, H.; Ota, Y.; Nishioka, K.; Yamaguchi, M. The Outdoor Field Test and Energy Yield Model of the Four-Terminal on Si Tandem PV Module. *Appl. Sci.* 10, 2529, 2020.
- [25] [https://www.nedo.go.jp/news/press/AA5\\_101150.html](https://www.nedo.go.jp/news/press/AA5_101150.html), last access: Aug. 13, 2020.
- [26] [https://www.nedo.go.jp/news/press/AA5\\_101326.html](https://www.nedo.go.jp/news/press/AA5_101326.html), last access: Aug. 13, 2020.
- [27] Home. <http://ecoship-pb.com/>.
- [28] <http://www.cea.fr/multimedia/Documents/infographies/energy-observer.pdf>
- [29] Solar electric catamaran. *Soel Yachts* <https://soelyachts.com/soelcat-12/>.
- [30] Dethleffs e.home: le camping-car 100% électrique est arrivé - Le monde du camping car. <https://www.lemondeducampingcar.fr/actualite/camping-car/dethleffs-e-home-le-camping-car-100-lectrique-est-arriv/60626>.
- [31] 2020 Hyundai Sonata Hybrid: What to expect from its mpg-boosting solar roof. *Green Car Reports* [https://www.greencarreports.com/news/1127957\\_2020-hyundai-sonata-hybrid-what-to-expect-from-its-mpg-boosting-solar-roof](https://www.greencarreports.com/news/1127957_2020-hyundai-sonata-hybrid-what-to-expect-from-its-mpg-boosting-solar-roof).
- [32] Everything About the Sonata Hybrid's Solar Roof - Hyundai Motor Group TECH. <https://tech.hyundaimotorgroup.com/article/everything-about-the-sonata-hybrids-solar-roof/>.
- [33] [https://www.autoklimaanlage.info/fileadmin/user\\_upload/Tagung\\_2013/PRO\\_KLIMA\\_Wecker\\_Potentials\\_of\\_Solar\\_Systems\\_in\\_Vehicles\\_for\\_Air\\_Conditioning\\_2013-12-04.pdf](https://www.autoklimaanlage.info/fileadmin/user_upload/Tagung_2013/PRO_KLIMA_Wecker_Potentials_of_Solar_Systems_in_Vehicles_for_Air_Conditioning_2013-12-04.pdf).
- [34] [Hot Item] Energy Saved Solar Electric Car Populr Vehicles. *Made-in-China.com* <https://gaiasolar.en.made-in-china.com/product/ASuQJdZbZPpO/China-Energy-Saved-Solar-Electric-Car-Populr-Vehicles.html>.
- [35] 2014 Nissan LEAF Press Kit. *Nissan News USA* <https://usa.nissannews.com/en-US/releases/us-2014-nissan-leaf-press-kit> (2013).
- [36] Kia and Hyundai reveal solar charging system technology to power future eco-friendly vehicles. [https://press.kia.com/ie/en/home/media-resouces/press-releases/2018/Kia\\_and\\_Hyundai\\_reveal\\_solar\\_charging\\_system.html](https://press.kia.com/ie/en/home/media-resouces/press-releases/2018/Kia_and_Hyundai_reveal_solar_charging_system.html).
- [37] Lambert, F. Hyundai and Kia unveil new solar roof to charge batteries in vehicles, launching next year. *Electrek* <https://electrek.co/2018/10/31/hyundai-kia-solar-roof-electric-vehicles/> (2018).
- [38] Lambert, F. Tesla Cybertruck will have solar roof option to add 15 miles of range per day. *Electrek* <https://electrek.co/2019/11/22/tesla-cybertruck-solar-roof-option-add-range/> (2019).



- [39] Une voiture à l'énergie solaire chez Fiat ? *Autoplus.fr* <https://www.autoplus.fr/actualite/make-Divers-model-Divers-659700.html>.
- [40] Fiat : Le projet Phylla en panne ? Non, seulement sur une dépanneuse... *Blog Automobile* <https://blogautomobile.fr/fiat-le-projet-phylla-en-panne-non-seulement-sur-une-depanneuse-19272> (2009).
- [41] Toyota shows off solar Prius with 860 W output from 34% efficient cells. *pv magazine International* <https://www.pv-magazine.com/2019/07/12/toyota-shows-off-solar-prius-with-860-w-output-from-34-efficient-cells/>.
- [42] Solar car tarp to recharge EV batteries – *pv magazine International*. <https://www.pv-magazine.com/2020/04/06/solar-car-tarp-to-recharge-ev-batteries/>.
- [43] Retractable car cover claimed to gain miles of EV range each day. [https://www.greencarreports.com/news/1127787\\_retractable-car-cover-claimed-to-gain-miles-of-ev-range-each-day](https://www.greencarreports.com/news/1127787_retractable-car-cover-claimed-to-gain-miles-of-ev-range-each-day).
- [44] Hanergy Solar R. *ACI* <https://www.allcarindex.com/concept/china/hanergy/solar-r/>.
- [45] China's Hanergy showcases 4 models of 100% solar cars. *Renewablesnow.com* [/news/chinas-hanergy-showcases-4-models-of-100-solar-cars-531316/](https://www.renewablesnow.com/news/chinas-hanergy-showcases-4-models-of-100-solar-cars-531316/).
- [46] Ford C-Max Solar Energi : la première vraie voiture solaire ? | *Automobile*. [https://www.lepoint.fr/automobile/innovations/ford-c-max-solar-energi-la-premiere-vraie-voiture-solaire-03-01-2014-1776499\\_652.php](https://www.lepoint.fr/automobile/innovations/ford-c-max-solar-energi-la-premiere-vraie-voiture-solaire-03-01-2014-1776499_652.php).
- [47] Home - BO | SolarCar. <https://www.bosolarcar.de/>.
- [48] Vehicles | Sunswift. <http://sunswift.com/vehicles>.
- [49] Salon EVER : Venturi présente l' Eclectic, une voiture électrique autonome. *CNET France* <https://www.cnetfrance.fr/cartech/salon-ever-venturi-presente-l-eclectic-une-voiture-electrique-autonome-39368366.htm>.
- [50] Solar car roof by a2-solar. *a2solar* <https://a2-solar.com/en/vw-tiguan-gte-concept-iaa-2015/> (2015).
- [51] ISRO Demonstrates Solar Hybrid Electric Car. *CarandBike* <https://www.carandbike.com/news/isro-demonstrates-solar-hybrid-electric-car-1688371>.
- [52] Peugeot : le BB1 électrique fait sa promo européenne – *Energzine*. <https://www.energine.com/peugeot-le-bb1-electrique-fait-sa-promo-europeenne/9355-2009-11>.
- [53] Gibbs, Y. NASA Dryden Fact Sheet - Helios Prototype. *NASA* <http://www.nasa.gov/centers/armstrong/news/FactSheets/FS-068-DFRC.html> (2015).
- [54] Zephyr. *Airbus* <https://www.airbus.com/defence/uav/zephyr.html>.
- [55] Stratospheric solar airplane. <https://www.solarstratos.com/en/plane/>.
- [56] Premier vol historique pour l'avion hybride Eraole - YouTube. <https://www.youtube.com/watch?v=MeTi2u3kkdc>.
- [57] Solar Ship | No roads. No fuel. No infrastructure. <http://fr.solarship.com/>.
- [58] Flixbus dote ses bus de panneaux CIGS ayant une efficacité de 18 %. *pv magazine France* <https://www.pv-magazine.fr/2020/02/14/flixbus-dote-ses-bus-de-panneaux-cigs-ayant-une-efficacite-de-18/>.
- [59] Mondialisation, M. Un premier « train solaire » en Inde : entre rêve de transition et limites. *Mr Mondialisation* <https://mrmondialisation.org/un-premier-train-solaire-en-inde/> (2017).



- [60] Famous Jetty Train. Busselton Jetty <https://www.busseltonjetty.com.au/jetty-train/famous-jetty-train/>.
- [61] Byron Bay Train » Sustainability. <https://byronbaytrain.com.au/sustainability/>.
- [62] Start reducing fuel consumption with green energy | IM Efficiency. <https://imefficiency.com/>.
- [63] SuperTruck | Volvo Trucks USA. <https://www.volvotrucks.us/innovation/supertruck/>.
- [64] Transports. Solar Cloth System <https://www.solar-cloth.fr/transports/>
- [65] International's CataLIST SuperTruck: The Features. <https://www.ccjdigital.com/international-catalist-super-truck/>.
- [66] Lockridge, D. How Fleets are Using Solar Power. <https://www.truckinginfo.com/157690/how-fleets-are-using-solar-power>.
- [67] SuperTruck. <https://freightliner.com/why-freightliner/industry-leading-results/supertruck/>.
- [68] macsworldwide. I-Cool Solar System tested in Japan. *Mobile Air Conditioning Society (MACS) Worldwide Blog* <https://macsworldwide.wordpress.com/2010/11/16/i-cool-solar-system-tested-in-japan/> (2010).



## 1.2 Overview and perspectives of the PV technologies for PV-powered vehicles

### 1.2.1 Overview of PV cell and module technologies

Photovoltaic solar power generation found its first commercial application in powering spacecraft starting in 1958, which heralded the first practical application for solar cells. Since then, a wide range of solar cell technologies have emerged and are manufactured in large quantities for terrestrial power generation. Today, the market for terrestrial photovoltaics dwarfs that of space with a generating capacity of 115 GWp installed globally in 2019 [1]. Market size for space photovoltaics is not accurately recorded but based on recorded launches in 2019, is estimated to be around 500 kWp per annum. These two established markets for photovoltaic solar cell products set boundaries for the photovoltaic technology that can be incorporated into a vehicle in the near future.

The strong disparity between cost and efficiency in these two photovoltaic technology markets is illustrated in Fig. 1.2-1, with terrestrial photovoltaic modules occupying the low-cost, low efficiency quadrant and space photovoltaic modules in the high-efficiency high cost quadrant. At the time of writing, the lowest solar module spot prices were around 0,2 USD/Wp for terrestrial modules with typical efficiencies of around 18%. These low prices are the result of very large-scale manufacturing and intense market competition within the terrestrial photovoltaic module manufacturing sector. By contrast, high efficiency solar cells used on spacecraft retail at significantly higher prices. A very high premium for photovoltaic efficiency is tolerated by spacecraft manufacturers who prize solar array reliability and weight over cost.

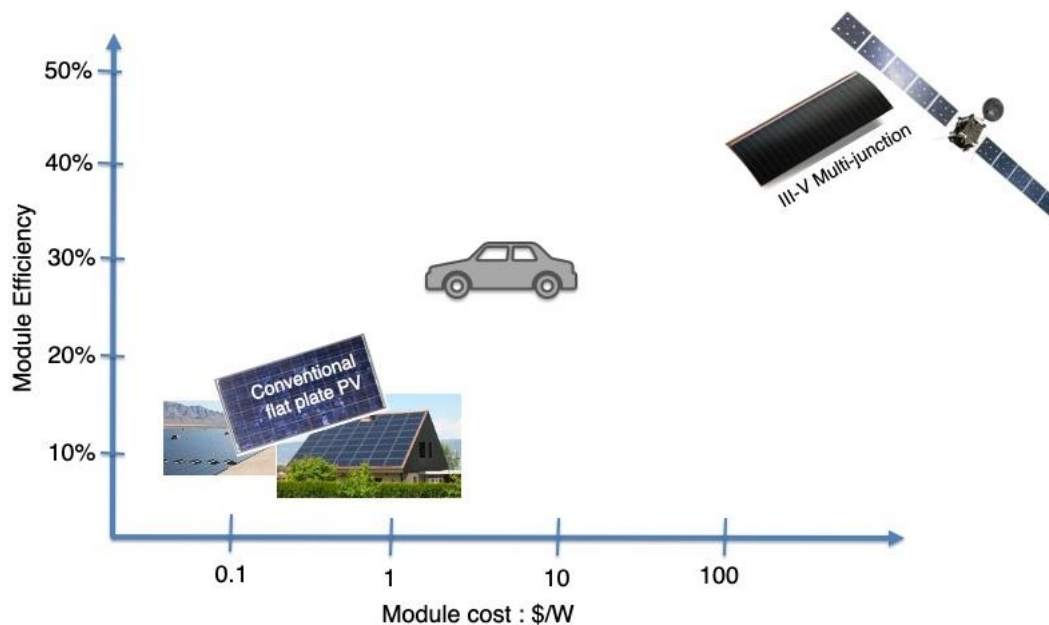
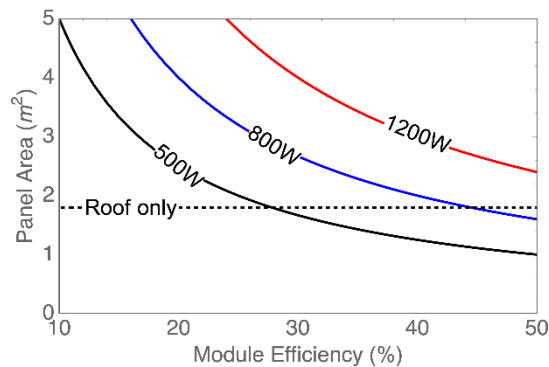


Fig. 1.2-1 Chart showing the module costs for conventional silicon PV and III-V multi-junction solar cells. The likely market for VIPV is anticipated to be for technologies that can attain premium efficiencies over conventional flat-plate PV with module costs in the range 1-10 USD/Wp.

This strong polarisation in photovoltaic technology has left an unoccupied middle ground shown in Fig. 1.2-1, where the efficiency is uncompetitive for spacecraft and prices too high for terrestrial flat-plate PV modules. It is in this area where there is an opportunity to develop PV technologies for vehicles, those with higher efficiency than conventional low-cost flat-plate PV but at a significantly lower cost than those used on spacecraft. The target efficiency module cost point is notionally illustrated by the passenger vehicle in Fig. 1.2-1, the size of this market is estimated to be 50 GWp by 2040 [2].



**Vehicle surface area places a lower bound on solar cell efficiency.** The limited area available on a vehicle places a strong premium upon PV cell efficiency. Fig. 1.2-2 shows how available area and module efficiency are constrained for a particular electrical power output under full sun conditions (1 000 W/m<sup>2</sup>). 500 W is taken as a practical minimum, since with a solar irradiance of 3 kWh/m<sup>2</sup>/day and in a vehicle with a drive efficiency of 10 km/kWh, this would deliver 15 km/day of solar range. Achieving 1 200 W increases this range proportionally to 36 km/day. In case of 6,7 km/kWh, the solar range would be 10 km/day by 500 W and 24 km/day by 1 200 W. Using just the roof, module efficiencies above 25% are required to achieve the minimum 500 W. If the engine hood is also used, this can increase the area to approximately 2,5 m<sup>2</sup> bringing the minimum efficiency down to 20%.



**Fig. 1.2-2 Relationship between the PV module area and efficiency required to deliver an electrical power output of 500 W, 800 W and 1 200 W under standard test conditions (1 000 W/m<sup>2</sup>). Diagram adapted from [2]**

### 1.2.2 Photovoltaic solar cell technologies

The present world record efficiencies for photovoltaic modules are shown in Table 1.2-1. The distinction between module efficiency and the more commonly cited cell efficiency is important since remarkably high solar cell efficiencies can be attained using very small cm<sup>2</sup> sized (or smaller) devices but do not scale well to larger areas. Since for VIPV we are interested in PV technologies capable of delivering power over many square metres in the short to medium term, module efficiencies are considered at this stage.

**Table 1.2-1 Terrestrial module efficiencies measured under global AM1,5 at 1 000 W/m<sup>2</sup> and 25 °C [3]**

Module format	Cell type	Module Type	Efficiency	Module Area / m <sup>2</sup>	Description
Wafer based	III-V thin-film	InGaP/GaAs/InGaAs thin-film	31,2%	0,97	Sharp
		GaAs thin-film	25,1%	0,87	Alta Devices
	Silicon	Silicon Mono-crystalline	24,4%	1,32	Kaneka 2016, HJT IBC cell
		Silicon Multi-crystalline	20,4%	1,48	Hanwa Q cells
Large format substrate	Chalcogenide thin-film	a-Si/nc-Si tandem	12,3%	1,43	TEL solar
		CIGS thin film	19,2%	0,84	Solar Frontier
		CdTe thin film	19,0%	2,36	First Solar
		Perovskite	17,9%	0,80	Panasonic
	Organic	8,7%	0,80	Toshiba	



The table is separated into two different module formats: Wafer based modules are those where a mosaic of solar cells are assembled into a larger module, usually as a series connected string. Large format substrate modules are those where the semiconductor material can be deposited directly onto metal or glass surfaces and which hold particular long-term promise for vehicle integrated photovoltaics. In principle, it should be possible to coat vehicle body parts using these photovoltaic materials and achieve power generation from the entire bodywork. Not shown in the table, but discussed for each cell technology below, is the reliability of the module, meaning the extent to which the photovoltaic material degrades over time. The operational lifetime of a typical EV is 10 years in accordance with the useful lifetime of the battery pack. While this is less than half the standard warranty for conventional solar modules, this does not mean high degradation rates in a VIPV module can be tolerated. Arguably, the role of PV in an EV nearing its end of life is more important since the battery range of the vehicle will have been reduced through wear to the battery pack. Losing PV capacity, in addition to battery capacity would compound driver dissatisfaction with a VIPV product.

**Crystalline silicon (c-Si)** photovoltaic modules made from crystalline silicon are the dominant module technology, with a 94% market share in 2019 [4]. The cells are formed from wafers that are sawn from either a single crystal ingot or from a multi-crystalline cast block, which results in two different cell types, monocrystalline and multi-crystalline silicon solar cells. Historically, multi-crystalline has held larger market share on account of the lower manufacturing costs, but is less efficient; evident from the entries in Table 1.2-1 and discussed further in recent review articles [5]. Recently, the ability to manufacture higher efficiency silicon solar cell architectures has tipped the balance back in favour of monocrystalline wafers, providing a pathway to achieve performance approaching the record values above in volume manufacturing. According to the 2020 International Technology Roadmap for PV (ITRPV), premium n-type back contact monocrystalline silicon solar modules are presently achieving 21% in mass production and are projected to reach 23% in 2020. High efficiency (>21,5%) silicon back contact cells were used to form the sun-facing body parts of the Lightyear One solar electric vehicle. Conventional silicon module assemblies usually employ thick front glass that makes the module rigid and inflexible. Recently polymer encapsulated modules have been developed that can be laminated onto curved surfaces. Both the rigid and flexible technology types have been successfully integrated into vehicles and are discussed further in section 1.2.3. The annual degradation rates for crystalline silicon modules are exemplary, losing only 0,5% of their rated power each year, marking the lowest rate for any photovoltaic technology.

**III-V thin film solar cells** represent the highest efficiency but also the highest cost photovoltaic technology. The cells are formed by depositing semiconductor onto a crystalline substrate (usually GaAs or Ge) in an epitaxial process that enables highly efficient multi-junction devices to be made. These solar cells are mainly manufactured for use on spacecraft or solar concentrator systems where efficiency is of paramount importance. The present costs of manufacturing have been detailed by Horowitz et al. [6], indicating that substrate cost, epitaxial deposition and metal contact formation represent the top three costs in fabricating the solar cell. Present costs of the technology are unacceptably high for VIPV but techno-economic analysis shows that capacity costs below 1 USD/Wp are potentially achievable with this technology with epitaxial lift-off and wafer reuse [6] or III-V on inexpensive silicon substrates [2]. There is insufficient terrestrial module reliability data to make a quantitative comparison of degradation, the target should be to match crystalline silicon, otherwise the efficiency premium offered by III-V technology risks being lost.

**Amorphous silicon modules** are composed of thin silicon films deposited onto glass. Once the dominant thin-film PV technology holding a 9% market share in 2000, they have since relinquished that lead to other chalcogenide thin film modules and held 0,2% market share in 2019 [4]. The highest efficiencies are obtained in a tandem configuration where an amorphous silicon cell is stacked on top of a nanocrystalline silicon cell resulting in a record efficiency just above 12%. This technology compares unfavourably in efficiency to other photovoltaic technologies and typically degrades faster in operation than crystalline silicon modules but has the virtue of enabling partially transparent, photovoltaic active windows to be made. Kaneka (JP) fabricates a 7% partially transparent amorphous photovoltaic product that has potential to generate power from vehicle windows. Degradation of amorphous silicon photovoltaics is generally higher than crystalline silicon, around 1% of power per annum [7].

**Chalcogenide thin-film modules** account for 6% of global photovoltaic manufacturing and are composed of either CdTe or Copper Indium Gallium Selenide (CIGS) semiconductors deposited onto glass or metal foil. While these thin-film materials are not as efficient as silicon, they represent the most efficient of the thin-film materials that can



be deposited onto glass or metal foil thereby providing the potential to fabricate curved PV active vehicle body parts directly. Degradation of chalcogenide photovoltaic modules has improved and are found to be similar to silicon [8] however momentary, partial shading during operation has been shown to impair the performance of commercial chalcogenide modules [9]; this degradation can likely be mitigated through careful module design.

**Perovskite and organic photovoltaic** modules share the benefit of chalcogenide thin-films of enabling conformal coating of a wide range of substrate types with the added advantage they are solution processable at low temperature. Both technologies are relatively new, having been developed over the last two decades and as a consequence, the long-term stability of these materials and module efficiency is inferior to crystalline silicon, although both are likely to determine the ultimate appeal of these technologies for VIPV.

**Module assembly** for VIPV will inevitably lead to additional costs over those used in conventional flat-plate modules used on buildings. Firstly, there will be additional module assembly costs associated with reliable encapsulation of a curved vehicle body part integrated with photovoltaic solar cells that will be manufactured in relatively small volumes for each vehicle design. The savings enjoyed by terrestrial flat-plate module manufacturing using a standard module size and cell layout will be lost with VIPV. The impact behaviour of a VIPV module will be substantially different from conventional modules, since terrestrial modules only need survive the IEC61215/10.17 hail test, but in addition to surviving this test, a vehicle body part must also deform appropriately to mitigate the damage in the event of a collision. VIPV modules will also be subject to vibrational environments that will be alien to any standard terrestrial module. Only space PV arrays are subjected to levels of vibration beyond that sustained on passenger vehicles.

**Coloured Modules:** The aesthetic appeal of a vehicle will be an important factor in any consumer purchase, so coloured modules may be one prioritised option. This necessitates a small loss in efficiency since light that would otherwise be absorbed by the solar cell must be reflected back to the observers' eye. With well-engineered optical coatings, in principle it is possible to deliver colour with relatively little efficiency loss [10]. Coloured PV modules are most commonly used on building facades where power conversion efficiency is not a primary factor [11]. For VIPV, automotive painting techniques have been shown to be compatible with a CIGS PV cell relatively small (5%) in power loss [12].

**Consumer Willingness to pay for VIPV:** To evaluate consumer attitudes, electrical vehicles equipped with on-board solar charging, a survey of over 2 000 individuals from all socioeconomic backgrounds in over eight cities was carried out in Australia [13]. The questionnaire was designed to determine the desire of the consumer towards a solar electric vehicle and by presenting them with a choice between vehicles that they might wish to purchase, as well as their willingness to pay for the technology. The study showed that the appeal of VIPV is highest among young adults with a willingness to pay for a solar electric range of up to 50 AUD/km among wealthy young adults and an average of 25 AUD/km for all participants. A further premium of 1 415 AUD was determined for colour coordination of the photovoltaic module with the vehicle bodywork and styling. This places the viable VIPV module cost in the region of a few USD/Wp as illustrated in Fig. 1.2-1.

**VIPV Market Potential:** Annual vehicle production statistics provide an approximate indication of the potential size of the VIPV market. In 2019, a total of 87 million passenger and light commercial vehicles were manufactured together with a total of 4,4 million buses and trucks. Assuming a 22% module efficiency, 4m<sup>2</sup> available on a passenger vehicle and 30 m<sup>2</sup> on buses and trucks, this amounts to a total annual capacity of approximately 100 GWp, similar to present terrestrial PV manufacturing market size. In the short term, the VIPV market will be serviced from photovoltaic technologies that can be adapted from terrestrial PV and space PV manufacturing, but this market is sufficiently large so that a new breed of VIPV products are likely to emerge that combine the unique requirements for this application, occupying the high-efficiency, moderate cost zone shown in Fig. 1.2-1.

**VIPV Safety:** The automotive industry is highly regulated in order to ensure the highest standards for safety. Typically, each country has its own road authority that verifies safety standards are met by a vehicle where the vehicle will be registered and used. The exact rules for authorization in each country can vary. Within a country, the rules may also change depending on the type of vehicle, the total number of that make and model produced, and other considerations. However, there is a move globally to try to make safety standards more universal in order to decrease manufacturing and homologation costs. As a general rule, when adding something to the vehicle, such as VIPV, it should not increase the risk to the driver, passengers, or others in the vicinity of the vehicle including



pedestrians, cyclists, or emergency responders. As such, the technology of VIPV must still be adapted and demonstrated to be safe in this context. Conventional PV modules (and most other applications) are designed for stationary applications. With VIPV, situations of higher velocity, more vibrations, impact incidents, and being inherently more accessible to the user or others make the safety of this type of integrated PV very important. For example, based on rules for consumer electronics limiting voltage and current in the system, as well as ensuring adequate electrical insulation layers or active control such that even in an accident, the PV panel can be rendered safe. In addition, full vehicle crash testing must also be performed with the active PV elements. This offers new technical challenges in terms of materials and design.

### 1.2.3 Perspectives on existing PV technologies and their suitability for the integration into the electric vehicles

Conventional flat-plate modules used for rooftop or utility scale power generation require some modification for integration into electric vehicles. Nevertheless, PV modules are available in different formats with different solar cell technology and module encapsulation methods that can allow for non-planar surfaces to be covered with photovoltaic cells.

**Curved PV technologies:** Glass-backsheet or Glass-Glass curved PV technologies have a similar structure to conventional flat-plate modules with a 2-3 mm glass front sheet. This technology use 3D curved glass; an illustrative example is shown in Figure 1.2-3.

**Flexible PV technologies:** Flexible PV modules can use several different technologies ranging from c-Si based cells to thin-film technologies such as organic or CIGS solar cells. An illustrative example is shown in Fig. 1.2-4.

**Light PV technologies:** A PV module technology that is not flexible but light and rigid is listed on Table 1.2-2. Such modules are not flexible but they may replace a vehicle's body parts. They also have the potential to be 3D-curved. An illustrative example is shown in Figure 1.2-5.

A non-exhaustive survey of commercial lightweight and/or flexible modules is shown in Table 1.2-A, at the end of this section. The table presents information such as manufacturer, model, cell technology, weight or module efficiency.



[HIT™ Photovoltaic Module for Automobile]

Fig. 1.2-3 Panasonic module for Toyota Prius [14]

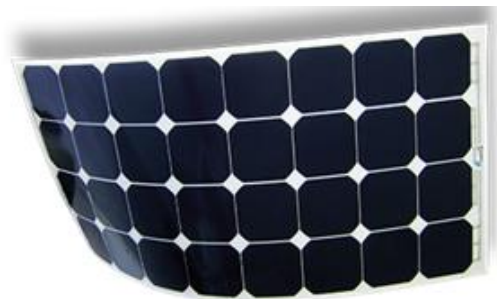


Fig. 1.2-4 Solbian flexible solar panels [15]



Fig. 1.2-5 Sunman light solar panel [16]



Among the PV modules listed in Table 1.2-A, 50% are classed as flexible PV (Fig. 1.2-6), followed by curved PV and Light PV. A histogram of the power density for flexible and lightweight modules (0,7 to 6,7 kg/m<sup>2</sup>) is presented in Fig. 1.2-7; for comparison a standard flat-plate glass-backsheet PV module is 12 kg/m<sup>2</sup>. The wide variation in power density arises from the diversity of cell technologies and encapsulation methods used. A histogram of the power density available (Fig. 1.2-8) shows a tighter distribution and broadly similar to that of standard flat-plate modules. A histogram of the modules classified as light PV is shown in Fig 1.2-9 with a density between 5,6 and 8,9 kg/m<sup>2</sup> but also down to ≤ 4 kg/m<sup>2</sup> (Fig. 1.2-9).

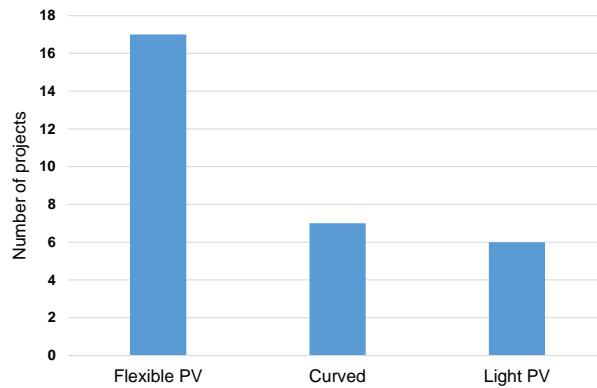


Fig. 1.2-6 Number of projects for each type module technology

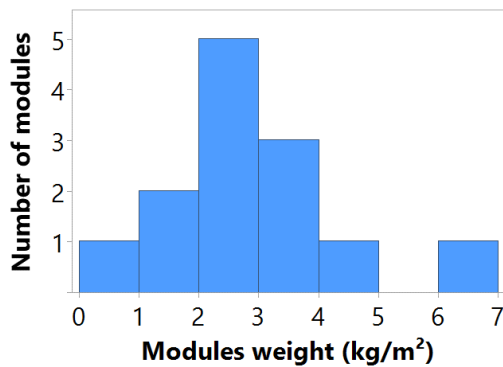


Fig. 1.2-7 Number of commercially available flexible modules in Table 1.2-2 (commercial brands) for each weight class

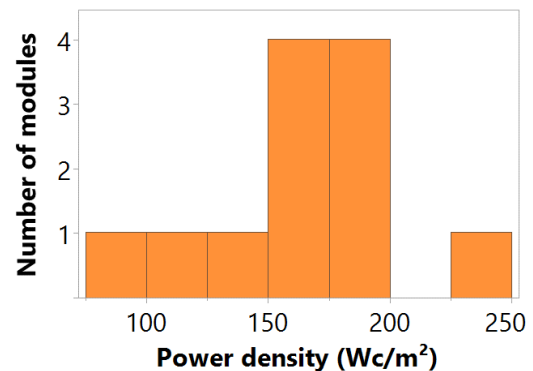


Fig. 1.2-8 Number of commercially available flexible modules in Table 1.2-2 (commercial brands) for each power density class

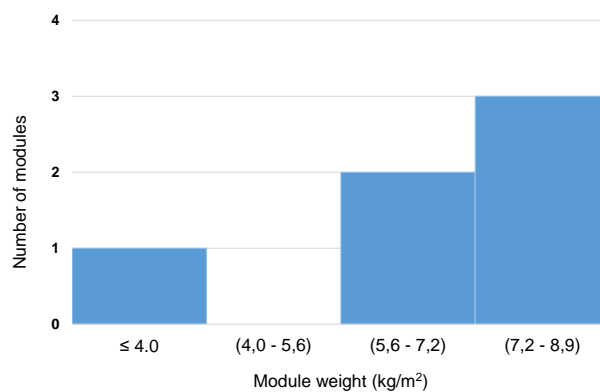


Fig. 1.2-9 Number of light modules for each weight class



Table 1.2-A Non-exhaustive list of light and/or flexible PV technologies and their performances

Manufacturer	Model/Project	Type	Stage	Year	Cell technology	Cell efficiency	Module efficiency	P_surf Wc/m <sup>2</sup>	P_mass Wc/kg	Weight kg/m <sup>2</sup>	Thickness (mm)	References
Panasonic		Curved	Commercial	2017	c-Si HIT							[14]
A2Solar		Curved	Commercial	2013	c-Si							[17]
Fuyao		Curved	Commercial									[18]
Sunpower		Curved	Commercial		c-Si mono IBC							[19]
LG	Neon 2 CELLO cells (6x9)	Curved	Prototype	2018	c-Si LG cell 12BB	23,0 %		167				[20][21]
LG	Neon R IBC cells (6x9)	Curved	Prototype	2018	c-Si LG cell BC	25,0 %		193				[20][21]
Fraunhofer		Curved	Prototype	2019	366 c-Si mono shingle cells							[22]
Gohermann		Flexible PV	Commercial	2014	c-Si mono IBC		22,9 %	229	327	0,70		[23]
SinoSola	SASF	Flexible PV	Commercial		c-Si mono IBC	22,0 %	18,7 %	187	56	3,36	3,00	[24]
Solbian	Flex SP	Flexible PV	Commercial		c-Si mono IBC	23,0 %	17,7 %	177	76	2,34	2,00	[25]
Sacred Solar		Flexible PV	Commercial		c-Si mono IBC	23,0 %	17,4 %	174	51	3,45	3,00	[25]
DAS Energy	Universal Module	Flexible PV	Commercial	2020	c-Si mono 5 BB		17,4 %	174	53	3,30	2,00	[26]
HighFlex	HF315	Flexible PV	Commercial		c-Si mono 3 BB	19,2 %	16,5 %	165	88	1,89	1,50	[27]
Armor	ASCA	Flexible PV	Commercial		Organic							[28]
Heliatek	HeliaSol	Flexible PV	Commercial		Organic							[29]
Opvius		Flexible PV	Commercial		Organic							[30]
Hanergy Miasolé	02WS	Flexible PV	Commercial	2018	CIGS	17,0 %	15,1 %	151	56	2,69	2,50	[31]



Manufacturer	Model/Project	Type	Stage	Year	Cell technology	Cell efficiency	Module efficiency	P_surf Wc/m <sup>2</sup>	P_mass Wc/kg	Weight kg/m <sup>2</sup>	Thickness (mm)	References
Sunware	20 series	Flexible PV	Commercial	2017	c-Si mono		14,3 %	143	21	6,74	5,00	[32]
Nanosolar	UltraLight	Flexible PV	Commercial		CIGS	11,7 %	11,2 %	112	43	2,56	4,00	[33]
Flisom	eFlex 3.1	Flexible PV	Commercial		CIGS		9,4 %	94	36	2,59	2,20	[34]
Couleenergy		Flexible PV	Commercial		c-Si mono shingle	22,4 %	17,7 %	177	70	2,53		[35]
Energy Mobile		Flexible PV	Commercial		c-Si mono IBC		18,3 %	183	43	4,31	3,00	[36]
Go Power	Solar Flex	Flexible PV	Commercial									[37]
Ocean Vital		Flexible PV	Commercial							1,60	0,8 - 1,5	[38]
Lumeta	Lynx 60 Comp	Light PV	Commercial	2018	Si mono 4 BB		18,3%	183	21	8,87	4,00	[39]
BenQ Solar		Light PV	Commercial		Si mono		16,5 %	165	27	6,00		[40]
Sunman	eArche 325	Light PV	Commercial	2017	Si mono 4 BB		16,1 %	161	42	3,82	5 60	[36]
SBM Solar		Light PV	Commercial					160	19	8,30		[41]
Fujjpream	Nozomi	Light PV	Commercial							6,50		[42]
Tulipps Solar		Light PV	Commercial							8,50		[43]



## [References]

- [1] IEA Report, Global Photovoltaic Market 2020
- [2] Yamaguchi, M., Masuda, T., Araki, K., Sato, D., Lee, K., Kojima, N. et al. (2020). Development of high - efficiency and low - cost solar cells for PV - powered vehicles application. *Prog Photovolt Res Appl*.
- [3] Green, M. A., Dunlop, E. D., Hohl-Ebinger, J., Yoshita, M., Kopidakis, N., & Hao, X. (2020). Solar cell efficiency tables (version 56). *Prog. Photovoltaics*, 28(7), 629-638.
- [4] “Photovoltaics Report” Fraunhofer Institute for Solar Energy Systems, ISE & PSE Projects GmbH, 16<sup>th</sup> September 2020.  
<https://www.ise.fraunhofer.de/content/dam/ise/de/documents/publications/studies/Photovoltaics-Report.pdf>
- [5] Green, M. A. (2019). Photovoltaic technology and visions for the future. *Progress in Energy*, 1, 013001.
- [6] Horowitz, Kelsey A. W., Timothy Remo, Brittany Smith, and Aaron Ptak. (2018). *Techno-Economic Analysis and Cost Reduction Roadmap for III-V Solar Cells*. Golden, CO: National Renewable Energy Laboratory. NREL/TP-6A20-72103. <https://www.nrel.gov/docs/fy19osti/72103.pdf>.
- [7] Jordan D C and Kurtz S R 2013 Photovoltaic degradation rates—an analytical review *Prog. Photovolt. Res. Appl.* 21 12–29
- [8] Ochoa, M., Buecheler, S., Tiwari, A. N., & Carron, R. (2020). Challenges and opportunities for an efficiency boost of next generation Cu(In,Ga)Se<sub>2</sub> solar cells: prospects for a paradigm shift. *Energy & Environmental Science*, 13(7), 2047-2055.
- [9] Silverman, T. J., Mansfield, L., Repins, I., & Kurtz, S. (2016). Damage in Monolithic Thin-Film Photovoltaic Modules Due to Partial Shade. *IEEE Journal of Photovoltaics*, 6(5), 1333-1338.
- [10] Halme, J., & Mäkinen, P. (2019). Theoretical efficiency limits of ideal coloured opaque photovoltaics. *Energy Environ. Sci.*, 3(6), 438-1285.
- [11] IEA-PVPS Report “Coloured BIPV: Market, Research and Development.” T15-97:2019.
- [12] Masuda, T., Hirai, S., Inoue, M., Chantana, J., Kudo, Y., & Minemoto, T. (2018). Colorful, Flexible, and Lightweight Cu(In,Ga)Se<sub>2</sub> Solar Cell by Lift-Off Process with Automotive Painting. *IEEE Journal of Photovoltaics*, 8(5), 1326-1330.
- [13] M.Ghasri, A.Ardeshiri, N.J.Ekins-Daukes, T.Rashidi, “Willingness to Pay for Electric Vehicles with Photovoltaic Solar Cells”, *Transportation Research Part C, under review (2020)*
- [14] Panasonic’s Photovoltaic Module HIT(TM) adopted for Toyota Motor’s New Prius PHV | Headquarters News. Panasonic Newsroom Global <http://news.panasonic.com/global/press/data/2017/02/en170228-3/en170228-3.html>.
- [15] SP series - Solbian. <https://www.solbian.eu/en/5-sp-series>.
- [16] SUNMAN. [http://www.sunman-energy.com/pro\\_38\\_show.html](http://www.sunman-energy.com/pro_38_show.html).
- [17] a2-solar - Advanced and Automotive Solar Systems for Facades, Vehicles and Special Applications. <https://a2-solar.com/en/>.
- [18] Photovoltaic Sunroof\_Fuyao Group. [https://www.fuyaogroup.com/en/products\\_list\\_14.html](https://www.fuyaogroup.com/en/products_list_14.html).
- [19] Panneaux solaires pour applications résidentielles et tertiaires | SunPower France. <https://www.fr.sunpower.com/fr>.



- [20] Solar panels for retailers and installers | LG Solar. [http://www.lg-solar.com/hu/media/news/news-2018\\_aug.jsp](http://www.lg-solar.com/hu/media/news/news-2018_aug.jsp).
- [21] LG solar panels and battery systems 2019. CLEAN ENERGY REVIEWS  
<https://www.cleanenergyreviews.info/blog/lg-solar-home-ess-battery-system>.
- [22] Fraunhofer ISE displays colored solar car roof at auto trade fair. pv magazine International <https://www.pv-magazine.com/2019/09/03/fraunhofer-ise-displays-colored-solar-car-roof-at-auto-trade-fair/>.
- [23] GoChermann Solar Technology – Development and Production of High Performance Solar Arrays.  
<https://www.gochermann.com/>.
- [24] Sinosola. <http://www.sinosola.cn/>.
- [25] High Efficiency Bendable PV Module-Sacred Industry|Sacred Solar Technology|Sacred New Energy.  
<http://www.sacredsolar.com/index.aspx?menuid=12&type=introduct&lanmuid=26&language=en>.
- [26] DAS Energy. DAS Energy <https://www.das-energy.com>.
- [27] HighFlexSolar. <https://www.highflexsolar.com/>
- [28] ASCA® | Film photovoltaïque organique transparent et souple. <https://www.asca.com/>.
- [29] Heliatek | Global leader for organic solar films. Heliatek <https://www.heliatek.com/>.
- [30] Home - Organic Photovoltaic Solutions. <http://www.opvius.com/>.
- [31] Products. MiaSolé <http://miasole.com/products/>.
- [32] SunWare Series-20. [https://en.sunware.solar/produkte/module\\_folie\\_20xxx](https://en.sunware.solar/produkte/module_folie_20xxx).
- [33] Nanosolar: <http://www.nanosolar.com/>.
- [34] eMetal, eRoll, eFlex & Customization | Flisom. <https://www.flisom.com/products/>.
- [35] IEC61215 & IEC61730 Certified Solar Panels. Coulee Limited <https://couleenergy.com/>.
- [36] Panneau solaire flexible, Electricité Autonome - Energie Mobile. <http://www.energiemobile.com/>.
- [37] Solar Flex Kits. Go Power <https://gpelectric.com/product-category/solar/solar-flex-kits-solar/>.
- [38] FONDATION OCÉAN VITAL. <https://agence-api.ouest-france.fr/societe/fondation-ocean-vital>.
- [39] For Shingle Roofs. Lumeta Solar <https://www.lumetasolar.com/service/shingle-roofs>.
- [40] AUO Solar. AUOEVENTS-AUOEVENTS <https://solar.auo.com/fr-FR>.
- [41] SBM Solar. <https://sbmsolar.com>.
- [42] Solar Photovoltaic System | Fuji Pream Corporation. <http://www.fujipream.co.jp/en/tech/tech2/>.
- [43] TULiPPS - Home. <https://www.tulipps.com/nl>.



## 1.3 Summary

In this chapter, recent trends regarding PV-powered vehicles and relevant PV technologies were overviewed.

In recent years, multiple projects, consortia and companies (both existing and start-ups) have been aimed at delivering PV-powered vehicles, especially on passenger vehicle-based PV integration. These vehicles offer more than just low emission transport but also options of convenience and autonomy. Market introduction of PV-powered vehicles can be important for uptake of electric transport and create opportunities for other PV applications in the transport sector, as well. Considering the direct usage of PV electricity for vehicles on-board, the available area for PV modules is limited. However, the PV even in a limited area will be able to work for the electricity supply with a battery equipped in the vehicle. All types of solar cells and encapsulation technology are being explored.

In Europe, as pioneer manufacturers of PV-powered vehicles, Sono Motors and Lightyear are developing PV-powered passenger vehicles equipped with crystalline Si solar cells, and their vehicles will be likely coming to the market. “Sion”, by Sono Motors, has lightweight PV modules at least 20% lighter than comparable metal body parts, which can generate 1 208 Wp. Sono Motors estimates up to 5 800 km/year using only solar energy and up to 34 km/day (in Munich). “Lightyear One”, by Lightyear, has been designed to be very light, with high performance materials. PV modules on 5 m<sup>2</sup> and 215 Wp/m<sup>2</sup> may provide up to 70 km/day. Additionally, the CEA-INES developed a demonstration vehicle equipped with 1,3 m<sup>2</sup> crystalline Si PV modules.

In Japan, two major car manufacturers, Toyota Motor Corporation (Toyota) and Nissan Motor Corporation (Nissan), engineered prototypes of PV-powered passenger vehicles using high-efficiency III-V multijunction solar cells, supported by NEDO, and started testing. PV capacity of Toyota’s PV-powered vehicle, Prius-HEV, is 860 Wp and that of Nissan’s PV-powered vehicle, e-NV200, is 1 150 Wp. It is noted that both vehicles are commercial passenger vehicles implying that the III-V multijunction solar cells are capable of being mounted on normal passenger vehicles without sacrificing elegant body shapes.

Silicon-based cells are the most common technologies for PV-powered vehicles. The modules using silicon-based cells show the best compromise between performances and price with an acceptable level of reliability. The weak point is their lack of flexibility in two-directional bending. III-V multijunction solar cells have also been applied to PV-powered vehicles due to higher power conversion efficiency. The disadvantages are higher price and spectrum mismatching loss compared with crystalline Si solar cells. For reducing such disadvantages, a four-terminal III-V on Si multijunction solar cells has also been demonstrated. Other thin-film solar cells, such as amorphous silicon and chalcogenide compare unfavourably in efficiency to other photovoltaic technologies. However, they represent the most efficient of the thin-film materials that can be deposited onto glass or metal foil providing the potential to fabricate curved PV active vehicle body parts directly and perhaps more cheaply. Perovskite cells have the potential of combining high efficiency, low-cost and flexibility, but this technology is not currently manufactured at large scale due to a lack of reliability/durability and, at present, lower efficiency than c-Si based PV at large scale.

From the viewpoint of PV module assembly, there are additional module costs associated with reliable encapsulation of photovoltaic solar cells in the curved vehicle body part. Compared to conventional flat-plate PV modules, these vehicle parts will be manufactured in relatively small volumes for each vehicle design. Curved, flexible and light weight module technologies with low cost and high reliability are required. The modules will also be subject to vibrational environments that will be alien to any standard terrestrial module. The aesthetic appeal of a vehicle will be an important factor in any consumer purchase, so the modules must not only be efficient but also coloured. With well-engineered optical coatings, it is possible to deliver colour with relatively little efficiency loss.



## 2. EXPECTED BENEFITS OF PV-POWERED VEHICLES

PV-powered electric vehicles substitute on-board PV generated electricity in place of grid or charging station electricity. This offers benefits for users in terms of reduction of CO<sub>2</sub> emissions during driving, cost savings, and reduction in the frequency of charging. In order to foresee the expected benefits, some case studies were carried out.

This chapter is focused on the results of case studies on PV-powered passenger vehicles, light commercial vehicles and trucks in various locations around the world.

- Case study on PV-powered passenger vehicles in Japan
  - : Expected CO<sub>2</sub> reduction and charging frequency
    - o Expected benefits of PV-powered passenger vehicles equipped with 1 000 Wp-PV, in terms of the reduction of CO<sub>2</sub> emissions, and comfort (charging frequency) are analysed.
    - o An hourly solar irradiance in Tokyo is used to estimate electricity generated by on-board PV.
    - o Six driving patterns obtained by a previous survey in Japan are used, and life-cycle CO<sub>2</sub> emissions of PV is considered to evaluate environmental benefits.
- Case studies on passenger vehicles in the Netherlands
  - : Reduction of charging, cost and CO<sub>2</sub> emission
    - o A detailed energy flow model is developed to balance the driving profile and use case as well as the vehicle energy demand, battery system, and local irradiance on a 10 minute time step.
    - o The model is used to analyze the performance of 3 different PV-powered vehicles in Amsterdam, the Netherlands.
    - o Eight driving patterns in Amsterdam are assumed.
    - o Expected benefits of PV-powered passenger vehicles equipped with 800 Wp-PV, in terms of the reduction of charging frequency, CO<sub>2</sub> emissions, and cost for charging are quantified..
- Case study on PV-powered light commercial vehicles in Germany
  - : Energy balance and expected CO<sub>2</sub> reduction
    - o PV-powered light commercial vehicles equipped with 2 180 Wp-PV is developed.
    - o Solar irradiance on vehicle's roof during driving is measured in the field, and energy balance for the PV-powered vehicle is analysed.
    - o In order to evaluate environmental impact, a life-cycle CO<sub>2</sub> emission of PV technology integrated into a vehicle is analysed.
- Case study on PV-powered reefer trucks in Spain
  - : Economic feasibility assessment
    - o It is expected that PV is installed on the roof of trailer and that PV electricity is used for refrigeration.
    - o PV electricity substitutes diesel fuel consumption and its economic feasibility is assessed.
- Case study on PV-powered truck trailers in the Netherlands
  - : PV electricity production on trailers
    - o It is expected that PV is installed on the roof and sides of trailer.
    - o PV electricity is used for auxiliaries and saves diesel fuel consumption.
    - o Expected PV electricity production is simulated, assuming both vertical and horizontal installation of PV systems.



## 2.1 Case study on PV-powered passenger vehicles in Japan: Expected CO<sub>2</sub> reduction and charging frequency

PV-powered vehicles substitute on-board PV electricity for grid electricity charged at stations. As one of benefits of PV-powered vehicles, reduction of CO<sub>2</sub> emissions compared to conventional electric vehicles will be expected. Additionally, frequency of electricity charging, for example, at charging stations will be decreased and users' comfort will be improved.

In this section, such benefits expected by PV-powered vehicles are analysed quantitatively.

### 2.1.1 Approaches and assumptions for analysis

#### 2.1.1.1 Fundamental approaches

Benefits of PV-powered vehicles will be derived from reducing fossil fuel based electricity from the grid.

Since expected benefits will differ depending on how the driver uses a vehicle and the on-board battery capacity, it may not be possible to always use 100% of the electricity generated by on-board PV.

The amount of electricity to be stored in an on-board battery is given by the difference between the generated electricity and the electricity consumed. When the generated electricity is greater than the consumed electricity, the remainder is stored in the on-board battery. However, when the on-board battery has been highly charged and there is little free capacity, it is not possible to charge the on-board battery with the electricity generated by on-board PV, resulting in the creation of surplus electricity that will be curtailed as shown in Fig. 2.1-1.

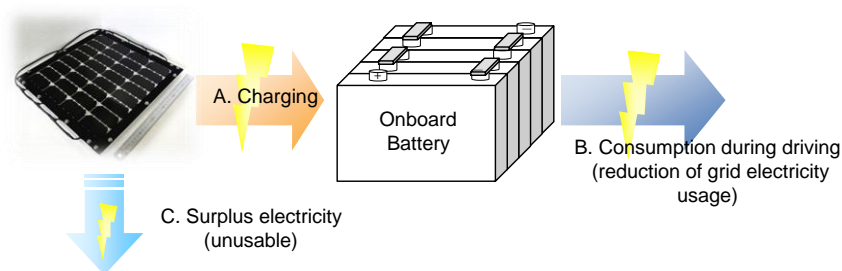


Fig. 2.1-1 Image of surplus electricity created due to battery capacity restrictions

During quantification, taking into account the battery constraints described above, as shown in Fig. 2.1-2, an amount of electricity given by subtracting unusable surplus electricity from the actual electricity generated by on-board PV was referred to as the “reduction of grid electricity usage” achieved through the introduction of an on-board PV system. The reduction in CO<sub>2</sub> emissions and the reduction in frequency of charging were evaluated based on this reduction of grid electricity usage.

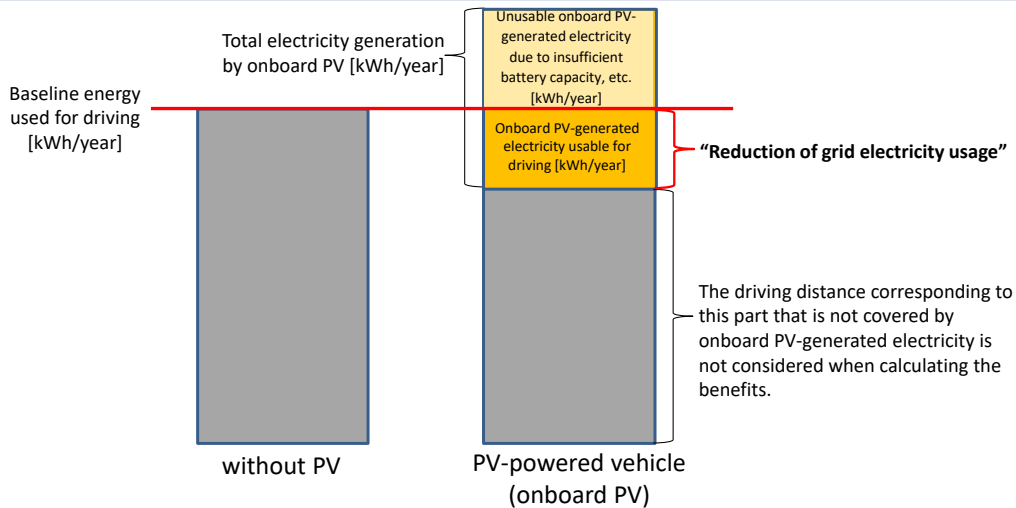


Fig. 2.1-2 Evaluation approach for reduction of grid electricity usage by on-board PV

The reduction of grid electricity usage will depend on the balance between the electricity generated by on-board PV and the surplus electricity that cannot be used for driving, with the unusable surplus electricity being decided by the charging state of the battery and the driving pattern.

Because the amount of electricity generated by on-board PV varies from hour to hour due to weather and season, the electricity generated per hour was calculated from hourly solar radiation in Tokyo for this analysis. The calculation flow of reduction of grid power usage is shown in Fig. 2.1-3. The effect of reducing charging frequency at the stations is analysed by this flow, too.

As electricity consumption by a vehicle will be influenced by driving patterns, the patterns used for this analysis are described later.

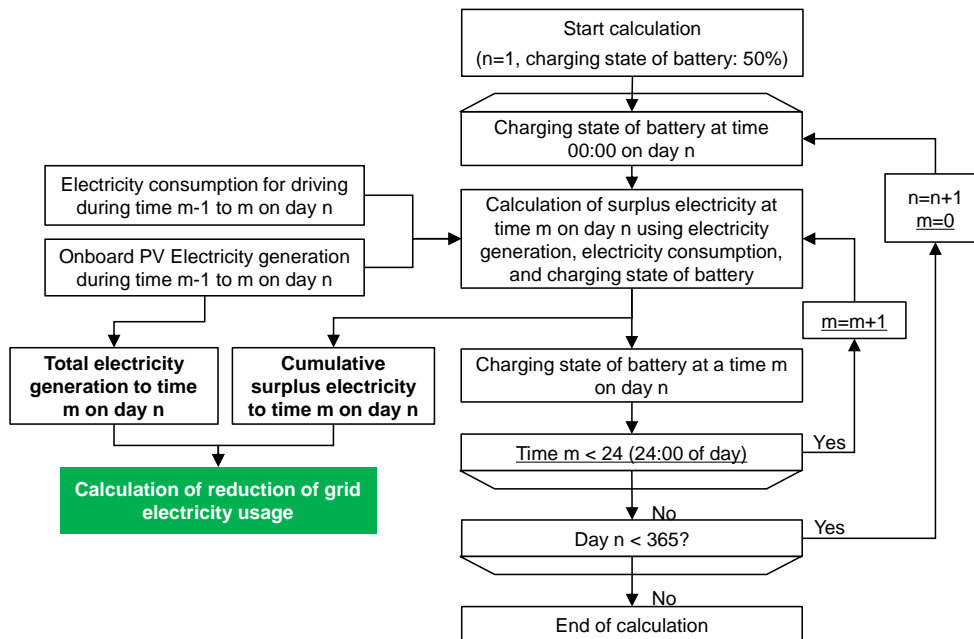


Fig. 2.1-3 Calculation flow of reduction of grid power usage



In this analysis, CO<sub>2</sub> emissions during driving were compared, and as shown in Fig. 2.1-4, only the effect of providing the PV system was evaluated without considering the CO<sub>2</sub> emissions caused by the manufacturing and disposal of the vehicle.

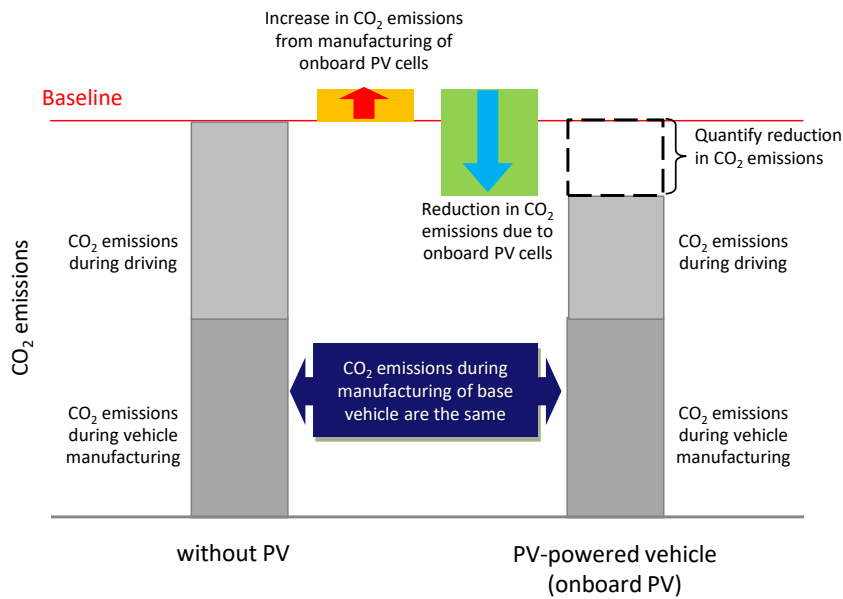


Fig. 2.1-4 Evaluation approach for reduction of CO<sub>2</sub> emissions by on-board PV

The reduction of CO<sub>2</sub> emissions was calculated by subtracting the amount of CO<sub>2</sub> emissions generated by adding on-board PV from the product of the reduction of grid power usage and the CO<sub>2</sub> emission factor for grid power. For the CO<sub>2</sub> emissions by on-board PV, a life-cycle CO<sub>2</sub> of a PV system was considered. On the other hand, although some automobile parts become unnecessary due to the installation of a PV system, and a reduction of CO<sub>2</sub> emissions relating to the manufacturing of such parts is conceivable, it was excluded from the reduction of CO<sub>2</sub> emissions used in this study.

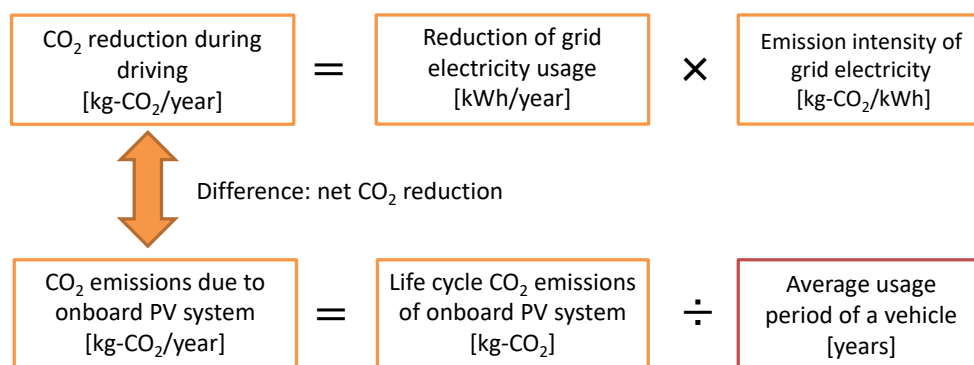


Fig. 2.1-5 Calculation of net reduction of CO<sub>2</sub> emissions

### 2.1.1.2 Representative driving patterns

Various driving patterns of vehicles are assumed according to the user's place of residence and user attributes. From past research, it is known that traffic volume on roads fluctuates on a yearly or weekly cycle.



In this analysis, six driving patterns, as shown in Fig. 2.1-6, which were reclassified from ten driving patterns (c1 to c10) of private passenger vehicles for a one-week cycle obtained by a previous survey in Japan were assumed. Table 2.1-1 includes details of these six types of driving patterns and user images corresponding to the respective driving patterns.

Also, hourly driving distance of these six patterns were assumed as shown in Figs. 2.1-7, 2.1-8 and 2.1-9.

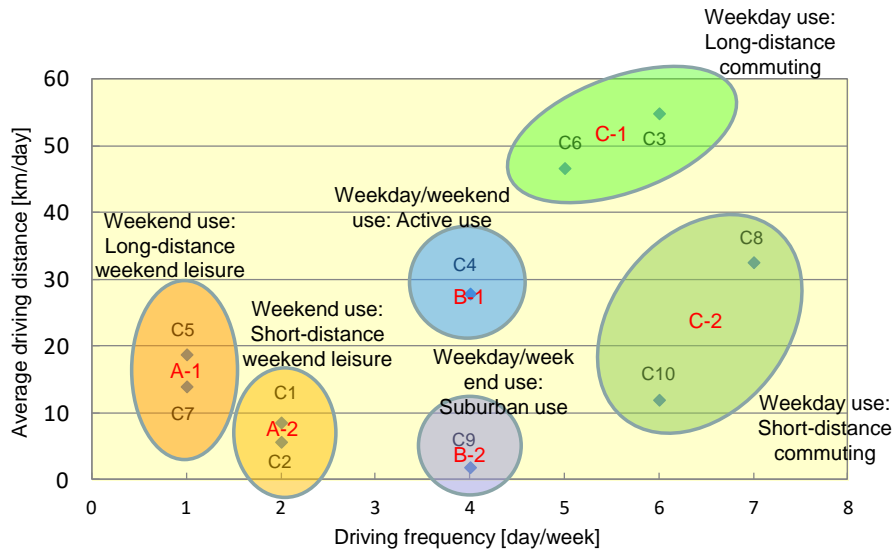


Fig. 2.1-6 Classification of driving patterns used in this analysis [1]

Table 2.1-1 Representative vehicle usage patterns and user images for evaluating introduction of on-board PV

Pattern	Type	Driving distance per journey (km)	User image	Annual driving distance (km/year)
A. Weekend use	A-1: Long-distance weekend leisure	150 km for 2 days (Sat. and Sun.)	Use only on weekends (Sat./Sun.) for visiting distant locations for leisure, etc.	15 600
	A-2: Short-distance weekend leisure	50 km for 2 days (Sat. and Sun.)	Use only on weekends (Sat./Sun.) for visiting nearby locations for leisure, etc.	5 200
B. Weekday /weekend use	B-1: Active use	50 km for 4 days (Mon., Wed., Fri., and Sun.)	Use actively on weekdays and weekends	10 450
	B-2: Suburban use	5 km for 4 days (Mon., Wed., Fri., and Sun.)	Use for visiting shops and local destinations, on weekdays and weekends	1 045
C. Weekday use	C-1: Long-distance commuting	50 km for 5 days (weekdays)	Use only on weekdays for commuting to distant workplace, etc.	13 050
	C-2: Short-distance commuting	15 km for 5 days (weekdays)	Use only on weekdays for commuting to nearby workplace, etc.	3 915

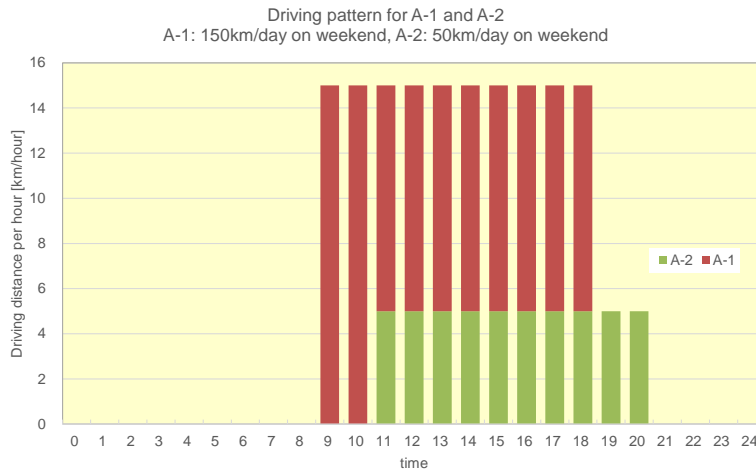


Fig. 2.1-7 Hourly driving patterns for A-1 and A-2

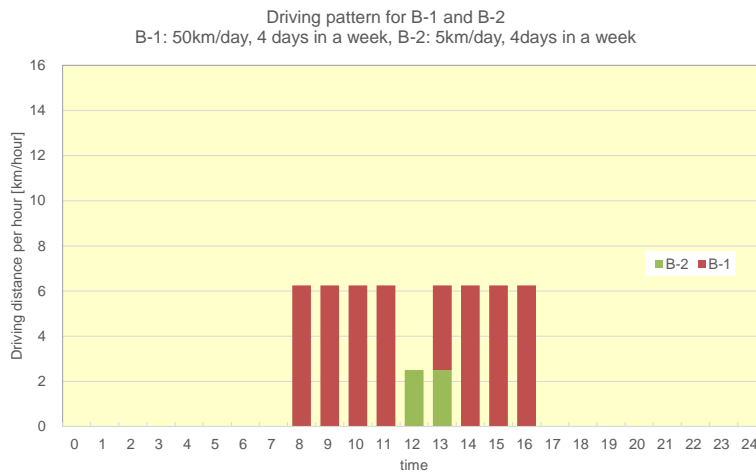


Fig. 2.1-8 Hourly driving patterns for B-1 and B-2

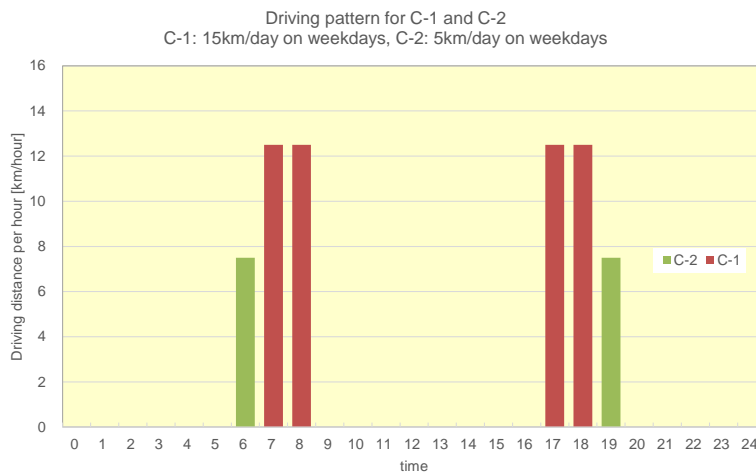


Fig. 2.1-9 Hourly driving patterns for C-1 and C-2



### 2.1.1.3 Assumption on PV and electric vehicle

Table 2.1-2 shows assumptions for analysing benefits.

PV capacity on-board was assumed to be 1 kW. The highest efficiency of current PV modules is 31,17% achieved by NEDO/SHARP Corporation [2], and thus 31% was set as a level that will be sufficiently attainable in the future when on-board PV come into practical use. With this condition, the installation area for PV modules required to achieve an output of 1 kW is 3,23 m<sup>2</sup> as the horizontally projected area, which is substantially equal to the combined area of the roof and hood of electric vehicles currently on the market.

The performance ratio of PV on-board was set at 0,805 [3], considering temperature correction coefficient of 0,91; with a maximum power point tracking (MPPT) loss factor of 0,95; DC/DC conversion efficiency of 0,95 by a power conditioner (PCS), and charging loss factor of 0,98 for the battery. Power consumption by the control unit (ECU) of 0,12 kWh/day [1] was also taken into account.

As to the amount of solar irradiation, the value for the Tokyo metropolitan area in the NEDO's solar irradiation database, METPV-11 [4] was used. The solar irradiation of PV on-board will depend on the environment during driving and parking, as well as on buildings and structures which will be shading the vehicles. A preliminary study implemented in Japan [5] showed that solar irradiation of a vehicle's roof might be 50-90% compared to solar irradiation of a reference point, such as building rooftop, as a tentative results. Therefore, in this analysis, a ratio of effective irradiation was set at 70%, e.g. 30% shading losses.

CO<sub>2</sub> emissions for PV manufacturing per kW was assumed by referring to a past study [6], supposing that PV is manufactured in Japan, with CO<sub>2</sub> emissions for residential PV system using poly-crystalline silicon PV modules, excluding mounting materials and spare parts.

The battery capacity of an electric vehicle was assumed to be 40 kWh. The vehicle efficiency, e.g. electricity consumption of an electric vehicle was set by referring to a catalogue data of the Nissan Leaf vehicle with JC08 mode in Japan [7].

CO<sub>2</sub> emissions of PV on-board per kWh is given by dividing CO<sub>2</sub> emissions of PV manufacturing by the amount of electricity generated during the usage period of vehicle. The average usage period of a vehicle was set at 12 years by referring to an existing study in Japan [1].

For analysing the charging state of a battery and how to charge from the grid, the initial charging state of battery was assumed as 50% of battery capacity (20 kWh), while the remaining electricity for grid charging was 20% of battery capacity (8 kWh), and the upper limit for charging electricity from the grid was 80% of battery capacity (32 kWh).

CO<sub>2</sub> content of grid electricity per kWh was set by referring to the GHG emission factor for electricity supplied from the utility companies, shown by the Ministry of Environment, Japan [8].



Table 2.1-2 Assumptions on PV and an electric vehicle for analysing benefits

PV	PV capacity	(kWp)	1,0	
	Performance Ratio [3]	(%)	80,5%	
		: temperature	(%)	91%
		: MPPT	(%)	95%
		: DC/DC conversion	(%)	95%
		: battery charging	(%)	98%
	Averaged Horizontal solar irradiation (Tokyo, Japan) [4]	(kWh/m <sup>2</sup> /day)	3,39	
	Ratio of effective irradiation considering shading loss	(%)	70%	
	Annual PV electricity	(kWh <sub>DC</sub> /kW/year)	696	
	Electricity consumption by ECU [1]	(kWh/day)	0,12	
	Effective PV electricity	(kWh <sub>DC</sub> /kW/year)	653	
	CO <sub>2</sub> emission for PV manufacturing in Japan [6]	(kg-CO <sub>2</sub> /kW)	1 008	
EV	Battery capacity	(kWh)	40	
	Electricity consumption/vehicle efficiency	(km/kWh <sub>AC</sub> )	8,33	
	AC/DC conversion efficiency	(%)	90%	
	Lifetime [1]	(year)	12	
Battery charging	Initial charging state (before driving)	(%)	50	
	Remaining electricity for grid charging	(%)	20	
	Upper limit for charging electricity at the charging station	(%)	80	
	CO <sub>2</sub> content of grid electricity in Japan [8]	(kg-CO <sub>2</sub> /kWh)	0,462	

### 2.1.2 Utilised PV electricity and PV contribution to electricity for driving

Fig. 2.1-10 shows a vehicle's electricity consumption for each driving pattern (six poles) and expected electricity generation for driving by 1kW-PV on-board (red line). Although electricity consumption for air conditioners are not considered, it seems PV electricity will cover the electricity required for driving for A-2, B-2 and C-2.

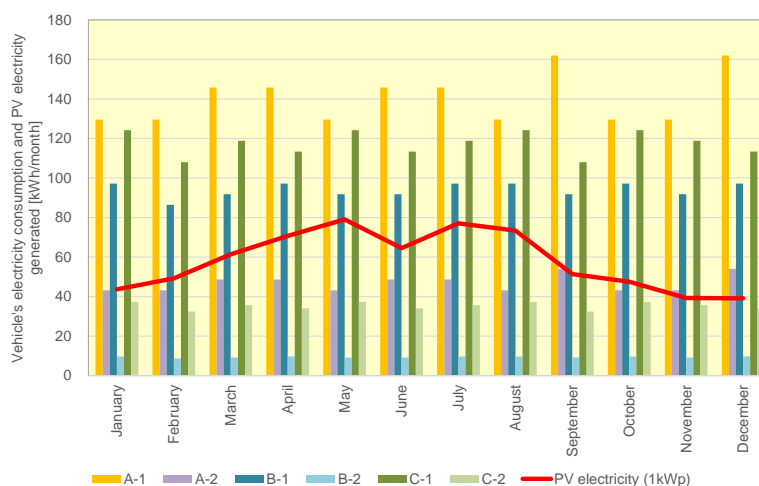


Fig. 2.1-10 Vehicle's electricity consumption and PV electricity generated

Fig. 2.1-11 shows the utilisation ratio of PV electricity (utilised PV electricity for driving/total PV electricity generated) and the contribution ratio of PV electricity (utilised PV electricity for driving/total electricity consumption for driving)



for six driving patterns. Additionally, Fig. 2.1-12 shows the utilised PV electricity and grid electricity for driving with ratios of PV utilisation and PV contribution.

For usage patterns such as A-1, B-1 and C-1 where the total driving distances are long, almost 100% of PV electricity is utilized. However, it will be difficult to drive by only PV electricity and will also be necessary to charge from the grid. The PV contribution ratio will be 38% in A-1, 58% in B-1 and 46% in C-1, respectively. On the other hand, for usage patterns such as A-2, B-2 and C-2 where the total driving distances are short, a vehicle will be driven only by PV electricity. However, surplus PV electricity will be generated and the utilisation ratio of PV will be 84% in A-2, 20% in B-2 and 67% in C-2, respectively.

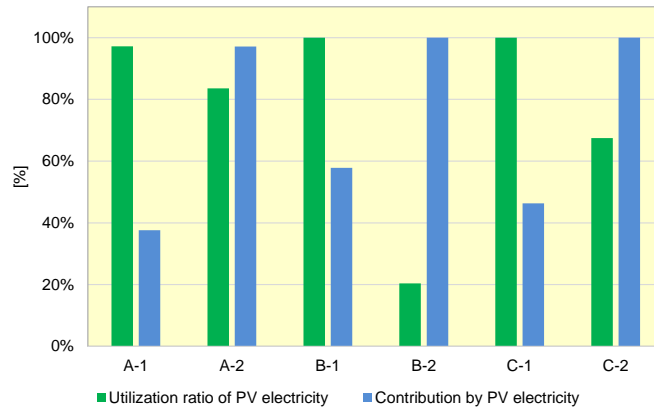


Fig. 2.1-11 Ratios of utilised PV electricity and PV contribution for electricity consumption

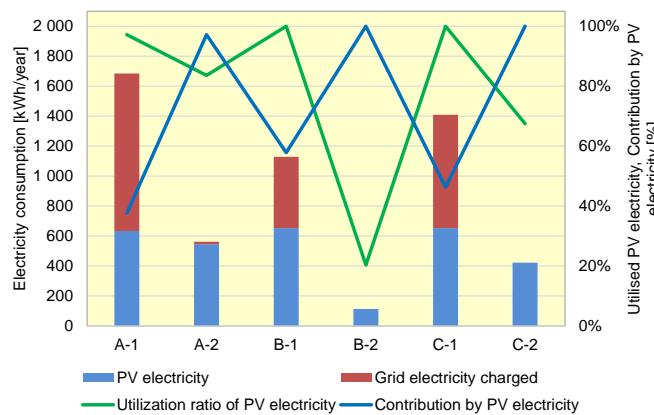


Fig. 2.1-12 Electricity consumption for driving and ratios of utilised PV electricity and PV contribution

## 2.1.3 Reduction of CO<sub>2</sub> emissions and frequency of electricity charging

### 2.1.3.1 Reduction of CO<sub>2</sub> emissions

Fig. 2.1-13 shows expected CO<sub>2</sub> emission for six driving patterns by conventional an electric vehicle (without PV) and a PV-powered vehicle (1kW PV). For five driving patterns except B-2, the PV-powered vehicle will realise reductions in CO<sub>2</sub> emissions. In the case of B-2, which driving distance is shorter and the PV utilisation ratio is lower, CO<sub>2</sub> emissions for PV manufacturing will not be covered by substituting grid electricity for charging.

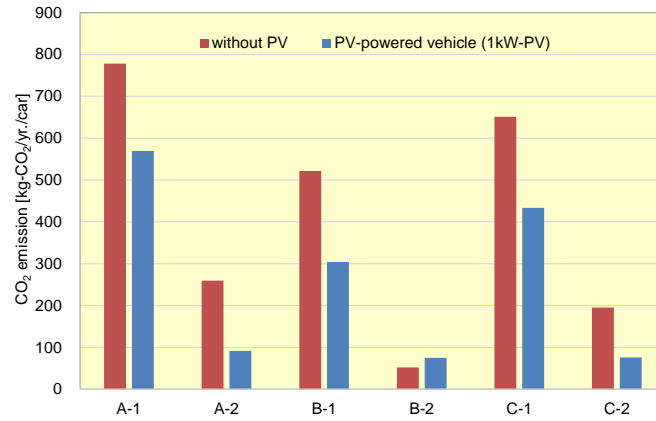


Fig. 2.1-13 Expected CO<sub>2</sub> emissions for six driving patterns

Fig. 2.1-14 shows expected CO<sub>2</sub> reduction by a PV-powered vehicle compared to a conventional electric vehicle without PV. For patterns A-1, B-1 and C-1 which will have 100% of PV utilised ratio, expected CO<sub>2</sub> reduction by PV-powered vehicle will be about 220 kg-CO<sub>2</sub>/year per vehicle.

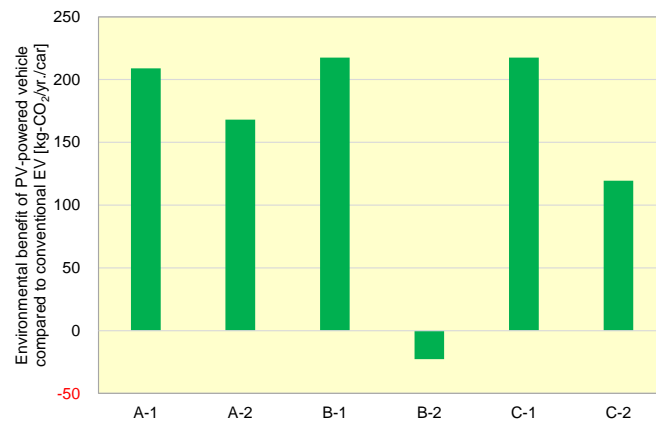


Fig. 2.1-14 Expected environmental benefit (CO<sub>2</sub> reduction) by a PV-powered vehicle compared to conventional electric vehicle

In Fig. 2.1-15, expected CO<sub>2</sub> emissions by electricity per 1km driving is shown. Although CO<sub>2</sub> emissions per 1 km driving for B-2, the shortest driving distance, will increase, the other five patterns will realise a reduction of the averaged CO<sub>2</sub> emissions during driving.

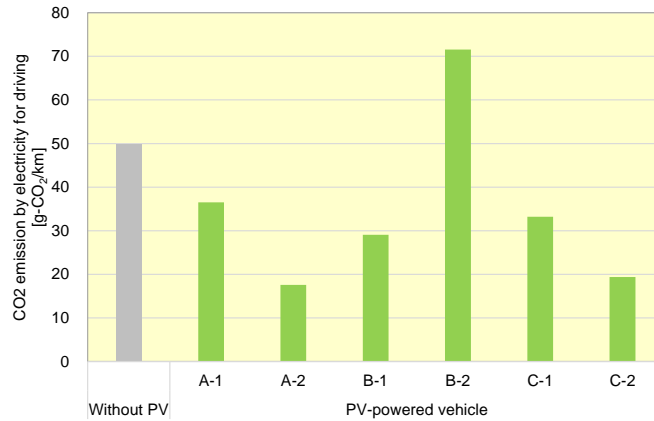


Fig. 2.1-15 Expected CO<sub>2</sub> emissions by electricity per 1km driving: without PV and a PV-powered vehicle (1kW-PV)

2.1.3.2 Frequency of electricity charging

Fig. 2.1-16 shows frequency of electricity charging for both a conventional electric vehicle (without PV) and a PV-powered vehicle (1 kW PV). For all driving patterns, frequency of electricity charging are significantly decreased. In the case of A-2, the required electricity charging will be only once a year, and especially, in case of B-2 and C-2, electricity charging will not be necessary. That is, short distance users/drivers will be free from electricity charging at the station when driving a PV-powered vehicle.

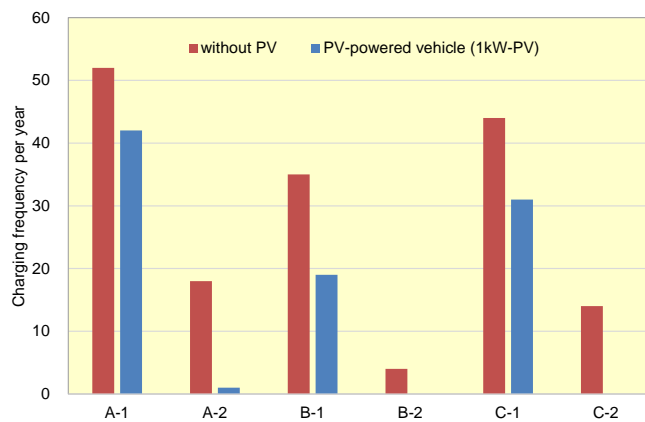


Fig. 2.1-16 Expected reduction of frequency of electricity charging

2.1.4 Impacts for expected benefits of a PV-powered vehicle by PV capacity and a vehicle’s efficiency

Expected CO<sub>2</sub> reduction and charging frequency by PV-powered vehicles will depend on the reduction of grid electricity usage, e.g. substitution by PV electricity. Then, a degree of reduction of grid electricity usage will be influenced by the amount of PV electricity utilised and the PV contribution, as well as the required electricity for driving.

In order to understand such a tendency, expected impacts by the following indicators are compared.

- PV capacity onboard : 0,5 kW, 0,75 kW and 1,0 kW
- Electricity consumption for driving : 6,67 km/kWh<sub>AC</sub>, 8,33 km/kWh<sub>AC</sub> and 10 km/kWh<sub>AC</sub>



### 2.1.4.1 Impacts by PV capacity

Figs. 2.1-17 and 2.1-18 show the utilisation ratio of PV electricity and PV contribution to a vehicle's electricity consumption for PV-powered vehicles by different PV capacity.

As for the PV utilisation ratio, for patterns A-2, B-2 and C-2, where the total driving distances are short, the utilisation ratio of PV electricity is greater, when the less PV capacity. In these patterns, surplus electricity is produced and the amount of surplus electricity will decrease with less PV capacity. On the other hand, contribution by PV electricity for five driving patterns except B-2 is smaller when the less PV capacity, corresponding to less amounts of PV electricity generated.

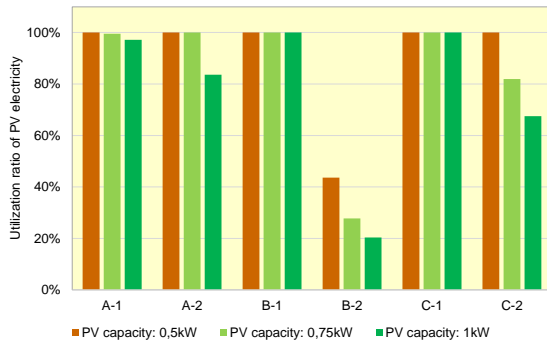


Fig. 2.1-17 Utilisation ratio of PV electricity by PV capacity

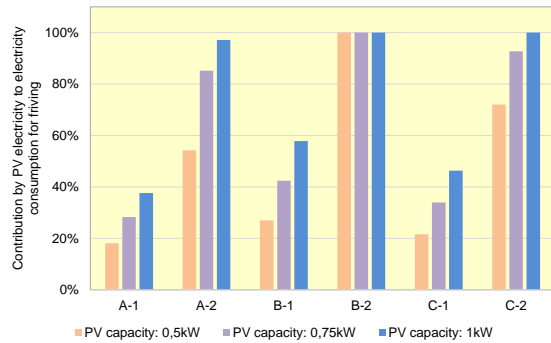


Fig. 2.1-18 PV contribution to electricity consumption by PV capacity

Figs. 2.1-19 and 2.1-20 show expected CO<sub>2</sub> reduction compared to a conventional electric vehicle without PV and charging frequency of a PV-powered vehicle with different PV capacities.

For patterns A-1, B-1 and C-1, where the total driving distances are long and almost 100% of PV electricity is utilized, the amount of CO<sub>2</sub> reduction will become small with the less PV capacity because of the less substitution by PV electricity. On the other hand, for patterns A-2 and C-2, CO<sub>2</sub> reduction for a PV-powered vehicle with 0,75 kW PV will be almost the same as a PV-powered vehicle with 1 kW PV. This means 1 kW PV will be redundant for these driving patterns. On the other hand, the charging frequency will increase with the less PV capacity.

In the case of B-2, the shortest driving distance among assumed patterns, additional CO<sub>2</sub> emissions will be reduced when the PV capacity is small, and the less PV capacity will produce environmental benefits, e.g. CO<sub>2</sub> reduction. This means that adequate PV capacity from a viewpoint of CO<sub>2</sub> reduction by a PV-powered vehicle will be less than 0,75 kW. Frequency of charging is not influenced by the PV capacity and charging electricity will not be necessary.

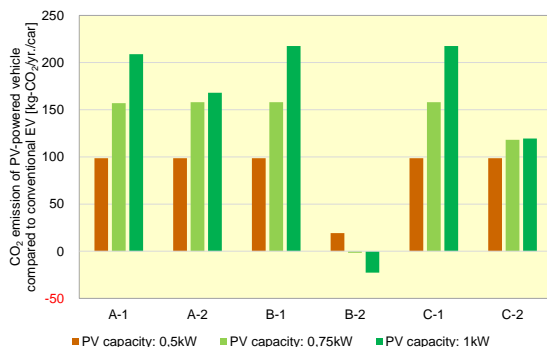


Fig. 2.1-19 Expected environmental benefit (CO<sub>2</sub> reduction) of a PV-powered vehicle by PV capacity

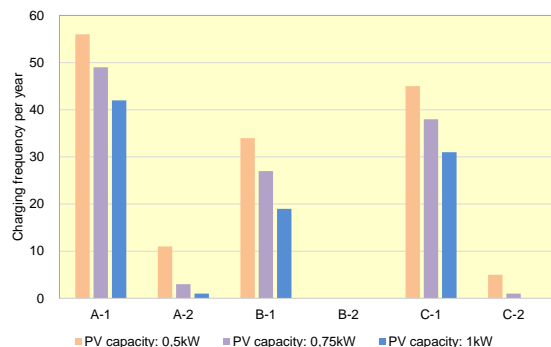


Fig. 2.1-20 Charging frequency of a PV-powered vehicle by PV capacity



### 2.1.4.2 Impacts by vehicle efficiency

Figs. 2.1-21 and 2.1-22 show the utilisation ratio of PV electricity and PV contribution to electricity consumption of a PV-powered vehicle by vehicle efficiency, e.g. electricity consumption for driving. Here, PV capacity for a PV-powered vehicle is 1 kW.

For patterns A-2, B-2 and C-2 where the total driving distances are short, the utilisation ratio of PV electricity is greater, when the vehicle efficiency is lower, while there will be no impacts for other driving patterns (A-1, B-1 and C-1).

On the other hand, as for PV contribution to electricity consumption for driving, that for patterns A-1, B-1 and C-1 becomes small when the vehicle efficiency is lower.

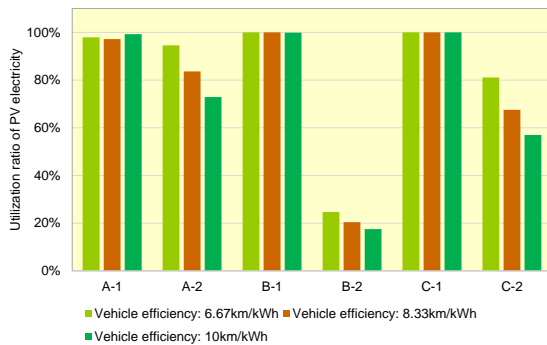


Fig. 2.1-21 Utilisation ratio of PV electricity by vehicle efficiency

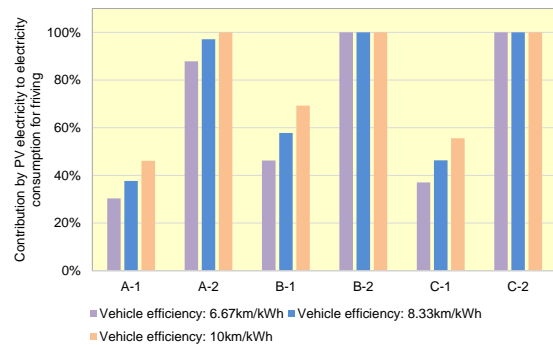


Fig. 2.1-22 PV contribution to electricity consumption by vehicle efficiency

In Figs. 2.1-23 and 2.1-24, expected CO<sub>2</sub> reduction by a PV-powered vehicle and charging frequency assuming there are different vehicle efficiencies (electricity consumption for driving) are shown.

For patterns A-1, B-1 and C-1, there will be no impacts for CO<sub>2</sub> reduction, as the total driving distances are long and almost 100% of PV electricity is utilised. For patterns A-2, B-2 and C-2, expected CO<sub>2</sub> reduction will be decreased with higher vehicle efficiency, because the required electricity for driving and utilised PV electricity will be reduced.

Additionally, the charging frequency will be decreased with higher vehicle efficiency. However, there will be no impacts with patterns B-2 and C-2.

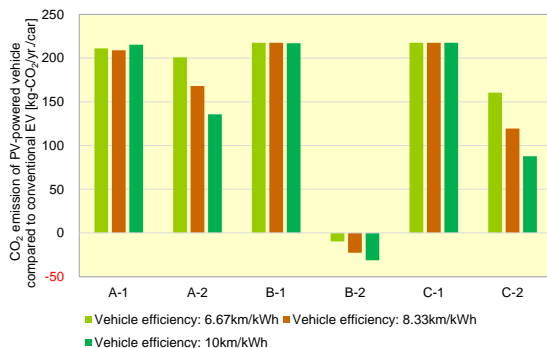


Fig. 2.1-23 Expected environmental benefit (CO<sub>2</sub> reduction) of PV-powered vehicles by vehicle efficiency

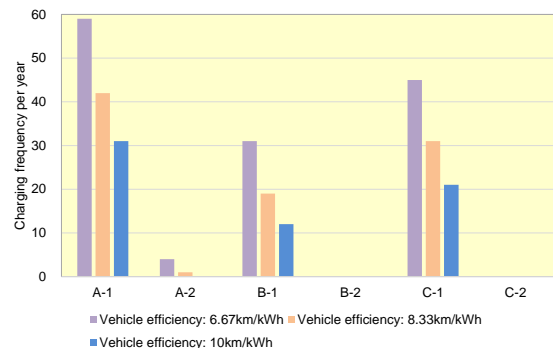


Fig. 2.1-24 Charging frequency of PV-powered vehicles by vehicle efficiency



### 2.1.5 Conclusions

In this section, expected benefits of PV-powered vehicles were analysed in terms of the reduction of CO<sub>2</sub> emissions, and comfort (charging frequency).

It was clarified that a PV-powered vehicle would produce environmental benefits, e.g. CO<sub>2</sub> reductions, compared to a conventional electric vehicle without PV, especially with longer driving distances, and that, however, 1 kW PV might be an excess capacity for shorter driving distances.

In order to increase environmental benefits by PV-powered vehicles, it is necessary to increase the utilised PV electricity. Therefore, in order to increase the utilised PV electricity, the optimised design of a PV-powered vehicle, such as its PV capacity while considering effective solar irradiation and vehicle efficiency, capacity and efficiency of a vehicle's battery and its operating condition will be required.

It was also clarified that a PV-powered vehicle will decrease charging frequency and that in case of a shorter driving distance, the PV-powered vehicle will be free from electricity charging. This benefit will make the vehicle more attractive, even if the expected environmental benefits will be slight.

### [References]

- [1] NEDO, PV-Powered Vehicle Strategy Committee Interim Report, January 2018
- [2] NEDO, News Release "Solar Cell Module with World's Highest Conversion Efficiency of 31.17% Achieved" (19 May 2016)
- [3] T. Hirota, Y. Kamiya and K. Komoto, Feasibility study of onboard PV for passenger vehicle application - Influence of vehicle usage condition on energy balance of PV and plug-in charging-, 2019 JSAE Congress (Autumn), October 2019
- [4] NEDO, Solar irradiation database "METPV-11" (2012)
- [5] NEDO, PV-Powered Vehicle Strategy Committee Interim Report (2) - Preliminary Study on Solar Irradiation of PV-Powered Vehicles -, April 2019
- [6] Mizuho Information & Research Institute, Inc., Research on life cycle assessment of photovoltaic power generation system, FY2007-2008 NEDO contract report, March 2009
- [7] Nissan Motor Corporation  
([https://www3.nissan.co.jp/content/dam/Nissan/jp/vehicles/leaf/1912/pdf/leaf\\_1912\\_specsheet.pdf](https://www3.nissan.co.jp/content/dam/Nissan/jp/vehicles/leaf/1912/pdf/leaf_1912_specsheet.pdf)).  
Accessed November 10, 2020.
- [8] Ministry of Environment, CO<sub>2</sub> emission coefficient for FY2018  
([https://ghg-santeikohyo.env.go.jp/files/calc/r02\\_coefficient\\_rev.pdf](https://ghg-santeikohyo.env.go.jp/files/calc/r02_coefficient_rev.pdf)). Accessed November 10, 2020.



## 2.2 Case study on PV-powered passenger vehicles in the Netherlands: Reduction of charging, cost and CO<sub>2</sub> emissions

The Netherlands, despite having lower annual irradiance than many other countries, is in position to benefit from vehicle integrated PV (VIPV) in terms of emission reductions and facilitating the energy transition. The Netherlands has one of the largest electric vehicle markets globally, at the time of this writing, and a government target that all new vehicles sold from 2030 onwards be zero-emission. Grid charged battery electric vehicles will meet the criteria for zero-emission; however, the production of electricity in the Netherlands is currently dominated by natural gas, a fossil fuel which will limit emissions' impact of such a transition to EVs. Several case studies in the Netherlands for PV-powered passenger vehicles have been considered and are reported in this section. Using an Energy Flow Model, investigations are done into the impact of PV-powered passenger vehicles in the Netherlands, specifically looking at the reduction in charging frequency, CO<sub>2</sub>-eq emissions, and estimating cost savings by the use of PV-powered passenger vehicles.

### 2.2.1 Electric passenger vehicles in the Netherlands

The Netherlands is one of the world leaders when it comes to the uptake of electric vehicles and the installation of charging infrastructure. Statistics are released each month by the Netherlands Enterprise Agency, RVO, showing the increase in electric vehicle registrations (Fig. 2.2-1), as well as the development of charging infrastructure (Fig. 2.2-2) [1]. Table 2.2-1 shows the 10 most popular makes and models of battery electric vehicles registered in the Netherlands.

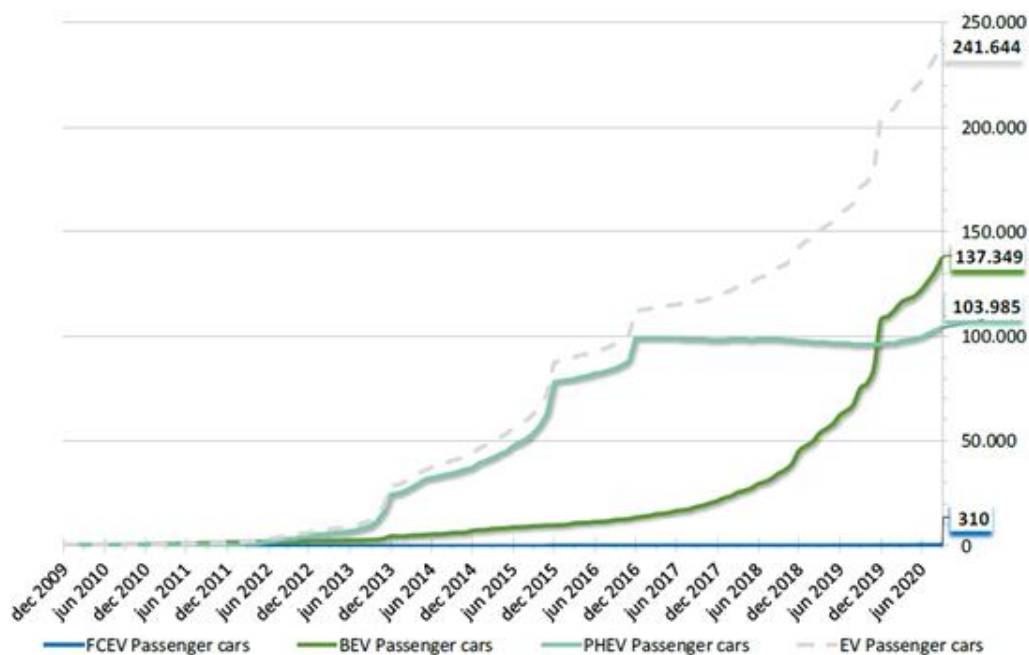


**Fig. 2.2-1 Monthly statistics from the Netherlands Enterprise Agency showing the development in the number of electric vehicles registered in the Netherlands**

(The graph shows Fuel Cell Electric Vehicles (FCEV), Battery Electric Vehicles (BEV) and Plug-in Hybrid Electric Vehicles (PHEV). Various incentives in road tax and lease arrangements have helped drive the recent more rapid increases in BEVs (After Netherlands Enterprise Agency, Statistics Electric Vehicles in the Netherlands up to and including September 2020)).

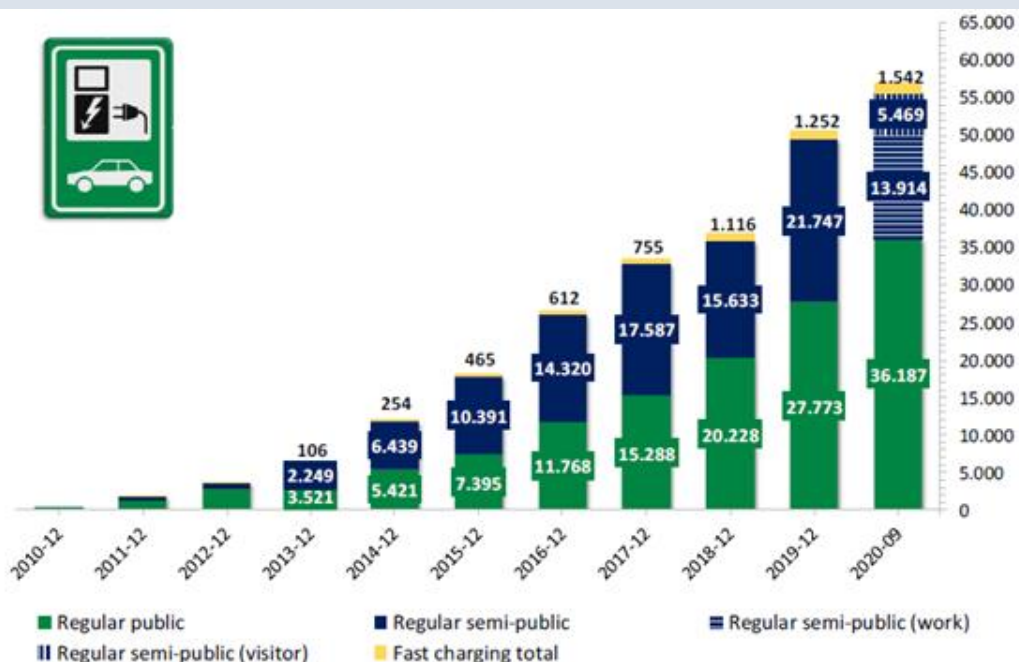


**Fig. 2.2-2 Development in the number of charging points in the Netherlands since 2010**  
 (according to the Netherlands Enterprise Agency, Statistics Electric Vehicles in the Netherlands up to and including September 2020 [1])

One of the paths to meeting the Netherlands climate targets from the Paris climate agreement, is to reduce greenhouse gas emissions in the mobility sector. The Dutch government has set a target in place that by 2030, all new passenger vehicles sold must be zero-emission, this translates to 1,9 million electric passenger vehicles on the Dutch roads by 2030. The National Agenda for Charging Infrastructure (Nationale Agenda Laadinfrastructuur), has been established to ensure that the required charging infrastructure does not present a barrier to these ambitions and to ensure that the required 1,7 million charging points for these 1,9 million private vehicles are installed by 2030 [2] [3].

**Table 2.2-1 Top 10 models of battery electric vehicles registered in the Netherlands**  
 (according to the Netherlands Enterprise Agency, Statistics Electric Vehicles in the Netherlands up to and including September 2020 [1])

Position	Brand/model	Number	Since previous month	Since the same month in the previous year
1	Tesla Model 3	34 241	986	20 635
2	Tesla Model S	12 802	23	110
3	Nissan Leaf	10 265	142	2 910
4	Volkswagen Golf	10 005	179	4 183
5	Hyundai Kona	8 874	419	4 673
6	Kia Niro	8 153	761	5 603
7	Renault Zoe	7 556	268	2 733
8	BMW i3	7 127	240	1 968
9	Tesla Model X	5 266	54	434
10	Jaguar I-Pace	4 339	-4	615



## 2.2.2 Driving habits in the Netherlands

According to open data from the Dutch Central Bureau of Statistics (CBS), the average Dutch passenger vehicle travels approximately 13 000 km/year, based on 2018 figures [4]. The most recent breakdown of reasons for travel also from the CBS, show 37% of driving is for travel to and from work [5]. A 2013 report published by Milieu Centraal and the Royal Dutch Touring Club (ANWB) [6], gave a breakdown of different driving profiles of Dutch drivers, with an average distance travelled of around 15 000 km, 41% of which was the home – work commute of 15 km one way Fig. 2.2-3.

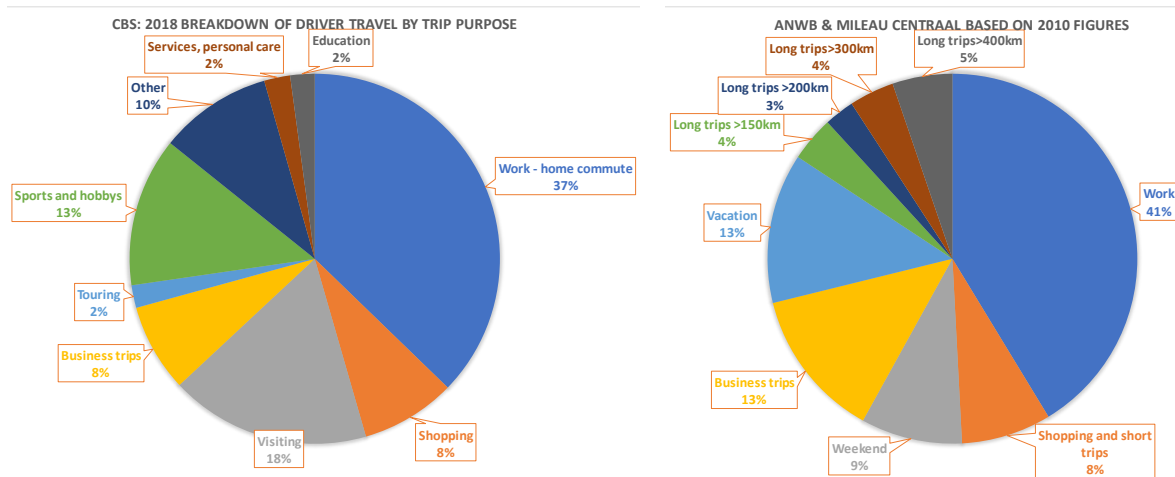
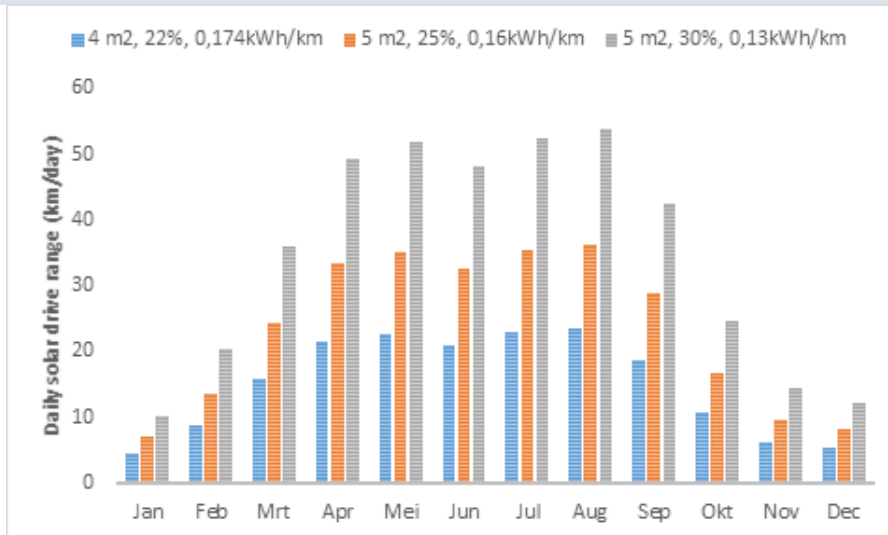


Fig. 2.2-3 Example driving profile breakdown by purpose; on the left, 2018 figures from CBS [4] [5] and right, 2010 figures from Mobiliteitsonderzoek NL 2010, as reported by ANWB and Milieu Centraal [6] (Both show around 40% of trips are for commuting to work.)

## 2.2.3 Approach to modelling case studies

A quick calculation of the potential benefit of integrated PV in the Netherlands reveals that, despite relatively low solar irradiance, the expected output from current PV technologies could generate enough power on a daily basis to support a short commute in the summer months. The blue bars in Fig. 2.2-4 show the average daily kilometres that could be driven from solar power in an average location in the Netherlands, with about 880 W of PV on a vehicle, with an average energy demand of 174 Wh/km. This suggests that with the technology available today, most electric vehicles could drive about 20 solar km/day. The orange and grey bars of Fig. 2.2-4 show the future potential of PV-powered vehicles in the Netherlands with more efficient PV and more efficient electric vehicles.



**Fig. 2.2-4 Average daily solar kms for a typical location in the Netherlands**

(The blue bars represent today's technology while the orange and grey bars represent the potential for future advances in PV and EV efficiency.)

To more accurately calculate the benefit of on-board integrated photovoltaics in electric passenger vehicles, a series of case studies have been made. Using an Energy Flow Model developed by TNO [7], and based on direct measurements of irradiance and driver behaviour with a Vehicle Irradiance Test Setup, the possible reduction in CO<sub>2</sub>-eq emissions, cost savings and reduction in the number of plug-in charging frequency, CMs, have been quantified. The key factors to consider in these assessments are: the available solar resource of the location and energy yield from the PV, the driving habits of the vehicle owners and the specifications of the electric vehicle.

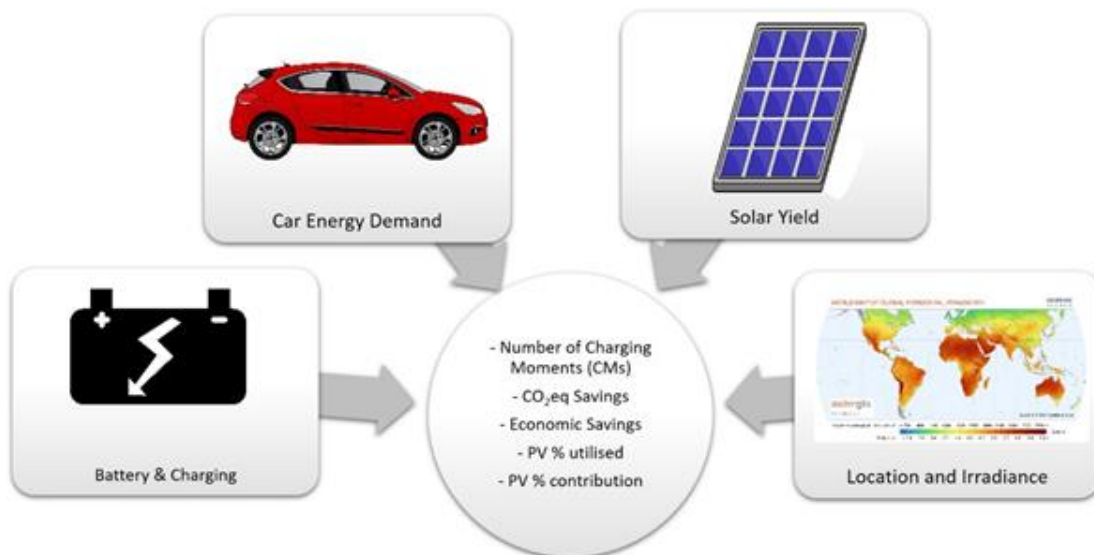


**Fig. 2.2-5 Key factors used in the Energy Flow Model, developed by TNO to determine the impact of vehicle integrated photovoltaics, VIPV, the specifications of the vehicle and driving habits of the owner, the available PV and the location and the available solar resource at the location**

Other impacts are the charging strategy or habits of the vehicle's owner, the cost of electricity and the carbon intensity, grams of CO<sub>2</sub>-eq/kWh, of the local grid electricity.



## 2.2.4 Measurements

### 2.2.4.1 Solar irradiance resource assessment and measurement of driver profiles – VITS

A Vehicle Irradiance Test Setup (VITS) has been built by TNO and has collected several months of data [7]. The system collects GPS and temperature values at 1 Hz and irradiance on four locations on the vehicle's roof at 100 Hz. The irradiance measurements have been validated by comparison with local weather station data and can be used to show the details of shading events. The data also provides realistic driver profiles to be used in the modelling. The collected data shows dynamic shading, driver profile and shading losses. The GPS data also allows precise analysis of shading events and where they occur.

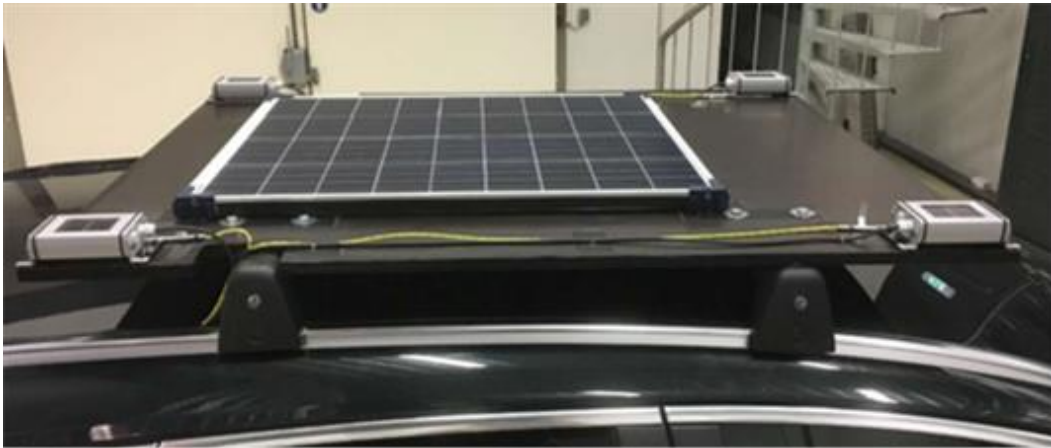


**Fig. 2.2-6 Vehicle Integrated Test System (VITS) with four irradiance sensors, the solar panel in the middle provides extra energy to power the data acquisition system**

(The VITS features its own battery (not visible in the image) to power the data acquisition system, so the vehicle's battery is not drained. The VITS battery is charged either from the grid, or from the solar panel.)

### 2.2.4.2 Validation of Irradiance measurements

Irradiance measured by the sensors on the vehicle are compared to nearby weather station measurements made by the KNMI (Royal Dutch Meteorological Institute). Using the measured GPS data the closest weather station can be selected dynamically for comparison along a driving route.

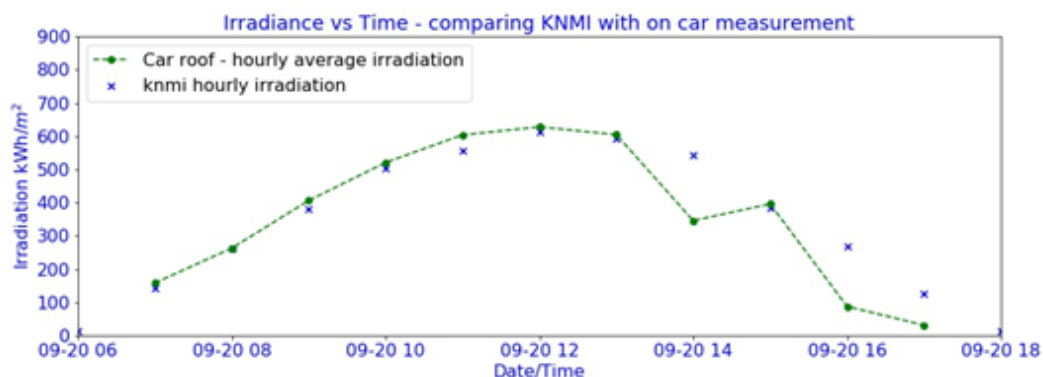


**Fig. 2.2-7 An example of hourly irradiance values measured with the VITS and at nearby KNMI weather stations**

(Large deviations are expected to be due to shading on the vehicle's roof. In this particular example, the KNMI daily total is 3,6% higher than what was measured on the vehicle.)

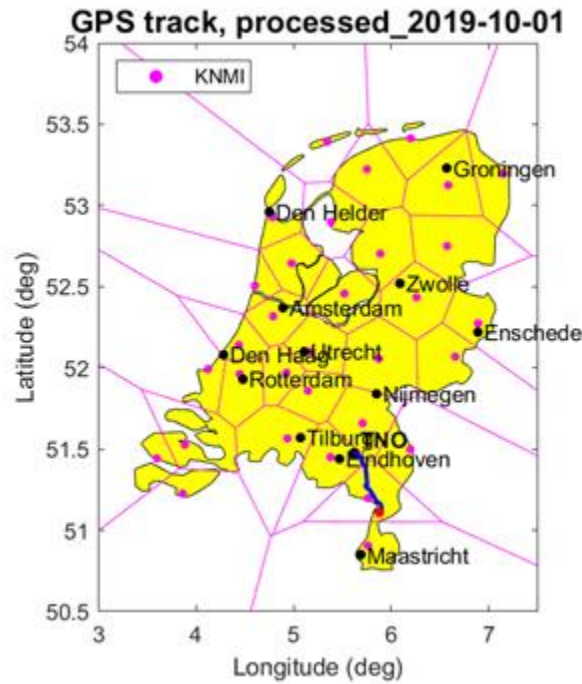


Fig. 2.2-8 Map of the Netherlands showing the network of KNMI weather stations measuring Global Horizontal Irradiance, the pink dots, and the route followed by the vehicle on the given day, the blue line. The pink lines delineate areas of points closest to a particular KNMI station.

### 2.2.4.3 Shading events

As well as providing an overview of the trips taken in the vehicle and the sunshine, the data also enables the investigation of shading events, which can reduce the output of the on-board PV; both when the vehicle is parked in the shade for a long time, but also when dynamic shading occurs during a drive. The figures below show instances of both effects.

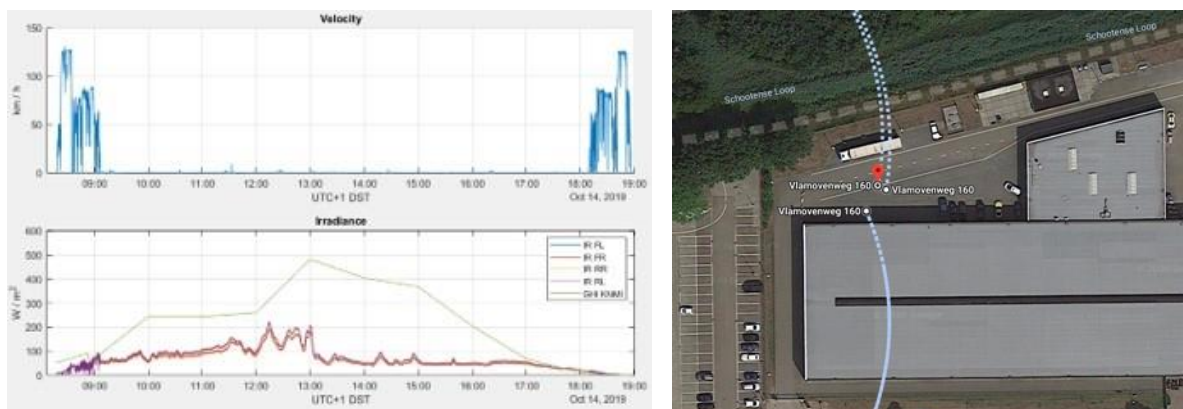
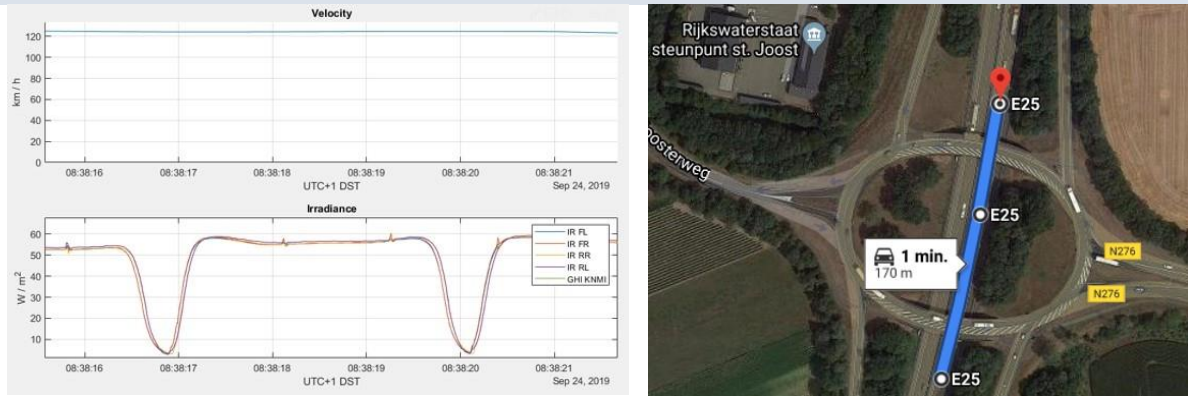


Fig. 2.2-9 The irradiance trace (bottom left) shows that the sunlight measured on the vehicle is far below that measured by the weather station, further investigation of the GPS data confirms the vehicle was parked on the North side of a tall building.



**Fig. 2.2-10 Results from monitoring showing dynamic shading as a vehicle travels beneath an overpass** (The vehicle is travelling at 120 km/h, the two dips in the irradiance trace (bottom left) occur as the vehicle goes under the two overhead roads.)

### 2.2.4.4 Measured driving profile

The GPS measurements made during the data collection period provide a real time driving profile of someone who lives and works in the Netherlands, having a 100 km round trip to work 4 days per week, some business trips, weekend driving and vacation trips. Their annual distance travelled is around 28 000 km, approximately double the Dutch average.

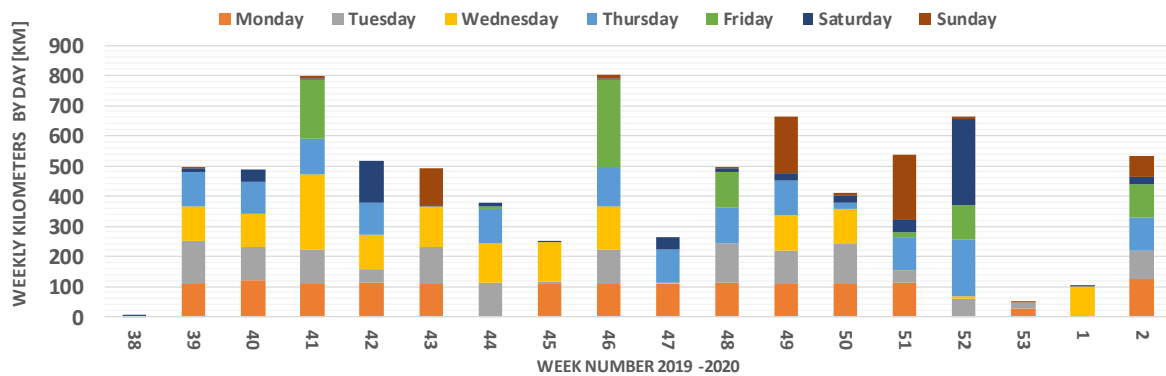


**Fig. 2.2-11 Measured driving profile - from GPS data, presented as kilometres travelled per week broken down into days of the week**

### 2.2.5 Modelling: The Energy Flow Model

The TNO Energy Flow Model inputs, processes and outputs are illustrated below, Fig. 2.2-12. The simulations are done for one full year of vehicle operation. They use time series inputs for the irradiance, ambient temperature and driving profile. The energy required by the vehicle and the state of charge (SOC) of the battery are calculated at each time step. The PV energy yield is simultaneously calculated along with any grid charging frequency that are required to meet the driving energy demand. The outputs of the model are derived from the balance of electricity generated by the PV as compared to the grid.

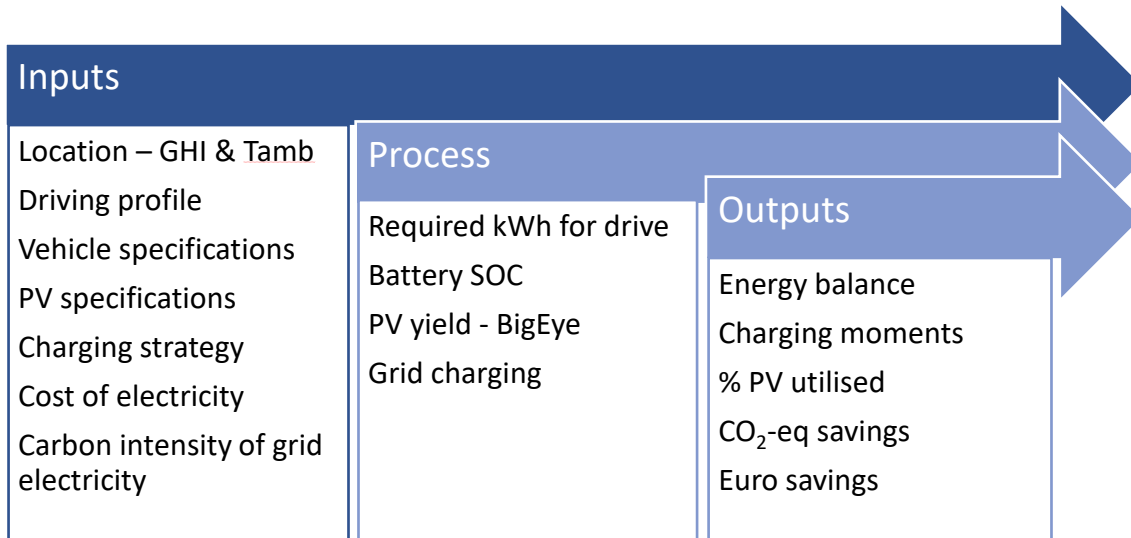


Fig. 2.2-12 Energy Flow Model, inputs as a time series, process calculations and model outputs

## 2.2.6 Inputs and data sources

### 2.2.6.1 Location meteorological data

The meteorological data used for the simulations is sourced using the software Meeonorm 7.3 [8], it can be downloaded per location as a 10 minute interval time series. The monthly radiation figures for Amsterdam can be seen in Fig. 2.2-13, the total global horizontal irradiance is shown with the diffuse proportion overlaid.

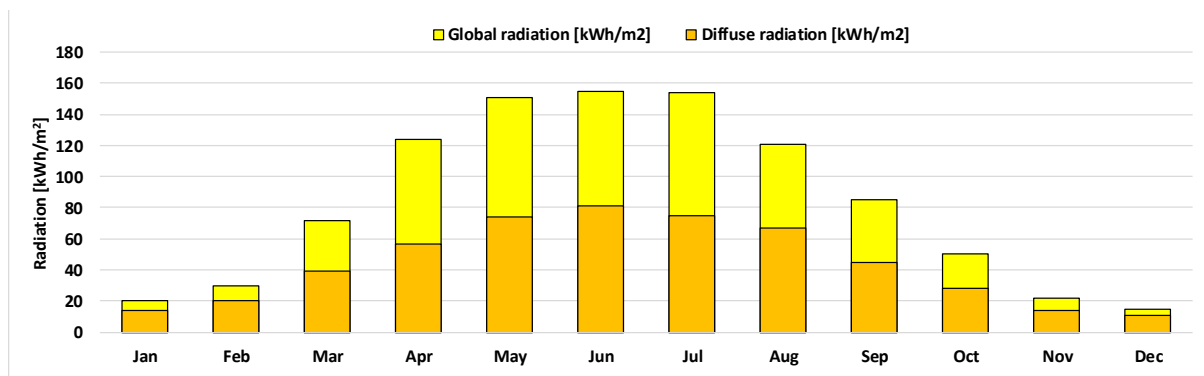


Fig. 2.2-13 Monthly radiation in Amsterdam based on Meeonorm data, showing both total GHI and the diffuse contribution [8]

### 2.2.6.2 Driving profiles

How a vehicle is driven, distances, frequency, road type, along with vehicle efficiency, determine the vehicle's energy requirements. Two driver profiles based on measured data have been constructed for a full year. These are a 50 km commute and a Dutch average 15 km commute. The 50 km profile is based on an extrapolation of the measured profile shown in Fig. 2.2-11 where the driver commutes 50 km to work and 50 km home on weekdays, as well as having many other trips. The Dutch average 15 km commute is constructed from the CBS data and the report from the ANWB and Milieu Centraal (Fig. 2.2-3) [4] [6]. Six synthetic driving profiles have also been created based on commuting to and from work on weekdays. These profiles are a 10 km each way commute, 15 km each way commute, 20 km, 30 km, 40 km and 50 km. Table 2.2-2 summarises the driving profiles used. In the cases of



the simple profiles, no one trip is longer than 50 km and daily travel is double that. However, in the Dutch average profile and the measured profiles the longest daily distance travelled is 200 km and 290 km respectively. In this way, the model is also able to account for the infrequent but often necessity of longer distance trips.

**Table 2.2-2. Driving profiles used in simulations**

(The simple profiles are synthetically created, and the Dutch average and measured profiles are based on real driving measurements.)

ID	Driving Profile	Commute distance each way [km]	Annual distance travelled [km]
a. s_10km	Simple 10k	10	5 220
b. s_15km	Simple 15k	15	7 830
c. s_20km	Simple 20k	20	10 440
d. s_30km	Simple 30k	30	15 660
e. s_40km	Simple 40k	40	20 880
f. s_50km	Simple 50k	50	26 100
g. 13k km/y	Dutch average	15	13 000
h. 28k km/y	Measured	50	28 000

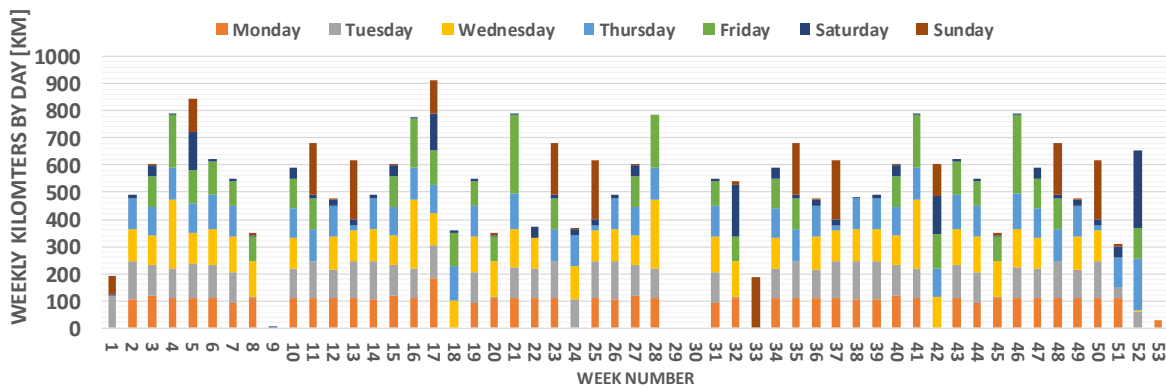


Fig. 2.2-14 Driving profile – 50 km one way commute based on measured data (28 000 km/year)

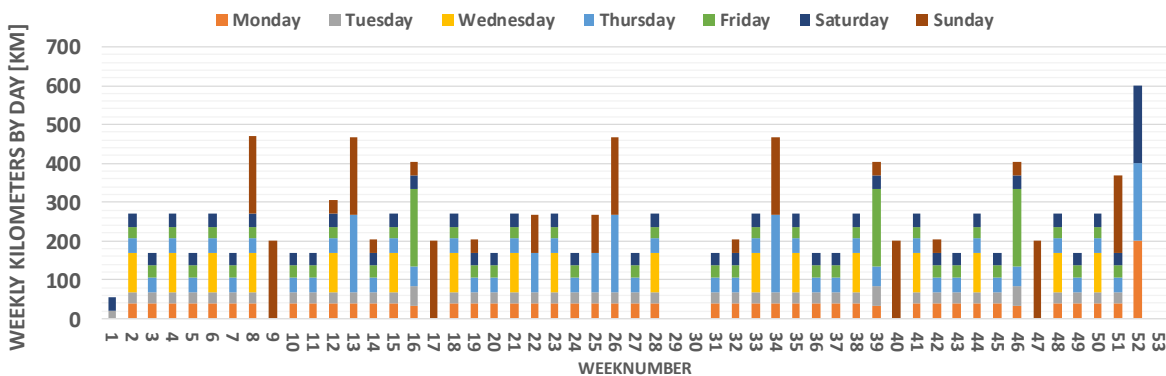


Fig. 2.2-15 Driving profile based on Dutch statistics and a 15 km one way commute (13 000 km/year)

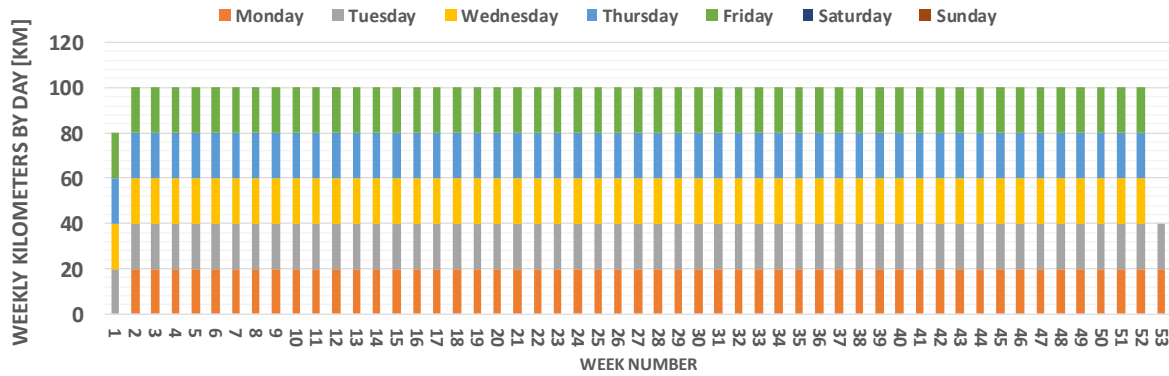


Fig. 2.2-16 Example of a synthetic driving profile, consisting of a 10 km each way commute on weekdays.

### 2.2.6.3 Vehicle choice and specifications

The vehicles selected for the case studies are based on the most popular EVs in the Netherlands, as reported in the monthly statistics [1], as shown in Table 2.2-1. The Electric Vehicle Database [9] has been used as a source for specifications of various electric vehicles. It presents real use efficiency and range values for the vehicles with respect to road type and weather type, as well as providing details on battery capacity. All of which are used in the EF model. The weather definitions are: Cold Weather: – ‘worst – case’ based on -10°C and use of heating, and Mild Weather: - ‘best-case’ based on 23 °C and no use of air conditioning [9]. Charging losses or factors (c.f.) are calculated by finding the relative difference between the two WLTP (World Harmonised Test Protocol Rating) values. The WLTP vehicle consumption value is equal to the calculated battery energy used by the vehicle for propulsion and on-board systems and the WLTP rated consumption value includes charging losses [9]. The charge factor (c.f.) is then calculated as follows:

$$c.f. = 1 - \left( \frac{WLTP \text{ Rated Consumption}}{WLTP \text{ Vehicle Consumption}} \right)$$

The c.f. is applied in the EF model both during PV charging and during grid charging. The battery charging limits have been taken to be between 20% and 80% state of charge. This means the low battery trigger is set to 20% of full capacity, and the maximum charge a battery will receive is 80% of capacity. This is the approach that is recommended to prolong battery life as described in [10].

For the simulations, three generic vehicles have been used, based on EV database parameters for three popular vehicles in the Netherlands. Given that the distance an electric vehicle can travel or its range between charging is directly related to the size of the vehicles battery. A short-range or small battery capacity vehicle, a mid-range or middle sized battery capacity vehicle and a long-range or large sized battery capacity vehicle have been selected for modelling. The specification of the three vehicles are presented in Table 2.2-3.

Table 2.2-3 Vehicle specifications used in the modelling including road types and weather definitions (EV Database accessed, June 2020)

Vehicle	Batt. Cap. (Usble) [kWh]	EVDB Real Range [km]	WLTP Veh. Cons. [Wh/km]	WLTP rated. Cons. [Wh/km]	Real Energy Use [Wh/km]					
					Cold Weather			Mild Weather		
					City	Hwy.	Cmb.	City	Hwy.	Cmb.
Long -range	72,5	460	129	160	167	220	188	109	167	136
Mid -range	56	330	145	180	172	243	204	115	187	149
Short -range	32	190	138	153	173	237	200	114	188	149



#### 2.2.6.4 PV specifications and yield predictions

The TNO PV yield model, originally developed to calculate the yield of bifacial PV installations, BigEye, [11] is used to calculate the energy yield of the vehicle integrated PV element. BigEye uses the GHI (Global Horizontal Irradiance) ambient temperature and 1-diode parameters for the PV modules. The simulations assume mono c-Si PV technology with approximately 21% module level efficiency.

#### 2.2.6.5 Charging strategies

To quantify the impact of different user behaviours, two different charging strategies have been used for comparison in the simulations: a conservative look-ahead strategy and PV optimised strategy. In both strategies the model looks to upcoming driving requirements for the day or the next day and compares the energy required for that drive with the current state of charge of the battery. If there is enough energy in the battery to complete the drive, then nothing occurs. If there is not enough energy in the battery, then in the conservative look-ahead strategy, the vehicle will be charged from the grid and charged to the allowed maximum (80%). For the PV optimised strategy, some space is left in battery (10%, PV reserve) such that the battery can accept PV energy produced during the drive the next day. This maximises the utilisation of the PV resource.

**Table 2.2-4 EV charging strategies applied in the EF model**

Strategy	Details
<b>Conservative - look ahead</b>	Battery SOC evaluated for next drive requirement – if SOC + buffer not enough – then battery is fully charged
<b>PV optimised</b>	Same as conservative – look ahead, except battery not fully charged, some space left to accommodate PV charging

#### 2.2.6.6 Cost of electricity and CO<sub>2</sub>-eq intensity of the local grid

To determine the environmental and financial benefits of PV integration in electric vehicles, the domestic electricity prices per kWh and carbon intensity in grams of CO<sub>2</sub>-eq per kWh for each country are used to calculate the reduction in CO<sub>2</sub>-eq emissions and financial savings. [12] [13].

The cost savings are based on the household electricity prices with the assumption that most charging will be done at home. Costs savings will vary (likely higher) if fast charging or en-route charging is used.

Net CO<sub>2</sub>-eq (ΔCO<sub>2</sub>-eq) emissions are calculated according to:

$$\Delta \text{CO}_2\text{-eq} [\text{kg}] = E_{\text{PV}}[\text{kWh}] \cdot C_{\text{grid}} [\text{kg/kWh}] - C_{\text{emb-PV}}$$

Where  $E_{\text{PV}}$  is the total energy generated by the PV each year;  $C_{\text{grid}}$  is the carbon intensity of the country grid; and  $C_{\text{emb-PV}}$  is the embedded CO<sub>2</sub> footprint of the PV, according to the LCA described in section 2.3.3.3 of this report (Kanz, et al. 2020) with an assumed 12 year VIPV system lifetime.

### 2.2.7 Simulations and results

The assumptions and inputs are summarised in Table 2.2-5. Initial study results presented are focused on the Netherlands, other locations are assessed for comparison in Chapter 4.1.

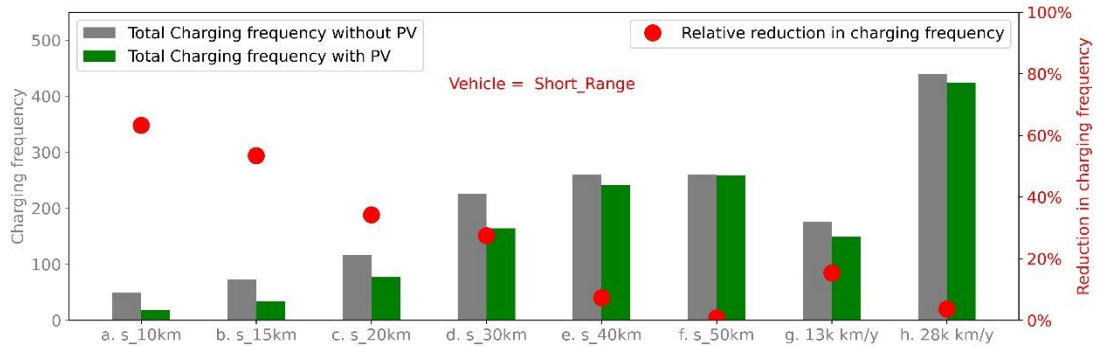


Table 2.2-5 Assumptions and inputs for Netherlands simulations

PV	PV	Wp	800
	Global Horizontal Irradiance [8]	kWh/m <sup>2</sup> /year	999,6
	Diffuse Horizontal Irradiance [8]	kWh/m <sup>2</sup> /year	522,5
	Ambient Temperature [8]	C° (average)	10,9
	Orientation	Tilt/azimuth	Horizontal
	Shade losses	%	0%
	CO <sub>2</sub> emission from manufacturing [14]	(kg-CO <sub>2</sub> /kWp)	1 229,16
	Annual CO <sub>2</sub> contribution from manufacturing for 800Wp, 12year lifetime	(kg)	81,9
EV	EV-database real energy consumption and charging losses (c.f.) [9]	Real Energy Consumption (average) (Wh/km)	Charging factor (c.f.)
	Long-range	158	0,24
	Mid-range	170	0,24
	Short-range	168	0,13
	Lifetime	(years)	12
Battery charging	Initial state (before driving)	(%)	100%
	Charging rate	(kW)	7,4
	CO <sub>2</sub> content local grid electricity [13]	(kg-CO <sub>2</sub> /kWh)	0,437 (Netherlands)
	Electricity price (household prices) [12]	(EUR/kWh)	0,221 (Netherlands)
	Low battery trigger	(%)	20 %
	Maximum limit for charging (grid)	(%)	80 %
	Maximum limit for charging (PV)	(%)	80 %
	Reserve for PV in PV opt strategy	(%)	10 % (charge to 70 %)

### 2.2.7.1 Reduction in charging frequency per driving profile and vehicle

Figs. 2.2-17, 18 and 19 show the total and relative reduction in charging frequency for the different vehicles and driving strategies. The biggest benefit (more than 60%) is gained in terms of reduction in charging frequency for any vehicle with the simple 10 km commute. As the driving distance increases, the relative reduction in charging frequency decreases for all vehicle types. In the case of a short-range vehicle with a small battery and a long driving distance (simple 50 km commute), there is almost no decrease in charging frequency as the necessary driving distances almost always require a full battery and perhaps even one or two stops on a trip. However, as the vehicle's range (battery capacity) increases, a relative benefit in charging frequency of at least 10% is calculated (except in the case of the 28 km driving profile). As a consumer will likely choose a vehicle with a nominal range that is equal to or greater than their daily commuting needs, the benefit of on-board PV will likely be at least a 10% decrease in charging frequency in the Netherlands. It should also be noted that for the measured driving profiles (g) and (h) the reduction in charging frequency is not as great as for the simple commute driving profiles with similar commute distance. This is due to some individual trips in (g) and (h) being longer than the simple profile trips which lead to the battery needing to be charged more often.



**Fig. 2.2-17 Total number of charging frequency with and without PV for Amsterdam and the relative reduction in charging frequency – right axis**  
(For all driving profiles and the short-range distance vehicle.)

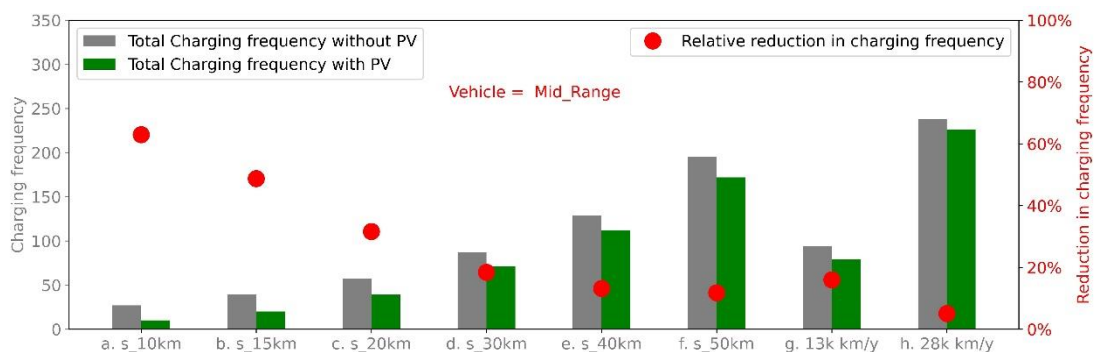


**Fig. 2.2-18 Total number of charging frequency with and without PV for Amsterdam and the relative reduction in charging frequency – right axis**  
(For all driving profiles and the mid-range distance vehicle.)

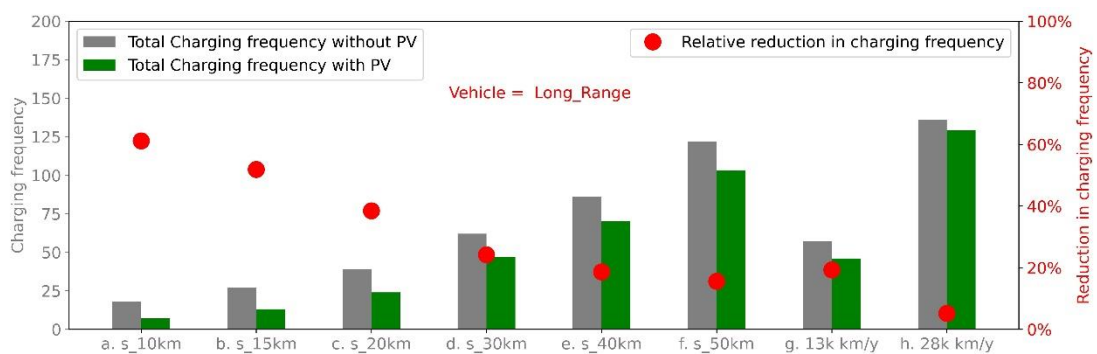


**Fig. 2.2-19 Total number of charging frequency with and without PV for Amsterdam and the relative reduction in charging frequency – right axis**  
(For all driving profiles and the Long-range vehicle.)

### 2.2.7.2 Charging and PV utilization

In order to have the most impact on cost savings and CO<sub>2</sub> emissions, the energy generated by the PV should be maximally utilized. Figs 2.2-20, 21, and 22 show the total number of kWhs from the grid and/or PV resource and the PV utilization (with an 800 W PV system). These simulations use the PV optimized charging strategy. It can be seen that the PV is almost always 100% utilized for all vehicle types. Interestingly, for a simple 10km commute, the PV is best utilized in the case of a mid-range vehicle, due partly to the larger battery being able to accept the PV



charge and partly due to the higher energy requirements of the mid-range vehicle. These higher energy requirements are due to the combination of a lower efficiency and higher charging losses when compared to the other two vehicles. For the more realistic driving profiles, (g) and (h), a lower PV utilization is caused again by longer individual trips in these profiles, draining the battery and requiring it to be recharged more often. As the battery size increases, the PV utilization also increases.

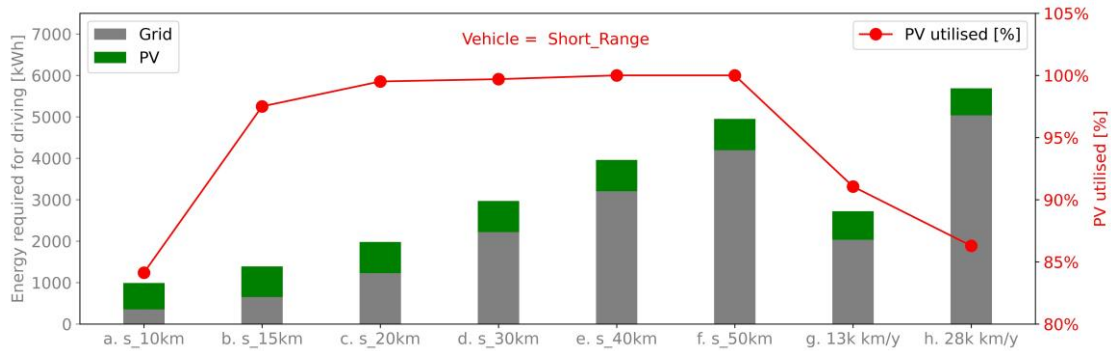


Fig. 2.2-20 The total kWh utilised for driving divided into Grid and PV charging (left axis) and the percentage of generated PV energy that has been utilised (right axis) for Amsterdam and the short range vehicle

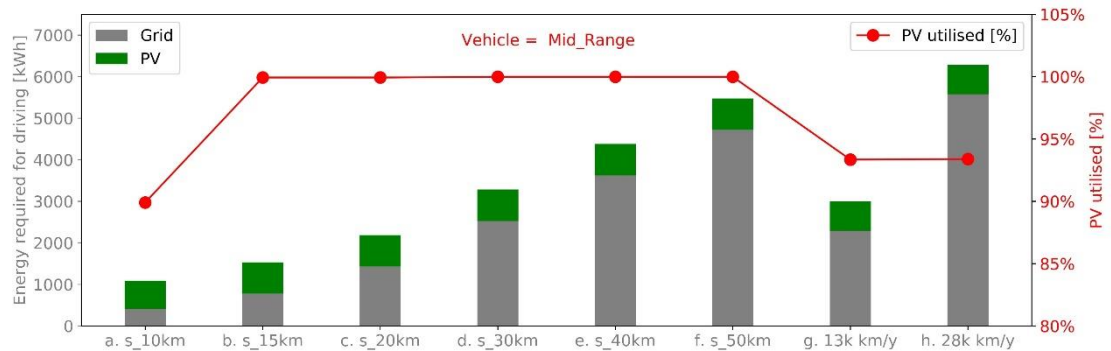


Fig. 2.2-21 The total kWh utilised for driving divided into Grid and PV charging (left axis) and the percentage of generated PV energy that has been utilised (right axis) for Amsterdam and the mid-range vehicle

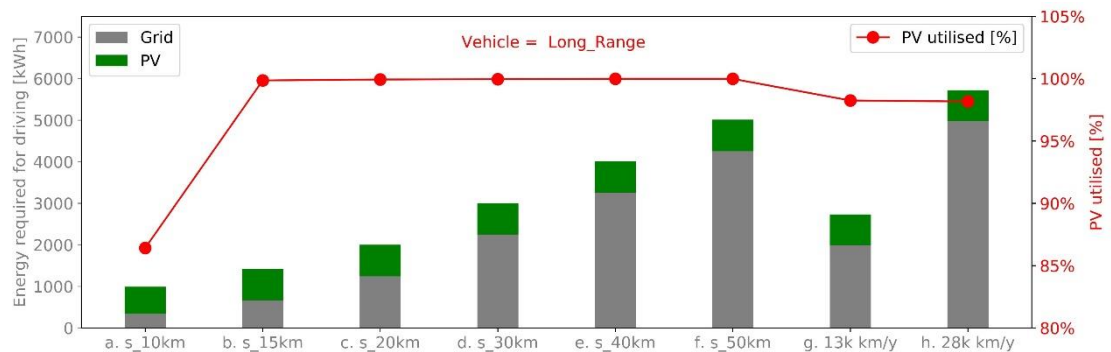


Fig. 2.2-22 The total kWh utilised for driving divided into Grid and PV charging (left axis) and the percentage of generated PV energy that has been utilised (right axis) for Amsterdam and the long-range vehicle



### 2.2.7.3 Solar kilometers

The total solar kilometers that can be driven each year in Amsterdam are shown in Fig. 2.2-23. For all vehicle types and driving profiles, the PV can supply energy for between 3 000 – 4 100 km/year with an average of approximately 3 650 km. This will scale with more PV and better (PV or EV) efficiency. The mid-range vehicle has notably lower solar kilometres, which is due to the higher energy requirements discussed earlier.

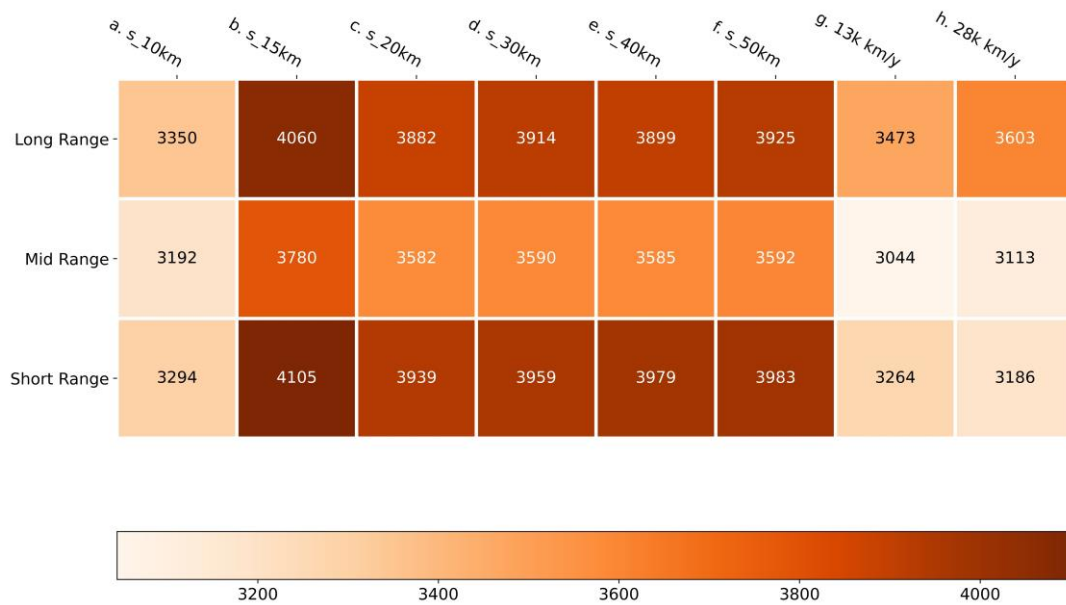


Fig. 2.2-23 Solar kilometres per year, all vehicles and all driving profiles in Amsterdam

### 2.2.7.4 CO<sub>2</sub> emission analysis

The highest PV utilisation and consequently the largest CO<sub>2</sub> reductions occur using the optimised for PV charging strategy. Fig. 2.2-24, Fig. 2.2-25 and Fig. 2.2-26 show the comparison of CO<sub>2</sub> emissions with and without PV for all driving profiles and Fig. 2.2-27 show the net CO<sub>2</sub> emissions for all vehicles and profiles. The calculations are made using the optimised for PV charging strategy. The CO<sub>2</sub> embedded in the PV is included in the ‘with PV’ values.

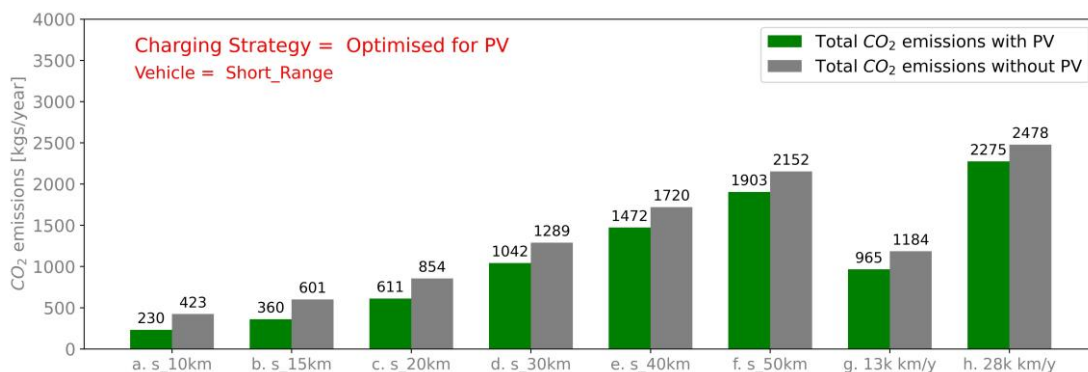


Fig. 2.2-24 Total CO<sub>2</sub> comparison without and with PV in Amsterdam with the short range vehicle and all the driving profiles and the PV optimised charging strategy, the values for with PV include the embedded CO<sub>2</sub> in the PV itself. For 800 Wp of PV this is around 82 kg/year

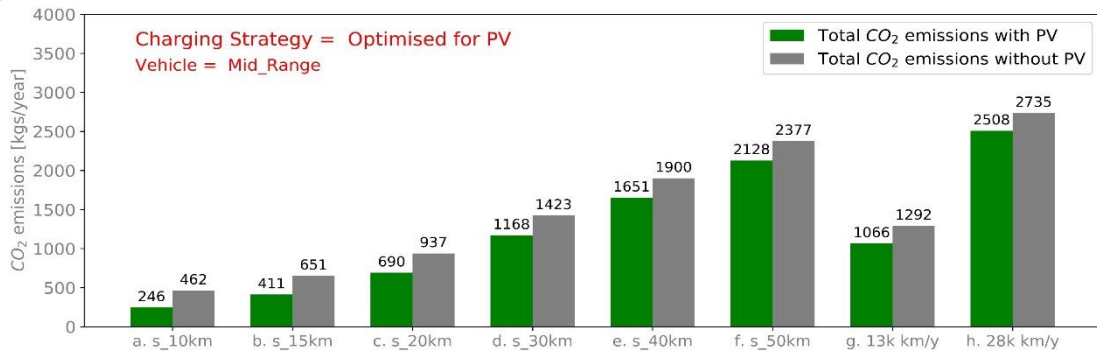


Fig. 2.2-25 A comparison of the total CO<sub>2</sub> emissions with and without PV for the mid-range vehicle and the optimised for PV charging strategy

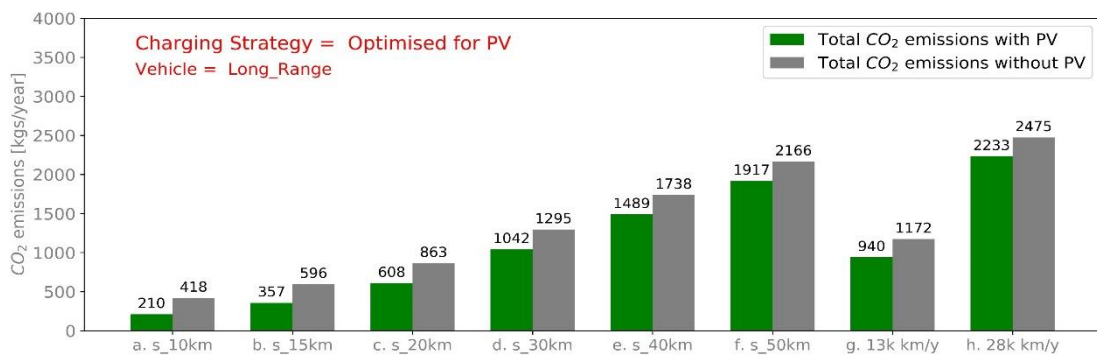


Fig. 2.2-26 A comparison of the total CO<sub>2</sub> emissions with and without PV for the long-range vehicle and the optimised for PV charging strategy

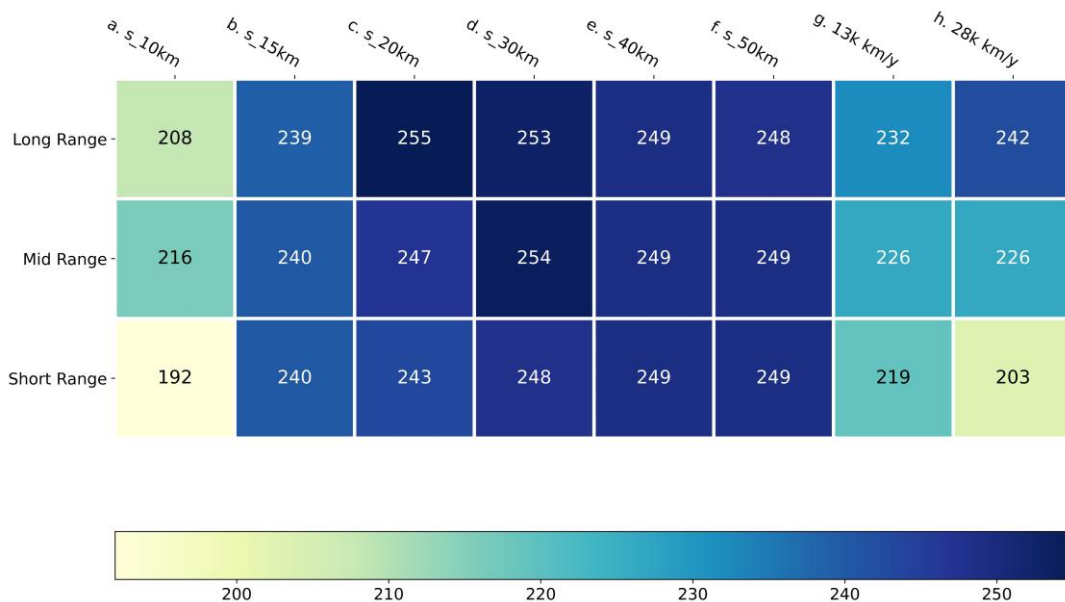


Fig. 2.2-27 Net CO<sub>2</sub>-eq savings in kg/year for Amsterdam, all profiles and all vehicles (The net value is calculated as the difference between the CO<sub>2</sub> emissions with and without PV.)



The net CO<sub>2</sub> savings are very similar for all driving profiles and all vehicles where the PV is optimally utilized. This is because they are directly related to the PV utilised. The net savings are between 192 and 255 kg-CO<sub>2</sub>/year across the profiles and vehicles.

### 2.2.7.5 Cost savings

The cost savings are directly related to the utilised PV, calculated by multiplying the kWh of PV utilised by the household electricity prices in EUR/kWh. For these calculations, the cost of the PV element itself is not considered.

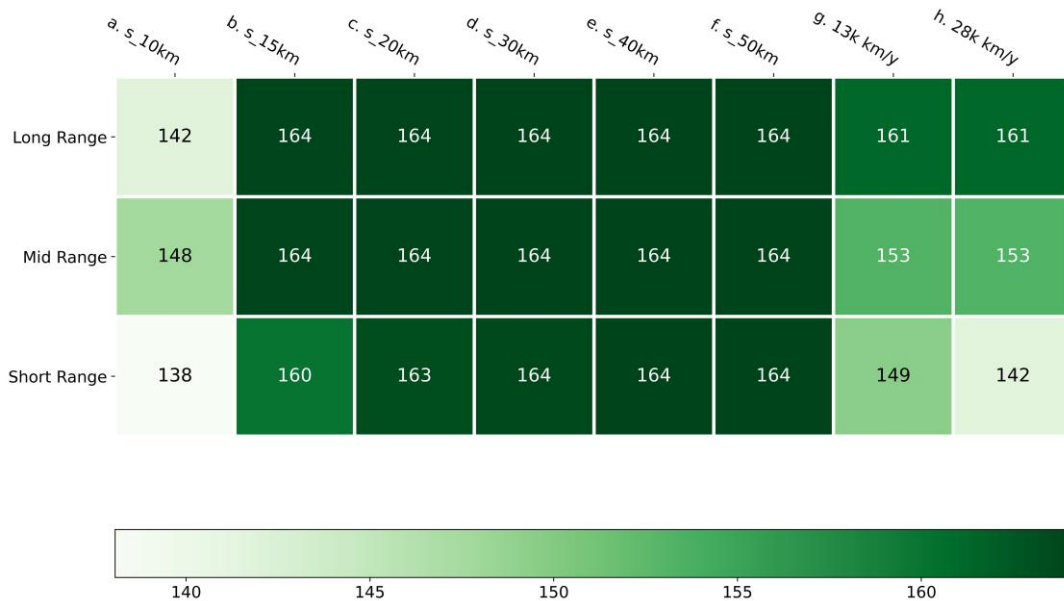


**Fig. 2.2-28 Predicted financial benefit, for Amsterdam, based on a household electricity price of 0,22 EUR/kWh**

(The savings range between 138 and 164 EUR/year.)

Like the CO<sub>2</sub> reductions, the cost savings have a direct correlation with the PV utilised, and range between 138 and 164 EUR/year for the profiles and vehicles examined here. These savings are most likely higher if the commercial charging pole prices were considered. In the Netherlands a figure of 0,35 EUR/kWh is not uncommon and so this would increase the above figures by 60%, making the savings up to 262 EUR/year. The Netherlands government has stated that the cost of charging electric vehicles must become much clearer by December 1, 2020 [15], but these figures were not available at the time of this writing.

### 2.2.8 Conclusions

The results of these case studies in this section show that even with a relatively low total irradiation, PV-powered vehicles can make a significant impact on electric vehicles in the Netherlands. As PV and EVs become more efficient the impact can increase. It is also shown that driver behaviour, in the form of charging strategies and driving profiles, can have a measurable effect on the benefits of PV-powered vehicles. Up to 60% reduction in charging frequency can increase autonomy and a feeling of security for the EV driver. And while CO<sub>2</sub> emission reduction will depend on the carbon intensity of the local grid, current values in the Netherlands mean that there can be an effective CO<sub>2</sub> reduction of about 200 kg CO<sub>2</sub>-eq/year. Finally cost savings are shown up to 164 EUR/year, but are more likely to be much higher as commercial EV charging rates are currently significantly higher than household electricity prices.



## [References]

- [1] RVO (Netherlands Enterprise Agency), "Statistics Electric Vehicles in the Netherlands (September 2020)," RVO (Netherlands Enterprise Agency), 2020.
- [2] ElaadNL, "Factsheet: Nationale Agenda Laadinfrastructuur [NAL], Winter 2020," ElaadNL, Arnhem, 2020.
- [3] RVO (Netherlands Enterprise Agency), "Factsheet: The National Charging Infrastructure Agenda," RVO (Netherlands Enterprise Agency), Utrecht, 2020.
- [4] Centraal Bureau voor de Statistiek, "Verkeersprestaties personenauto's; eigendom, brandstof, gewicht, leeftijd," 17 September 2019. [Online]. Available: <https://opendata.cbs.nl/statline/#/CBS/nl/dataset/71107ned/table?ts=1596182351376>. [Accessed 27 July 2020].
- [5] Centraal Bureau voor de Statistiek, "Mobiliteit; per persoon, vervoerwijzen, motieven, regio's," 21 February 2020. [Online]. Available: <https://opendata.cbs.nl/statline/#/CBS/nl/dataset/84710NED/table?ts=1596186613938>. [Accessed 27 July 2020].
- [6] ANWB & Milieu Centraal, "Factsheet Elektrisch autorijden," ANWB & Milieu Centraal, Utrecht, 2013.
- [7] A. J. Carr, E. van den Tillaart, A. R. Burgers, T. Köhler and B. K. Newman, "Vehicle Integrated Photovoltaics - evaluation of the energy yield potential through monitoring and modelling," in *37th European Photovoltaic Solar Energy Conference and Exhibition*, online, 2020.
- [8] Meteotest AG, "Meteonorm V7.3.4.21143 Climate Data Software," Bern, 2020.
- [9] EV Database, "Electric Vehicle Database," 2020. [Online]. Available: <https://ev-database.org/>. [Accessed 23 July 2020].
- [10] E. D. Kostopoulos, G. C. Spyropoulos and J. K. Kaldellis, "Real-world study for the optimal charging of electric vehicles," *Energy Reports*, vol. 6, pp. 418-426, 2020.
- [11] G. J. Janssen, A. R. Burgers, A. Binani, A. J. Carr, B. B. van Aken, I. G. Romijn, M. Klenk, H. Nussbaumer and T. Baumann, "How to Maximize the kWh/kWp Ratio: Simulations of Single-Axis Tracking in Bifacial Systems," in *35th European Photovoltaic Solar Energy Conference and Exhibition*, Brussels, 2018.
- [12] Global Petrol Prices.com, "electricity\_prices," 17 July 2020. [Online]. Available: [https://www.globalpetrolprices.com/electricity\\_prices/](https://www.globalpetrolprices.com/electricity_prices/). [Accessed 17 July 2020].
- [13] IEA, "Statistics - CO2 Emissions from fuel combustion," IEA, Paris, 2019.
- [14] O. Kanz, A. Reinders, J. May and K. Ding, "Environmental Impacts of Integrated Photovoltaic Modules in Light Utility Electric Vehicles," *Energies*, vol. 13, no. 19, p. 5120, 2020.
- [15] M. d. J. Baas, "ACM: prijs van laden elektrische auto moet op 1 december overal duidelijk zijn," *Dé Duurzame Uitgeverij*, 26 October 2020. [Online]. Available: <https://nederlandelektrisch.nl/actueel/i1583/acm-prijs-van-laden-elektrische-auto-moet-op-1-december-overal-duidelijk-zijn>. [Accessed December 2020].



## 2.3 Case study on PV-powered light commercial vehicles in Germany: Energy balance and expected CO<sub>2</sub> reduction

In Germany, integration of photovoltaics (PV) into electrically-driven vehicles is currently investigated within the framework of public funded research projects (e.g. within the project “PATOS” [1], “Street” [2] and “Lade-PV” [3] – all funded by the German Ministry for Economic Affairs and Energy), by the Start-Up company Sono Motors [4], and by a few automotive companies such as Audi [5].

This section reports on the case study within the project “Street”. In “Street”, on-board application of PV specifically in electrically powered light commercial vehicles (LCV) is investigated. Besides the need for de-carbonization of the entire transport sector, the transition from combustion engine-driven LCVs to electrically-driven LCVs is also motivated by the necessity to improve the air quality in inner cities. In numerous cities of Germany, for example, the EU limit for nitrogen oxide concentration (below 40 µg/m<sup>3</sup> of outside air) has yielded a driving ban for older diesel vehicles with high NO<sub>2</sub> emissions. On the other hand, delivery service in the inner cities is increasing more and more, in particular due to the increased importance of internet trade. Electrification of the “last delivery mile” is therefore desirable. In Germany, electrically powered LCVs are commercialized for example by Streetscooter (WORK), Volkswagen (E-Crafter) and MAN (eTGE).

Exemplary differences to the situation for passenger vehicles are that for LCVs, the rather high cuboid compartment relaxes the requirements on aesthetics such as curvature or color of the PV modules. In addition, the electricity provided by the PV modules can not only be used for driving but also for on-board functions such as a refrigerated box. Finally yet importantly, the driving pattern for LCV, such as delivery vehicles, exhibits stops with significant time for PV-based recharging. Exemplary differences to the situation for heavy trucks and truck trailers are that for LCVs, both the available roof areas and the energy consumption during driving are smaller, shading issues are probably more pronounced in urban environments than on highways [6], and electrically-driven vehicles are more established so that the PV energy can more likely be utilized for driving rather than for on-board functions only.

Therefore, one may expect significant differences for the integration of photovoltaics in LCVs as compared to the user case of passenger vehicles and heavy trucks / truck trailers.

The general objective of Street is to demonstrate experimentally a high solar coverage rate > 20% of the energy required by electrically powered light commercial delivery vehicles, and to demonstrate an economic viability of VIPV for this application. For this purpose, a demonstration vehicle – a Streetscooter WORK L (see Fig. 2.3-1) – is equipped with photovoltaics. Street is a research project with a duration of three years, and started on 1<sup>st</sup> August 2018. The consortium members of Street are: StreetScooter – an electric vehicle manufacturer located in Aachen, Germany, owned by Deutsche Post DHL Group; Continental – a German automotive manufacturing company specialized in, among other fields, interior electronics, automotive safety and powertrain; a2-solar – a German PV module manufacturer specialized in vehicle integrated and building integrated applications; Meyer-Burger - a Swiss PV equipment manufacturer specialized in, among other technologies, deposition tools for Silicon Heterojunction (SHJ) cells, operating a SHJ pilot line in Hohenstein-Ernstthal, Germany; the Institute for Solar Energy Research Hamelin (ISFH); the Institute for Electronic Materials and Devices from Leibniz University Hannover (MBE); JÜLICH; Helmholtz-Zentrum Berlin (HZB) - research institutes with expertise in PV cell development. Street is coordinated by ISFH.



Fig. 2.3-1 Streetscooter: WORK L



### 2.3.1 Energy balance analysis for LCV

Regarding vehicle types, the Street project has chosen the electrically driven light commercial vehicle “WORK L” from the company StreetScooter (see Fig. 2.3-1). More than 10 000 of these are already in use in the fleet of Deutsche Post DHL Group.

When integrating solar modules into the compartment of the WORK L (roof, sides, rear-side), a total area of ~15 m<sup>2</sup> can be used. The maximum peak power available from this area would be 3 000 W<sub>p</sub> for an assumed module efficiency of 20% under standard testing conditions STC (25°C, AMG 1,5 spectrum, vertical light incidence). The first generation VIPV modules actually realised in the Street project have a total peak power of 2 180 W<sub>p</sub> under STC. The modules designated for the roof accounts for 875 W<sub>p</sub> under STC.

Of course, this poses an upper limit since light incidence is by far not vertical (in particular for the modules mounted on the side and on the rear), there is no direct irradiation on the sides facing away from the sun, and transient partial shading can occur. Besides an effectively reduced time-averaged irradiation, the transient effects may also be relevant for on-board electronics such as maximum power point trackers (MPPTs), since they can occur at significantly higher frequencies compared to stationary use.

In order to assess time-averaged aspects such as the roof-to-side ratio of the irradiation as well as the abovementioned transient aspects, the solar irradiance on the roof and the side of a vehicle while driving was measured with very high time resolution [7][8]. Three Kipp & Zonen SP2 Lite 2 pyranometers on a Renault Kangoo are attached with a modified roof rack. The used pyranometers are silicon based and have a spectral range of 400 nm to 1 100 nm and a response time lower than 500 ns. They are directed to the left, right and upwards with respect to the direction of driving. The output signal is an analogue voltage, which is proportional to the solar irradiance on the sensor with a sensitivity of 72 fV/W/m<sup>2</sup> and is recorded by a digital oscilloscope with a sampling rate of 10 kHz. GPS was used to track the location and speed with a sampling rate of 1/s.

The test route represents many different situations that can typically occur while driving in an urban environment with light commercial delivery vehicles. The route features sections with a high building density with narrow streets and low speed limit, as well as sections with medium wide streets such as alleys and wide streets with higher speed limit, such as city highways. The route was also chosen so there were about equally long sections in predominantly north-south (or south-north) direction as in predominantly east-west (or west-east) direction. The route is depicted in the satellite image in Fig. 2.3-2. The data used in this work was collected in a total of six runs in autumn 2019, in winter 2019/2020 and in summer 2020, on a sunny and on a cloudy day, respectively.



Fig. 2.3-2 The GPS track of the test route. The direction of driving is counter clockwise with the start/end-point in the northwest (Google Earth Pro 7.3.3.5776, 52°22'33,53" N 9°43'55,15" E, Imagery date 4/1/2019, © 2019 Google, © 2009 GeoBasis-DE/BKG)



The measured maximum irradiance on the vehicle’s roof was consistent with stationary irradiance measurements of the Institute of Meteorology and Climatology of the Leibniz University Hannover [9] at a location close to the test route. Fig. 2.3-3 shows the average irradiance on the side of the vehicle relative to the irradiance on the roof. It was found that this side-to-roof ratio is about 40% in average, which is similar to [10] considering the different degrees of latitude of the respective locations. However, it can vary from 26% to 93%, heavily depending on the solar altitude, the weather conditions and the type of the street. The significantly higher side-to-roof ratio in winter at sunny weather due to low solar altitude and little diffuse light is noteworthy.

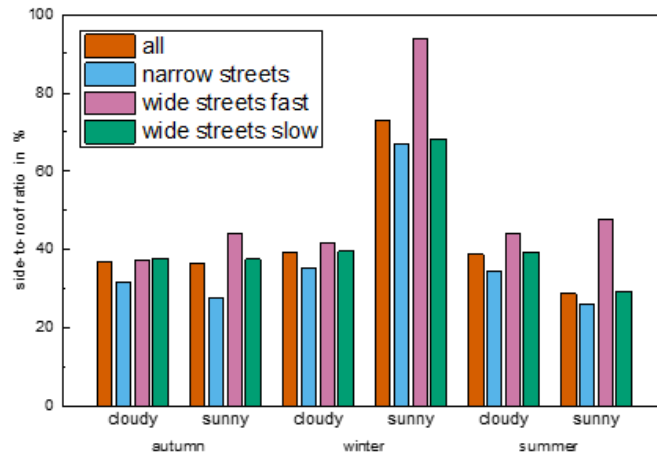


Fig. 2.3-3 Average irradiance on the side of the vehicle relative to the irradiance on the roof (side-to-roof ratio)

The collected data provides not only information about the overall solar irradiance on the vehicle while driving, but the high sample rate also allows an analysis of the transient behavior of illumination. Fig. 2.3-4 exemplarily shows a 10-minute extract of the measured irradiance over time from 09/05/2019 (a sunny day). The test run was performed between 13:00 and 14:00 UTC.

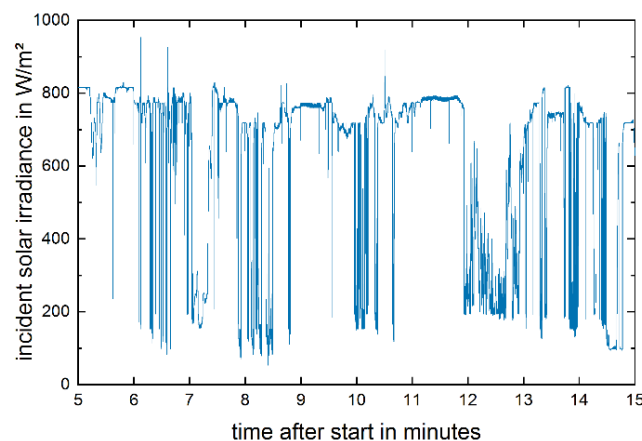
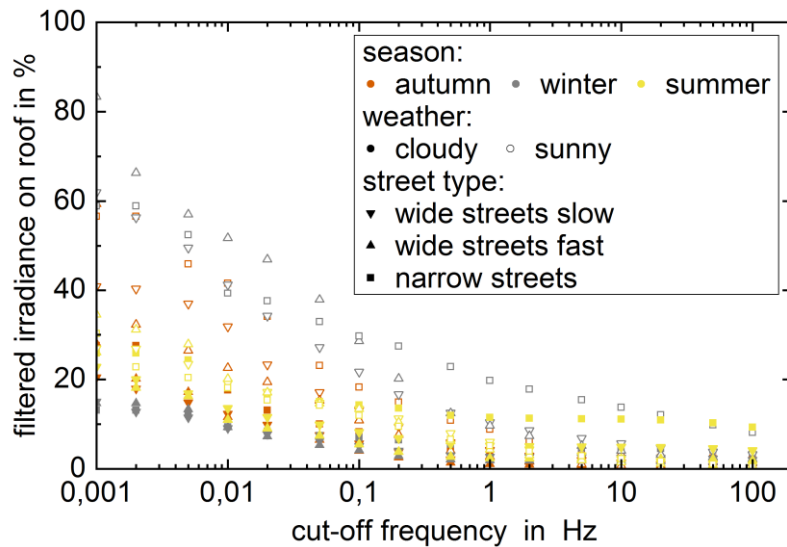


Fig. 2.3-4 A 10-minute extract of the measured irradiance on the roof of the vehicle over time from 09/05/2019, recorded between 13:00 and 14:00 UTC

Fourier transform (FFT) was performed on the recorded data. The FFT converts a waveform from time domain to frequency domain, enabling a subsequent filtering. Fig. 2.3-5 shows the high pass filtered irradiance for the roof relative to the maximum irradiance for different seasons, weather conditions and street types over cut-off frequency. It was found that the frequencies at which irradiance changes occur heavily depend on the solar altitude, the



weather conditions and the type of the street. There is a trend to higher frequencies for sunny weather and streets with high speed limit. It was also found that higher frequencies occur more often on the sides of the vehicle, although not shown here.



**Fig. 2.3-5 High pass filtered irradiance on the roof over cut-off frequency for different environmental conditions**

For all environmental conditions, Fig. 2.3-5 shows a continuous decrease of the filtered irradiance with increasing cutoff frequency. On cloudy days, the decrease is much steeper. This can be explained by the more direct light on the sunny days which causes more hard edge shades which in turn cause more abrupt dark-light or light-dark transitions. The most relevant frequency range is below 1 Hz for most conditions, while higher frequencies contribute very little to the overall irradiance. For example, for a cloudy day in autumn, only 1,5% of the incident irradiance occur above a cutoff frequency of 1 Hz, and for sunny day in autumn, only 4% of the incident irradiance occur. For a cutoff frequency of 5 Hz, only 1,2% and 1,9% of the irradiance would be “filtered out” at these days.

In conclusion, the solar irradiance on the roof and the side of a vehicle while driving with high time resolution was measured. It was found that the side-to-roof ratio is about 40% in average, but it can vary from 26% to 93%, heavily depending on the solar altitude, the weather conditions and the type of the street. The transient behavior of the irradiance with high time resolution was also investigated and it was found that more than 98% of the incident energy occur at frequencies below 5 Hz. A control rate of the MPPT is not required to exceed 5 Hz as illumination changes at higher frequencies are negligible for the overall energy yield – at least for the test routes investigated.

While these irradiation measurements on specific test routes provide valuable insights aspects such as roof-to-side ratio and transient shading, they are not directly generalizable for longer periods (e.g. annual average), other routes and different locations. This generalization is addressed by JÜLICH. JÜLICH is developing a methodology to forecast the energy yield on different timescales (days to annual average) based on metrological and satellite data. This model is currently validated by a comparison of its predictions with the results from experimental test drives. JÜLICH is also performing a Life Cycle Assessment to quantify the ecological benefit of VIPV for this specific user case (see below).

Another approach is to estimate the ratio between the annual energy yield and the peak power for modules mounted horizontally and vertically on a vehicle based on practical experience. a2-solar has many years of practical experience in VIPV and has determined this ratio already in previous projects. For the modules mounted on the Streetscooter “WORK L” vehicle - 2 180 W<sub>p</sub> (875 W<sub>p</sub>) in total (on the roof) under STC - a2-solar estimates a total energy yield from 1 170 kWh/a (Hamburg, Germany) to 2 210 kWh/a (Rome, Italy), as shown in Table 2.3-1.



**Table 2.3-1 Estimation of annual energy yield from the modules on the Streetscooter “WORK L” vehicle for exemplary latitudes and longitudes, and the respective solar energy coverage fraction**

(The (weighted) ratio between module peak power mounted roof and on the sides to the energy yield is based on a2-solars many years practical VIPV experience.)

City	Estimated annual energy yield (in total 2 180 W <sub>p</sub> mounted on vehicle) [kWh/a]	Solar energy coverage fraction (assuming an energy consumption of 19,2 kWh/100 km and an annual driving distance of 20 000 km) [%]
Hamburg (53,5511 ° north, 9,993682 ° east)	1 170	31
Erfurt (50,9787 ° north, 11,03283 ° east)	1 300	34
Munich (48,1351 ° north, 11,581981 ° east)	1 430	37
Rome (41,9028 ° north, 12,496365 ° east)	2 210	58

For the specified energy consumption for driving for this vehicle (19,2 kWh / 100 km according to NEFZ), this would correspond to a PV powered distance from 6 094 km/a (Hamburg, Germany) to 11 510 km/a (Rome, Italy). Referring to an average annual driving distance of ~20 000 km /a for these delivery vehicles, a solar energy coverage fraction from 30% to > 50% seems therefore achievable (see Tale 2.3-1). These numbers would definitely be significant. Currently, the Street consortium is working on the experimental verification of this prediction. For this purpose, the integration of the PV modules – as well as of the electrical components from Continental (fast maximum power-point tracker, DC/DC converter) - into the StreetScooter “Work L” vehicle is ongoing work. First test drives were planned for end of 2020.

### 2.3.2 Identified requirements, barriers and solutions for PV powered LCVs

For the solar cells, the crystalline Si (c-Si) technology is chosen. As the application for VIPV, c-Si is in competition with thin-film and III-V based photovoltaic [5][11]. Thin film PV might be applied on flexible substrates and thus facilitates at least one-directional curved and lightweight modules. For III-V PV, very high efficiencies up to 29,1% are reported for single junction cells [12]. However, it is expected that for VIPV, c-Si provides the best trade-off between efficiency and costs. The a-Si:H/c-Si heterojunction technology (SHJ) based on double-side contacted cells was chosen. Meyer-Burger Germany provided 1 000 Si heterojunction (SHJ) cells on n-type doped, Czochralski-grown Si pseudo-square shaped wafers with a size of 156,75 mm × 156,75 mm and a thickness of 150 μm. The median cell energy conversion efficiency (CEE) of SHJ cells from the pilot line at Meyer-Burger is currently 24,1% (standard testing conditions, busbarless measurement on full area). Due to the excellent surface passivation quality of the amorphous Si (median open circuit voltage 742 mV), the temperature coefficient of the CEE is only -0,2 %/K.

These cells were connected to strings at ISFH using the Smart-Wire Cell Interconnection Technology (see Fig. 2.3-6(a)). Besides many other positive aspects, one major advantage of this concept for the application VIPV is mechanical robustness and its tolerance against micro-cracks in the solar cells. The MB- Smart Wire Technology with In-free low-temperature solder material were used, and the latest generation of transparent foils for the foil-wire assembly. These strings were integrated into modules by a2-solar (see Fig. 2.3-6(b)), and further integrated into the vehicle (see Fig. 2.3-6(c)).

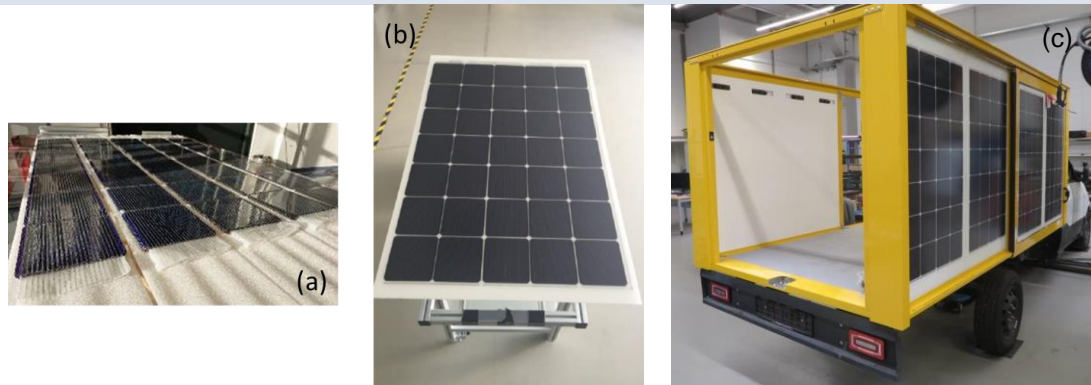


**Fig. 2.3-6 (a) Photo of SHJ cell strings interconnected by the Smart-Wire Cell Interconnection Technology at ISFH. (b) Integration of these strings into final VIPV modules (a2-solar). (c) Integration of the PV components into the vehicle (Photo: Continental Engineering Services).**

For a second module generation, a2-solar will work on further reduction of the module weight, since a minimum of reduction of the payload is crucial for LCV applications. However, the durability requirements of automotive applications (high maximum temperatures, huge temperature gradients, vibrations and mechanical shocks, hail, etc.) are harsh and challenging to meet by foil-based light-weight modules. Therefore, a2-solar performs aggressive mechanical and accelerated aging tests.

The integration of the PV modules – as well as of the electrical components from Continental (fast maximum power-point tracker, DC/DC converter) - into the Streetscooter “Work L” vehicle is ongoing work. It already became obvious that feed-in of the energy converted by the PV modules into the high-voltage system of the electrically driven vehicle is not trivial. Besides the highly efficient DC/DC-converter from Continental, an appropriate adaption of the on-board communication system is required for this purpose.

The integration of the PV components into the demonstrator vehicle were completed at the end of 2020, with a total nominal peak power of 2 180 W (see Fig. 2.3-7). The PV-converted energy is transferred into the high-voltage board net and utilized for range extension.



**Fig. 2.3-7 PV-powered light commercial vehicle, developed by the Street project (Photo: Institute for Solar Energy Research Hamelin)**

### **2.3.3 Analysis of expected benefits: reduction of CO<sub>2</sub> emission**

Though prior studies have often indicated that VIPV will result in lower CO<sub>2</sub> emissions, actual LCAs of VIPV are barely available, and most claims until now have not been quantified or validated for the specific situation of VIPV of LCVs [13][14][15]. Thus, the goal of this work is to analyze how PV-powered vehicles can contribute to sustainable mobility. Therefore, an LCA focused on determining the CO<sub>2</sub> emissions of the abovementioned VIPV LCV “WORK L” from StreetScooter is conducted. The results of this research could be useful for car manufacturers, to calculate emissions per vehicle, for political institutions to estimate environmental impacts for the transport sector and for business parties in the solar market to identify further application possibilities and yield useful data to identify critical areas for the improvement of VIPV for LCVs.

This section presents the general methodology used to execute the LCA, defines the efficiency of the VIPV investigated and quantifies the resulting CO<sub>2</sub> emissions. Additionally, key parameters that limit the environmental performance of the electricity produced by the PV system integrated into the vehicle are identified. Assumptions about these critical parameters for the reference case are clarified.



### 2.3.3.1 Life Cycle Assessment Method

LCA is a useful tool to quantify environmental performance, considering a holistic perspective. LCA is generally understood as a compilation and evaluation of the inputs, outputs and potential environmental impacts of a product system throughout its life cycle [16]. LCA studies always consist of four main phases, which are covered through ISO standards (DIN 14044; ISO 14040:2006). The first step of the LCA is used to define the goal and scope of the study. The second step is a life cycle inventory (LCI) model through which data is collected and organized. The third step is the life cycle impact assessment (LCIA), used to understand the relevance of all the inputs and outputs in an environmental framework. The fourth step is the interpretation, which is a systematic technique to identify, check, and evaluate information resulting from the LCIA (see Fig. 2.3-8).

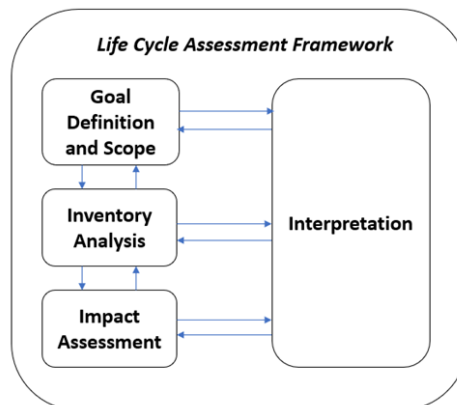


Fig. 2.3-8 LCA Framework (DIN 14044; ISO 14040:2006)

The environmental impact assessment for this study has been completed at the mid-point level. Midpoints are considered to be connections in the cause-effect chain of different impact categories, also known as the problem-oriented approach or classical impact assessment method. Greenhouse gas emissions (kg CO<sub>2</sub>-eq) were used as an indicator of climate change contribution. 100-year global warming potentials based on the IPCC 2013 were assumed, according to their radiative, forcing capacity relative to the reference substance CO<sub>2</sub>. Global Warming Potential (GWP) during the life cycle stages of a PV system is estimated as an equivalent of CO<sub>2</sub> containing all the significant emissions CO<sub>2</sub> (GWP=1), CH<sub>4</sub> (GWP=25), N<sub>2</sub>O (GWP=298) and chlorofluorocarbons (GWP = 4 750-14400). The calculations are performed using LCA software GaBi with Ecoinvent v2.2+ as background database. GaBi is a process-oriented software, examining the material and energy flows of each step in the production chain.

### 2.3.3.2 Input Parameters of the LCA

The use case is the light commercial battery electric vehicle WORK L of StreetScooter. The functional unit for this study is 1 kWh of electricity supplied by the PV system to the battery of the StreetScooter. In comparison to the functional unit of 1 km driven, the emissions of 1 kWh can be calculated more accurately. Furthermore, the chosen functional unit of 1 kWh allows for a direct comparison of effects of charging by PV modules to those due to charging by the grid. Thus, the emissions of VIPV and grid charged BEV can be evaluated more precisely referring to the same functional unit. The operation of the electrical vehicle is set in Cologne, Germany and started in 2017. Within the scope of this project, the environmental impacts of VIPV are to be studied according to the standard of life cycle assessment ISO 14040:2006. The PV system configuration is based on the first generation of the VIPV panels for the STREET Project with heterojunction silicon PV modules. Due to the lack of availability of LCA input data for the specific cell and module manufacturing chain described above, the input data for modules manufactured in China is assumed here. The analysed VIPV configuration includes three panels and three control units, including the cables mounted on the vehicle's roof. The VIPV system's overall capacity is assumed to 930 Wp (corresponding to an envisage second module generation on the roof of the WORK L vehicle). Due to the uncertainties regarding the irradiation on the sides, so far the modules mounted there have been disregarded. The VIPV electricity system



includes raw material extraction, wafers, crystalline silicon-based heterojunction solar cells and module manufacturing, mounting structures manufacturing, inverters manufacturing, system installation and the operation. The production process of a typical commercial crystalline silicon solar cell is modelled based on the existing datasets describing the supply chain [17] (see Fig. 2.3-9). Input parameters of the manufacturing of the PV control unit (PVCU), as well as the vehicle integration process were added based on internal communication in the project STREET. The electricity consumption on all process levels is modelled following specific electricity mixes corresponding to China (CN) or Germany (DE) respectively, based on the Ecoinvent data sets.

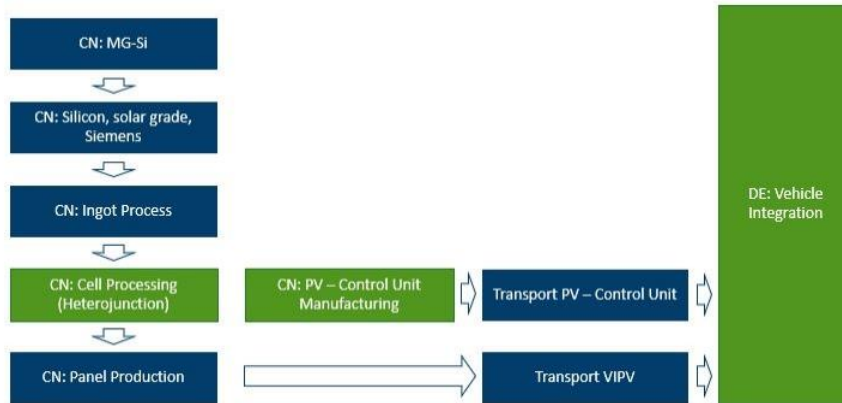


Fig. 2.39 VIPV system value chain: Process flow diagram; CN means China, DE means Germany

The exact location of manufacturing plants is undocumented and unknown. However, it can be assumed that the location of these plants is somewhere within China. Modelling of the transportation was based on the standard distances as suggested in the Guideline for PC LCA [16]

The main factor for the estimation of PV electricity generation is the effective solar irradiance, which depends on the route and location, season, time and module configuration and orientation. For the reference case of the LCA, the location for the operation was set in Cologne, Germany. The hourly global horizontal solar irradiance has been defined by averaging hourly incident global horizontal radiation data extracted from the PVGIS database. The on-board generation of electricity was simulated based on degradation, system losses and shading factor (see Table 2.3-2). A 19,7% module efficiency is assumed [18]. This can be considered as a conservative estimate of the lower case: efficiencies well above 22% have been demonstrated for “stationary” heterojunction modules but specific VIPV requirements such as foil-based front sides might reduce the module efficiencies in our scenario. In line with the IEA PVPS methodology guidelines [16], degradation of 0,7% per year is applied. Operation time of the reference case was set to eight years, based on data of LCVs in delivery services [19].

Table 2.3-2 Input Parameters for the Operation of the VIPV

Parameter	Value	Unit
Capacity	930	[Wp]
Efficiency	19,7	[%]
Degradation	0,7	[%]
Operation lifetime	8	[a]
Location	Cologne [50,938/6,954]	[Lat/Lon]
Database	PVGIS-CMSAF	-

According to the literature guidelines, the VIPV system’s efficiency was estimated. Due to dynamic shading, an average 70% performance compared to residential PV is assumed. Furthermore, generated energy cannot be used directly for traction of the vehicle and must be stored in the battery, where a DC-charging/discharging loss of 2% appears. An additional loss of 5% is considered due to the DC/DC converter. The loss of the MPP tracking additionally limits its efficiency in the model to 95%. A performance loss of 9% due to temperature increase and



low irradiance is assumed [20]. The overall average efficiency losses of the VIPV system is to be found in Table 2.3-3.

**Table 2.3-3 VIPV System Efficiency**

Loss Coefficient	Changes in output [%]
MPPT Loss	-5
Temperature/low irradiance	-9
DC/DC conversions	-5
DC Charging/ Discharging loss	-2
Average shading factor	-30

The grid mix in the location of the charge is analysed regarding its carbon intensity. The grid’s emissions can vary massively depending on the different power plants. Fossil power plants dominate the power generation in Germany. Acknowledged studies usually consider annual average carbon footprints of the grid power plants caused by the life cycle (construction, fuel production, operation, etc.) [21]. Hourly average emissions of the German electricity mix vary depending on the day and night times. The German electricity mix was modelled using SMARD electricity generation data from 2017 and utilised for the projection of the future scenario [22]. The reference scenario follows the pathway of technological development as far as possible, according to the goals set by politics.

The targeted total amount of CO<sub>2</sub> emissions of the electricity sector for the year 2030 in Germany is 180-186 million t CO<sub>2</sub>. Until 2028, the annual electricity mix GWP is expected to decrease by 2 % per year [23].

**2.3.3.3 Results of the LCA**

The results of the analysis of the manufacturing phase [*kg CO<sub>2</sub>-eq*] demonstrate the impact before the operation starts. The manufacturing process VIPV shows similar results to other PV systems. The most dominant contributor to this phase is the Solar-Grade Process. It is responsible for 444,30 kg CO<sub>2</sub>-eq, a third of total emissions. The process of integration of the cells into the panel emits 235,24 kg CO<sub>2</sub>-eq. The calculated total amount of emissions during the manufacturing process is 1 143,12 kg CO<sub>2</sub>-eq (see Fig. 2.3-10).

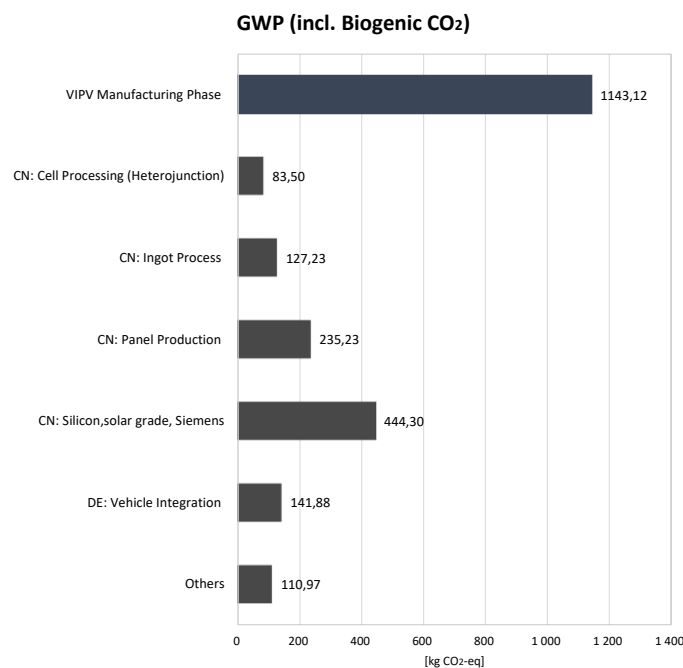


**Fig. 2.3-10 Results of the LCA, the manufacturing phase GWP = 1 143 [kg CO<sub>2</sub>-eq]**



The on-board generation of electricity was simulated based on the assumptions on degradation, system losses and shading factor. While driving the EV, the batteries will discharge and will recharge again using the on-board PV modules. The degree of VIPV's impact was expected to vary with the usage patterns: different daily driving distances have different depths of discharge corresponding to daily driving durations. In this study, all incoming irradiance during the day is used, assuming energy is being collected and the battery is being charged, even if not driving. For the reference scenario of eight years operation and a shading factor of 30%, the VIPV contribution is 3 738,116 kWh. Prolonged operation of 12 years generates 5 526,702 kWh in total. For the same amount of energy, if the grid would be used, 1 630 kg CO<sub>2</sub>-eq for eight years and 2 267 kg CO<sub>2</sub>-eq for 12 years were calculated. The losses appearing due to grid distribution are not calculated, because the emission factor is already based on an energy consumption perspective.

Main findings of the comparison with grid electricity show: VIPV can improve the carbon footprint for the reference case of an average shading factor of 30% and eight years of operation time. For the functional unit of 1 kWh of on-board generated PV electricity, the emission factor of 0,357 kg CO<sub>2</sub>-eq/kWh is calculated for the reference case. In comparison, the average grid emissions for the operation time are expected to be 0,435 kg CO<sub>2</sub>-eq/kWh.

Considering the data quality of the LCA, reduction of emissions of the functional unit for the reference case compared to the grid is about 18%. The holistic view of the results for the reference case shows 3 738 kWh VIPV contribution. For the functional unit of 1 kWh of on-board generated PV electricity, the emission factor of 0,357 kg CO<sub>2</sub>-eq/kWh is calculated. In comparison, the average grid emissions for the operation time are expected to be 0,435 kg CO<sub>2</sub>-eq/kWh. Compared to the estimated grid average, about 18% less emissions per kWh are caused by VIPV. The projected contribution of VIPV was replaced by grid charging to find out in which operation year VIPV have fewer emissions than the grid and thus calculate the "ecological break-even point". In the previously described reference case, this point is achieved in the year 2022. That means that after 6,5 years of operation, the ecological impact of VIPV equals the impact of the grid charge. However, an increasing shading factor of mobile application causes a significant growth of emissions per kWh.

The study's results are wide-ranging. The variations mainly arise from system operating assumptions (e.g. solar irradiation, system lifetime, shading factors) and technology improvements (e.g. electricity consumption for manufacturing processes). PV-generated power is an essential variable for the reduction in emissions. By increasing the shading factor, emissions per kWh grow significantly. An emission factor of 0,357 kg CO<sub>2</sub>-eq/kWh is calculated for the reference case. The increased shading factor of 40% results in 0,435 kg CO<sub>2</sub>-eq/kWh, which equals the average emissions of the future grid electricity. The ecological benefit over the grid charge disappears completely when the shading factor reaches 40%. Sensitivity analysis shows that if the VIPV is used for a prolonged life of 12 years, the emission factor of the produced electricity decreases to 0,221 kg CO<sub>2</sub>-eq/kWh. A reduction of 38 % (0,136 kg CO<sub>2</sub>-eq/kWh) compared to the reference case of eight years is noted. The average grid mix emissions of prolonged use decrease to 0,409 kg CO<sub>2</sub>-eq/kWh.

As mentioned above, the electricity consumption was so far modelled according to China's grid mix data. The emission factor of 0,831 kg CO<sub>2</sub>-eq/kWh for China's electricity mix was used for the simulation of the reference case. With the increasing share of renewable energy in the electricity mix, lower GWP impact will arise from the production phase of the VIPV. Assuming "green" electricity is used for the manufacturing process, as is the case in Norway, the amount of emissions can be reduced. Using green electricity has the potential to be almost carbon-free, as is the case for hydropower already in use today. "Green" electricity assumptions of hydro plants with average emissions of 0,003 kg CO<sub>2</sub>-eq/kWh were used to cover the energy need of the manufacturing phase (Memmler et al. 2018). For manufacturing of the whole system, 566,019 kWh are needed. If instead of the grid mix of 0,831 kg CO<sub>2</sub>-eq/kWh hydro plants with 0,003 kg CO<sub>2</sub>-eq/kWh are used in the reference case of 30% shading, the emissions fall from 0,357 kg CO<sub>2</sub>-eq/kWh to 0,230 kg CO<sub>2</sub>-eq/kWh. The transport emissions from China are responsible for around 10% of the overall emissions of VIPV. Assuming transport of the wafers from Norway instead of China, the emissions arising from transport can be extremely reduced. The reason is shorter distance to Germany (1 100 km from Oslo, Norway, instead of 19 994 km from Shanghai).

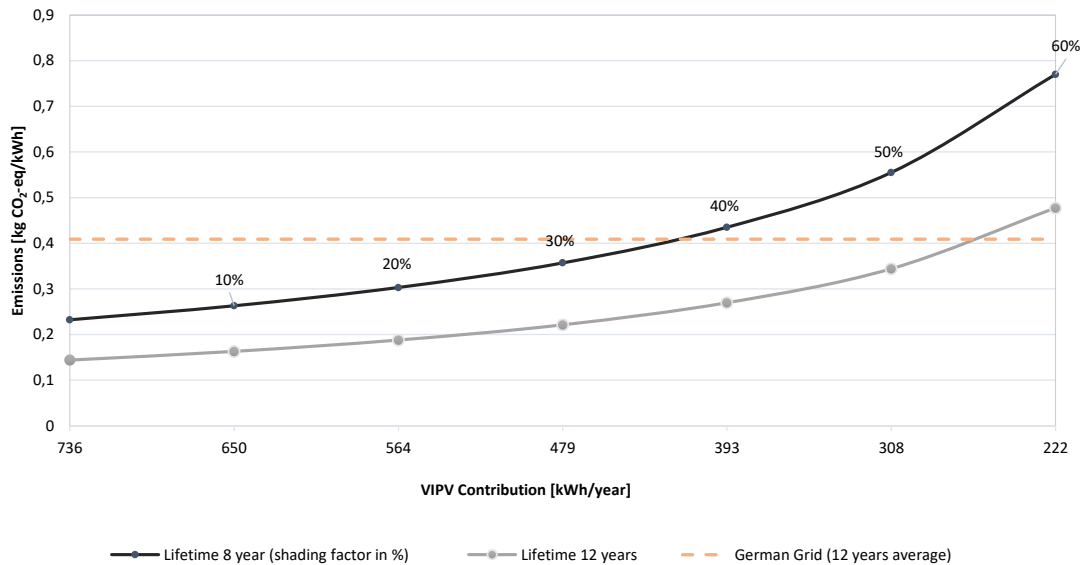


Fig. 2.3-11 Emissions depending on the shading factor and prolonged lifetime

For the recycling process, no established and reliable routes were found. As to the knowledge of the author, no study provides details on the LCI with the input and output of every process stage. However, if material depletion is considered, recycling is crucial, and further research should include recyclability options. Since second use is an important issue, the mounting structure, removable and light-weighted, must become a priority for the research. Furthermore, a scenario of VIPV connection to the public grid while parking during weekends, in which the surplus of unused electricity can be fed into the grid, seems to be realistic. Vehicle-to-Grid (V2G) concepts can be very profitable, but first, the dependence on the state of charge (SOC) of the battery including an ageing model of the battery with charging and discharging losses should be analysed. To contribute to the growth of the VIPV market, governments willing to achieve emission goals must support the standardisation of the technology. To solve this problem, international methods of evaluating added value on the reduction of grid power and ecological benefits are required.

## [References]

- [1] <https://www.enargus.de/pub/bscw.cgi/26?op=enargus.eps2&q=patos>
- [2] <https://www.enargus.de/pub/bscw.cgi/26?op=enargus.eps2&m=0&v=10&p=0&s=0&q=street>
- [3] <https://www.enargus.de/pub/bscw.cgi/26?op=enargus.eps2&m=0&v=10&p=0&s=0&q=lade-pv>
- [4] <https://sonomotors.com/>
- [5] <https://www.pv-magazine.com/2017/08/23/audi-hanergy-unit-to-jointly-develop-pv-for-vehicles/>
- [6] M. Kühnel et al., Prog. Photovolt: Res. Appl. 25 (7) p. 1099 (2017)
- [7] Gustav Wetzel, Leon Salomon, Jan Krügener, Robby Peibst, "Specifications for maximum power point tracking in vehicle-integrated photovoltaics based on high-resolution transient irradiance measurements", Proc. of the 46<sup>th</sup> IEEE PVSC (2020)
- [8] Gustav Wetzel, Jan Krügener, and Robby Peibst, "For VIPV applications: Investigation of transient shading with high time resolution under different environmental conditions", to be presented at the 30<sup>th</sup> PVSEC (2020)



- [9] Institute of Meteorology and Climatology Leibniz University Hannover, accessed July 14, 2020, <https://www.muk.uni-hannover.de/258.html?&L=1>
- [10] Kenji Araki et al. PVSEC-29 Proceeding, pp. 2592-2598 (2019)
- [11] T. Masuda *et al.*, presented at the 33rd EUPVSC (2017)
- [12] Press release from Alta Device, Dec. 12<sup>th</sup> (2018): <https://www.altadevices.com/solar-world-record-nasa-selects-alta-devices/>
- [13] New Energy and Industrial Technology Development Organization, “NEDO, PV-Powered Vehicle Strategy Committee,” 2018.
- [14] R. G., “Automotive application of solar energy,,” 6th IFAC Symposium Advances in Automotive Control , , Munich, Germany, 2010.
- [15] L. J. G. K. a. M. Y. Kenji Araki, “To Do List for Research and Development and International Standardization to Achieve the Goal of Running a Majority of Electric Vehicles on Solar Energy,” 2018.
- [16] D.-N. G. d. Umweltschutzes, *Environmental management - Life cycle assessment - Requirements and guidelines (ISO 14044:2006 + Amd 1:2017); German version EN ISO 14044:2006 + A1:2018*, 2006.
- [17] R. Frischknecht, R. Itten, P. Sinha, M. d. Wild-Scholten and J. Zhang, Life Cycle Inventories and Life Cycle Assessments of Photovoltaic Systems, IEA PVPS Task 12, Subtask 2.0, LCA Report IEA-PVPS 12. INTERNATIONAL EN-ERGY AGENCY, 2015.
- [18] C. Olson, M. d. Wild-Scholten and M. Scherff, “Life Cycle Assessment of Hetero-junction Solar Cells,,” 2013.
- [19] F. Hacker, R. Waldenfels and M. Moschall, Wirtschaftlichkeit von Elekt-romobilität in gewerblichen Anwendungen. Betrachtung von Gesamtnutzungskosten, ökonomischen Potenzialen und möglicher CO<sub>2</sub>EQ -Minderung im Auftrag der Begleitforschung zum BMWi Förderschwerpunkt IKT für Elektromobilität, 2015.
- [20] L. J. G. K. a. M. Y. Kenji Araki, “To Do List for Research and Development and International Standardization to Achieve the Goal of Running a Majority of Electric Vehicles on Solar Energy,” 2018.
- [21] P. Icha, Entwicklung der spezifischen Kohlendioxid-Emissionen des deut-schen Strommix in den Jahren 1990 - 2018. 29., 2019.
- [22] Bundesnetzagentur für Elektrizität, Gas, Telekommunikation, Post und Eisenbahnen; , “SMARD,” 2020. [Online]. Available: SMARD.de. [Accessed 22 06 2020].
- [23] European Environment Agency (EEA), “Progress of EU transport sector towards its environment and climate objectives,” 2018.



## 2.4 Case study on PV-powered reefer trucks in Spain: Economic feasibility assessment

### 2.4.1 Introduction

Solar Photovoltaics is expected to contribute to the necessary decarbonisation in the transport sector by providing green electricity for the transport of persons and goods, offering increasing arguments for its imminent deployment, as explained in this report. Traditionally, PV modules have been placed on passenger vehicles, integrated into solar roofs, basically as an auxiliary power source for air conditioners and other uses powered by traditional electric batteries. It contributes to recharge batteries in motor-powered vehicles or support power generated by an internal combustion engine (ICE).

Road transport vehicles have mostly been using ICE for the past few decades, because of high reliability. Due to the increase in diesel and petrol prices, as well as environmental pollution and depletion of fossil fuels, most of the vehicle manufacturers are looking for alternative fuels for vehicle propulsion. The electrical vehicle (EV) is the best solution to reduce the global warming gases emission in the transport sector [1][2] and includes battery electric vehicles, hybrid electric vehicles, plug-in hybrid vehicles and fuel cell electric vehicles. The main challenge for the electric vehicle is the cost of energy source and renewable energy generation. In all of these configurations and also in the traditional ICE vehicles, photovoltaics can provide additional power to the battery and extend its driving range, thereby allowing (important) savings in 'fuel costs' which will provide significant benefits for companies and end-consumers. In these vehicles, the available surface for the integration of PV cells is quite limited.

As opposed to passenger vehicles, the transport of goods by road, mainly depending on diesel-powered trucks, offers other alternatives for PV with larger surfaces available, free of obstacles (heavy-duty road transport, e.g. trucks, or passengers transport in intercity long-distance and urban buses) for instance using the roof of trailers, or the bodywork for buses, including also the lateral parts, and with potential to power not only auxiliary services, but other important uses such as goods refrigeration or for driving.

The economic viability of Vehicle Integrated PV (VIPV) might be achieved earlier in commercial trucks than in passenger vehicles due to their predictable routes and times [3]. Other factors are directly linked to the transport company's specific business activity. One example can be found in the Spanish company GRUPO PRIMAFRIO, the leading transport company in Europe for refrigerated goods.

GRUPO PRIMAFRIO (<https://www.primafrio.com/en/>) was set up over 50 years ago with the goal to become a global road refrigerated transport company. In line with this, GRUPO PRIMAFRIO is an excellent example and leader in the innovation field as shown in their headquarters with more than 300 000 m<sup>2</sup> surface area (15 000 m<sup>2</sup> for a cross-docking refrigerated warehouse) as well as 106 loading and unloading docks and all kinds of services (laundry, hotel, restaurant 24/7, playroom and gym among others). The company has the logistical and operational capacity, as well as the flexibility required for the transport demand of today's market.

PRIMAFRIO is leading the energy transition in the transport and logistics sector being the first fleet using LNG trucks on international routes crossing more than 25 countries and working directly with the most reputed consortiums in Europe on the EU development programs for decarbonisation, automation, safety and connectivity of the transport sector in the H2020 and Green Deal calls.

PRIMAFRIO's main activity is road transport of refrigerated goods, thanks to the hermetically sealed trailers equipped with the latest safety technology, offering a full load and groupage service from the production areas in Spain and Portugal to the major points across Europe. The most important transported goods are:

- Fruit and vegetable transport and food freights across Europe. The refrigerated transport solutions have been adapted, ensuring the characteristics of these perishable goods and securing their cold and traceability chain. The company is a benchmark for the transport of berries (strawberries, raspberries, blackberries, blueberries and cranberries), exporting more than 80% of Spain's berry harvest.
- GRUPO PRIMAFRIO also covers transport of the so-called "added-value products", specific items (technological gadgets, industrial, cosmetics and telecommunication devices) requiring a higher level of safety and a lower number of hours in a vehicle.
- Through PRIMAVIA, GRUPO PRIMAFRIO is leading the intermodal transport combining railways and heavy-duty long-haul transportation.



- Finally, transport of pharmaceutical products and medicinal products through some diversification lines such as PRIMAPHARMA.

GRUPO PRIMAFRIO has a fleet of near 2 500 vehicles equipped with live tracking and safety systems, which allow for the constant monitoring of location, consumption, driving times, emissions and temperature of each truck in real time. Through cutting-edge temperature control devices and real-time alerts, predictive and preventive maintenance in order to prevent any incidents are carried out, ensuring adequate maintenance of the cold chain and traceability of the items being transported.



**Fig. 2.4-1 New acquisition of 600 VOLVO TRUCKS (latest technology) (Photo: PRIMAFRIO)**

The main objective of PRIMAFRIO is the OPEX costs (Energy cost reduction in diesel for driving and cooling of goods), thanks to the green electricity provided by a PV system integrated in the trailer roof.

One of GRUPO PRIMAFRIO's commitments is to ensure its sustainability and complies with the highest standards of environmental care and protection. Thanks to the company's annual fleet renewal programme, sustainability goals have been met, reducing nitrogen oxide (NOx) emissions by 80% and particulate pollutant emissions by 66%, as well as achieving an 8% fuel economy by using Euro VI engines. Transport alternatives such as gas (LNG)-fuelled trucks have also incorporated, thus furthering the commitment to reducing pollutant emissions. In this context, the VIPV is seen as a key factor for achieving its environmental sustainability and reducing emissions from the heavy-duty transport sector. Technology acquires a great role in this field since, thanks to the advances that are being made in topics so conventional for the transport sector, GRUPO PRIMAFRIO can implement predictive models and the simplification of large-scale operations that, in combination with strategic collaborations from national and European projects, allows them to develop new and more efficient measures such as active aerodynamics, biodegradable components or electrical traction, among others, which will realise the reduction of polluting and acoustic emissions, while combining, at the same time, more advanced and efficient operation.

### **2.4.2 Economic feasibility assessment**

This subsection summarises the cost-benefit analysis of adding a PV system on top of PRIMAFRIO's refrigerated trailers, by comparing the potential of PV production with the truck's energy consumption, for different PV module technologies. The study also determines under which circumstances there is a profitable business case for the transport company, considering the multiple factors and parameters that have influence on the economic profitability.

The exercise in the analysis has consisted of consumption loads, both for refrigeration of goods and for the truck's motion; then in the analysis of the potential PV generation, assuming specific boundary conditions such as the route followed by the truck, different PV module providers, etc. Finally, the payback time (PBT) has been calculated, considering the CAPEX, OPEX, savings in diesel, losses due to non-delivered goods caused by the reduction of payload or increase of diesel consumption due to extra weight. Given parameters and variables that affect the



economic analysis, a sensitivity analysis is presented to identify which parameters are key factors in reducing the PBT and making the business case with PV feasibility for the truck's company.

As a previous step for this analysis, it is worth highlighting different restrictions imposed by Grupo PRIMAFRIO which come from the day-to-day activity of the company. Some of them are summarised below:

- The trailers are replaced every 66 months (every five and a half years), so that the PV system should be mounted and dismantled with every change of trailer, if the maximum lifetime of PV modules is considered.
- Maximum height of the set composed by the supporting structure and PV modules should be less than 10 cm thick, and ideally less than 3 cm thick.
- Maximum weight of the PV system, including modules and BOS (electronic devices, wiring, supporting structure) is suggested not to surpass 200 kg, approx. 1% of payload: (Payload: 22 ton).

#### 2.4.2.1 Consumption analysis

PRIMAFRIO's trucks' consumption is powered at present by diesel EURO VI engines on trucks and standard diesel engine for the refrigeration of goods (note that such engines do not respect any EURO contaminant legislation). The efficiency of a diesel engine for refrigeration is estimated at 27% (based on electricity consumptions for the compressor measured by PRIMAFRIO). For these engines, 1 litre of diesel is equivalent to 2,96 kWh of electricity. On the contrary, the average efficiency for the ICE used for motion is hardly 10%, thus 1 litre of diesel is equivalent to 0,9 kWh (source: TECNALIA for hybrid heavy-duty vehicles). Additional data provided by PRIMAFRIO regarding the consumption can be found below:

- Annual driving: 180 000 kms per truck.
- Refrigeration consumption: Two working modes: fix and automatic. On average, 70% of time reefer trucks work in fixed mode, and 30% in automatic mode, with a weighted consumption of 2,5 l/hour of diesel type B. Moreover, according to the information provided, 48 min/hour the compressor is ON, and 12 min OFF. This parameter depends on the working modes and it determines the percentage of direct self-consumption that solar PV system can provide to the refrigeration engine, without using the batteries. The consumption also depends on the external temperature, if the trucks drive at day/night, and the temperature set for the refrigeration.
- As an additional parameter, on average, 60% of consumption is produced in absence of sunlight, whilst the remaining 40% is produced during daylight, thus 40% potential direct self-consumption

The truck has two different batteries, one for the truck, auxiliary services, etc., another for the reefer. As a conclusion, the energy contained in both batteries is very limited compared with the production capacity of PV panels, which make them almost useless in ICE trucks.

- 24V:  $2 \times 220 \text{ Ah} \times 12\text{V} = 5,28 \text{ kWh}$
- 12V:  $1 \times 55 \text{ Ah} \times 12\text{V} = 0,66 \text{ kWh}$

#### 2.4.2.2 Generation analysis

The starting point for the energy production analysis is the available surface on top of the trailer, free of obstacles. According to data provided by PRIMAFRIO, a maximum surface of 13,6 m × 2,6 m could be occupied with PV panels, though the usable surface is reduced to 13 m × 2,5 m, 32,5 m<sup>2</sup>. Two different module providers have been considered for this application, lightweight Solbian (Sun Power back contact c-Si cells), DAS ENERGY (monocrystalline 5BB solar cells, ETFE front sheet), additionally, TECNALIA's SOLARFACE® encapsulation technology (with c-Si cells) and standard 72-cells glass-based crystalline silicon technology to complete the benchmarking.



Table 2.4-1 PV module technologies parameters

<u>PV module</u>	<u>Solbian</u> <u>(back-</u> <u>contact c-Si)</u>	<u>DAS Energy</u> <u>(mono c-Si)</u>	<u>Solarface®</u>	<u>c-Si (20%)</u> <u>front</u> <u>glass</u>
Efficiency (%)	17,17	17,45	16,5	20,0
Wp/module (Wp)	104	350	330	400
Lenght (mm)	1 109	2 024	2 000	2 000
Width (mm)	546	991	1 000	1 000
Weight/panel (kg)	1,4	6,02	6,4	25
No. modules	44	12	12	12
Total peak power (Wp)	4 576	4 200	3 960	4 800

The highest peak power is achieved with c-Si, totalling 4,8 kWp, 25 kg/panel, meaning 300 kg extra on the roof (without considering DC-DC converter weight). With lighter solutions, offering less than 4 mm thickness, e.g. SOLARFACE® (fibre glass reinforced composite encapsulation material for PV cells, TECNALIA’s in-house technology), the installed power is reduced to 3,96 kWp and around 75 kg (3,2 kg/m<sup>2</sup>); DAS Energy, SOLBIAN, around 4,5 kWp, and 60-70 kg.

The company offers transport services starting from Spain / Portugal with destination Europe. The route selected for the analysis starts in Murcia, and arrives at La Junquera, a 10-hour trip that can be made 100% in daylight. With 0° inclination, the PV panels will produce an average daily production of 3,62 kWh/kWp/day along the Mediterranean coast, including the energy losses (PR=0,72), which means 14-17 kWh/day (average annual value), with peak values of approx. 26 kWh/day in July. No shade losses have been considered as the truck and trailers travel almost 100% of the time on the road.

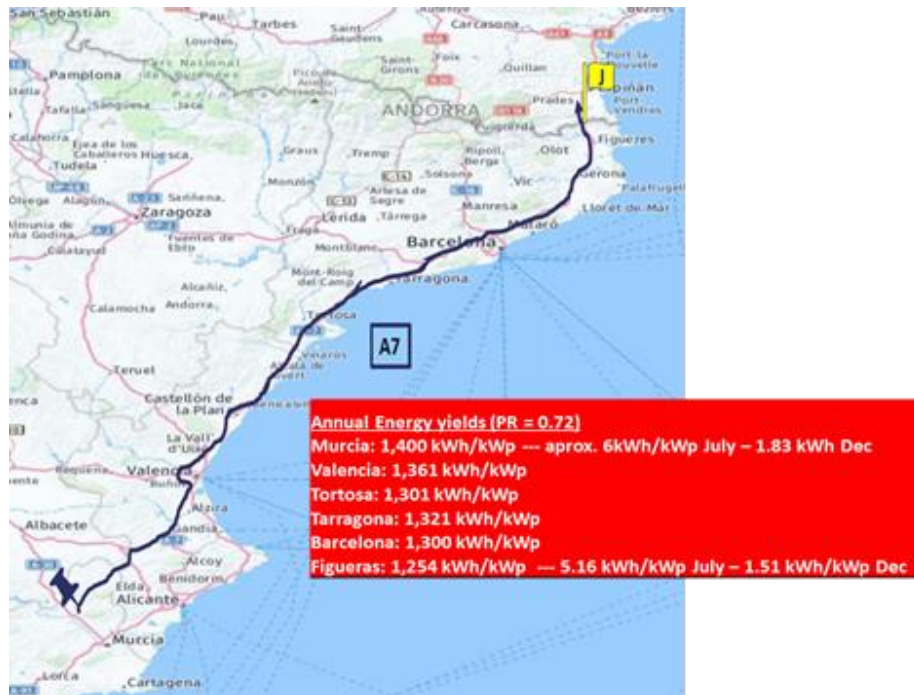


Fig. 2.4-2 Route for analysis, from Murcia to La Junquera, 10-hour trip



Table 2.4-2 Energy production for each PV technology

		Solbian	DAS Energy	Solarface	cSi
Total daily production (kWh/day)	Maximum	25,2	23,1	26,4	21,8
	Minimum	7,6	6,9	7,9	6,5
	Average	16,6	15,2	17,4	14,4

### 2.4.2.3 Economic feasibility assessment

The CAPEX for the analysed PV solutions ranges from 3 500 EUR for the glass-based c-Si to almost 7 000 EUR for certain lightweight solutions, including DC-DC converters and installation works (mounting and dismounting of supporting structure included).

OPEX is not considered, as the cleaning of PV modules (top part of trailers) is already included within the activities usually carried out by PRIMAFRIO. The costs for diesel considered for this analysis are: 0,75 EUR/litre of diesel A (used for motion) and 0,45 EUR/litre of diesel B (used for industrial or agricultural activities, here used for cooling). Every kWh provided by PV systems and self-consumed by each truck involves a saving of 0,833 EUR/kWh if used for motion and 0,152 EUR/kWh if used for refrigeration.

On the other hand, in case the company cannot deliver full load due to the weight of the PV system, it will lose incomes due to non-transported goods. The PV system's weight also has an impact on the fuel consumption of the truck, being both the most important factors related to the weight of PV panels. Other factors such as the loss of aerodynamics are discarded in this study.

It is assumed that out of the overall kWh generated during a day by the PV system, 100% are self-consumed in refrigeration: 81,1% in a direct way, without using batteries (mode ON reefer) and 19,9% stored in batteries (assuming energy losses close to 20% in the charging / discharging process).

The annual incomes (savings in diesel) will account for 1 165-1 412 EUR, depending on the PV solution. The annual losses (missing incomes due to goods not transported): 520-1 480 EUR. This leads to a minimum simplified payback time of 9,28 years (SOLBIAN), thus, not representing a successful business case for PRIMAFRIO. However, there are multiple variables and restrictions, whose modification could make this payback time more attractive.

### 2.4.2.4 Sensitivity analysis and discussion

By modifying the most important parameters that affect the PBT, the individual effect on this value can be analysed, providing useful information that will help PRIMAFRIO to make the decision of being committed to PV in trailers as a cost-effective green measure to reduce their diesel consumption. Next, some of the cases analysed are described. Some of them make PV systems profitable for PRIMAFRIO's business, given the imposed conditions:

- % time that refrigeration works in a fixed mode. By default, 70%. In case 100% is considered, the PBT is reduced to 8,75 years payback. This improvement can be easily explained given that in a fixed refrigeration mode, the compressor is working 100% of the time (time ON), thus improving the self-consumption ratio for the electricity generated by the PV modules, making the use of batteries almost residual.
- If diesel for refrigeration is the one used for driving (diesel EURO VI), the PBT is automatically reduced to 4,43 years. This is a situation that will come in the very near future due to environmental restrictions. Again, this conclusion is much-anticipated, since the benefits for the transport company are derived from the reduction of diesel consumption. If the diesel consumption avoided is almost twice more expensive (0,75 Vs 0,45 EUR/l), then the PBT is deeply reduced. This effect can be seen in Fig. 2.4-3 for a 100 % of time at full-load.



- % of time that the trailer is fully loaded, reaching its Maximum Authorised Weight (MAW). By default, PRIMAFRIO's trucks deliver always their maximum payload, so if additional weight is placed on top of the trailer, that means less goods transported and thus, less revenues for the transport company. With just 75% of the time at its MAW, the PBT is improved up to 8,15 years and with 50%, 7,27 years PBT. See Fig. 2.4-3 for more details on the evolution; on the left side with diesel costs for refrigeration at 0,45 EUR/litre and on the right, at 0,75 EUR/litre. In both cases, the evolution is clearly dependant on the % of time at full load, with minimum values leading to PBT below four years if the trucks never travel at full payload.
- Lost freight charges. For a value of lost freight charges set at 1 000 EUR/ton and year, the PBT is reduced significantly to 3,84 years, resulting in a key factor. See Fig. 2.4-4 for more details on the evolution, by considering annual freight values in the range of 1 000 - 4 000 EUR.
- In the present analysis, ICE trucks have been considered, the great majority of PRIMAFRIO trucks. In case of hybrid trucks, the electricity provided by the PV system could be used to fill the EV battery, contributing to the truck driving. In the case under analysis, 100% of the energy produced by the PV system is used to feed the refrigeration, but, if this electricity is entirely used for motion in hybrid electric trucks (100% for motion, 0% for cooling), a PBT of 0,66 years is achieved. More details on the dependence of the PBT with the use of PV electricity can be found in Fig. 2.4-5. 100% means that all the PV electricity is used for refrigeration; 50% means that half of the electricity goes for refrigeration, and half for the truck's motion. In the following figure, the PRIMAFRIO SMARTRUCK is presented, as an evolution of the actual ICE model (see Fig. 2.4-6).

The sensitivity analysis could be completed by considering the variation of different parameters at the same time, leading to more complex results and conclusions, and out of the scope of the present study. Just as an example, if the same diesel is used both for motion and refrigeration (0,75 EUR/l), considering that 75% of time the trucks travel in full load, the best PBT is reduced to 3,62 years.

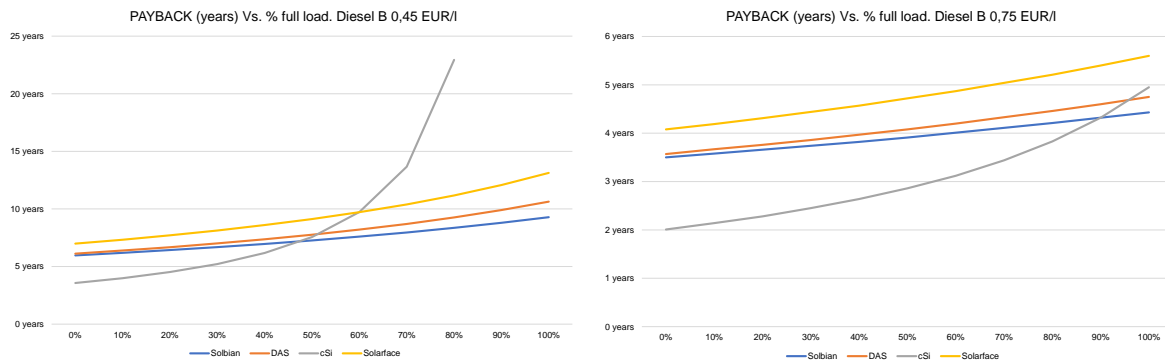


**Fig. 2.4-3 PBT Vs % time that the trucks go fully loaded for different diesel prices (0% never full, 100% always full): Left 0,45 EUR/l, Right: 0,75 EUR/l**

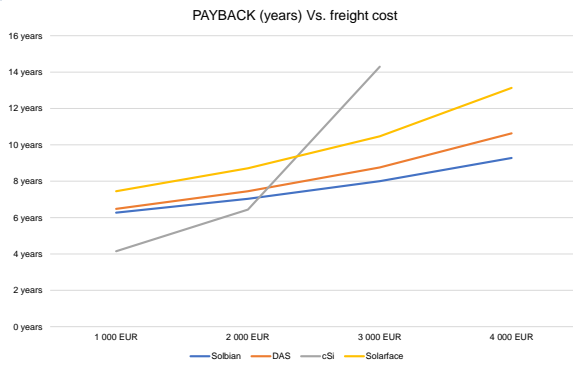


Fig. 2.4-4 PBT Vs freight cost of delivering 1 000 kg of goods per year

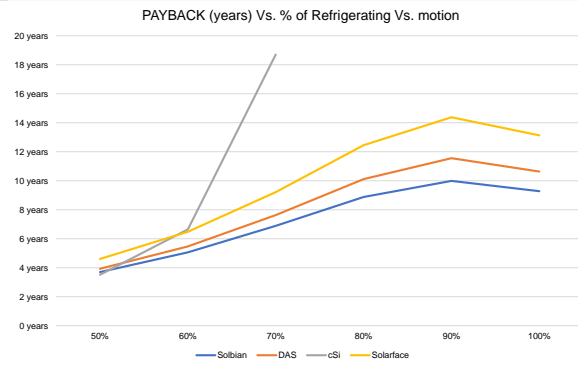


Fig. 2.4-5 PBT Vs % PV production that feed the refrigerating Vs motion (100% means all the electricity feed the refrigeration)



Fig. 2.4-6 Truck of the Future: PRIMAFRIO SMARTRUCK, hybrid model

### 2.4.3 General concepts for PV in the road transport

By analysing the existing options for the road transport of passengers and goods, and focusing on heavy duty vehicles, two main alternatives can be found: trucks for goods and buses for travellers. The needs, requirements and specific conditions derived from each vehicle’s usage make the integration of PV different from one case to another. In Fig. 2.4-7, a tree diagram represents a simple classification of heavy-duty vehicles and describes key features for each category, addressing the implications for the integration of PV systems.

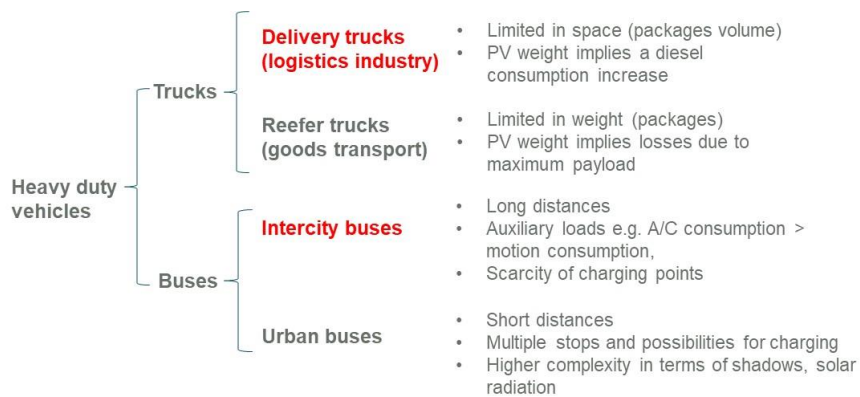


Fig. 2.4-7 Classification of heavy-duty vehicles and main features that affect the integration of PV systems



As can be observed, trucks for the logistics industry fit better for the integration of PV, given that the most frequent limitation for these vehicles comes from the space that goods delivered occupies (usually packages and boxes) and not from the weight of these packages, which makes the PV system's weight represent much less of an impact on the incomes losses, and thus, getting a much better PBT for the investment in the PV systems. In the case of buses and coaches, long-distance lines or occasional use buses make the best business case. In some of these coaches, and depending on weather conditions, season of the year, etc. the auxiliary load, especially the air conditioning, represents even more consumption than the bus motion for hybrid models. This would make a perfect use of the electricity provided by PV systems, instantaneously. On the contrary, urban buses suffer from more difficult conditions for the PV systems, e.g. continuous shading, vibrations and reducing the availability of PV electricity on-board.

Despite easier integration than in passenger vehicles, PV in trucks / buses still show challenges to overcome, most of them shared with lighter and smaller vehicles:

- Incorporation of new and high efficiency cell technologies and encapsulation materials
- PV in movement → quick changes in the I-V curve, which implies the need of ultra-fast MPPT algorithms
- Shades on the EV → mismatching in I-V curves, need of specific lay-out for the interconnection of cells, ad-hoc DC-DC converters.
- Repair in case of small impacts, scratches, damages
- Recycling of components
- Cleaning of bodywork, sometimes with abrasive products

All in all, the business case for each vehicle is a case by case exercise; there are no general rules, and the PBT can be as low as 1 year or as high as > 50 years, depending on application, country, size of transport, routes, weights, diesel prices, etc. Nevertheless, the conclusion is doubtlessly positive, and PV systems in trucks or buses could be useful and not just for auxiliary consumptions, offering also additional benefits for the brand/company linked to sustainability and green image.

## [References]

- [1] Energy sources and multi-input DC-DC converters used in hybrid electric vehicle applications e A review. international journal of hydrogen energy 43 (2018) 17387 e1 7408
- [2] Richardson DB. Electric vehicles and the electric grid: a review of modelling approaches, impacts, and renewable energy integration. Renew Sustain Energy Rev 2013;19:247e54.
- [3] Putting solar in the driver's seat. Solar Mobility report. SPE Solar mobility Task force, Nov. 2019.



## 2.5 Case study on PV-powered truck trailers in the Netherlands: PV electricity production on trailers

IM Efficiency from the Netherlands [1] will commercialise the so-called ‘SolarOnTop’ system for use in semi-trailers of trucks. The SolarOnTop system contains three main elements: thin film solar PV Panels of about 30 m<sup>2</sup> which are integrated on top of a semi-trailer, a battery pack and a sophisticated energy control unit. Product development started in 2016, which resulted in early prototypes. By the end of 2020, the final product tests and approvals were completed. Since 2021, commercial sales take place in the Benelux. Simulations have shown that using a SolarOnTop system on certain routes can decrease diesel consumption with more than 5% and prevent CO<sub>2</sub> emissions of 6 000 kg per year per truck-trailer combination.



Fig. 2.5-1 PV truck trailers (Photo: IM Efficiency)

PV electricity produced by the SolarOnTop can typically be used at three main moments during a road trip by a truck:

- During driving, the solar energy is supplied to the truck to power its auxiliaries. At those times, the alternator doesn't exert a load on the engine, thereby reducing fuel consumption of the vehicle.
- During resting-time of the driver, the SolarOnTop can supply clean electricity to the truck to power electrical appliances for the driver's comfort, such as cooling, heating, a fridge, a TV, etc. Thanks to the power supply of the SolarOnTop, there is no need for the driver to idle the truck's diesel engine for electricity generation. In this manner, noise and unhealthy emissions on the parking spot will be avoided.
- In case of electrical equipment in the semi-trailer (e.g. tailgates or other), the SolarOnTop system charges this semi-trailer's batteries both during a trip and stationary moments. By acting like a mobile charger, the SolarOnTop system guarantees that the driver can utilize electrical equipment at all times, therefore it improves the operational reliability of the vehicle.

In 2019/2020, a study has been executed in collaboration with University of Twente to simulate the effectiveness of solar PV panels attached to the sides of the semi-trailer, in addition to those on top of the semi-trailer. The assumed sizes of the PV modules were just like those on top and 30 m<sup>2</sup> on each side of the trailer. In this simulation study, four different routes have been evaluated, which were driven every day of the week. The directions of the evaluated patterns were similar (starting northwest and after 50 km going north), but the departure cities have different latitudes; they were Stockholm, Utrecht, Budapest and Madrid. Above, a scheme of the model and a characteristic route in Sweden are shown.

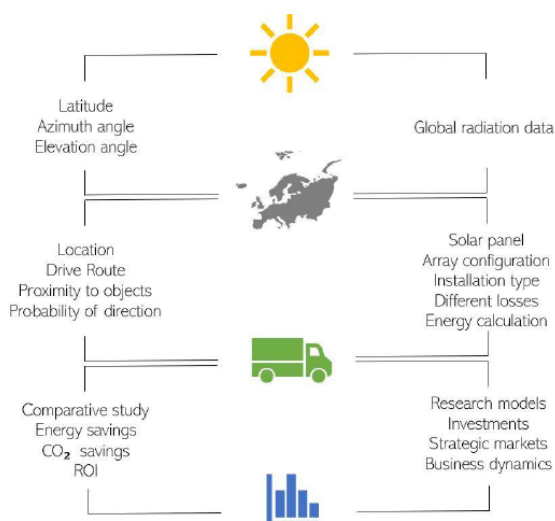




Fig. 2.5-2 Approach for the simulation study

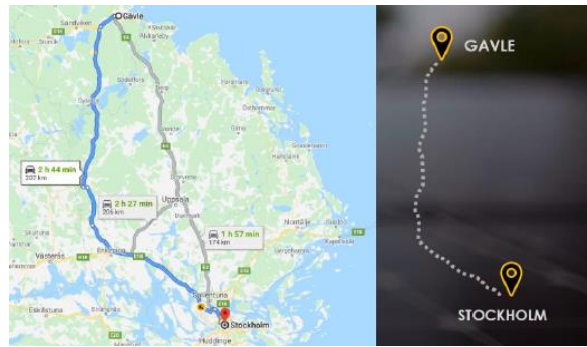


Fig. 2.5-3 Example of driving route in Sweden

Fig. 2.5-4 shows some preliminary results of the energy production study where the vertical installation represents two vertically oriented PV panels attached to the sides of a semi-trailer, and the horizontal installation just one horizontally oriented PV panel with similar size as one of the two vertically oriented PV panels.

- In general, two vertically oriented PV panels attached to the sides of a semi-trailer results in as much energy per year as a horizontally aligned PV module of the same size on top.
- However, detailed daily graphs show that during seasons or moments with a reduced elevation of the sun such as – in the Northern Hemisphere – fall and winter, vertically oriented PV panels will have a higher yield depending on the location, date, time.
- In Spain, due to the high elevation angle of the sun the whole year through, the horizontally oriented solar PV panel outperforms the two vertical ones.
- The general conclusion could be drawn that the higher the latitude, the more suitable vertically oriented PV panels will be for solar power production by semi-trailers.

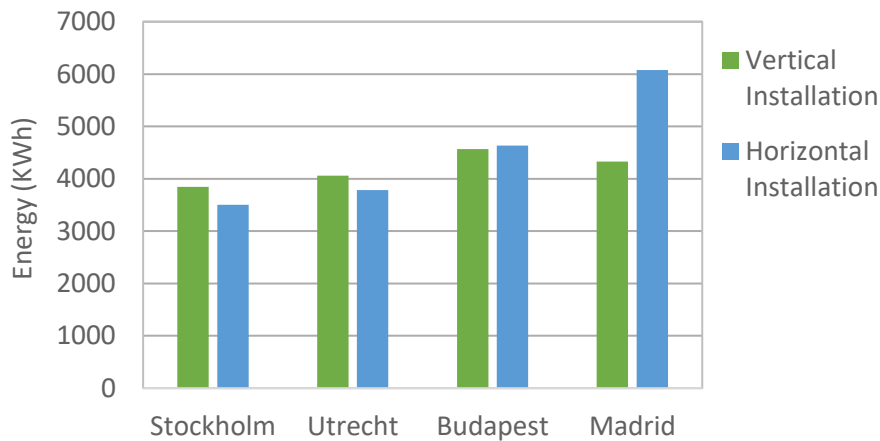
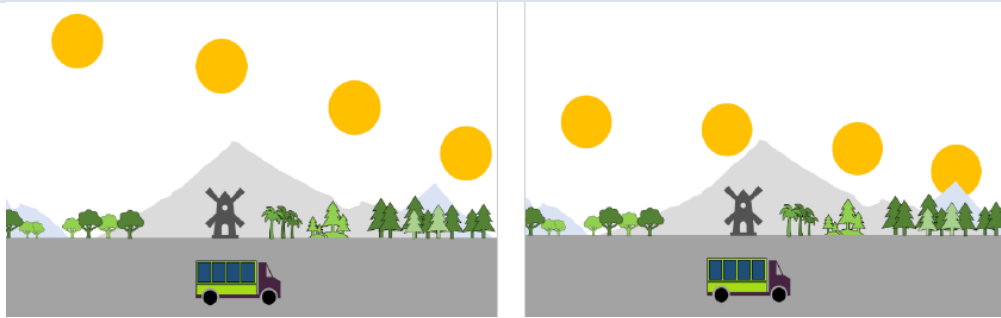


Fig. 2.5-4 Preliminary results of annual PV electricity production in some cities in Europe

The effect of surroundings on the performance of both horizontally and vertically oriented PV panels on trailers is illustrated in Fig. 2.5-5, where on the left, the elevation angle of the sun is high and at the right, it is low. Depending on objects in the surroundings, the position of the sun and the drive speed, the trailers' surfaces will be subjected to alternating shades which will be a challenge.



**Fig. 2.5-5 Effect of surroundings on the performance of PV panels on trailers**  
(left: high elevation angle, right: low elevation angle)

Given the promising results shown above and also given some challenges in relation to surrounding objects along routes, in the coming period IM Efficiency will further study possibilities, technical solutions and business cases for vertical solar panels on the sides of the trailer. Preliminary studies have indicated that the effectiveness of vertical solar panels on trailers, is about 50% of that of horizontal panels. Obviously this is highly dependent on the latitude, the route the truck-trailer drives, the locations the truck visits, the surroundings on those locations, the changeability of the weather and the date/time. Therefore, it will be essential to develop tools and methods to forecast the possible power and energy production during a journey ahead of the actual trip itself.

Further studies will possibly be executed together with other partners of the newly started ASOM.solar, the Association of Solar Mobility [2].

## [References]

- [1] IM Efficiency (<http://www.imefficiency.com>)
- [2] the Association of Solar Mobility (<http://www.ASOM.solar>)



## 2.6 Summary

PV-powered vehicles offer several benefits for users. In order to foresee the expected benefits, two case studies on PV-powered passenger vehicles and three case studies on PV-powered commercial vehicles and trucks were included in this chapter.

As these case studies use different approaches and assumptions, the results shown are summarised as below.

### Case studies on PV-powered passenger vehicles

Detailed case studies of PV-powered passenger vehicles used in Japan and the Netherlands have identified and quantified benefits for on-board PV in terms of reduced lifetime CO<sub>2</sub> emissions, lower operating costs, and decreased dependence on the grid. For a wide range of vehicles, use cases, and locations suggest that 800 – 1000 W<sub>p</sub> of PV on a standard passenger car will provide benefits for most users as compared to electric vehicles without PV. These benefits can be increased with both technology development and optimized driver behaviours.

The case study in Japan clarified that a PV-powered vehicle would produce environmental benefits, e.g. CO<sub>2</sub> reductions up to about 220 kg CO<sub>2</sub>-eq/year, compared to a conventional electric vehicle without PV, especially with longer driving distances, and that, however, 1 kW PV might be an excess capacity for shorter driving distances. In order to increase environmental benefits by PV-powered vehicles, it is necessary to increase the utilised PV electricity. In order to increase the utilised PV electricity, the optimised design of a PV-powered vehicle, such as its PV capacity while considering effective solar irradiation and vehicle efficiency, capacity and efficiency of a vehicle's battery and its operating condition will be required. It was also clarified that a PV-powered vehicle will decrease charging frequency and that in case of a shorter driving distance, the PV-powered vehicle will be free from electricity charging. This benefit will make the vehicle more attractive, even if the expected environmental benefits will be slight.

The case study in the Netherlands showed that even with a relatively low total irradiation, PV-powered vehicles can make a significant impact on electric vehicles in the Netherlands. As PV and EVs become more efficient the impact will increase. It is also shown that driver behaviour, in the form of charging strategies and driving profiles, can have a measurable effect on the benefits of PV-powered vehicles. Up to 60% reduction in charging frequency can increase autonomy and a feeling of security for the EV driver. While CO<sub>2</sub> emission reduction will depend on the carbon intensity of the local grid, current values in the Netherlands mean that there can be an effective CO<sub>2</sub> reduction of about 200 kg CO<sub>2</sub>-eq/year. Finally cost savings are shown up to 164 EUR/year based on household electricity prices, and are likely to be higher in practice as commercial EV charging rates are currently more expensive. It is noted that in order to have the most impact on cost savings and CO<sub>2</sub> emissions, the energy generated by the PV should be maximally utilized.

Based on these case studies, expected benefits of PV-powered passenger vehicles in IEA PVPS Task17 countries are estimated and included in Chapter 4.1. Additionally, the relationship between such expected benefits and utilisation ratio of PV electricity is further discussed.

### Case studies on PV-powered commercial vehicles and trucks

A second important use case is the deployment of on-board PV on electric commercial vehicles and trucks (diesel).

A Case study in Germany focused on PV-powered light commercial electric vehicles. Based on the solar irradiance measurements on specific test routes, it was found that this side-to-roof ratio is about 40% on average. Also, it was estimated a total energy yield for the modules mounted on the roof and side (2 180 W<sub>p</sub> in total) to be from 1 170 kWh/a (Hamburg, Germany) to 2 210 kWh/a (Rome, Italy). In parallel, a life cycle assessment (LCA) of PV components, assuming production in China and integration in Germany, found that PV-powered vehicles can improve the carbon footprint for the case of an average shading factor of 30% and eight years of operation time. The emission factor of on-board generated PV electricity is to be 0,357 kg CO<sub>2</sub>-eq/kWh, and the average grid emissions for the operation time are expected to be 0,435 kg CO<sub>2</sub>-eq/kWh. The lower shading factor and the longer operation time result in greater environmental benefits.



A case study in Spain discussed the economic feasibility of PV-powered reefer trucks; PV integration on the roof of a refrigerated trailer. Fuel consumption in diesel engine trucks varies by a load, and costs for diesel differ according to the use such as driving and refrigeration. The economic feasibility of on-board PV depends on how to PV electricity is used, and how to substitute fuel and freight load, in addition to the cost and performance of PV. As an example, if the same diesel is used both for motion and refrigeration (0,75 EUR/l), considering that 75% of time the trucks travel in full load, the best cost payback time is estimated to be 3,62 years, very reasonable from the investment point of view. Based on the understandings, preliminary concepts for PV-powered heavy duty vehicles, especially trucks were indicated.

A case study on PV-powered truck trailers in the Netherlands estimated PV electricity production on the tops and sides of semi-trailers. The considered system is composed of vertically oriented PV panels attached to the sides of a semi-trailer, and one horizontally oriented PV panel with similar size as one of the two vertically oriented PV panels. The preliminary studies indicated that the effectivity of vertical solar panels on trailers, is about 50% of that of horizontal panels. This is highly dependent on the latitude, the route the truck-trailer drives, the locations the truck visits, the surroundings on those locations, the changeability of the weather and the date/time. It will be essential to develop tools and methods to forecast the possible power and energy production during a journey ahead of the actual trip itself.

These case studies have given a clear potential and substance of depth study regarding PV-powered trucks and trailers that have integrated PV systems. Taking into account the possible use of PV electricity for auxiliary demand, PV integration in trucks and trailers may be closer to realisation and coming into the market. Further research seems to be needed, especially in view of promoting more sustainable transport.



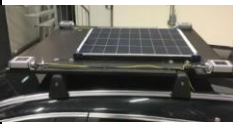
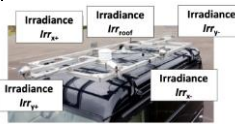
### 3. VEHICLE SOLAR IRRADIANCE MEASUREMENTS

In order to promote development and adoption of PV-powered vehicles, it is also necessary to understand the effects of the dynamic environment of the vehicle for optimal design of on-board PV energy generation systems. The amount of PV electricity generated on-board depends on factors such as available solar irradiance and temperature. The solar irradiance falling on a PV-powered vehicle depends on the specific location and direction during parking and driving. Additionally, the solar irradiance during use is always changing; due to the surrounding environment of the route, such as whether buildings, structures or foliage are shading or even reflecting light on the vehicle. In response to this situation, several different methodologies have been developed for measuring the real irradiance falling on vehicles.

Table 3-1 shows measurement methods of TNO in the Netherlands, ISFH in Germany, University of Miyazaki in Japan, Bern University of Applied Sciences in Switzerland and UNSW in Australia. As shown in Chapter 2.2, TNO in the Netherlands have developed a four-point horizontal irradiance measurement that can capture dynamic shading events as shades quickly sweep across the vehicle while it is in motion. In Germany, ISFH has made fast, sub-microsecond irradiance measurements to evaluate the stability of maximum power point tracking algorithms during rapidly changing irradiance conditions experienced when in motion, as shown in Chapter 2.3. Besides, in Japan, preliminary measurements in Sapporo and Miyazaki were conducted by NEDO and continuously, the University of Miyazaki has made precise irradiance measurements on five planes, one horizontal and four vertical while the vehicle is in motion. This has enabled the irradiance available to different surfaces of the vehicle to be evaluated precisely for a couple of occasions. In Switzerland, Bern University of Applied Sciences has measured solar irradiance in five directions with five reference cells directly attached to the vehicle’s body. Furthermore, in Australia, the UNSW has developed a low-cost solar irradiance data logger that has been developed to crowdsource data from passenger vehicles capturing real-world conditions experienced while driving and parking habits.

Although, there has not yet been enough data collected to make generalisations on the characteristics of the solar irradiance experienced by a vehicle, this chapter overviews these approaches and some data measured.

**Table 3-1 Solar irradiance measurement of TNO in the Netherlands, ISFH in Germany, University of Miyazaki in Japan, Bern University of Applied Sciences in Switzerland and UNSW in Australia**

TNO, Netherlands	ISFH, Germany	Univ. of Miyazaki, Japan	Bern University of Applied Sciences, Switzerland	UNSW, Australia
Four horizontal pyranometers and PV module on roof rack	10 kHz irradiance measurements	Five direction pyranometers on roof rack	Five reference cells on two types of vehicles	Low-cost, autonomous irradiance sensor installed on a large number of vehicles
	<p>Pyranometer SP Lite 2 from Kipp&amp;Zonen with readout time &lt; 500ns</p> 			
High fidelity irradiance measurements on horizontal plane. Partial and dynamic shading quantified	High fidelity irradiance measurements with high temporal accuracy	High fidelity irradiance measurements in all directions.	High fidelity irradiance measurements in all directions.	Crowdsourced irradiance and driving data under ‘real-world’ conditions, including parking behaviour



### 3.1 Solar irradiance measurements in the Netherlands and Germany

Solar irradiance measurements in the Netherlands and Germany were described in Chapter 2.2 and Chapter 2.3, respectively. In this section, these approaches are summarised briefly.

#### 3.1.1 Solar irradiance measurements in the Netherlands

In the Netherlands, a Vehicle Irradiance Test Setup (VITS) has been built by TNO, which collects GPS and temperature values at 1 Hz and irradiance on four locations on the vehicle’s roof at 100 Hz. The irradiance measurements have been validated by comparison with local weather station data and can be used to show the details of shading events. The collected data shows dynamic shading, driver profile and shading losses. The GPS data also allows precise analysis of shading events and where they occur.

Although a quantitative analysis was not made in Chapter 2.2, the data also enables the investigation of shading events, which can reduce the output of the on-board PV; both when the vehicle is parked in the shade for a long time, but also when dynamic shading occurs during a drive. Instances of both effects are shown in Figs. 3.1-1 and 3.1-2.

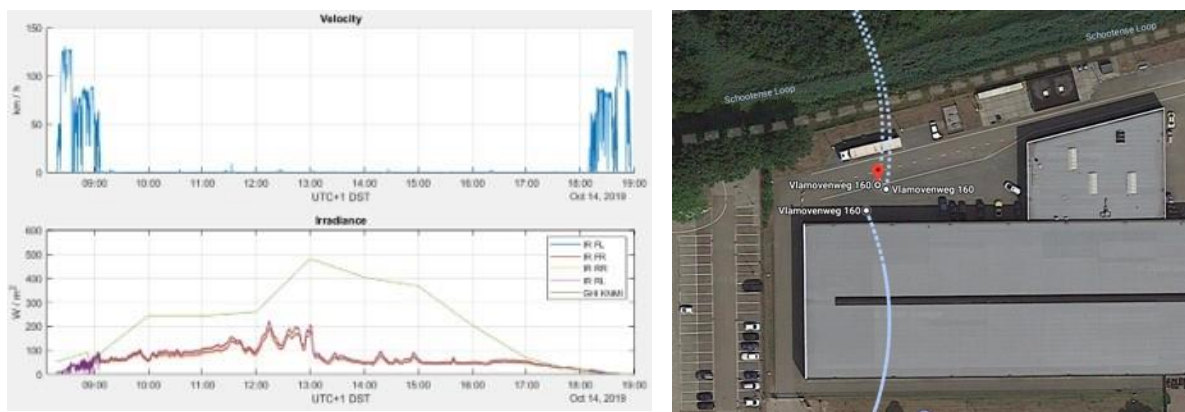


**Fig. 3.1-1** The irradiance trace (bottom left) shows that the sunlight measured on the vehicle is far below that measured by the weather station, further investigation of the GPS data confirms the vehicle was parked on the North side of a tall building. (see Fig. 2.2-9)

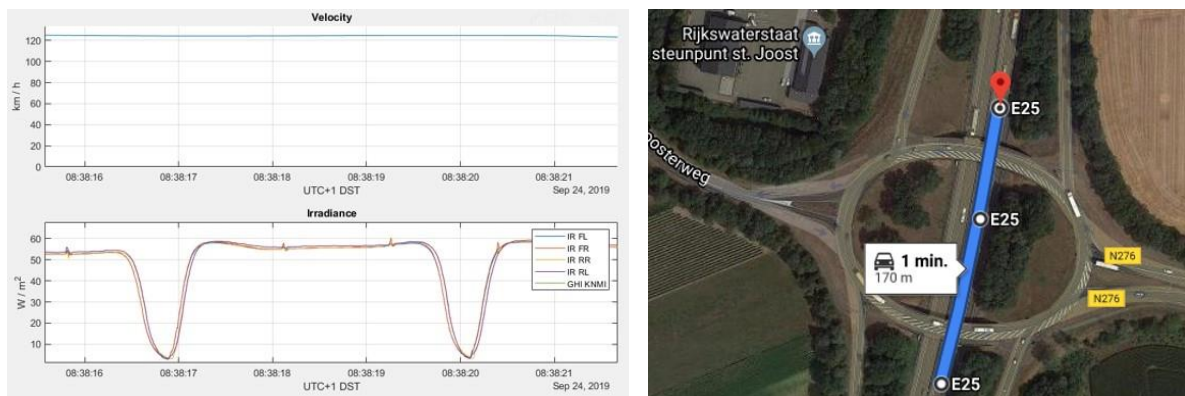


**Fig. 3.1-2** Results from monitoring showing dynamic shading as a vehicle travels beneath an overpass (The vehicle is travelling at 120 km/h, the two dips in the irradiance trace (bottom left) occur as the vehicle goes under the two overhead roads.) (see Fig. 2.2-10)



### 3.1.2 Solar irradiance measurements in Germany

In Germany, in order to assess time-averaged aspects such as the roof-to-side ratio of the irradiation, the solar irradiance on the roof and the side of a vehicle while driving was measured with very high time resolution. The used pyranometers are silicon based and have a spectral range of 400 nm to 1 100 nm and a response time lower than 500 ns. They are directed to the left, right and upwards with respect to the direction of driving. The pyranometer was measured using an oscilloscope with a 10 kHz sampling rate. GPS was used to track the location and speed with a sampling rate of 1/s.

The test route represents many different situations that can typically occur while driving in an urban environment with light commercial delivery vehicles. The route features sections with a high building density with narrow streets and low speed limit, as well as sections with medium wide streets such as alleys and wide streets with higher speed limit, such as city highways. The route was also chosen so there were about equally long sections in predominantly north-south (or south-north) direction as in predominantly east-west (or west-east) direction.

As shown in Fig. 3.1-3, it was found that a ratio of irradiance on the side of the vehicle relative to the irradiance on the roof was about 40% in average. However, it can vary from 26% to 93%, heavily depending on the solar altitude, the weather conditions and the type of the street. The significantly higher side-to-roof ratio in winter at sunny weather due to low solar altitude and little diffuse light is noteworthy.

The collected data provides not only information about the overall solar irradiance on the vehicle while driving, but the high sample rate also allows an analysis of the transient behavior of illumination. Fig. 3.1-4 exemplarily shows a 10-minute extract of the measured irradiance over time from 09/05/2019 (a sunny day).

While these irradiation measurements on specific test routes provide valuable insights aspects such as roof-to-side ratio and transient shading, they are not directly generalizable for longer periods, other routes and different locations. This generalization will be addressed under the German project.

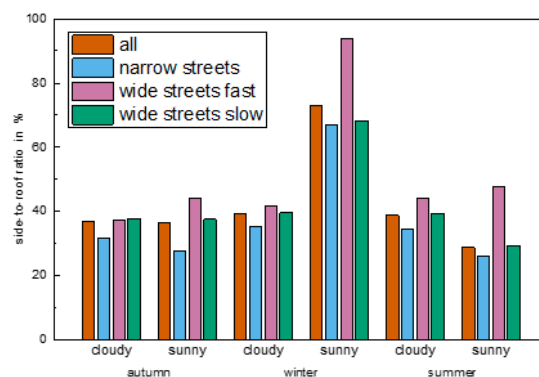


Fig. 3.1-3 Average irradiance on the side of the vehicle relative to the irradiance on the roof (see Fig. 2.3-3)

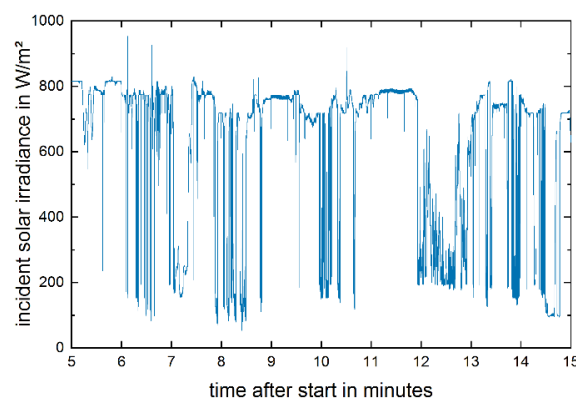


Fig. 3.1-4 A 10-minute extract of the measured irradiance on the roof of the vehicle over time from 09/05/2019, recorded between 13:00 and 14:00 UTC (see Fig. 2.3-4)



## 3.2 Solar irradiance measurements in Japan

### 3.2.1 A preliminary measurements of solar irradiance of PV-powered vehicles

#### 3.2.1.1 Method of measuring solar irradiance

As a preliminary study on a PV-powered vehicle's solar irradiance, the solar irradiance acquired by actual vehicles in motion was measured in Japan. The measurement was implemented at two locations, Sapporo City in Hokkaido (hereinafter, simply "Sapporo") and Miyazaki City in Miyazaki Prefecture (hereinafter, simply "Miyazaki"). These locations are positioned in the north and south of the Japanese archipelago that extends in the north-south direction.

Table 3.2-1 shows the method for measuring solar irradiance. Note that since this is a preliminary study that precedes a full-scale investigation, to make effective use of existing equipment, there were some differences in measurement methods and measurement conditions between the two locations.

Solar irradiance was measured at one position on the roof of a vehicle in Sapporo using three pyranometers that have different response speeds. In Miyazaki however, measurements were performed at a total of five positions which were the four sides of the vehicle, that is, the front, rear, right and left, in addition to the roof. The sampling interval of the measurement data was set at 0,1 seconds in Sapporo and at 1 second in Miyazaki. Measurement was conducted in the fall of 2018, and solar irradiance was measured three times a day (sometimes just once a day in Miyazaki) to investigate the influence of solar elevation.

To examine the influence of the environment, a measurement route including an urban section, a high-rise section, and an open-air section was chosen. The measurement route in Sapporo also included an underpass section.

**Table 3.2-1 Method of measuring solar irradiance of vehicles [1]**

Measurement Location	Sapporo City, Hokkaido (near N43°04', E141°21')	Miyazaki City, Miyazaki Prefecture (near N31°53', E131°25')
Insolation Measurement Positions	One (Horizontal irradiance on vehicle's roof)	Five (Horizontal irradiance on vehicle's roof and four upper side surfaces of vehicle: on front, rear, left, and right sides)
Pyranometer	- Secondary standard (x1) - Second class (x1) - Silicon type (x1)	- Second class (x5)
Sampling Interval	0,1 seconds	1 second
Measurement Period	Mid-September to late October, 2018	Mid-September to early October, 2018
Measurement Time of Day	First run: around 08:15 to around 09:15 Second run: around 11:15 to around 12:15 Third run: around 14:15 to around 15:15	First run: around 09:00 to around 10:00 Second run: around 11:30 to around 12:30 Third run: around 15:00 to around 16:00
Measurement Route	About 18km including the following: - Urban section - High-rise section - Open-air section - Underpass section	About 30km including the following: - Urban section - High-rise section - Open-air section
Insolation reference Point	Japan Meteorological Agency (JMA), Sapporo Regional Headquarters - Kita 2-Jo Nishi 18-Chome, Chuo-ku, Sapporo - near N43°3,6', E141°19,6' - Pyranometer type: secondary standard *Data produced as one-minute totals for every-second measurements (one-minute values of surface observation data produced by JMA)	University of Miyazaki (National University Corporation) - 1-1 Gakuen Kibanadai-nishi, Miyazaki - near N31°49', E131°24' - Pyranometer type: second class *Data produced as 10-second averages for data measured every second
Measured by	Japan Weather Association	University of Miyazaki



### 3.2.1.2 Measurement results in Sapporo

The measurement conditions used in Sapporo are shown in Table 3.2-2. In Sapporo, measurements were taken on five days between September 20, 2018 and October 22, 2018. Solar irradiance acquired by a vehicle is influenced by the shades of surrounding buildings and the like. Since it was assumed that this influence depends on solar elevation, measurements were taken three times a day at different time of day.

To identify the fall in solar irradiance due to shades and the like, comparisons were performed with the insolation at a reference point (JMA Sapporo Regional Headquarters). Since it was assumed that this fall would also be affected by irradiance components (whether direct solar irradiance or diffuse solar irradiance), measurement was performed on both fine and cloudy days.

**Table 3.2-2 Measurement dates and weather in Sapporo [1]**

Date of measurement	Route	Weather		
		First run (around 8:15 to around 9:15)	Second run (around 11:15 to around 12:15)	Third run (around 14:15 to around 15:15)
Sep. 20, 2018 (Thursday)	Clockwise	Sunny	Sunny	Clear
Sep. 25, 2018 (Tuesday)	Anticlockwise	Slightly cloudy	Slightly cloudy	Cloudy
Sep. 28, 2018 (Friday)	Clockwise	Sunny, partly cloudy	Cloudy, occasionally scattered showers	Cloudy, occasionally scattered showers
Oct. 19, 2018 (Friday)	Anticlockwise	Very clear	Clear	Clear
Oct. 22, 2018 (Monday)	Clockwise	Clear	Clear	Clear

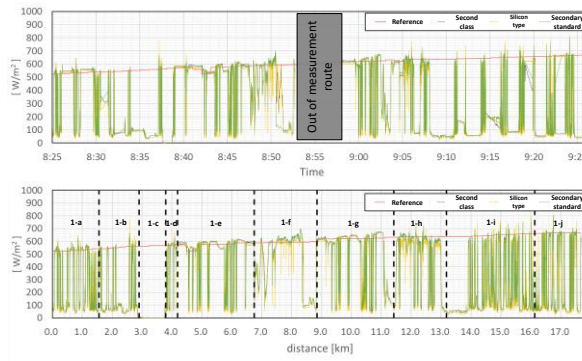
As examples of measurement results, Figs. 3.2-1 to 3.2-3 show the measurement results of the first to third runs on September 20, 2018 (Day 1).

In urban sections and high-rise sections, solar irradiance fell and fluctuated due to the shades of buildings and trees along the road, with this especially frequent in high-rise sections. Even in open-air sections, solar irradiance sometimes fell due to the shades of buildings, trees, and power poles along the road. Although the fall in solar irradiance due to the shades of buildings, trees, and the like may be smaller than the influence of clouds in terms of cumulative solar irradiance over a certain period, the variations in solar irradiance that occur on a vehicle's roof have a characteristic of occurring at extremely short cycles and with a large range of fluctuation. In urban sections and high-rise sections, solar irradiance sometimes exceeded the solar irradiance at the reference point, and it is thought that this could be due to an increase in acquired insolation caused by reflections from buildings.

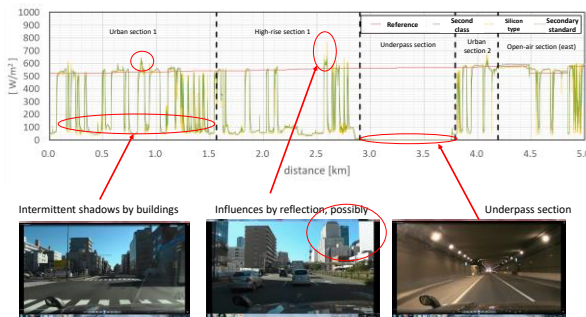
Looking at the characteristics according to time of day, shades from buildings, trees, power poles, and the like occur in urban sections, high-rise sections, and partly in open-air sections, causing a fall in solar irradiance. During the second run (when the sun is substantially due south), the solar elevation is high, which means that the frequency of falls in solar irradiance due to shades is low. The range of fluctuations in solar irradiance though is larger. During the first and third runs when the solar elevation is low, solar irradiance falls frequently due to shades, but when the sun is oriented close to the direction of the road (i.e., the direction of travel), shades that affect solar irradiance are produced less frequently.



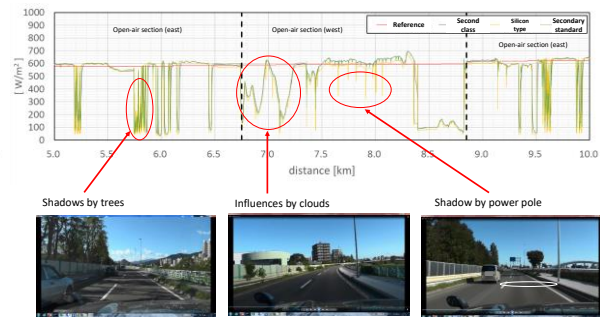
### Day 1 – First run



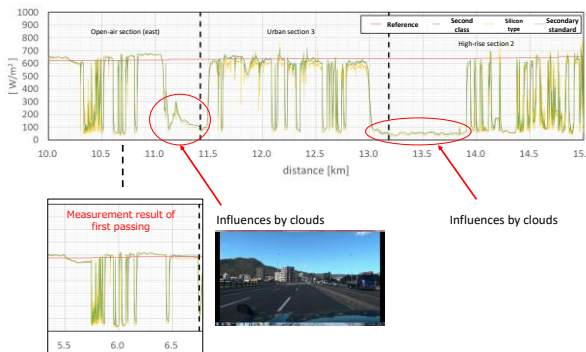
#### Day 1 – First run [0.0 to 5.0km]



#### Day 1 – First run [5.0 to 10.0km]



#### Day 1 – First run [10.0 to 15.0km]



#### Day 1 – First run [15.0 to 17.69km]

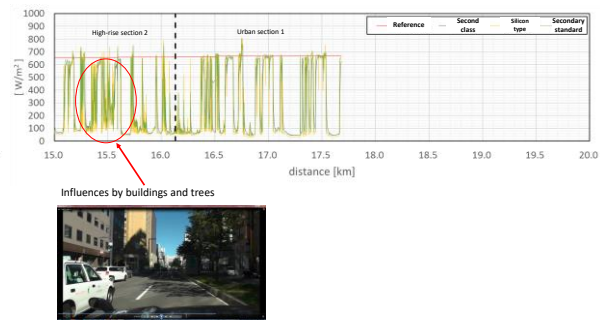
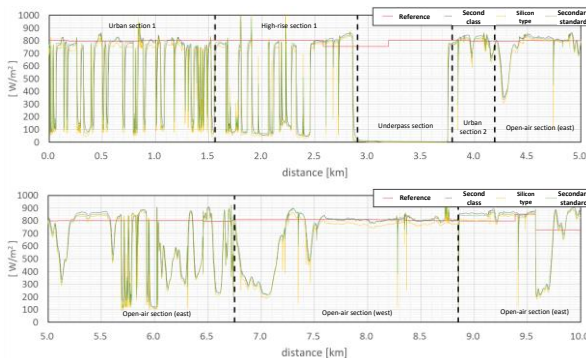


Fig. 3.2-1 September 20, 2018 (Day 1) in Sapporo: Measurement results for solar irradiance during the First run [1]

#### Day 1 – Second run [0.0 to 10.0km]



#### Day 1 – Second run [10.0~17.69km]

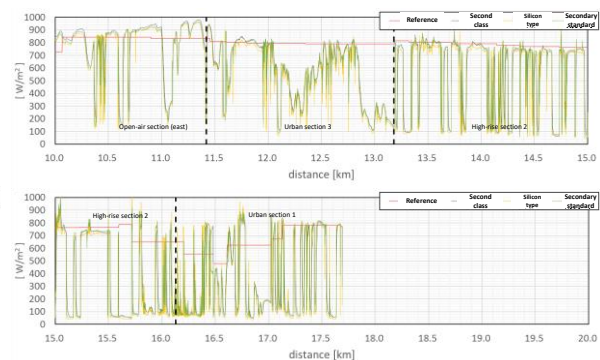


Fig. 3.2-2 September 20, 2018 (Day 1) in Sapporo: Measurement results for solar irradiance during the Second run [1]

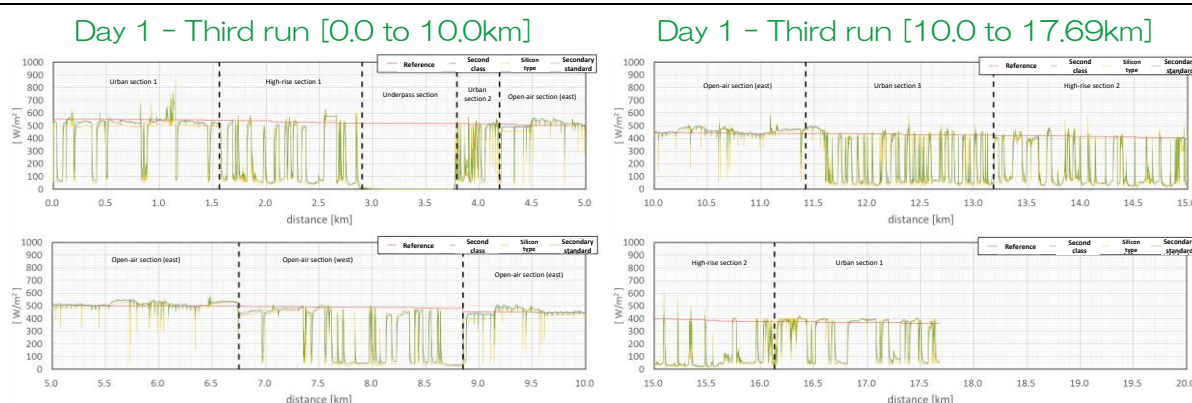


Fig. 3.2-3 September 20, 2018 (Day 1) in Sapporo: Measurement results for solar irradiance during the Third run [3]

Table 3.2-3 shows the ratio between total solar irradiance in every section (measured with a secondary standard pyranometer) and irradiance at the reference point for the measurement results on Day 1 to Day 5.

On fine days, there was a tendency for a ratio of around 50% on the first and third runs and 70% on the second run. On cloudy days, the ratio was over 70% irrespective of time of day. This is thought to be due to cloudy days having a low solar intensity and a low amount of direct solar irradiance that could be shaded by buildings or the like.

Table 3.2-3 Measurement results for solar irradiance in Sapporo (Comparison with reference: Summary) (Pyranometer: Secondary standard)[1]

			First run (around 8:15 to around 9:15)	Second run (around 11:15 to around 12:15)	Third run (around 14:15 to around 15:15)
Day 1	Sep 20, 2018	Weather	Sunny	Sunny	Clear
		Irradiance on vehicle's roof	308,0 Wh/m <sup>2</sup>	462,5 Wh/m <sup>2</sup>	264,6 Wh/m <sup>2</sup>
		Reference irradiance	564,2 Wh/m <sup>2</sup>	666,4 Wh/m <sup>2</sup>	462,2 Wh/m <sup>2</sup>
		Vehicle roof/reference	54,6%	69,4%	57,2%
Day 2	Sep 25, 2018	Weather	Slightly cloudy	Slightly cloudy	Cloudy
		Irradiance on vehicle's roof	323,1 Wh/m <sup>2</sup>	336,9 Wh/m <sup>2</sup>	143,2 Wh/m <sup>2</sup>
		Reference irradiance	444,5 Wh/m <sup>2</sup>	469,3 Wh/m <sup>2</sup>	196,8 Wh/m <sup>2</sup>
		Vehicle roof/reference	72,7%	71,8%	72,8%
Day 3	Sep 28, 2018	Weather	Sunny, partly cloudy	Cloudy, occasionally scattered showers	Cloudy, occasionally scattered showers
		Irradiance on vehicle's roof	410,6 Wh/m <sup>2</sup>	204,6 Wh/m <sup>2</sup>	120,4 Wh/m <sup>2</sup>
		Reference irradiance	546,8 Wh/m <sup>2</sup>	214,3 Wh/m <sup>2</sup>	222,3 Wh/m <sup>2</sup>
		Vehicle roof/reference	75,1%	95,5%	54,2%
Day 4	Oct 19, 2018	Weather	Clear	Clear	Clear
		Irradiance on vehicle's roof	231,5 Wh/m <sup>2</sup>	430,6 Wh/m <sup>2</sup>	121,1 Wh/m <sup>2</sup>
		Reference irradiance	451,3 Wh/m <sup>2</sup>	598,1 Wh/m <sup>2</sup>	270,3 Wh/m <sup>2</sup>
		Vehicle roof/reference	51,3%	72,0%	44,8%
Day 5	Oct 22, 2018	Weather	Sunny	Clear	Clear
		Irradiance on vehicle's roof	198,4 Wh/m <sup>2</sup>	317,3 Wh/m <sup>2</sup>	117,2 Wh/m <sup>2</sup>
		Reference irradiance	382,7 Wh/m <sup>2</sup>	528,0 Wh/m <sup>2</sup>	232,0 Wh/m <sup>2</sup>
		Vehicle roof/reference	51,8%	60,1%	50,5%



### 3.2.1.3 Measurement results in Miyazaki

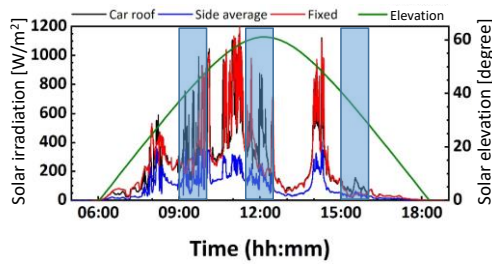
The measurement conditions in Miyazaki are shown in Table 3.2-4. In Miyazaki, measurements were taken on four days between September 13, 2018 and October 1, 2018. Solar irradiance acquired by a vehicle is influenced by the shades of surrounding buildings and the like. Since it was assumed that this influence depends on solar elevation, measurements were taken three times a day in different time of day on two out of the four days.

To identify the fall in solar irradiance due to shades and the like, comparisons were performed with the insolation at a reference point (the rooftop of a University of Miyazaki building). The insolation and solar elevation at the reference point on the date of measurement are shown in Fig. 3.2-4, as well as for the vehicle's roof and side surfaces (the average of four directions).

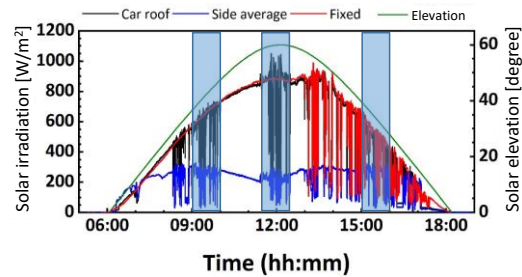
Table 3.2-4 Measurement dates in Miyazaki [1]

Date of Measurement	Route	First run (around 9:00 to 10:00)	Second run (around 11:30 to 12:30)	Third run (around 15:00 to 16:00)
Sep. 13, 2018 (Thu.)	Anticlockwise	√	√	√
Sep. 16, 2018 (Sun.)	Anticlockwise	√	√	√
Sep. 22, 2018 (Sat.)	Anticlockwise	-	√	-
Oct. 1, 2018 (Mon.)	Anticlockwise	-	√	-

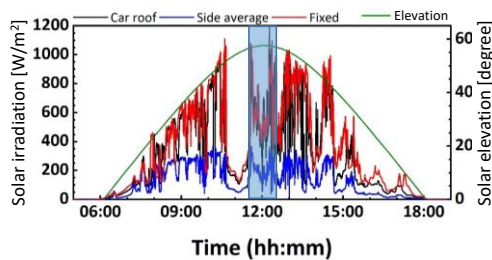
<Sep. 13, 2018>



<Sep. 16, 2018>



<Sep. 22, 2018>



<Oct. 1, 2018>

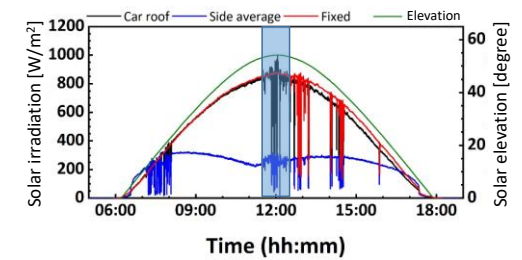


Fig. 3.2-4 Solar irradiance at University of Miyazaki (reference point) [1]

Table 3.2-5, Fig. 3.2-5 and Fig. 3.2-6 show the measurement results for solar irradiance on the vehicle's roof and vehicle's sides (the value for the sides is an average of four directions) in the urban section (residential area) on September 16, 2018 (Day 2). Although the measurement periods were short at two to four minutes, vehicle's roof solar irradiance relative to irradiance at the reference point was high at 92,0% in the morning (9:40-9:42) (First run) and 83,6% at midday (12:17-12:21) (Second run), which shows that there was little loss due to the shades of buildings, trees, and power poles along the road. On the other hand, the ratio was rather low at 62,5% during the afternoon (15:48-15:51) (Third run).

As shown in Fig. 3.2-5, there were large falls in solar irradiance for 30 to 40 seconds during 12:20 to 12:21 and 15:49 to 15:51, resulting in reduced ratios to the reference. Although this is thought to be caused by the shades of

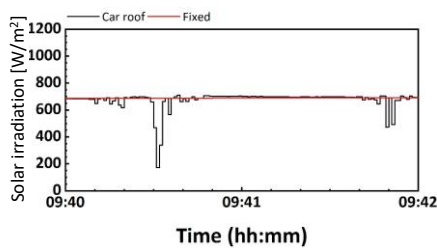


buildings, when the vehicle is stopped at an intersection or the like, the effect of shades will continue for several tens of seconds.

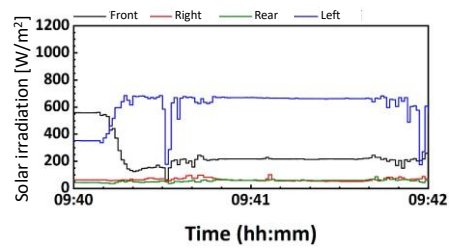
Fig. 3.2-6 shows measurement results of the solar irradiance on the sides of the vehicle. The timing at which the falls in solar irradiance were observed were the same as for the roof of the vehicle. When the vehicle is driving on a south-to-north road, insolation is high on the east side (mainly the left side of the vehicle) in the morning, the south side (mainly the front of the vehicle) at midday, and the west side (mainly the right side of the vehicle) in the afternoon, with a characteristic that solar irradiance is a similar level to the vehicle’s roof in the morning and afternoon. The average solar irradiance in the four directions was 35% of the vehicle’s roof in the morning, 25% at midday, and around 67% in the afternoon.

**Table 3.2-5 Measurement results for solar irradiance of vehicle roof in urban section on September 16, 2018 in Miyazaki [1]**

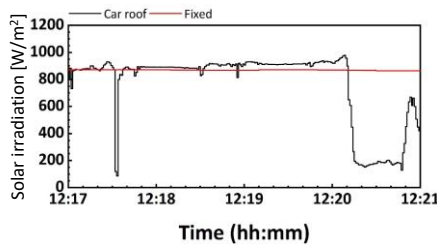
Measurement time of day	Vehicle’s roof irradiance (vehicle-roof)	Side irradiance (average of four sides)	Irradiance at reference (rooftop: fixed)	Ratio of vehicle’s roof irradiance to reference
9:40 – 9:42	23 Wh/m <sup>2</sup>	8 Wh/m <sup>2</sup>	25 Wh/m <sup>2</sup>	92,0%
12:17 – 12:21	51 Wh/m <sup>2</sup>	13 Wh/m <sup>2</sup>	61 Wh/m <sup>2</sup>	83, %
15:48 – 15:51	15 Wh/m <sup>2</sup>	10 Wh/m <sup>2</sup>	24 Wh/m <sup>2</sup>	62, %



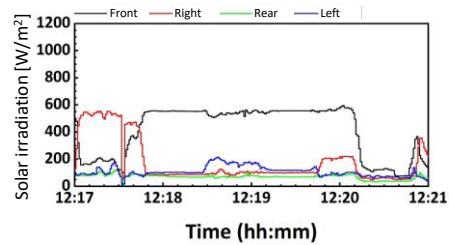
Time (hh:mm)



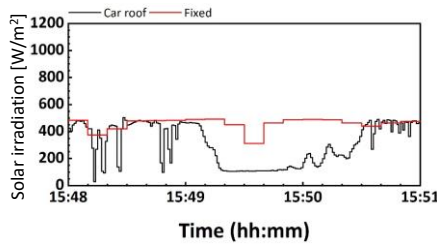
Time (hh:mm)



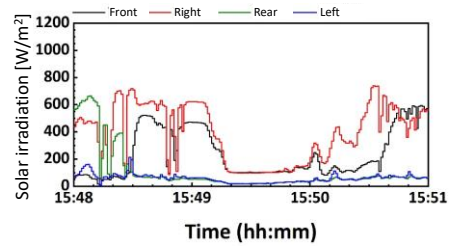
Time (hh:mm)



Time (hh:mm)



Time (hh:mm)



Time (hh:mm)

**Fig. 3.2-5 Measurement results for solar irradiance of vehicle’s roof in urban section on September 16, 2018 in Miyazaki [1]**

**Fig. 3.2-6 Measurement results for solar irradiance of vehicle’s roof in urban section on September 16, 2018 in Miyazaki [1]**

Tables 3.2-6 and 3.2-7 show the measurement results for the solar irradiance on the vehicle’s roof and sides (the value for the sides is the average in four directions) in the high-rise section and open-air section.

In the high-rise section (commercial buildings and downtown area), although the measurement periods were short at two to four minutes, vehicle’s roof insolation relative to insolation at the reference point was 73,9% in the morning



(9:22-9:24) (First run), 63,1% at midday (11:58-12:02) (Second run), and 58,8% in the afternoon (15:29-15:33) (Third run).

In the open-air section, the vehicle's roof solar irradiance relative to insolation at the reference point was extremely high at 95,2% in the morning (9:05-9:07) (First run) and 96,7% at midday (11:31-11:35) (Second run).

Table 3.2-8 shows solar irradiance on the vehicle's roof and side surfaces (the value for the side surfaces is an average of four directions) for all sections of travel and the ratios with the irradiance at a reference point. The values are cumulative solar irradiance for a route including an urban section, a high-rise section, and an open-air section.

The weather was fine on Day 2 (September 16, 2018), if a little cloudy in the afternoon. Day 1 (September 13, 2018) was very cloudy, with very little solar irradiance in the afternoon. Out of these two days, the ratio of the solar irradiance to irradiance at the reference point was 87,5% to 92,4% for the vehicle's roof on the second day, so only slightly lower than the reference point. On the first day, solar irradiance on the vehicle's roof exceeded the reference point. Regarding the solar irradiance on the side surfaces of the vehicle, the ratio was higher on the first day. Although there is the possibility that there were different cloud conditions between the reference point and the route of travel, the presence of less direct irradiance and more diffuse irradiance is also believed to be a factor. In addition, the ratio with the reference point was lower on the second run (at midday) compared to the morning and afternoon. It is presumed that the greater difference on the second day was due to a difference in solar elevation.

Regarding the measurement of solar irradiance at midday, it was cloudy on Days 1 and 3 but fine on Days 2 and 4. On Days 2 and 4, there were falls in solar irradiance (short period fluctuations) that would appear to be shades of buildings, trees, power poles, and the like along the road, but the ratio of solar irradiance on the vehicle's roof to the reference point was 87,5% and 92,0% on the two days, indicating that there was little loss due to shades. There were also times where the solar irradiance on the vehicle's roof exceeded the insolation at the reference point. There is the possibility that this was due to reflections from surrounding buildings and the like, but since the conditions may have differed between the reference point and the route of travel, it is not possible to make any definite judgment on this. The solar irradiance on the vehicle's sides was below 30% of the reference point on Days 2 and 4 when the weather was clear. There was also a tendency that when the ratio of the solar irradiance on the vehicle's roof to the irradiance at the reference point was low, the ratio for the vehicle's sides was also low.

**Table 3.2-6 Measurement results for solar irradiance of vehicle roof in high-rise section on September 16, 2018 in Miyazaki [1]**

Measurement time of day	Vehicle roof irradiance (vehicle-roof)	Side irradiance (average of four sides)	Irradiance at reference (rooftop: fixed)	Ratio of vehicle roof irradiance to reference
9:22 – 9:24	17 Wh/m <sup>2</sup>	7 Wh/m <sup>2</sup>	23 Wh/m <sup>2</sup>	73,9%
11:58 – 12:02	48 Wh/m <sup>2</sup>	13 Wh/m <sup>2</sup>	76 Wh/m <sup>2</sup>	63,1%
15:29 – 15:33	20 Wh/m <sup>2</sup>	11 Wh/m <sup>2</sup>	34 Wh/m <sup>2</sup>	58,8%

**Table 3.2-7 Measurement results for solar irradiance of vehicle roof in open-air section on September 16, 2018 in Miyazaki [1]**

Measurement time of day	Vehicle roof irradiance (vehicle-roof)	Side irradiance (average of four sides)	Irradiance at reference (rooftop: fixed)	Ratio of vehicle roof irradiance to reference
9:05 – 9:07	20 Wh/m <sup>2</sup>	10 Wh/m <sup>2</sup>	21 Wh/m <sup>2</sup>	95,2%
11:31 – 11:35	58 Wh/m <sup>2</sup>	16 Wh/m <sup>2</sup>	60 Wh/m <sup>2</sup>	96,7%
15:04 – 15:08	41 Wh/m <sup>2</sup>	20 Wh/m <sup>2</sup>	33 Wh/m <sup>2</sup>	124,2%



**Table 3.2-8 Measurement results for solar irradiance in Miyazaki (Comparison with reference: Summary)**  
[1]

			First run (around 9:00 to around 10:00)	Second run (around 11:30 to around 12:30)	Third run (around 15:00 to around 16:00)
Day 1	Sep. 13, 2018	Vehicle's roof solar irradiance	404 Wh/m <sup>2</sup>	393 Wh/m <sup>2</sup>	88 Wh/m <sup>2</sup>
		Vehicle's side surface solar irradiance	169 Wh/m <sup>2</sup>	146 Wh/m <sup>2</sup>	36 Wh/m <sup>2</sup>
		Irradiance at reference point	346 Wh/m <sup>2</sup>	329 Wh/m <sup>2</sup>	51 Wh/m <sup>2</sup>
		Vehicle roof/reference	114,3%	118,2%	180,0%
		Vehicle sides/reference	48,8%	44,4%	70,6%
Day 2	Sep. 16, 2018	Vehicle's roof solar irradiance	617 Wh/m <sup>2</sup>	775 Wh/m <sup>2</sup>	450 Wh/m <sup>2</sup>
		Vehicle's side surface solar irradiance	258 Wh/m <sup>2</sup>	205 Wh/m <sup>2</sup>	243 Wh/m <sup>2</sup>
		Irradiance at reference point	659 Wh/m <sup>2</sup>	879 Wh/m <sup>2</sup>	459 Wh/m <sup>2</sup>
		Vehicle roof/reference	92,4%	87,5%	91,8%
		Vehicle sides/reference	39,2%	23,3%	52,9%
Day 3	Sep. 22, 2018	Vehicle's roof solar irradiance		578 Wh/m <sup>2</sup>	
		Vehicle's side surface solar irradiance		203 Wh/m <sup>2</sup>	
		Irradiance at reference point	-	613 Wh/m <sup>2</sup>	-
		Vehicle roof/reference		95,1%	
		Vehicle sides/reference		33,1%	
Day 4	Oct. 1, 2018	Vehicle's roof solar irradiance		804 Wh/m <sup>2</sup>	
		Vehicle's side surface solar irradiance		248 Wh/m <sup>2</sup>	
		Irradiance at reference point	-	867 Wh/m <sup>2</sup>	-
		Vehicle roof/reference		92,0%	
		Vehicle sides/reference		28,6%	

#### 3.2.1.4 Characteristics of solar irradiance of vehicle

The solar irradiance on a vehicle's roof and on a vehicle's side surfaces has the following characteristics.

##### [Horizontal solar irradiance on vehicle's roof]

- Shades are caused by buildings, trees, power poles, and the like along the road, so that compared to the reference point, solar irradiance falls in corresponding locations and sections.
- Shades occur by buildings frequently in high-rise sections and intermittently in urban sections. Although infrequent, shades also occur in open-air sections.
- Due to shades from buildings and the like, fluctuations in insolation occur in extremely short cycles (several hundred W/m<sup>2</sup> in 0,1 seconds).
- Although the solar intensity has a similar level to the reference point in sections with no shades, there is a fall of around 50 to 100 W/m<sup>2</sup> in sections where shades occur, with the range of fluctuations in solar irradiance increasing as solar elevation increases.
- The fall in cumulative solar irradiance depends on the length of the period where shades occur. This was longest in the high-rise section and shortest in the open-air section, with the urban section in between.
- Although the buildings along the road may cast shades across the entire vehicle's roof, shades produced by trees and power poles do not cover the entire roof and correspond to partial shading.



- The occurrence of shades on the vehicle largely depends on the relationship between the direction of the road (the direction in which the vehicle travels) and the orientation of the sun, and when these almost match, the influence of shades is small, even in a high-rise section.
- The occurrence of shades on the vehicle caused by buildings along the road is thought to be influenced by road width and the lane in which the vehicle is traveling.
- In high-rise sections and urban sections, solar irradiance on the vehicle may exceed irradiance at the reference point. It is believed that solar irradiance may increase due to reflections from buildings along the road.

#### **[Insolation on the vehicle's sides]**

- Shades are by buildings, trees, and power poles along the road, and as with the roof of the vehicle, there is a fall in solar irradiance in corresponding locations and sections.
- Solar irradiance and the occurrence of shades on the vehicle greatly depend on the relationship between the solar orientation and the direction of the road. Surfaces that face the orientation of the sun (one or two out of the front, rear, left, and right of the vehicle) are hardly affected by shades of buildings and the like along the road, but other surfaces will receive no direct solar irradiance and irradiance is low.
- The surface(s) where insolation is high will change as the direction in which the vehicle is traveling changes.
- Although the average value (per square meter) of solar irradiance in the various directions is less than the vehicle's roof, the solar irradiance of the surface facing the sun may exceed the solar irradiance on the vehicle roof when the solar elevation is low.
- In high-rise sections and urban sections, it is believed that solar irradiance increases due to reflections from buildings along the road. In open-air sections also, it is believed that solar irradiance increases due to reflections from the surroundings.

Data on solar irradiance acquired by a vehicle is a first step or gateway toward the use of PV in automobiles and is vital information for evaluating the significance and effect of mounting a PV system. It is also important for the design and operation of a control system for using generated power as power for driving the vehicle.

This preliminary study, a trial that measured the solar irradiance of a vehicle, was conducted at limited locations and times, and has therefore produced fragmentary data. Although it would not be appropriate to make generalizations on the characteristics of the solar irradiance acquired by a vehicle or to conduct quantitative evaluations into the expected level of generated power from only the results given here, the following characteristics and trends were observed as indicated above.

- Shades of buildings, trees, power poles, and the like occur, causing a fall in solar irradiance in affected locations and sections.
- Shades by a building or the like may cover an entire surface, such as the vehicle's roof, or may only partially shade the surface.
- Due to reflections from buildings and the like, the solar irradiance by a vehicle in some locations and sections may exceed the insolation on a roof or rooftop of a building.
- Fluctuations in solar irradiance due to shades and reflections often occur with very short cycles (less than 0,1 seconds).



### 3.2.2 High fidelity irradiance measurements in all directions

As a preliminary study on solar irradiance of a PV-powered vehicle, the solar irradiance acquired by actual vehicles in motion was measured in Japan. The measurement was implemented at two locations, Sapporo City in Hokkaido (hereinafter, simply “Sapporo”) and Miyazaki City in Miyazaki Prefecture (hereinafter, simply “Miyazaki”). These locations are positioned in the north and south of the Japanese archipelago that extends in the north-south direction.

The shading influence that frequently degrades the output of the solar panels on the vehicle’s roof or the vehicle’s side is complicated and varies by the position and the relative orientation (to the sun position) of the panel. In the case of the vehicle’s roof PV, the location (orientation) of the panel cannot be predicted. One practical approach is to rely on the probability model, supposing that some statistical model randomly distributes the distribution of height and density of the shading objects, and the orientation of the vehicle is independent and random as well. Another approach is to monitor the solar irradiance around the vehicle in three-dimensionally [2].

For a definition of the angle of the solar irradiance and module orientation, the reference axis should be local to the automobile [3]. Each axis moves by the movement of the vehicle and is independent of the orientation of the sun. On the other hand, the relative position is unchanged, and thus a linear coordinate conversion dynamically synchronized to the location, direction, and speed of the vehicle, monitored by a GPS, handles this situation [4]. The coordinate is an orthogonal one (Fig. 3.2-7).



Fig. 3.2-7 Three-dimensional irradiance around the vehicle’s body [2]

The advantage of the monitoring solar irradiance in the local axis of the vehicle, using five pyranometers are:

1. Direct indication of the solar irradiance for the PV panels on the vehicle’s roof and vehicle’s side(s)
2. Shading detection by comparison with the information of the direction by comparison of four monitored irradiances on the side(s) of the vehicle
3. Three-dimensional solar resource monitoring, including the angular distribution of the solar resource on the vehicle’s roof that is essential to the characterization of the curved module.
4. Secured validation of the performance model and solar irradiance model for the vehicle integrated PV by the check of more than two orthogonal axes using the monitored data in five orthogonal directions.

The measurement system consists of five pyranometers mounted on the vehicle’s roof, along with a GPS; thus, it could be moved on the road. The pyranometer axes  $Q_{x+}$ ,  $Q_{x-}$ ,  $Q_{y+}$ ,  $Q_{y-}$ , and  $Q_z$  are defined, as shown in Fig. 3.2-7. One pyranometer is placed horizontally on the vehicle’s roof ( $Q_z$ ), and four pyranometers are placed vertically facing each side of the vehicle ( $Q_{x+}$ ,  $Q_{x-}$ ,  $Q_{y+}$ ,  $Q_{y-}$ ). The global irradiance onto the vehicle’s roof ( $I_z$ ) is measured using a pyranometer  $Q_z$ . The global irradiance onto the sides of the vehicle ( $I_{x+}$ ,  $I_{x-}$ ,  $I_{y+}$ ,  $I_{y-}$ ) are measured using pyranometers  $Q_{x+}$ ,  $Q_{x-}$ ,  $Q_{y+}$ ,  $Q_{y-}$ . The direction of the moving vehicle is equal to that of  $Q_{y+}$ . An ambient temperature meter (Pt 100 temperature sensor) is also placed on the vehicle’s roof. The GPS is incorporated into the data logger, and data are recorded in 1 s intervals. The total number of hours of sun radiation (more than  $10 \text{ W/m}^2$  in  $I_z$ ) received over the year was 3 374 h, while the number of hours the vehicle was running was approximately 6% of this [2].

To acquire a dataset for comparison, a conventional static irradiance measurement system with a pyrliometer, a tracking pyranometer mounted onto a sun tracker, a horizontal pyranometer, and two vertical pyranometers facing eastward and westward was installed at the University of Miyazaki, Japan ( $31^\circ 49' \text{ N}$ ,  $131^\circ 24' \text{ E}$ ). The elevation



angle and azimuth angle of the sun's position are calculated based on the conventional method, including the day angle, declination angle, time equation, hour angle, latitude, and longitude [2].

The city of Miyazaki, Japan, is one of the capitals of local government in Japan (Miyazaki prefecture) with a population of approximately 200 000. Thus, this area contains an urban zone, a residential district, and a rural district. In a way, it may be a representative zone in the solar environment (shading frequency and shading height). We did not constrain the driving course of the one-year monitoring of the solar irradiance on the vehicle, but the most frequent driving course of this vehicle is shown in Fig. 3.2-8 since it was used for commuting between the University of Miyazaki and the driver's residence.

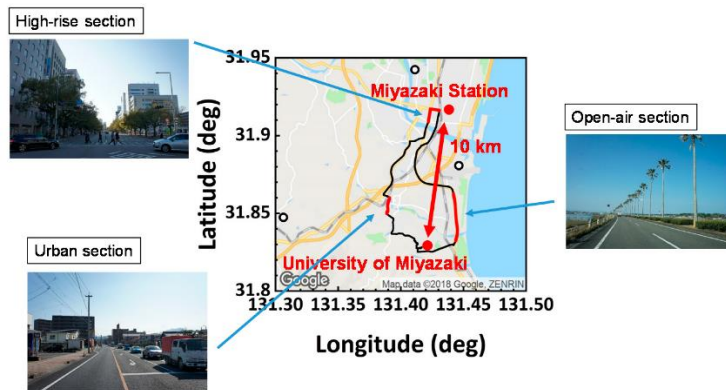


Fig. 3.2-8 The most frequent driving course of the dynamic solar irradiance measurement in the vehicle [2].

The typical monitored result of the route in Fig. 3.2-8 is shown in Fig. 3.2-9 (clear sky day) with comparison to the global horizontal irradiance (GHI) of fixed pyranometers (mounted on a roof of one of the buildings of the University of Miyazaki).

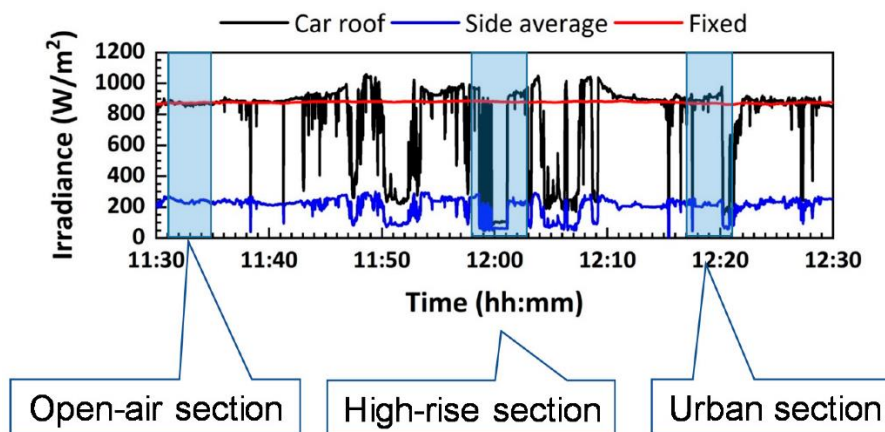


Fig. 3.2-9 Monitored result of the solar irradiance on the vehicle's roof and vehicle's sides in the driving route in Fig. 3.2-8 [2].

In the region of the open-air section, the solar irradiance on the vehicle's roof is almost identical to the GHI by the fixed pyranometers. However, that of other areas had frequent dips in the irradiance on the vehicle. The timestamp and position data taken by GPS confirmed that these are because of the shading effects by buildings and mountains. The vehicle's roof irradiance often exceeded GHI. It is also confirmed because of the reflectance of the structures [2].



The above model was compared with the one-year observation result of the solar irradiance on the vehicle, including seasonal (monthly) fluctuation. After fitting to the measurement irradiance dataset, the fitted average shading height is  $18,7^\circ$  in the direction along the road (local axis) and  $12,3^\circ$  in the direction orthogonal to the road (local axis), and  $15,5^\circ$  as the average. The averaged shading height after data fit was  $15,5^\circ$ , and it is very close to the value of the rough physical measurement ( $15^\circ$  on average). The average reflectance from the road is also fit to the measured data and obtained as 0,088, also a reasonable value for aged asphalt (typical value is 0,07). The annual ratio of the solar irradiance on the vehicle's roof relative to GHI (Global horizontal irradiance) was 0,925 (both modeled and measurement), and that of the vehicle's side was 0,412 (both modeled and measurement) [2].

The validation is also done by a one-month integration (seasonal fluctuation). The model met the modeled values in every month (Fig. 3.2-10). The trend of the residual errors could be explained by the difference in climate from the regular year (for example, cloudy in summer) [2].

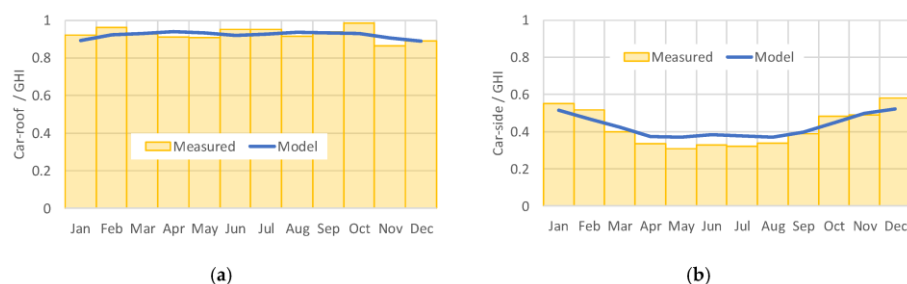


**Fig. 3.2-10 Monthly-based comparison between the measured solar irradiance around the vehicle (bar chart) and modeled (typical year from the METPV-11 solar database, namely, MEteorological Test data for PhotoVoltaic system) solar irradiance on the vehicle (line-chart): (a) vehicle's roof irradiance; (b) vehicle's side irradiance [2].**

Assuming that the density and height distribution of the shading objects are the same to that of Miyazaki, Japan, namely the average shading height is about  $15,5^\circ$ , it may be possible to anticipate the energy yield of the VIPV in various area in the world; which is useful to predict the merits of the introduction of solar-driven vehicles.

Fig. 3.2-11 indicates the map of the practical solar resource on the vehicle's roof normalized to the GHI, affected by climate conditions. They are calculated using the METPV-ASIA solar irradiance database. Due to the shading impact and curved surface, the practical solar resource for the vehicle's roof is less than the typical installation. The rough value may be  $3/4$  of the GHI.

Generally speaking, both the shading impact and curve impact increases with the decrease of the sun height, namely, increasing the latitude. However, both the curve-correction factor and effective solar resource on the vehicle's roof normalize to GHI (including the loss by the curved surface), do not show a strong correlation to latitude (thus sun height), and unlike other typical solar resource parameters, is affected by local meteorological conditions. Also, note that both the curve-correction factor and the effective solar resource relative to GHI are strongly influenced by the distribution (both special and height) of shading objects.

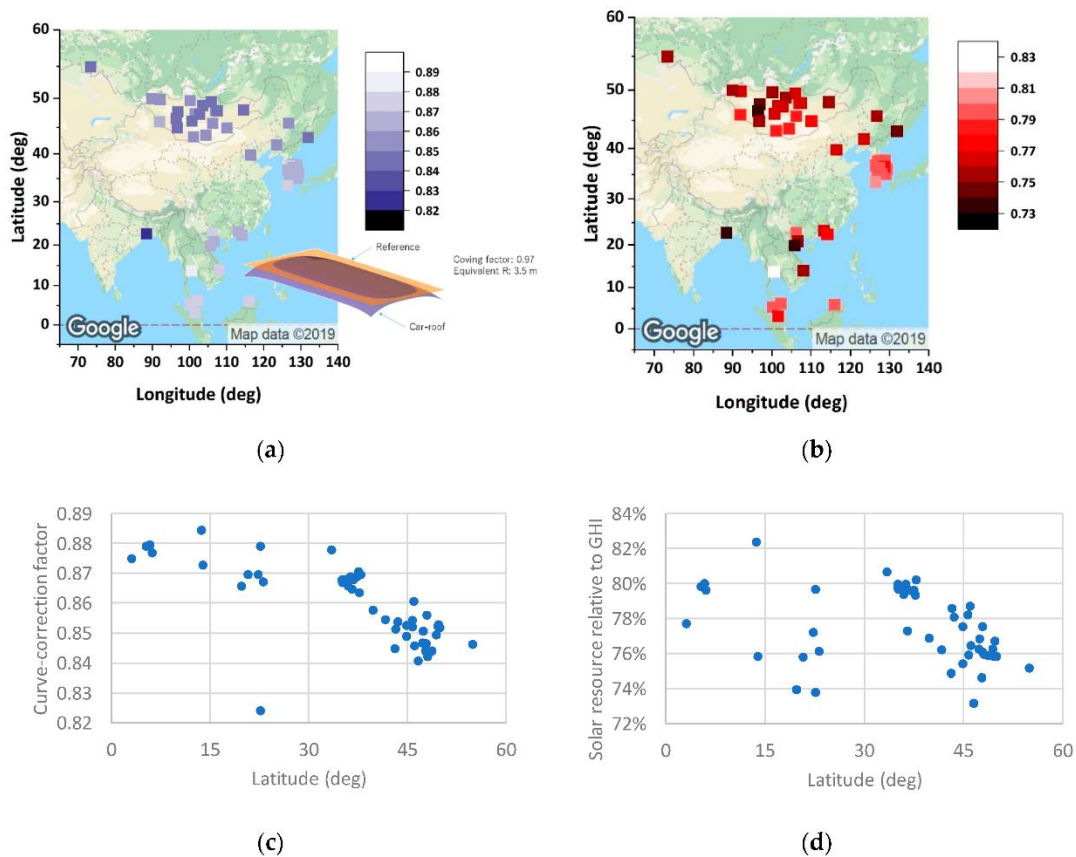


**Fig. 3.2-11** Map of the effective solar irradiance for the vehicle's roof: (a) curve-correction factor in a typical vehicle's roof; (b) effective solar resource to the vehicle's roof normalized to GHI, including the loss by the curved surface; (c) correlations between latitude (related to the sun height) and the curve correction factor; (d) correlations between latitude (related to sun height) and the effective solar resource to the vehicle's roof normalized to GHI, including the loss by the curved surface [2].

## [References]

- [1] NEDO, PV-Powered Vehicle Strategy Committee Interim Report (2) - Preliminary Study on Solar Irradiation of PV-Powered Vehicles -, April 2019
- [2] Araki, K.; Ota, Y.; Yamaguchi, M. Measurement and Modeling of 3D Solar Irradiance for Vehicle-Integrated Photovoltaic. *Appl. Sci.* 10, 872, 2020.
- [3] Araki, K.; Ji, L.; Kelly, G.; Yamaguchi, M. To Do List for Research and Development and International Standardization to Achieve the Goal of Running a Majority of Electric Vehicles on Solar Energy. *Coatings*, 8, 251; 2018.
- [4] Ota, Y.; Masuda, T.; Araki, K.; Yamaguchi, M. A mobile multipyranometer array for the assessment of solar irradiance incident on a photovoltaic-powered vehicle. *Sol. Energy*, 184, 84–90, 2019.



## 3.3 Solar irradiance measurements in Switzerland

### 3.3.1 Measurement of the irradiance on a Nissan Leaf

Solar irradiance was measured on all sides of a Nissan Leaf in 2020. The estimated useful surface for mounting PV on the vehicle is 5,3 m<sup>2</sup> and obtains 3-6 kWh/day on average from April to June, with an estimated module efficiency of 20%.

#### 3.3.1.1 Method

In total, five mono-crystalline reference cells have been mounted on five different sides of the Nissan Leaf: one on the hood, on the roof, on both side panels and one on the rear of the vehicle. Mono-crystalline, 5-inch cells from JA Solar were used, which provide an efficiency of 20%. Setting up the measurement system, the cells in our sun-simulator were calibrated using 500 W/m<sup>2</sup>.

Furthermore, two temperature loggers were installed, one beneath the cell on the vehicle's roof for measuring cell temperature and one beneath the spoiler in the rear for the logging of the ambient air-temperature. The data is collected using a Campbell Scientific CR1000X Logger which was connected to a 12 V battery inside the vehicle.

For reference irradiance levels, the BFH's longtime-measurement system was used on a building right next to the vehicle's parking lot at the campus. It measures global horizontal irradiance using a pyranometer. The location of the vehicle is logged using a GPS sensor from Garmin (GPS 18x). A measurement frequency of 1 Hz was used.

Fig. 3.3-1 shows the Nissan Leaf on the parking spot of BFH in Burgdorf, exposing one of the mounted reference cells on the vehicle's right-hand side panel.

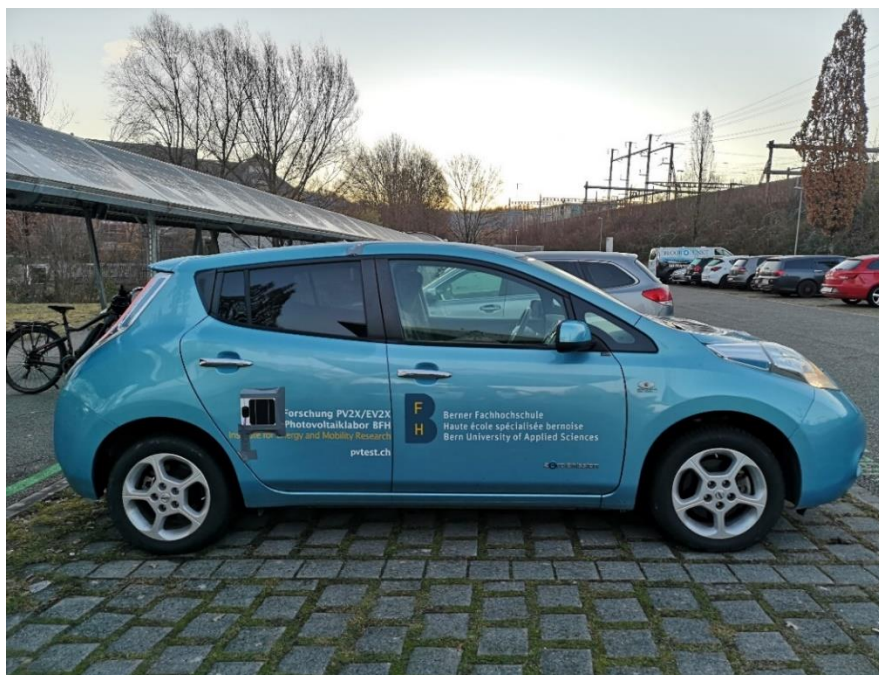


Fig. 3.3-1 Nissan Leaf with one of the reference cells on the right-side panel

Most of the time the vehicle is parked in the parking lot of Tiergarten Campus in Burgdorf. It is an open space parking place which gets a lot of sun during the day. Fig. 3.3-2 shows the parking lot and exact place where the vehicle is usually parked. The vehicle is usually parked facing northeast, as the plug for charging is integrated in its front.

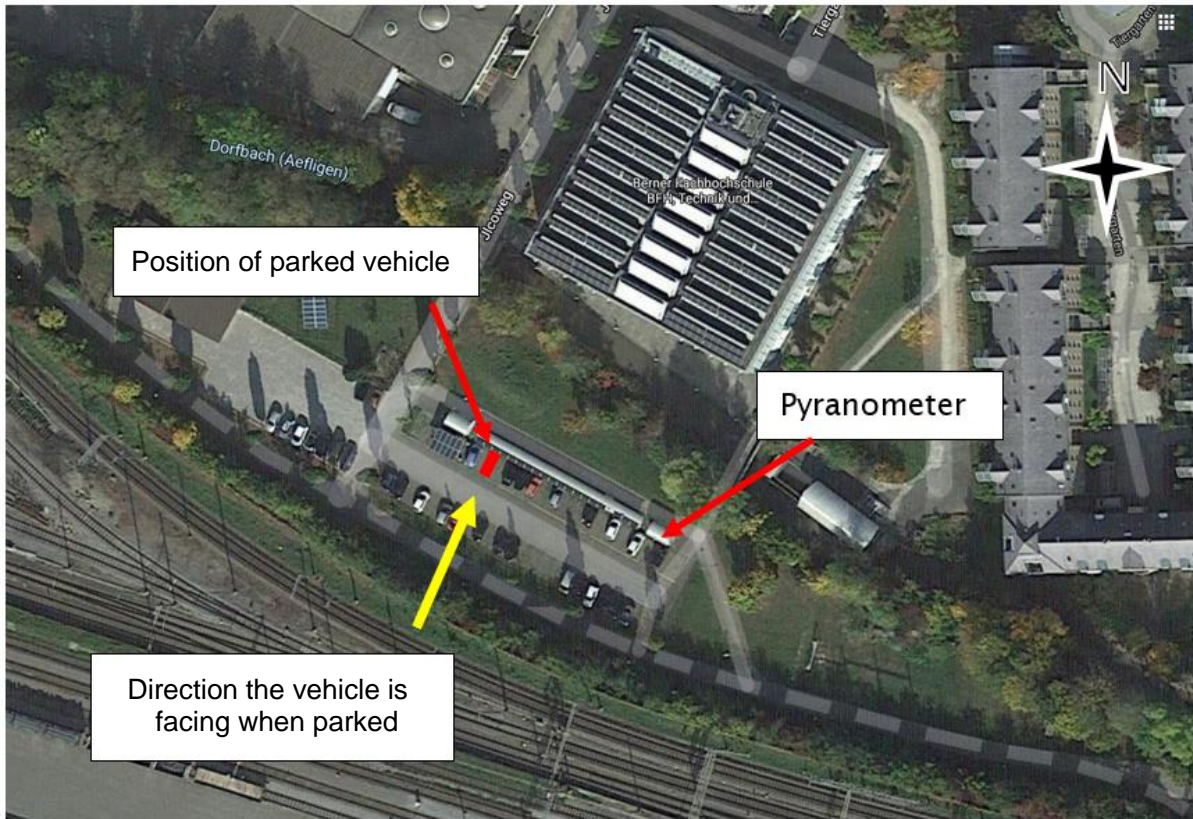


Fig. 3.3-2 Position of the parking lot at BFH in Burgdorf, where the measured Nissan Leaf is usually parked

### 3.3.1.2 Results

For every cell mounted on the vehicle a certain surface has been defined on which it would be possible to mount PV panels. The five surfaces cover a total surface of 5,3 m<sup>2</sup> on the vehicle. To estimate the amount of generated electricity a cell-efficiency of 20% has been defined for the mounted PV panels. Fig. 3.3-3 shows some of the defined “active” surfaces.

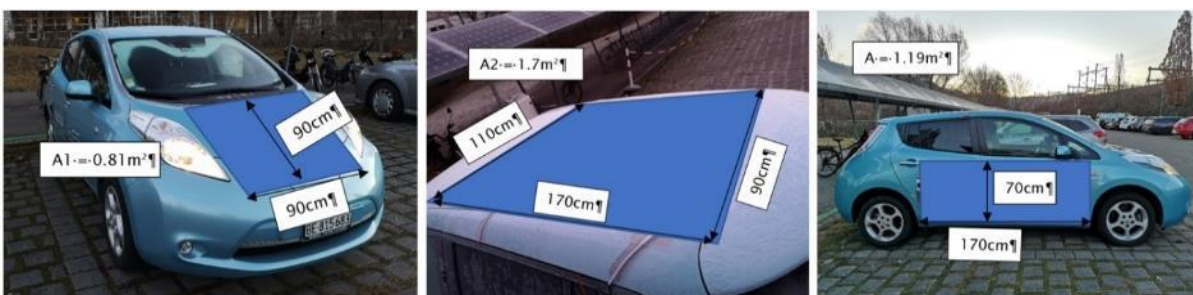


Fig. 3.3-3 Examples of defined surfaces apt to mount PV panels on

Fig. 3.3-4 shows an example of the diurnal irradiance levels of all irradiance sensor on the parked vehicle on a very sunny day in April. Here, the latitude of Burgdorf is: 47°3'21". The sensor on the rear of the vehicle (G5) shows the highest irradiance levels, as it is perfectly exposed to the sun and has a steep inclination of about 45°. The sensor on the hood (G1) shows very low irradiance levels as it is facing northeast with an inclination of around 10°. Some shading on the vehicle in the morning and in the evening can be observed.

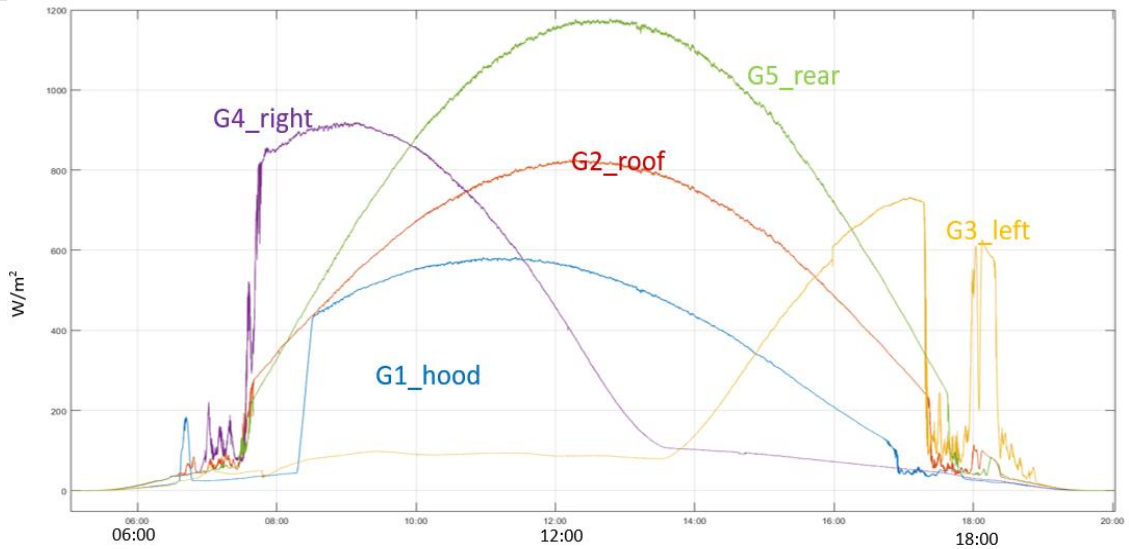


Fig. 3.3-4 Diurnal variations of irradiance levels on April 14th, 2020 [W/m<sup>2</sup>].

The measured irradiance levels were combined with the corresponding surfaces to calculate the possible energy yield. Fig. 3.3-5 shows the yield that has been measured so far on each surface of the vehicle (assuming 20% cell-efficiency and no conversion losses for battery charging, etc.).

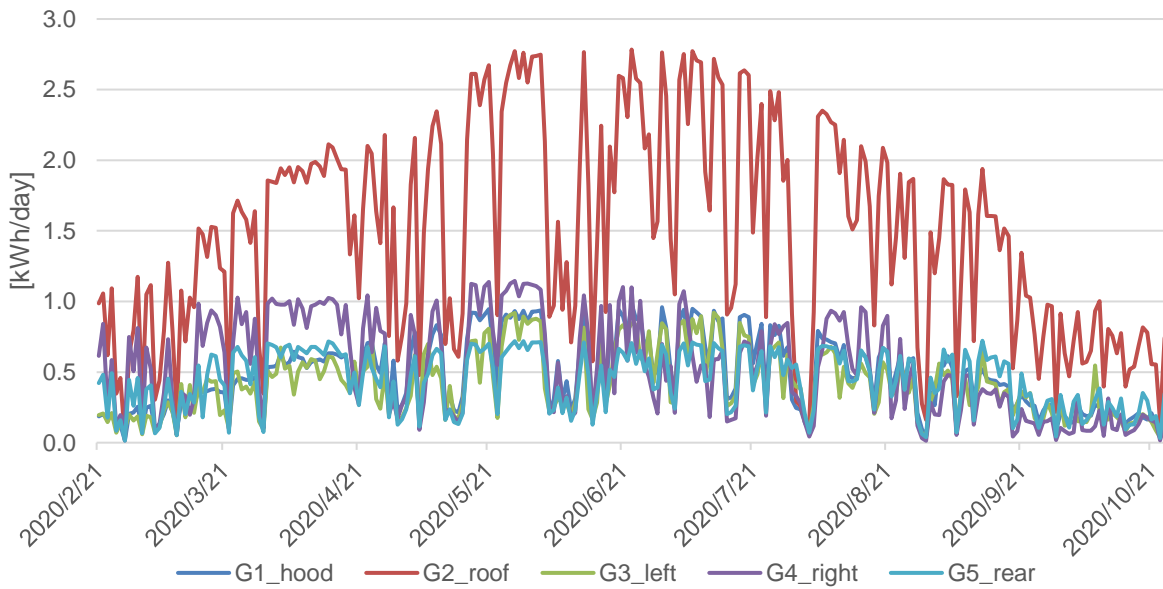


Fig. 3.3-5 The measured energy yield on each surface of the vehicle in kWh/day and per surface

Fig. 3.3-6 shows the same data, but the energy yield of the sum of all measured surfaces. The record yield so far has been measured in May and June, showing an output of 6,5 kWh in one day. A very sunny April provided more than 4 kWh/day on average. A Nissan Leaf has a mileage of around 17 kWh/100km and would therefore do 38 km for free with 6,5 kWh/day of sunshine on May 29<sup>th</sup> and around 23 km/day during a sunny April.

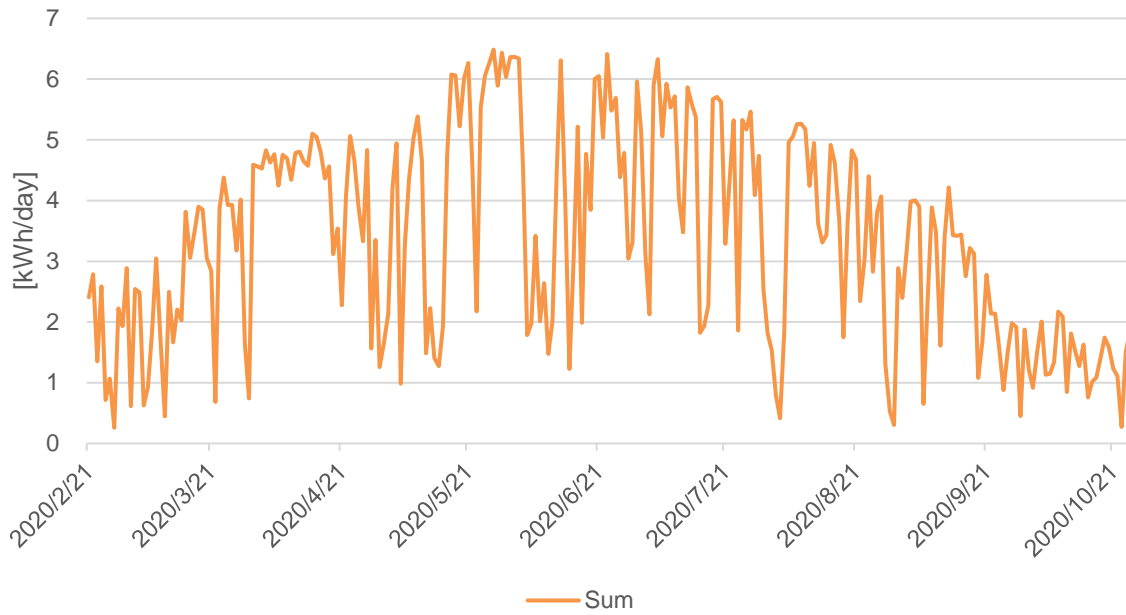


Fig. 3.3-6 Total energy yield per day (cell-efficiency: 20%, 5.3 m<sup>2</sup> in total) on Nissan Leaf

The yield of the defined surfaces on the vehicle is also compared with the theoretical yield which would be obtained using the reference-measurement-data: the global horizontal irradiance (GHI) up-scaled to the same surface (5,3 m<sup>2</sup>) has been defined for the vehicle. It can be described how much sunlight is incident on a “box-like” surface compared to a horizontal surface. The ratio between GHI and the sum of the measured irradiance on the vehicle is around 70%. A decline to around 60% towards the newest data can be seen. Fig. 3.3-7 shows the development of the vehicle / GHI – ratio over time.

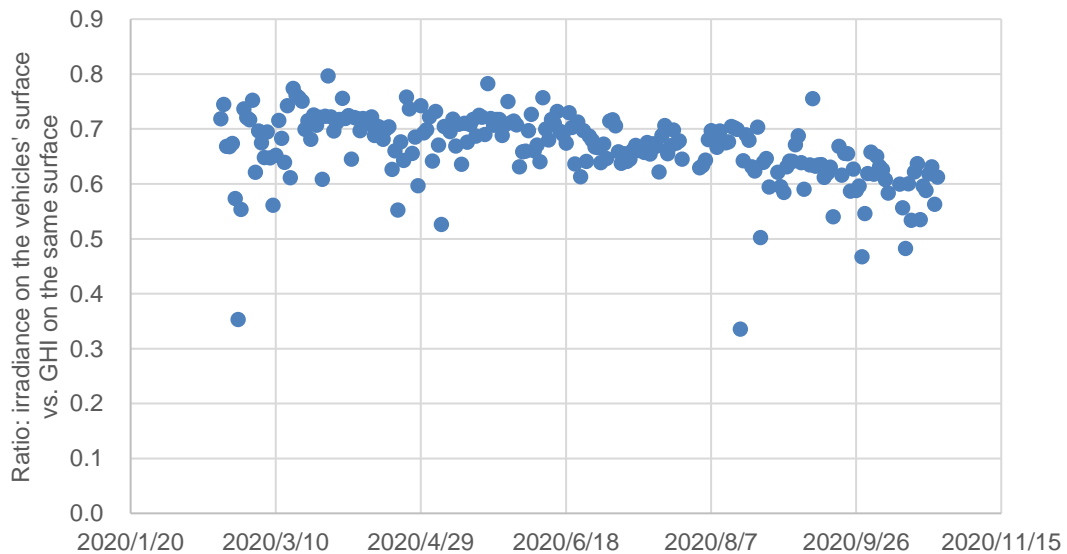


Fig. 3.3-7 Ratio between the measured Global Horizontal Irradiance and the sum of the measured irradiance on the Nissan Leaf (GHI normalized to the vehicle’s surface of 5.3 m<sup>2</sup>)



### 3.3.1.3 Findings

The irradiance measurements on the Nissan Leaf lead to interpretable results but also shows limiting aspects for interpretation. The energy yield of PV panels mounted on a vehicle is highly dependent on its parking spot. In this case, the vehicle has very good sun exposure during the whole day. It's rarely affected by shading from trees or other buildings. Nevertheless, it can be stated that its surface gets around 70% of the irradiance a flat area of the same extent would receive. Of course, this value needs to be confirmed in the months to come as it appears to differ with the position of the sun throughout the year.

It is stated, that in summer months, an EV with PV on a large part of its surface might be able to commute (average commuting distance in Switzerland is 35 km) on its own generated electricity on sunny days. The best days measured so far showed energy yields of around 6,5 kWh/day which correspond to a driving distance of around 38 km on a Nissan Leaf. This number needs to be treated with care, as it doesn't include conversion and charging losses from the battery.

### 3.3.2 Measurement on an electric Rikscha

In July 2020, irradiance measurements on a cargo tricycle from Rikscha Taxi Schweiz AG began. This company is working in city logistics with electrically assisted cargo bikes in the city of Bern. The same measurement concept as the Nissan Leaf above was applied as a different user case. The measured vehicle is on the road five days a week for about five to six hours per day and needs a lot less energy per km. Fig. 3.3-8 shows the "Rikscha Taxi" used for analyzing and measuring in July and August 2020.



Fig. 3.3-8 The «Rikscha Taxi» with a cargo box showing the left irradiance sensor.

#### 3.3.2.1 Method

The measurement method for the Rikscha is basically the same as described in the previous section (3.3.1), except that the power source for the logger is coming from the vehicle's 12V-plug. In addition, the energy consumption for charging the batteries of the Rikscha during two weeks in August has also been measured. The measurements for the irradiance levels have been carried out from July 13<sup>th</sup> to August 31<sup>st</sup>, 2020. For reference irradiance levels measurement data from a weather station in the city center of Bern was used. It measures global horizontal irradiance using a pyranometer. The location of the weather station and of the logistics center where the Rikschas operate from is shown in Fig. 3.3-9. It also shows the irradiance levels recorded on the roof of the Rikscha on August 17<sup>th</sup>, 2020. The mean operational time of the Rikscha was 5,8 hours per day. It usually started operating at



around 8 o'clock in the morning. When not in operation, the Rikscha was parked in a garage underground with the logger disconnected from power. The Rikscha is powered by an exchangeable battery with a capacity of 2,3 kWh. The battery swap is usually done around midday, when the vehicle is loaded for another run at the logistics center.

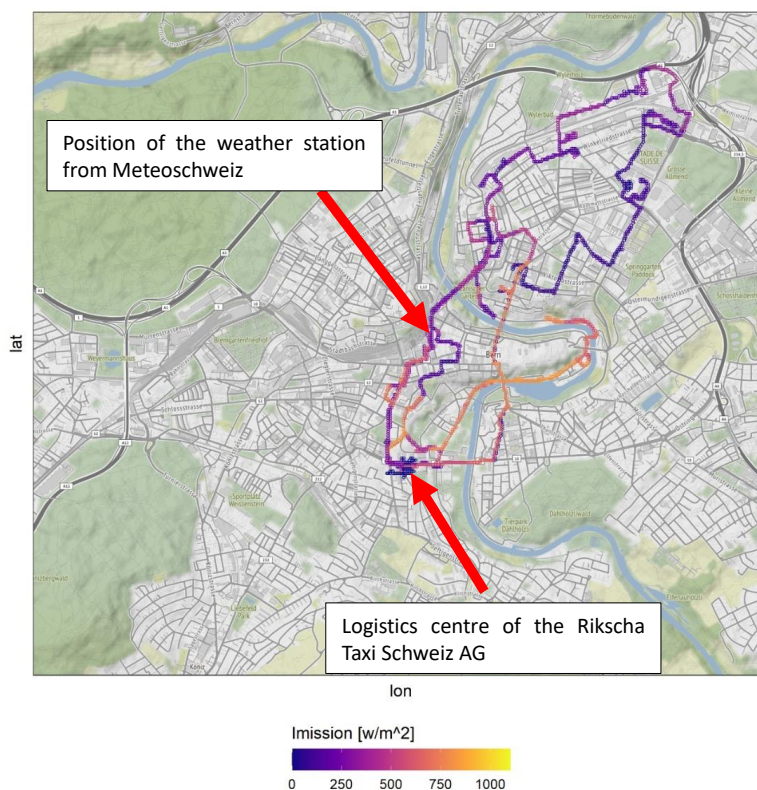


**Fig. 3.3-9 Map of Bern with the GPS-track of the Rikscha on the 17<sup>th</sup> of August 2020 showing different irradiance levels of sensor “G2” on the roof of the cargo box**  
 (The two red arrows point at the positions of the weather station and the logistics centre of Rikscha Taxi Schweiz AG)

For every cell mounted on the Rikscha, a certain surface has been defined on which it would be possible to mount PV panels. The five surfaces cover a total surface of 5,065 m<sup>2</sup> on the Rikscha. To estimate the amount of generated electricity a quote from “Solbian Energie Alternative srl.” in Italy was requested – they produce lightweight semi-flexible and highly efficient modules for mobile application. Although the cells used in the modules have an efficiency of 24%, an average efficiency of 15-16% was only obtained per surface used. In total, 793 Wp can be fitted on the Rikscha’s surface. Table 3.3-1 shows power, area and efficiency per surface.

**Table 3.3-1 Power and efficiency per surface (G1-G5)**

Surface	Module Power [Wp]	Area [m <sup>2</sup> ]	Efficiency of whole surface
G1 Drivers roof	65	0,42	15,5%
G2 Roof of cargo box	156	1,00	15,6%
G3 Left	234	1,44	16,3%
G4 Right	234	1,44	16,5%
G5 Back doors	104	0,77	13,5%
Sum	793	5,07	15,7%



### 3.3.2.2 Results

Fig. 3.3-11 and 3.3-12 show two examples of the diurnal irradiance measured by the weather station (GHI) and the five sensors (G1-G5) on 27<sup>th</sup> July 2020 and 13<sup>th</sup> of August 2020. GPS-tracks were also generated for every day the Rikscha was on duty (example shown on Fig. 3.3-9). Unfortunately, the possibilities to make proper use of these has not been realised until now.

**Irradiation measured on 27.7.2020**

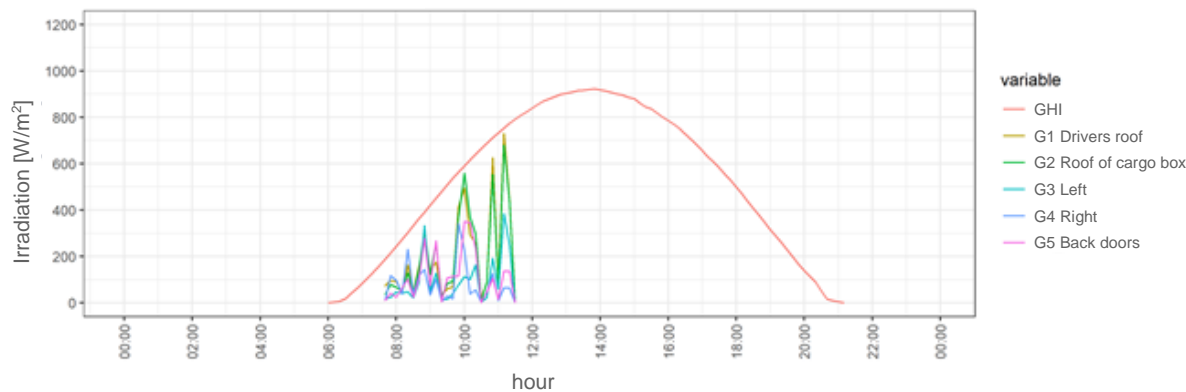


**Fig. 3.3-11 Diurnal variations of irradiance levels on July 27<sup>th</sup>, 2020 [W/m<sup>2</sup>]**  
(Data measurement (G1-G5) in the morning: not available)

**Irradiation measured on 13.8.2020**

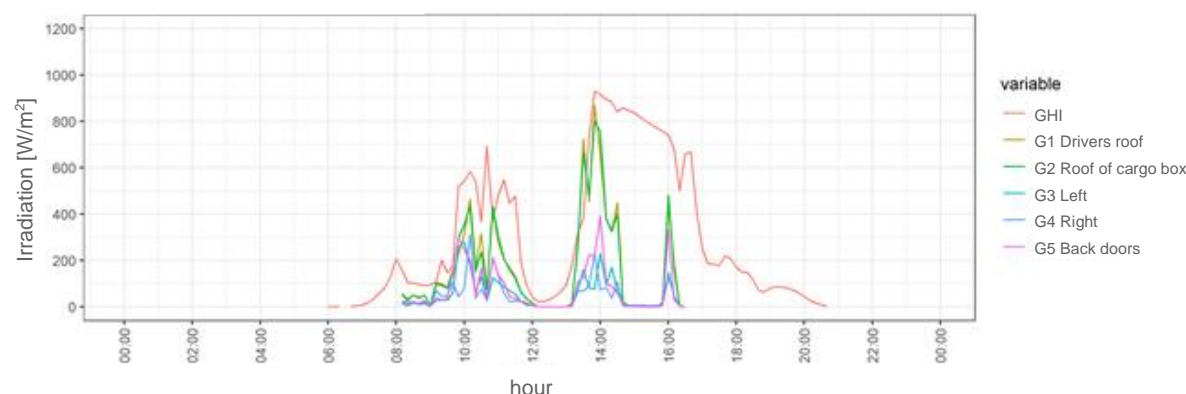


**Fig. 3.3-12 Diurnal variations of irradiance levels on August 13<sup>th</sup>, 2020 [W/m<sup>2</sup>]**  
(Data measurement (G1-G5) after 16:00: are not available)

Fig. 3.3-13 shows the energy yield of the sum of all measured surfaces. The record yield so far has been measured on August 27<sup>th</sup> with an output of 1 kWh in one day. The mean value of the generated energy per day was 0,48 kWh/day. Compared with the daily consumed energy which is 2,09 kWh/day on average, as shown in Fig. 3.3-14, the PV system on the Rikscha could cover less than 25% of the daily energy consumption. Fig. 3.3-15 shows the measured daily values of both consumed and generated energy by the Rikscha from August 12<sup>th</sup> to August 31<sup>st</sup>.

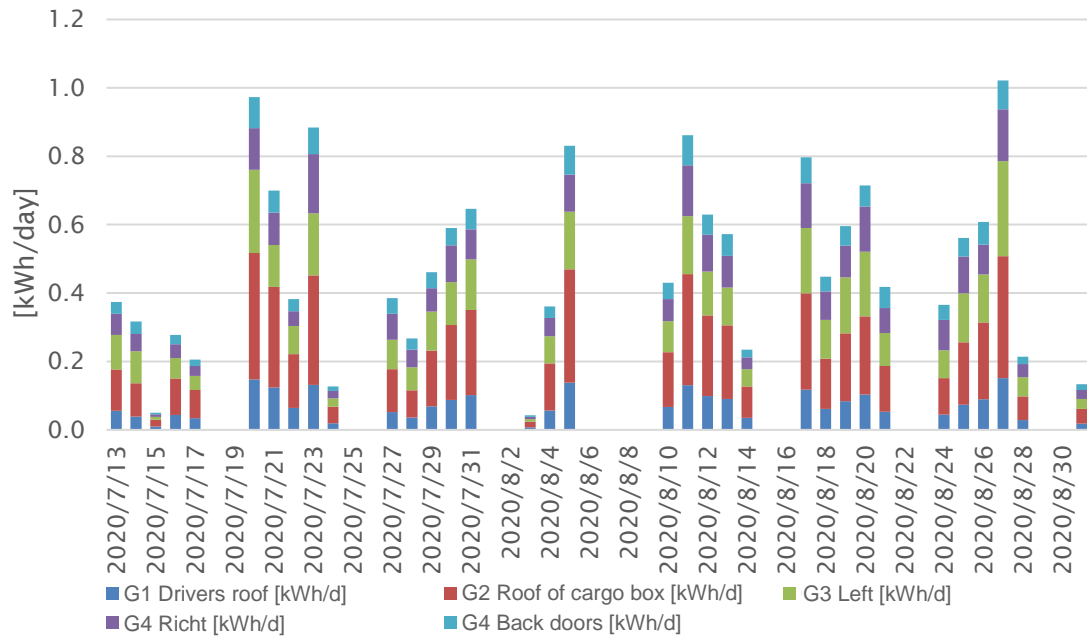


Fig. 3.3-13 Generated energy per day in kWh broken down by sensor G1-G5 (area = 5,1 m<sup>2</sup> & 15,6% module efficiency)

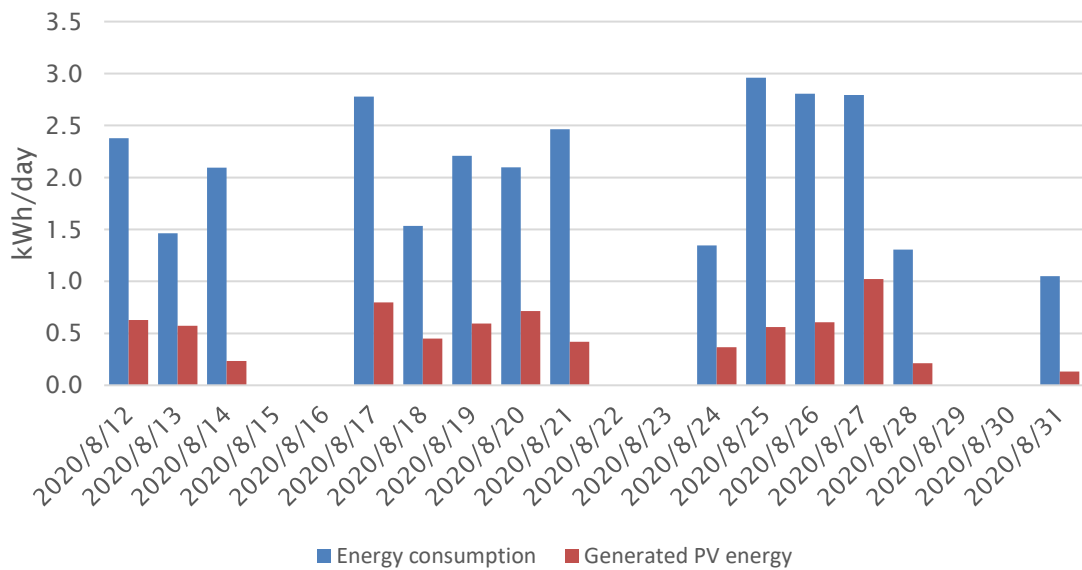


Fig. 3.3-14 Daily generated PV energy and consumed energy (the energy for battery charging has been measured.)

Fig. 3.3-15 shows the hourly averaged irradiation on all measured days of the roof sensor (G2). An orange or yellow square means that the average measured irradiance during that hour was between 500 and 800 W/m<sup>2</sup>. If the squares are dark blue, a minimum hourly average of 100 W/m<sup>2</sup> was recorded. It is visible, for example, that on the dates July 15<sup>th</sup>, 2020, July 24<sup>th</sup>, 2020 and August 3<sup>rd</sup>, 2020, weak irradiation conditions were measured. This is visible with all sensors. It is also visible that the average irradiation between 11 a.m. and 2 p.m. is higher than during the other times of day.

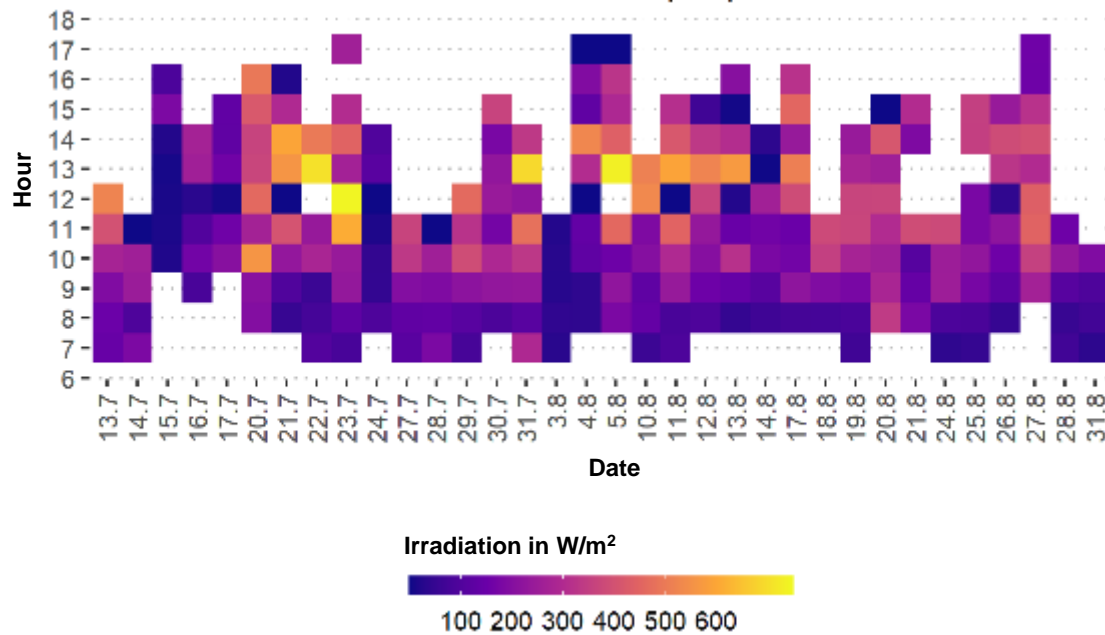


Fig. 3.3-15 Hourly averaged irradiation of the roof sensor on all measured days (G2)

### 3.3.2.3 Findings

With an average of only 5,8 operational hours a day (on weekdays) and being parked inside a garage the rest of the day, the generated daily PV-energy will be very low. The ratio between the measured Global Horizontal Irradiance and the sum of the measured irradiance on the Nissan Leaf (GHI normalized to the vehicle's surface of 5,3 m<sup>2</sup>) is around 0,7 on average, while the same ratio is around 0,21 for the Rikscha. This corresponds to less than one third of the ratio the Nissan Leaf obtains. The Rikscha uses just a fraction of the available irradiance due to the fact it is parked in the dark most of the time. This happens not only when it is not in use but also when it is unloading delivery and loading new packages (to be seen on Fig. 3.3-12 at around 13:00 and again at 14:30). If the Rikscha was in operation the whole day or parked outside, when not operating, it would generate much more PV-energy.

This means, that if Rikscha Taxi Schweiz AG decides to build a prototype of a "Solar Rikscha" they should look for a way the Rikscha can spend more time outside. The type of application for PV on EVs is crucial. Whether it is worth to use PV on vehicles depends very much on where the vehicle is parked when it's not in use. One user case for the "Solar Rikscha" would be to use it as a taxi. It could be waiting for customers on squares and public places which often offer some sunny spots.

### 3.3.3 Outlook

The measurements on the Nissan Leaf will be continued until the end of 2020, in order to make statements on the possible energy yields and driving distances on solar power throughout the year. The measured values to standard irradiance levels measured in the past 20 years in order to eliminate statistical deviances will also be normalized. And finally, an economic analysis of a PV-system for vehicles will be made.



### 3.4 Solar irradiance measurements in Australia

The concept developed at UNSW for vehicle irradiance measurements is shown in Fig. 3.4-1 where a fleet of vehicles (passenger vehicles, public buses and trucks) are equipped with irradiance sensors that send the data they measure to a central database over the mobile data network. The irradiance sensor (Solar Jinie, EnerJIN Pty), measures irradiances from 0 - 1 200 W/m<sup>2</sup> with 20 W/m<sup>2</sup> accuracy, location is also measured via GPS and achieves autonomous operation in Sydney (average irradiance 5 kWh/m<sup>2</sup>/day) using a 3 W silicon solar panel. The irradiance sensor is presently being deployed on a number of vehicles in Australia; here, two case studies where it has been deployed are reported on.

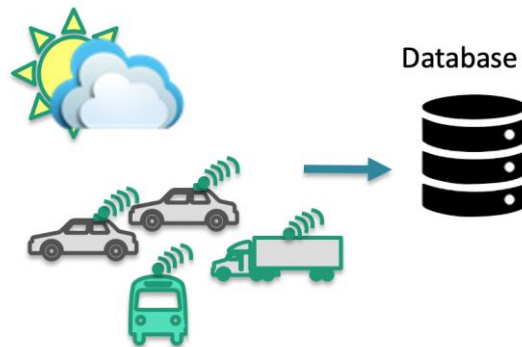


**Fig. 3.4-1 Solar irradiance concept developed by UNSW, Australia**

(Solar irradiance is measured from vehicles and sent via mobile data network to a central database.)

The first trial of the irradiance sensor involved a return journey from UNSW in Sydney to the ITP Battery Test Centre in Canberra in February 2020 which, in Australia, corresponds to mid-summer. The round-trip is shown in Fig. 3.4-2(a) measuring a total of 568 km on a day with mixed irradiance conditions throughout. The journey was undertaken in a Tesla Model S electric vehicle that averaged 6,25 km/kWh over the journey. The irradiance measured is shown in Fig. 3.4-2(b) which integrates to a daily total of 5,4 kWh/m<sup>2</sup> falling on the vehicle during that journey. While this EV is a conventional commercially battery electric vehicle, a solar range for this journey of 30 km if 4 m<sup>2</sup> of the vehicle were covered with 22 % PV modules has been estimated.

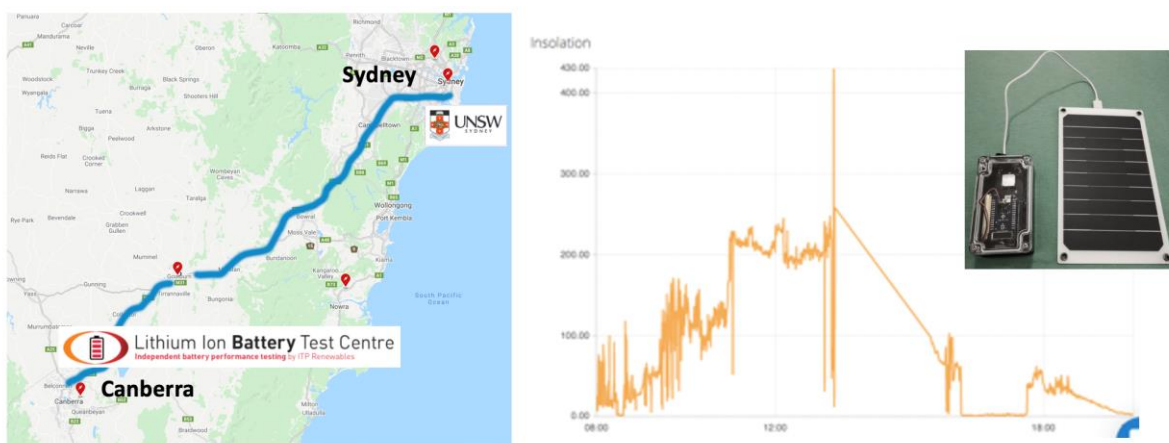


**Fig. 3.4-2 (a) Vehicle route from Sydney to Canberra, mostly on open country roads with a clear view of the sky. (b) The irradiance measured over the day. (c) The ‘Solar Jinie’ irradiance sensor used to measure the irradiance**



From April 2020 up to the time of writing (August 2020) an irradiance measurement trial in Melbourne, Australia's second largest city has been conducted on a private passenger vehicle. The period of measurement reported here coincides with the autumn and winter in Australia and during two lockdown periods due to the COVID-19 pandemic, so the data reported here is not representative of normal driving patterns but serves to illustrate the efficacy of this measurement. Driving conditions are mainly on wide open boulevards in the city suburban regions, depicted in Fig. 3.4-3(a), the annual average irradiance in Melbourne is 5 kWh/m<sup>2</sup>/day. The Solar Jinie irradiance sensor takes measurements every minute during daylight hours, the dataset of over 64 000 datapoints is summarised in Fig. 3.4-3(b) where each red spot indicates an irradiance measurement, with the size of the spot indicating the magnitude of the irradiance.

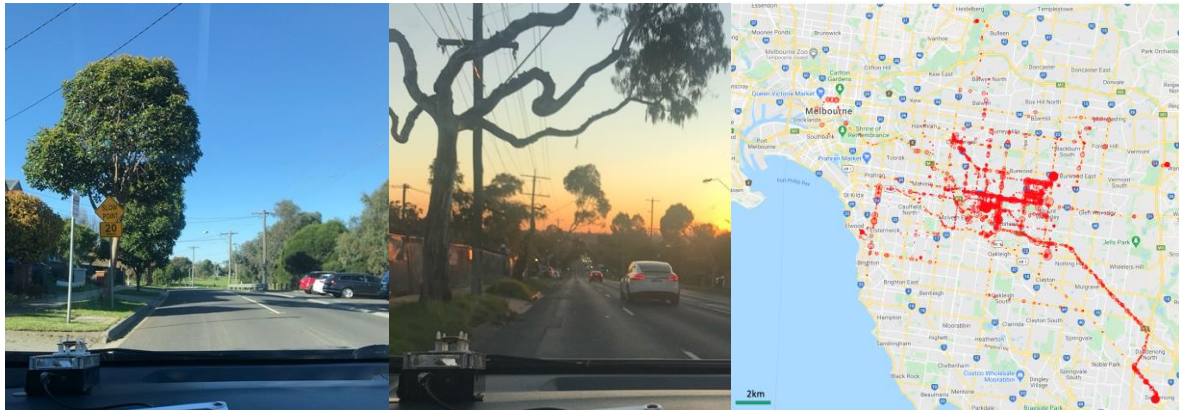


**Fig. 3.4-3 (a) Photographs of typical driving conditions on sub-urban streets and boulevards in Melbourne. (b) Map of S.E.Melbourne showing irradiance measurements made, the size of each datapoint represents the irradiance value**

During the period of measurement, the GPS data shows that the vehicle drove an average of 25 km per day on short trips, rarely exceeding 10 km. The vehicle was parked for 97% of the time and was housed in a garage when unused. In this particular example, the irradiance falling on the vehicle represents one of the most pessimistic case since the vehicle only received solar irradiance when it was being used, away from the home (and during a virus pandemic with restrictions on mobility). Fig. 3.4-4(a) shows a histogram of all the measurements made during daylight hours. The vast majority of the irradiance measurements are zero since the vehicle was parked in a garage. The remaining data appears to follow a roughly linear trend on this log-linear scale, indicating that the irradiance available to this vehicle can be approximated by a single exponential relationship. The total irradiance measured on this vehicle amounts to 0,35 kWh/m<sup>2</sup>/day. Further detail is presented in Fig. 3.4-4(b) where all irradiance values measured while the vehicle is stationary are plotted, excluding those when the irradiance is zero. 80% of the solar irradiance was collected while the vehicle was parked with the majority at irradiances below 200 W/m<sup>2</sup>. The irradiance levels experienced while moving shown in Fig. 3.4-4c were found to be marginally higher with a mean value of 136 W/m<sup>2</sup> vs 127 W/m<sup>2</sup> when stationary.

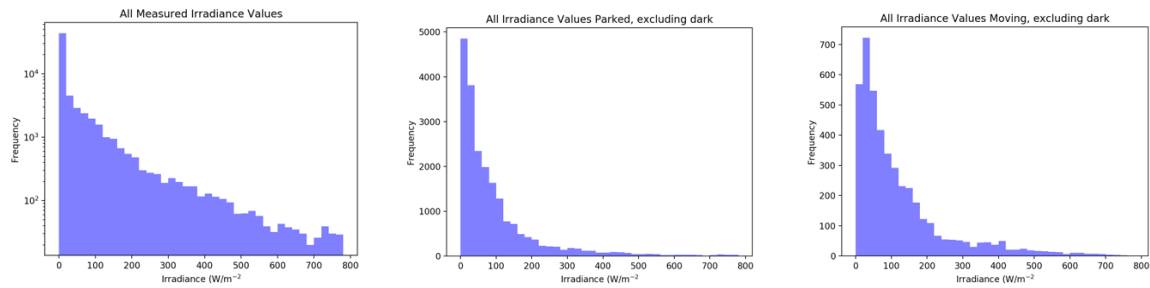


**Fig. 3.4-4 Irradiance histograms showing (a) total irradiance measured including when parked in a garage (log scale), (b) irradiance measured when the vehicle is stationary but not dark and (c) irradiance measured while the vehicle is moving, again excluding all measurements made in darkness**

In summary, two initial vehicle irradiance surveys have been carried out at UNSW Sydney. In the case of a long road trip, a total of 5,4 kWh/m<sup>2</sup> was estimated to fall on the vehicle during the journey that is estimated to add 30 km of solar range to that journey. Long term monitoring of a passenger vehicle during the autumn and winter in Melbourne (and during a period of restricted mobility due to the COVID-19 pandemic) showed that the vehicle was parked 97% of the time and that 80% of the irradiance falling on a passenger vehicle took place while the vehicle was stationary.



### 3.5 Summary

In this chapter, approaches for measuring the real irradiance falling on vehicles in some organisations/countries were overviewed. Although there has not yet been enough data collected to make generalisations on the characteristics of the solar irradiance, each approach showed varying results and from these, a few trends and similarities were found.

A preliminary studies in Japan, which was conducted at limited locations (Miyazaki city and Sapporo city) and times, observed the following characteristics and trends:

- Shades of buildings, trees, power poles, and the like occur, causing a decrease in solar irradiance in affected locations and sections
- Shade from a buildings or the like may cover an entire surface, such as the vehicle's roof, or may only partially shade the surface
- Due to reflections from buildings and the like, the solar irradiance by a vehicle in some locations and sections may exceed the insolation on a roof or rooftop of a building
- Fluctuations in solar irradiance due to shades and reflections often occur with very short cycles (less than 0,1 seconds)

Fluctuations in solar irradiance on vehicle's roof were observed by measurements in the Netherlands and Germany, as well. Solar irradiance on the vehicle's roof during driving relative to GHI will range from 50% to 90%, e.g. from high-rise section to urban and open-air sections. Such a wide range indicates that it is currently difficult to make generalizations on the characteristics of the solar irradiance on vehicles and more data is needed as it will depend highly on the location. A ratio of roof-to-side measured in Miyazaki was from 30% to 50%, averagely 40%, which was relatively close to the measured ratio in Germany.

Measurements in Burgdorf, Switzerland found that a vehicle's roof gets around 70% of the irradiance a flat area of the same extent would receive. This value needs to be confirmed in the months to come as it appears to differ with the position of the sun throughout the year. Also, in this case, the vehicle has very good sun exposure during the whole day. In the case of another vehicle, which is parked in the dark most of the time, the ratio was around 21%. This result means a worth to use PV on vehicles depends on where the vehicle is parked when it's not in use.

In Australia, two initial vehicle irradiance surveys have been carried out. In the case of a long road trip from Sydney do Canberra, a total of 5,4 kWh/m<sup>2</sup> was estimated to fall on the vehicle during the journey that is estimated to add 30 km of solar range to that journey. Long term monitoring of a passenger vehicle during the autumn and winter in Melbourne (and during a period of restricted mobility due to the COVID-19 pandemic) showed that the vehicle was parked 97% of the time and that 80% of the irradiance falling on a passenger vehicle took place while the vehicle was stationary.

In addition to the impact of environmental shading, the impact of the inherent curvature of on-board PV increases with the decrease of the sun height, namely, increasing the latitude. However, the model-based study in Japan found that both the curve-correction factor and effective solar resource to the vehicle's roof, normalized to GHI, do not show a strong correlation to latitude, and, unlike other typical solar resource parameters, is more affected by local meteorological conditions. Also, both the curve-correction factor and the effective solar resource relative to GHI, are strongly influenced by the specific distribution of shading objects.

More irradiance measurements are needed in order to more accurately quantify the possible energy yields and driving distances on solar power throughout the year in specific locations and driving routes. Additionally, within the data set, measured values need to be normalized to standard irradiance levels measured in the past decades in order to eliminate statistical deviances.

Data on solar irradiance acquired by a vehicle is a first step or gateway toward the use of PV in automobiles and is vital information for evaluating the significance and effect, as well as optimal design, of an on-board PV system.



## 4. NEXT STEPS FOR REALISING PV-POWERED VEHICLES

This report overviewed recent trends of PV-powered vehicles in the world, and discussed expected benefits of PV-powered vehicles and measurement of solar irradiance on vehicles. Although more and more PV-powered vehicles' projects are identified over time, further actions will be necessary to realise practical deployment of PV-powered vehicles.

In this chapter, as the most impressive findings coming from this report, potential benefits of PV-powered passenger vehicles are discussed. Also, as important issues for realising PV-powered vehicles, standardisation of solar irradiance and module design, and combination with PV-powered infrastructures are discussed preliminary. Finally, conclusions and the way forward are described.

### 4.1 Potential benefits of PV-powered vehicles

This section shows potential benefits of PV-powered passenger vehicles in the IEA PVPS Task 17 member countries, based on the approaches at Chapters 2.1 and 2.2. As discussed in these chapters, the degree of expected benefits depends on various conditions, especially utilisation ratios of PV electricity generated on-board. Relations between expected benefits and utilisation ratios of PV electricity are also discussed.

#### 4.1.1 Expected benefits in IEA PVPS Task 17 countries

The IEA PVPS Task 17 member countries are shown in Table 4.1-1 and Fig. 4.1-1.

They are mostly confined to the Northern Hemisphere, but with a variety of latitudes representing a range of climates and range of expected energy production from photovoltaics. The solar resource in kWh/m<sup>2</sup>/year for the locations is shown in Fig. 4.1-2, and this can be translated directly to expected PV energy production. The largest solar resource values are seen in Rabat, Morocco and Canberra, Australia, followed by Madrid, Spain and Beijing, China. The smallest solar resource is in Amsterdam, the Netherlands.

**Table 4.1-1 IEA PVPS Task 17 member countries (as of March 2021)**

Australia, Austria, China, France, Germany, Japan, Morocco, the Netherlands, Spain, and Switzerland
---



**Fig. 4.1-1 IEA PVPS Task 17 member countries in red**

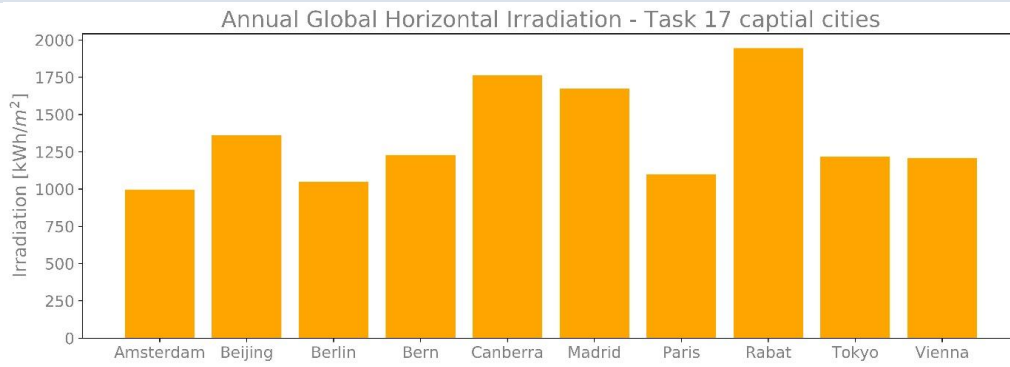


Fig. 4.1-2 PV potential - Annual Global Horizontal Irradiation of the capital cities of Task 17 countries [1]

The household electricity prices [2] and the carbon intensity of the local grid [3], are shown for all Task 17 locations in Fig. 4.1-3. It shows that Australia, Morocco and China have the highest carbon intensity, and that Switzerland and France have very low carbon intensities. Germany has the highest price for household electricity, and China the lowest. These differences are related to the potential impact that a PV-powered vehicle would have in each of the locations and can be seen in the results of the simulations.

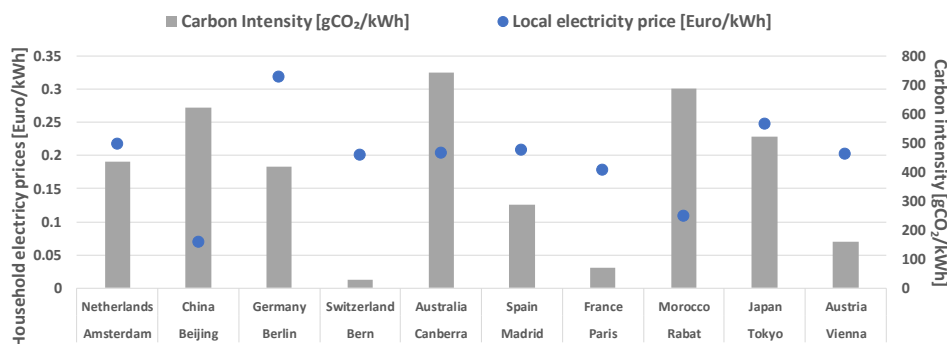


Fig. 4.1-3 Comparison of Household electricity prices and carbon intensity of electricity generation of Task 17 countries

(These values are used as input to the Energy Flow model to determine cost and CO<sub>2</sub>-eq savings for each location for a PV-powered vehicle [2][3])

Based on the methodologies used in Chapter 2.2, simulations have been done to quantify the impact of VIPV for the other Task 17 member countries, using the long -range vehicle and the 15 km simple commute driving profile as the base case. The reduction in charging frequency, PV contribution and utilisation, CO<sub>2</sub> emissions and solar kilometres travelled in a year have been examined. The carbon intensity of the local grid and local electricity prices used in the simulations are shown in Fig. 4.1-3. The value for the embedded CO<sub>2</sub> in the PV is based on the same values used in Chapter 2.2, where it is assumed that the PV has been manufactured in China, as this will be the case for most countries<sup>1</sup>.

As shown in Fig. 4.1-4, the total and relative reduction in charging frequency for the different locations is directly related to the amount of PV energy generated, a small secondary effect is the ambient temperature at the different locations which has an impact on the vehicle/battery efficiency and is included in the model. However, as can be seen in Fig. 4.1-5, the total kWh needed is very similar for each location. In the locations with very high PV

<sup>1</sup> The results shown in this section for Tokyo differ from the results reported in Chapter 2.2. There, the PV is assumed to be manufactured in Japan rather than China, with a different embedded CO<sub>2</sub> value; and a 30% shading factor has been assumed reducing the amount of PV energy generated.



generated energy the utilisation is lower. In these cases, the PV makes a significant contribution to the required energy (the green bar is much larger than the grey bar). However, more energy is generated by the PV than can be absorbed by the battery or used by the vehicle with the 15 km simple commuting profile. Therefore the utilisation is very low.

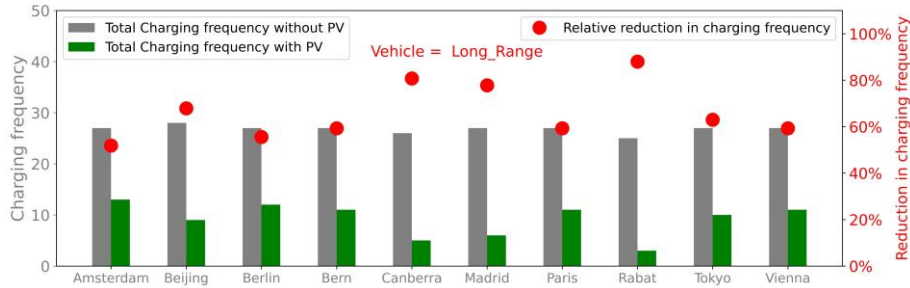


**Fig. 4.1-4 Comparison of total charging frequency for the long-range vehicle (left axis) and the relative reduction in charging frequency (right axis), for the simple 15 km commute profile and all Task 17 locations**

(Without PV the number of charging frequency are very similar. With PV the locations with higher irradiance, Canberra, Madrid and Rabat see the largest reduction in charging frequency as the PV contributes more to driving energy.)



**Fig. 4.1-5 The total kWh utilised for driving divided into Grid and PV charging is shown on the left axis, the right axis shows the percentage of generated PV energy that has been utilised for all Task 17 locations, the long-range vehicle and the simple 15 km commute profile**

(The locations with the largest PV contribution can also have lower utilisation as the battery, in some cases, is unable to absorb all the generated PV energy.)

As shown in Figs. 4.1-6 and 4.1-7, the CO<sub>2</sub>-eq emissions are very different for each location. The combination of high carbon intensity and high PV generated energy mean that Canberra, Beijing, and Rabat have the largest CO<sub>2</sub>-eq emissions without PV and the largest net CO<sub>2</sub>-eq savings with PV. Bern, Switzerland and Paris, France have very low carbon intensity grids, and because of this they have a net increase in CO<sub>2</sub>-eq emissions due to the embedded CO<sub>2</sub> in the PV element. They still have benefits in terms of more nearly 80% reduction in charging frequency and financial savings.



**Fig. 4.1-6 Comparison of CO<sub>2</sub> emissions for each location with and without PV**

(The locations with the lowest local grid carbon intensity, Bern and Paris, both have no CO<sub>2</sub> benefit from the 800 Wp PV on the long-range vehicle for the simple 15 km commute driving profile.)

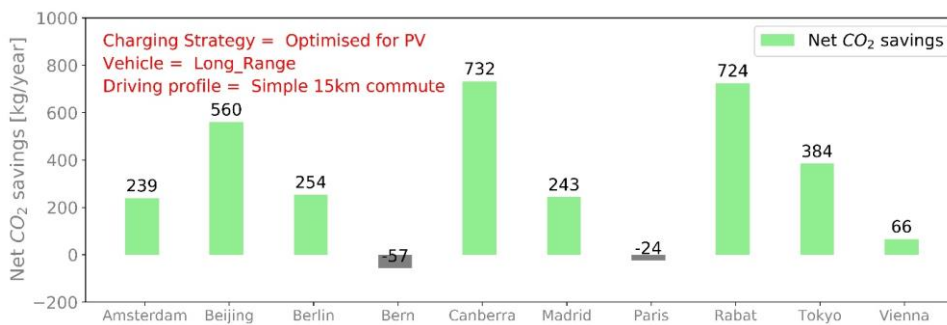


**Fig. 4.1-7 Net CO<sub>2</sub> savings per location for the simple 15 km commute driving profile and the long-range vehicle**

(Bern and Rabat show a negative value due to their already clean grid power.)

Fig. 4.1-8 shows the number of kilometres that are travelled each year in each location purely on energy from the PV. This result is based on the contribution of the PV generated energy to the total required energy seen in Fig. 4.1-5. It shows that in the high irradiance countries PV-powered vehicles can travel more than 6 000 km/year on PV. With higher efficiency electric vehicles this number will increase.



**Fig. 4.1-8 Total distance travelled using PV energy in one year by location, for the simple 15 km commute and the long-range vehicle**

### 4.1.2 Discussion on expected CO<sub>2</sub> reduction by PV-powered vehicles

As shown in the previous section, PV-powered vehicles will be able to contribute to CO<sub>2</sub> reduction compared to conventional electric vehicles without PV, although the degree of CO<sub>2</sub> reduction will depend upon the driving



patterns and the carbon intensity of the local grid. This should be a promising benefit produced by PV-powered vehicles.

However, it should be noted that if the carbon intensity of PV electricity (kg-CO<sub>2</sub>/kWh) is greater than that of grid electricity, a PV-powered vehicle will not realise CO<sub>2</sub> reduction compared to a conventional electric vehicle. In addition, even if the expected carbon intensity of PV electricity, supposing that all electricity generated could be used effectively, is less than that of grid electricity, a lower utilisation ratio of PV electricity or an excess PV capacity may cause an increase in CO<sub>2</sub> emission.

In this section, the expected CO<sub>2</sub> reduction by PV-powered vehicles will be discussed comprehensively.

#### 4.1.2.1 CO<sub>2</sub> emission of PV electricity

In general, CO<sub>2</sub> emission due to PV electricity is shown in Fig. 4.1-9, dividing the life cycle CO<sub>2</sub> emissions by the electricity generated during the lifetime of the PV.

Life cycle CO<sub>2</sub> emissions will be mainly dominated by the manufacturing process, and the emission by manufacturing process will depend on the manufacturing site. The main reason is that PV manufacturing processes, including purifying and refining semiconductor materials, require a lot of electricity and the CO<sub>2</sub> emissions caused by the electricity used at the site, provided from grid, will be different by region or country.

Electricity generated by PV during its lifetime will depend on solar irradiance, the performance ratio and the length of lifetime. Higher solar irradiance, higher performance ratio and a longer lifetime will result in smaller net CO<sub>2</sub> emissions from the PV electricity.

$$\boxed{\begin{array}{c} \text{CO}_2 \text{ emissions due to PV} \\ \text{electricity} \\ \text{[kg-CO}_2\text{/kWh]} \end{array}} = \boxed{\begin{array}{c} \text{Life cycle CO}_2 \text{ emissions} \\ \text{of PV system} \\ \text{[kg-CO}_2\text{]} \end{array}} \div \boxed{\begin{array}{c} \text{Electricity generation} \\ \text{during lifetime [kWh]} \end{array}}$$

Fig. 4.1-9 CO<sub>2</sub> emission of PV electricity

In the case of PV electricity for on-board PV (PV-powered vehicle), compared to conventional stationary PV systems, the expected solar irradiance may become small because of shading, the expected performance ratio may become small because of battery charging/discharging loss, and expected lifetime may be short because the vehicle's lifetime may be shorter than the PV's technological lifetime. Therefore, it is expected that electricity generation by an on-board PV system will be less and CO<sub>2</sub> emission by an on-board PV system will be greater than a conventional stationary PV system.

CO<sub>2</sub> emissions from on-board PV per kWh is calculated as shown in Fig. 4.1-10. Instead of expected electricity generation during the lifetime shown in Fig. 4.1-9, PV electricity effectively used for a vehicle during its lifetime should be taken into account. The PV electricity used for the vehicle is estimated by considering the expected on-board PV electricity generation during the vehicle's lifetime and the utilisation ratio of PV electricity for vehicle.

$$\boxed{\begin{array}{c} \text{CO}_2 \text{ emissions due to} \\ \text{onboard PV electricity} \\ \text{[kg-CO}_2\text{/kWh]} \end{array}} = \boxed{\begin{array}{c} \text{Life cycle CO}_2 \text{ emissions} \\ \text{of onboard PV system} \\ \text{[kg-CO}_2\text{]} \end{array}} \div \boxed{\begin{array}{c} \text{PV Electricity used} \\ \text{for vehicle during} \\ \text{lifetime [kWh]} \end{array}}$$
$$\boxed{\begin{array}{c} \text{Expected electricity} \\ \text{generation during} \\ \text{lifetime} \\ \text{[kWh]} \end{array}} \times \boxed{\begin{array}{c} \text{Utilisation} \\ \text{ratio of PV} \\ \text{electricity} \\ \text{[%]} \end{array}}$$

Fig. 4.1-10 CO<sub>2</sub> emission of PV electricity on-board, e.g. PV on a PV-powered vehicle



Fig. 4.1-11 shows an image of the relationship between CO<sub>2</sub> emissions of the PV generated electricity normalised to the 100% PV utilisation and the utilisation ratio of PV electricity. Compared to the 100% utilisation ratio, meaning that all electricity is used effectively, the CO<sub>2</sub> emissions at the 50% utilisation ratio is doubled. At 20% utilisation ratio, it is five times bigger, and at the 10% utilisation ratio the CO<sub>2</sub> emissions have increased by a factor of 10 compared to the 100% utilisation ratio. Therefore, when estimating the CO<sub>2</sub> emissions of PV-powered vehicles and comparing them with the CO<sub>2</sub> emissions of grid charging, it's necessary to pay attention to the utilisation ratio of PV electricity.

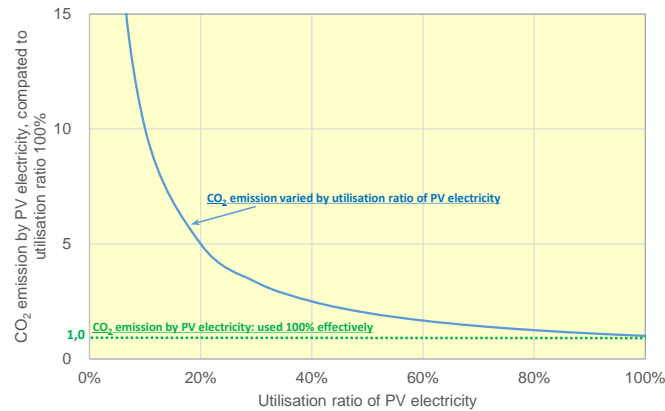


Fig. 4.1-11 Image of relations between CO<sub>2</sub> emissions by PV electricity and utilisation ratio of PV electricity

#### 4.1.2.2 Reduction of CO<sub>2</sub> emissions by PV-powered vehicles

Fig. 4.1-12 also shows an image of the relationship between the CO<sub>2</sub> emission from PV electricity generated on-board and that from grid electricity (or a charging station). An environmental benefit (CO<sub>2</sub> reduction) from a PV-powered vehicle will be realised when the CO<sub>2</sub> emissions from the PV electricity is less than the CO<sub>2</sub> emission from the grid. On the other hand, if CO<sub>2</sub> emissions by PV electricity are greater than grid electricity, because of a lower utilisation ratio of PV electricity, the PV-powered vehicle will have a negative impact, e.g. an increase in CO<sub>2</sub> emissions. It should be noted that when the CO<sub>2</sub> emissions from grid generated electricity are less than from the PV generated electricity, the benefit of a net reduction in CO<sub>2</sub> emissions will not be realised with a PV-powered vehicle even if the 100% utilisation ratio of PV electricity.

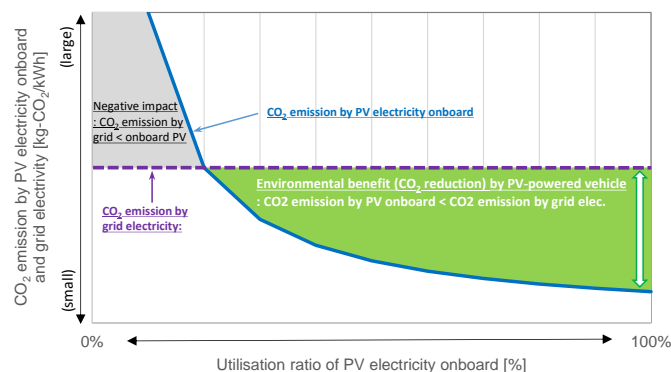


Fig. 4.1-12 Relationship between CO<sub>2</sub> emissions of PV electricity on-board and grid electricity



The value of the PV utilisation ratio where the CO<sub>2</sub> emissions from PV electricity are equal to the CO<sub>2</sub> emissions from the grid corresponds to a cross over point where the PV powered vehicle goes from producing an increase in CO<sub>2</sub> emissions to providing a decrease or an environmental benefit. This point is equal to the ratio of 'CO<sub>2</sub> emission by PV electricity with 100 % utilisation ratio' to 'CO<sub>2</sub> emission by grid'. As shown in Fig. 4.1-13, when the utilisation ratio of PV electricity is more than the ratio: 'CO<sub>2</sub>-PV<sub>100</sub>/CO<sub>2</sub>-grid', the PV-powered vehicle will produce an environmental benefit. However, if the utilisation ratio is less than 'CO<sub>2</sub>-PV<sub>100</sub>/CO<sub>2</sub>-grid', the PV-powered vehicle will not have that benefit.

That is, when the ratio, CO<sub>2</sub>-PV<sub>100</sub>/CO<sub>2</sub>-grid, is a small value, a lower utilisation ratio will still provide a benefit. However if the ratio is greater, e.g. CO<sub>2</sub> emission by PV electricity will be less than, but close to that of grid electricity, utilisation ratio of the PV electricity will need to be higher, ex. close to 100% to achieve a benefit.

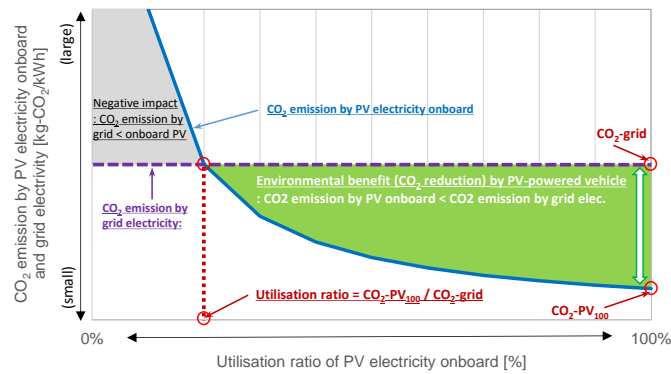


Fig. 4.1-13 Image of relations between CO<sub>2</sub> emissions of PV/grid electricity, utilisation ratio of PV electricity, and CO<sub>2</sub> reduction by PV-powered vehicle

Fig. 4.1-14 shows an example of the relationship between CO<sub>2</sub> reductions from a PV-powered vehicle and the utilisation ratio of PV electricity, based on the case study in Japan (Chapter 2.1). In the case study, the CO<sub>2</sub> emission from the grid electricity was assumed to be 0,462 kg-CO<sub>2</sub>/kWh, and the CO<sub>2</sub> emission from the PV electricity (1 008 kg-CO<sub>2</sub>/kW) supposing a lifetime of 12 years, 30% shading loss and 100% utilisation ratio was 0,129 kg-CO<sub>2</sub>/kWh. Then, the ratio: 'CO<sub>2</sub>-PV<sub>100</sub>/CO<sub>2</sub>-grid' will be 0,28 and the utilisation ratio of PV electricity required to produce an environmental benefit will be over 28%.

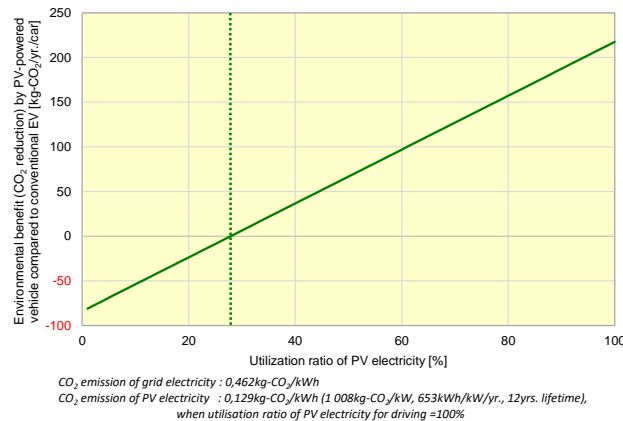
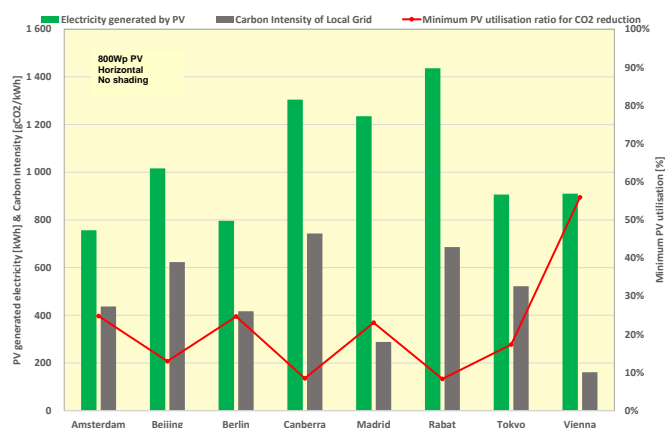


Fig. 4.1-14 Example of the relationship between the utilisation ratio of PV electricity and CO<sub>2</sub> reduction for the Japanese case study (Chapter 2.1)



This cross-over, or minimum PV utilisation ratio, has been calculated for each of the Task 17 countries' locations using results from the previous section 4.1.2.1. Fig. 4.1-15 compares the minimum PV utilisation ratio required to achieve a CO<sub>2</sub> reduction for each of the Task 17 countries, it also shows the annual PV generated electricity in kWh and the local grid carbon intensity in kg-CO<sub>2</sub>/kWh for each location. The minimum utilisation ratio required varies between locations, when the grid carbon intensity is very low, as in Paris and Bern, the utilisation ratio is above 100% and while this is not in reality possible it indicates that much more PV generated electricity is required to achieve a CO<sub>2</sub> reduction in these locations and even with a 100% utilisation ratio they are producing an increase in CO<sub>2</sub> emissions from the PV powered vehicle. Among the other locations the higher the grid carbon intensity and PV generated electricity the lower the required utilisation ratio, and it can be seen that a range from 8% utilisation ratio required in Canberra and Rabat, where both grid carbon intensity and PV production are high, to 56% in Vienna, with a relatively low grid carbon intensity and PV production, to realise an environmental benefit.



**Fig. 4.1-15 PV generated electricity and carbon intensity of the local grid (left axis) and the minimum utilisation ratio of PV electricity to begin achieving a CO<sub>2</sub> reduction (right axis)**

(Bern, Switzerland and Paris, France are omitted as they will not have a CO<sub>2</sub> reduction for the given example.)

In order to increase the CO<sub>2</sub> reduction achieved by PV-powered vehicles, one promising approach is that the CO<sub>2</sub> emission from the on-board PV electricity become smaller. As shown in Figs. 4.1-9 and 4.1-10, the CO<sub>2</sub> emission of PV electricity is calculated by dividing the life cycle CO<sub>2</sub> emissions of electricity generation by its lifetime. Therefore, the expected approaches for increasing CO<sub>2</sub> reduction is to reduce the life cycle CO<sub>2</sub> emission of PV and to increase PV electricity generation during the lifetime. Especially, in the case of a PV-powered vehicle, increasing PV electricity effectively used for the vehicle is important, as well as installing low carbon PV components.

As well-integrated PV technologies such as curved, flexible and light weight PV modules, in addition to higher efficiency PV technologies, will contribute to increasing PV electricity generation, in order to further increase PV electricity used for a vehicle, the utilisation ratio of PV electricity generated on-board should be increased.

In order to increase the utilisation ratio of the PV electricity, PV powered electric vehicles will require an optimised design. Factors to be considered include: the PV capacity with respect to effective solar irradiation and vehicle efficiency, the efficiency, capacity and operating condition of the battery, the driver's behaviour and charging strategies.

Here, increasing the utilisation ratio of PV electricity will be equal to avoiding surplus PV electricity. One of the most promising approaches will be to provide PV electricity to surroundings when the PV-powered vehicle is parked, e.g. V2X. Although this report is focusing on expected benefits led by PV-powered vehicles alone, effective and intelligent integration between PV-powered vehicle and V2X will be a focus of the next Task 17 report.

Another approach considered will be to manage the state-of-charge (SOC) of battery for PV electricity. When reserved capacity for PV electricity is well-managed, charging electricity at the stations will be restrained and PV electricity generated on-board will be effectively used more.



It is also expected that a large capacity battery will be effective to increase the utilisation ratio of PV electricity. Although enlarging battery capacity for PV on-board will become a reason for additional environmental burdens like CO<sub>2</sub> emission, PV integration with a vehicle which has a large capacity battery will be feasible.

### 4.1.3 Discussion on financial benefit

A PV-powered vehicle can also bring a financial benefit to the user. In addition to the cost reduction of running the vehicle, by considering an initial cost for PV installation, the net cost saving can be seen. Here, the PV installation cost has been set based on current rooftop system prices of ~1 000 EUR/kWp in Germany [4] and then multiplied by two to approximate the extra manufacturing and integration costs for the on-board PV.

Using the same approach as for the CO<sub>2</sub> emission analysis, the cost is taken for the PV element in EUR/kWp, and examined for the breakeven PV utilisation ratio where the cost savings realised from avoiding grid charging over the lifetime of the vehicle are greater than the original cost of the PV element. To achieve a benefit the minimum utilisation ratio for the PV electricity will be equal to the lifetime EUR/kWh for PV generated electricity to EUR/kWh of the local grid.

Fig. 4.1-16 shows an example of cost saving vs the PV utilisation ratio for Amsterdam, assuming a PV element cost of 2 000 EUR/kWp, and a local electricity cost of 0,217 EUR/kWh. The PV lifetime electricity cost is 0,1763 EUR/kWh, and resulting in a minimum PV utilisation ratio of 81,2% to achieve a cost benefit. If the cost of grid electricity is increased to typical commercial EV charging costs this breakeven point will be much lower.

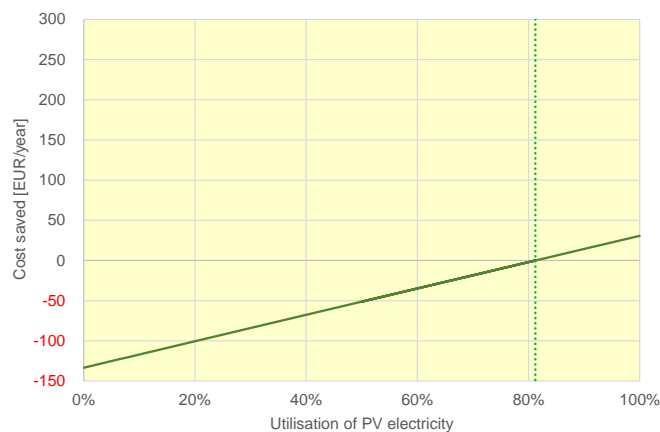


**Fig. 4.1-16 Example of cost savings vs PV utilisation ratio for Amsterdam; the point at which cost savings can be made is 81% PV utilisation.**

(PV element cost: 2 000 EUR/kWp, local electricity cost: 0,217 EUR/kWh)

Fig. 4.1-17 shows the PV energy generated per year and the household electricity price for each location, as well as the minimum PV utilisation ratio for achieving a cost benefit. While France and Switzerland did not achieve CO<sub>2</sub> reductions for the simulated case, due to the low carbon intensity of their respective grids, they both can realise cost savings if they achieve more than 91% and 53% PV utilisation ratio respectively. With the assumed PV cost and grid electricity cost, all locations except Beijing can achieve cost savings.

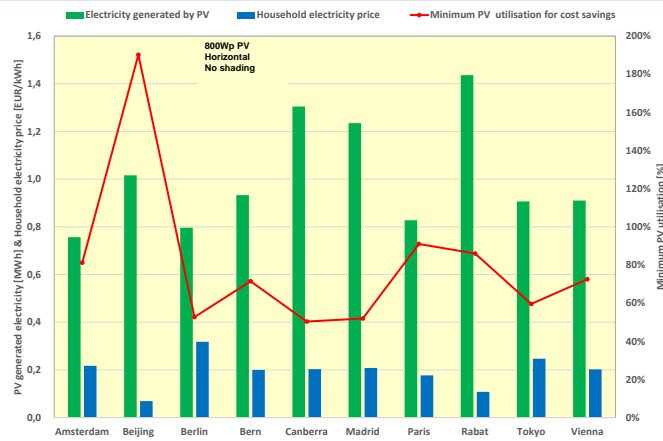


Fig. 4.1-17 Comparison of Task 17 countries for PV generated electricity and local household electricity prices (left axis) and the minimum utilisation ratio of PV electricity to begin achieving a cost saving (right axis).

### [References]

- [1] Meteotest AG, "Meteonorm V7.3.4.21143 Climate Data Software," Bern, 2020.
- [2] Global Petrol Prices.com, "electricity prices," 17 July 2020. [Online]. Available: [https://www.globalpetrolprices.com/electricity\\_prices/](https://www.globalpetrolprices.com/electricity_prices/). [Accessed 17 July 2020].
- [3] IEA, "Statistics - CO2 Emissions from fuel combustion," IEA, Paris, 2019.
- [4] Fraunhofer Institute for Solar Energy Systems, ISE, "Photovoltaics Report," Fraunhofer ISE, Freiburg, 2020.



## 4.2 Preliminary discussions for standardisation of solar irradiation and module design

Vehicle integrated photovoltaic is one of the photovoltaic systems, and simultaneously it is one of the components of vehicles. The product will be tested and rated by both two standards. For example, the performance of the PV module is to be verified by way of a photovoltaic system with necessary corrections by the different usage such as moving, frequently shaded, etc. At the same time, it is to be tested as an exterior component of vehicles, such as different types of glass. And also, it is to be tested as vehicles' electrical components due to different environments and requirements for vehicles, including EMC. For the moment, there is no published standard as well as no record of publications of official activities for the international standardisation. However, several open-access works of literature have been published by testing engineers and scientists.

In this section, the activities and "to-do" of the standardisation of the vehicle integrated photovoltaic are discussed.

### 4.2.1 Demanded in standardisation work and difference from typical solar panels and their installation

Several experts in photovoltaic standardisation published a list of items [1]. The structure of the proposed standardisation is shown in Table 4.2-1.

The conventional IEC 60904 international standard series for PV electrical characterization focusing on a 2-D flat panel [2], will need to expand to 3-D shaped PV modules. The vehicle's roof is three-dimensionally curved, and its curvature may induce power loss by increased cosine loss and self-shading loss. All the formulas and protocols for measurement of the performance of the PV module is based on the preconditions that the PV modules are flat. Determination of the output power and other fundamental electrical parameters such as short-circuit current and open-circuit voltage of the PV modules are essential to determine the input solar energy to the product of the irradiance and aperture area. On the other hand, the definition of the aperture area for the curved PV is not identical to the surface of the module. The vehicle's roof is three-dimensionally curved, and its curvature may induce power loss by increased cosine loss and self-shading loss [1]. Another aspect that needs to be considered is that the vehicle's roof PV is not in the installation of the standard slope angle and orientation. The orientation of the vehicle's roof changes with time without correlation to the sun's direction. Surrounding buildings and other objects often shade both. These factors have a different impact on the curve shape. Such interaction needs to be taken into account.

The standard PV modules are installed to avoid shades. However, the vehicle's roof PV is not oriented for the utilization of solar energy. The driver's convenience often shades the PV. The relative orientation of the PV on the vehicle to the sun's position is not fixed but frequently changes by driving. The PV on the vehicle's body and the vehicle's roof is curved. It is often shaded by its own surfaces.

The position and height of the shading objects are often difficult to predict. For predicting the total solar energy to a vehicle (either annual or monthly basis) in a specific area, not in a particular driving course, it is convenient to predict the shading influence using rough indicators of the roughness of the land. The value of the annual or monthly solar irradiance value in a specific area is valuable to predict the driving performance of vehicles mounting the PV panel.

It is necessary to consider the following vehicle-specific issues:

1. Greater chance of shading by objects around the vehicle (trees and buildings)
2. Curved surface
3. The orientation angle randomly varies
4. Mismatching loss by partial shading



**Table 4.2-1 List of standardisation items discussed among scientists and testing engineers [1]**

Rating test	Standard solar irradiation for standard testing condition solar resource around the vehicle is different from a typical PV installation	Definition of the standard solar irradiation Spectrum Value of irradiance – 1 kW/m <sup>2</sup> ?
		Solar simulation onto the vehicle’s roof Orientation/declination of the artificial light Representation of various levels of the sun height The standard (diffused) / (direct) of the sunlight Simulation of partial shading
	Testing facility	Light Source and the Testing Room Is the collimated light source necessary? Color and reflectance of the testing room
		Fixture supporting the PV (deflection by gravity)
	Curved surface	Repeatability of the tested result onto the curved surface
		Requirements of the solar simulator
		Testing protocols for repeatable measurement results
		Curve-correction factor: Definition, calculation protocol standard angular condition of the sunlight.
	Robustness to partial shading	Is the mismatched output from strings included in the curve-correction?
		Testing method for the sensitivity of partial shading (mismatching loss)
	Robustness to dynamic shading	Testing method for the sensitivity of partial shading (dynamic mismatching loss)
	Misc.	How about the door and engine hood? Same conditions to the vehicle’s roof?
		The temperature of the standard testing condition: Is it 25 °C, 60 °C or other temperature?
Is the flexible PV tested before mounting or after mounting?		
Design qualification	Standardisation body	IEC, ISO, or other standardisation bodies?
	Environmental test	List of the testing items and their conditions. Preferably with pass/fail criteria. Note the typical environmental chamber test for the vehicle-components is more intensive than PV products,
		The necessity of vehicle-specific tests including weight, dimensions, aerodynamics, safety, robustness to vehicle-wash, and so forth.
	Requirements for qualification	Definition of the minimum requirement and its background.
		Label, specification sheet, and its required item list;
		Retest guideline, namely when the vehicle’s roof PV undergoes a minor design change to fit a new or customized vehicle design, what kind of retest items need to be required to keep qualification recognition?
		Range of resembles as the criteria for the necessity of retests;
	Misc.	List and definition of terms;
Specification of the vehicle-interface like cables and connectors.		



Power Modeling	Is this the issue of standardisation?	
	Simplified parameters	Curve-correction factor
		Curve-shape representation (90% edge angle for example)
		Representative curve (or group of the curved surfaces)
		Representative distribution of the shading objects
		Representative solar irradiance for modeling calculation
		Representative distribution of the surface temperature
		Unit element vs. Shape calculation
	Modeling by rigorous calculation	3D curve issue
		mismatching issue
		stress issue
		dynamic shading issue
	Interaction to the string orientation	Current mismatching loss by non-uniform illumination
		Voltage mismatching loss by non-uniform temperature
	Outdoor measurement validation	Mode of outdoor operation
		Validation criteria
Parameter measurement for modeling	3D AOI (Angle of incidence) measurement	
	PV color (automobile painting)	
Solar modeling for vehicle	Three-Dimensional solar modeling	
	Climate correction of the power modeling	
Energy Prediction (km/kWh issue)	Difference between GHI and vehicle-roof irradiance (GHI: global horizontal irradiance)	The standard way of conversion
		Necessary parameters for the conversion
	Energy Nowcasting	High-speed calculation algorithm
		Link to the drive recorder image (dynamic shading)
		Map integration
		The requirement of the dataset
	Standard Smart Administration	Standard data format
		Standard procedure using a satellite or camera in the vehicle?

#### 4.2.2 Curve-correction

As it was mentioned in the previous section, the official standardisation activity has not been published, and the publication of the international standards will be done after intensive discussion among experts throughout the world, as well as voting by the national committees of member countries. However, remarkable progress was seen in these years in characterization and testing the vehicle's roof PV by intensive discussions among scientists and testing laboratories. The approach that is mentioned in this section is not the agreed standard, but one of the best candidates.

Before discussing the curve correction, it should be clarified where the standard measurement method has a problem [3]. The curved modules are often overestimated in efficiency measurements. It is because the input energy is often underestimated during the measurement by the indoor solar simulator.

To explain this, here again is the definition of efficiency measurement of the solar cells and modules (Equation (1)).

$$\eta = \frac{P_{out}}{P_{in}} \quad (1)$$

where  $\eta$  is the measured energy efficiency of the solar cell or module using the solar simulator.  $P_{in}$  is the input power to the solar cell or the module.  $P_{out}$  is the output power of the solar cell or the module. The measurement of  $P_{out}$  of the curved module is the same as the standard flat PV modules, and it is a simple electrical measurement. However, the difficult measurement is  $P_{in}$ .



In the standard measurement of the solar cell and module,  $P_{in}$  is calculated by Equation (2).

$$P_{in} = A \cdot Irr \quad (2)$$

where  $A$  is an aperture area.  $Irr$  is irradiance in the aperture window. In the solar simulator measurement,  $Irr$  is adjusted as  $1 \text{ kW/m}^2$  and uniform in the entire area of the aperture area  $A$ . For the standard flat PV module, the aperture area  $A$  is the same as the module active area. However, this definition is not applied to the curved PV module because the aperture area is defined as the window of the flat plane, and not the curved surface.

The first cause of the overestimation is that the curved PV module often collects more light than is defined by the aperture window. Since the illumination area of the solar simulator is always more extensive than the PV module, the curved module receives more unexpected light coming from the outer region so that it generates more unexpected power. Alternatively, it is an excellent way to place an aperture mask on the curved PV module. However, it is often eliminated because the multiple reflections between the aperture mask and optics in the solar simulator disturb the uniform illumination in the zone of the aperture window, and the solar simulator often and repeatedly requires time-consuming adjustment in the optics. Besides, there are no agreed standards in the position of the aperture mask for the curved PV module. Depending on the curved shape, the aperture mask interferes with the body of the curved module [3].

The second cause is the aperture area; namely, the module area in the active region of the curved module is not defined clearly and may have multiple definitions. It is a cause of fatal error in the estimation of the module efficiency in the dividing area of the module (Equations (1) and (2)) [3].

The third cause is the difference in the angular distribution in the indoor measurement (typical solar simulator) and outdoor operation. The curved surface generates more loss in the illumination by a higher incident angle. Unlike the case of the flat PV module, it cannot be applied to the indoor module efficiency to the outdoor operation. Correction by the curved shape is essential [3].

A PV module with a curved surface is different from a flat plate module on power output. Specifically, the self-shading effect of shading a part of the incident from a shallow angle on its convex surface, the local cosine loss at each point of the solar cell is not constant, and due to the above factors, a mismatching loss further reduces the power output. That is, the output of the curved module has a different output value from the performance test with a conventional solar simulator designed for a flat plate, as discussed in the previous section. Nonetheless, the exact test method of synthesizing the separately measured outputs by decomposing the curved surface into little surface elements (approximating each surface element to a very flat plate) is scarce in reality [5]. Therefore, a method of considering the power generation output on the 3D curved surface by multiplying the value measured by assuming the curved module as a 2D flat plate by the curve correction factor was studied. This curve correction factor is convenient because it can be uniquely determined for each curved surface given the incidence angle characteristics of the module and the incidence angle distribution of the solar cell if the mismatching loss is neglected [3].

The curve correction factor can be calculated by numerical, geometric calculation [6], or ray-tracing simulation [1]. For the geometrical calculation, it is important to add two conditions for avoiding complexity. First, the module does not absorb the light in the backside. Second, the curved surface is simple convex (no two or more peaks), namely the partial derivative functions of the profile function of the curved surface concerning  $x$  and  $y$  have no more than two points of the zero-crossing.

The curve correction factor  $f$  is defined as Equation (3).

$$P_{out} = AIf\eta \quad (3)$$

where  $P_{out}$  is the output of the module,  $A$  is a flattened area of the panel (not projected area),  $I$  is irradiance of the curved roof,  $f$  is the curve-correction factor, and  $\eta$  is the module efficiency measured by the flat condition by the conventional solar simulator. The curve correction factor  $f$  is a unique value depending on the 3D curve shape of the panel if the angular distribution of the solar irradiance is given. It is typically calculated by a numerical calculation (calculation algorithm should be open, transparent, and repeatable within some acceptable numerical errors, *i.e.*,



use of the Monte Carlo method). It should apply to the 3D CAD (computer-aided design) interface (most of the vehicle's roof 3D shapes were not simple polynomials but segmented smooth functions) [3].

The curve correction factor  $f$  can be expressed as the product of two parameters (Equation (4)).

$$f = f_1 f_2 \quad (4)$$

where,  $f_1$  is the coving factor, or in another way, geometrical curve correction factor corresponding to the ratio of the projected area by surface area,  $f_2$  is the irradiance ratio due to the local cosine loss and self-shading loss, in other words, optical curve correction factor. The parameter  $f_1$  may represent the overall shape of the curved surface [3].

The basic idea of the curve correction factor is the ratio of the absorbed flux and that of the light source with the area of the projected area of the curved PV panel that is placed just on the curved PV panel (Fig. 4.2-1). The line segment around the light source (semi-transparent light-blue area) corresponds to the rays emitted from the light source. The short line segments correspond to the ray that does not reach to the curved surface. The longer line segments correspond to the one that hits the curved PV panel (curved opaque gray surface), namely the ray that is absorbed by the PV. Note that some rays just above the curved PV panel do not hit the curved module due to its curvature. To avoid the situation, the real light-source was placed on the surface of the virtual source plane (semi-transparent light-blue area) with a ten times larger area than the virtual light source. A detector is placed on the virtual light source and measures the total flux that passes the aperture zone (corresponding to the projected area) and compares the total flux absorbed by the curved PV surface (opaque gray surface). Note that the absorption at the backside surface is disabled in this calculation. The angular characteristics of the absorption are assumed as a Lambertian surface [3].

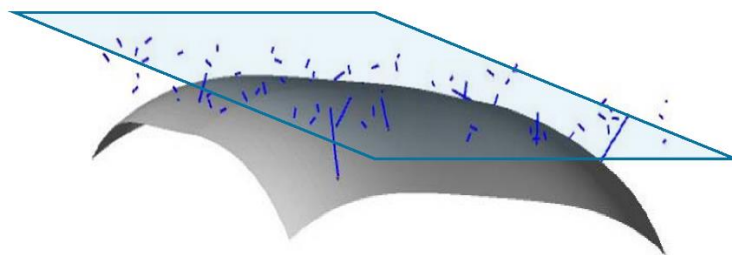


**Fig. 4.2-1 Geometrical relation between the curved PV panel (curved detector, opaque gray surface) and light source (corresponding to the projected area, semi-transparent light-blue area) [3].**

The line segment around the light source (semi-transparent light-blue area) corresponds to the rays emitted from the light source. The short line segments correspond to the ray that does not reach the curved surface. The longer line segments correspond to the one that hits the curved PV panel (curved opaque gray surface), namely the ray that is absorbed by the PV.

Note that rays just above the module do not always hit the module due to its curvature [1].

The curve correction factors of the various shape of the vehicle's roof are calculated and plotted in Fig. 4.2-2; each corresponding marker in the plot was given by the random numbers. The curve shape of the vehicle's roof widely varies. Random numbers model each surface with an approximation of the bi-cubic spline function structured by the power function of the tangent lines. The curve shape profile is approximated as the segmented (symmetrical to left-right direction, but asymmetrical to front-back direction) power function constrained by the maximum slope at the edges. Specifically, it keeps symmetry in the X direction, but allows asymmetry in the Y direction, considering that the curve shape of the vehicle's roof may vary in the front and tail of the vehicle's body.

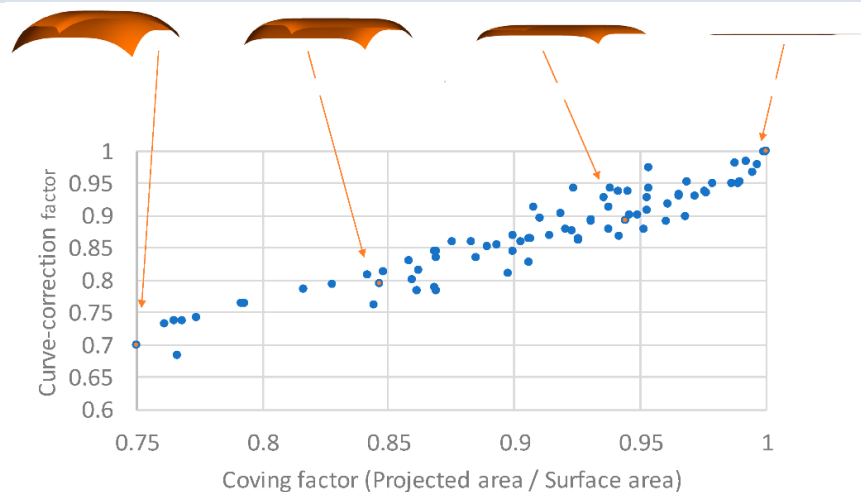


**Fig. 4.2-2 Curve correction factor vs. representative curve shape parameter [3]**

The curve correction factor decreases by the increase of curvature of the surface [4], corresponding to the ratio of the projected area by surface area (Fig. 4.2-2). The geometrical factor  $f_1$  dominates it, but the optical curve correction also decreases by the increase of the curvature as well. However, the optical influence depends on the surface shape, and it is essential to calculate its factor to every curve surface [3].

The above approach can simulate the distribution of the solar irradiance of the curved vehicle's roof PV panel. To do this, it is necessary to specify the orientation of the panel, the sun's height, and ratio of the direct and scattered components. It is not appropriate to use the statistical distribution of the incident angle data because the distribution depends on the direction of the direct sunlight [3].

The distribution of the irradiance varies by both the sun's height and orientation angle. The orientation angle of the vehicle's roof PV varies by time. Such non-uniformity is observed by the measurement of the mini-module attached to various places on the vehicle's roof [3,7].

The above-mentioned mismatching loss is handled separately by a Monte Carlo simulation. Although the mismatching loss due to non-uniformity may be expected, it will be significantly relaxed by the appropriate string design [8], and thus less significant than the reduction of the total flux [3].

The curve correction factor is also affected by the angular distribution of the solar irradiation. Roughly, the angular distribution of the sunlight in the horizontal surface moves to the higher incident angle when the sun height is low, thus higher latitude, the lower average height of the shading objects, and seasonal fluctuation of the sunshine duration are high in winter, as the area of the south-east side of mountains in Asian monsoon regions [3].

The curve correction factors,  $f$  and  $f_2$ , significantly vary by the site conditions, including latitude, climate pattern, and shading environment (urban zone or rural zone). This is because of the difference in the distribution of the incident angle onto the curved surface (Fig. 4.2-3) [3]

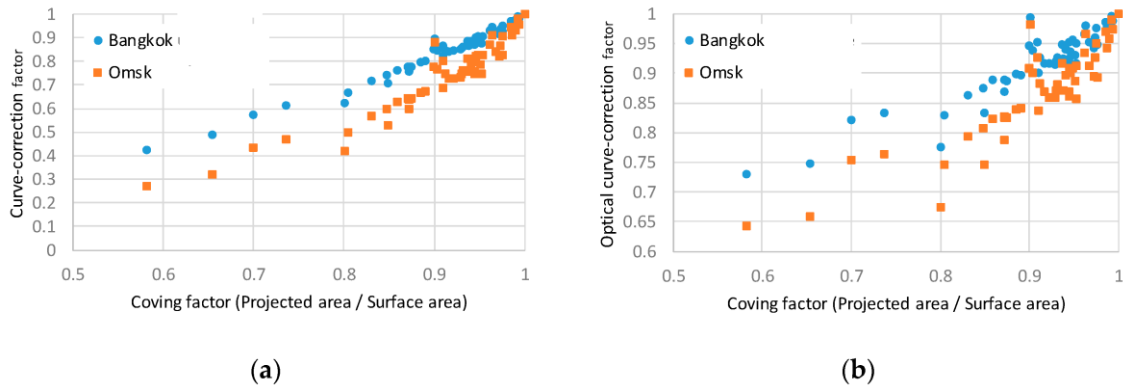


**Fig. 4.2-3 Correction factor vs. representative curve shape parameter (coving factor as  $f_1$ ) in two extreme cases, estimated by simulation [3]**

One is the urban zone in Bangkok (N 13,7° and 4,87 kWh/m<sup>2</sup>/day global horizontal irradiance, GHI), drawn by a blue line. The other is a rural zone of Omsk (N 54,9° and 3,34 kWh/m<sup>2</sup>/day GHI) drawn in an orange line: (a) curve-correction factor  $f_1$ ; (b) optical curve correction factor  $f_2$  [3].

### 4.2.3 International collaboration

Besides the international collaboration for accurate measurement of the curved PV panels, a web meeting group for brain-storming discussions on the preliminary standardisation was created by the voluntary contribution of scientists, manufacturers, and testing engineers. The activities of preliminary discussion for the standardisation through a series of web meetings have been done by 57 volunteer scientists and engineers from 16 different countries with a good mixture of scientists, manufacturers, and testing laboratories (Fig. 4.2-4). The discussion started in 2017 between Japan (Toyota Technological Institute) and China (Trina Solar) with a question on how to measure the performance of the curved vehicle’s roof PV. This technological problem and future potential of the vehicle’s roof PV has attracted many scientists and engineers, and registered people for the web meetings increased monthly. Up to November 16, 2020 (three years after the first question), 25 web meetings were held, including several face-to-face meetings. Specifically, the webinars covered (1) Irradiance modeling onto the vehicle’s roof; (2) Curve correction of the PV output; (3) Quantification and modeling of partial shading loss; (4) Performance testing conditions; (5) Effective solar resource on the vehicle’s roof impacted by shades of surrounding buildings; (6) Environmental testing conditions; (7) Minimum requirement of the solar simulator for testing curved PV [9].

The meeting contents were frequently published by open-access papers or conference proceedings [1, 9-13].

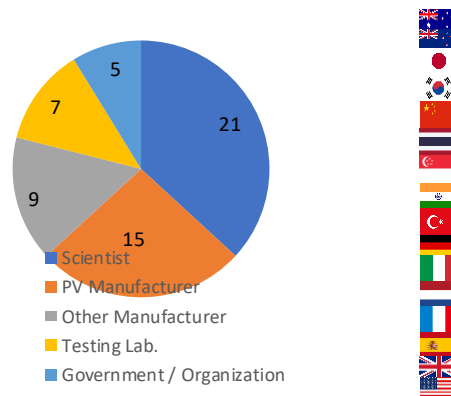


**Fig. 4.2-4 Members of the web meeting group for the vehicle’s roof standardisation and modelling (up to November 16, 2020)**



## [References]

- [1] Araki, K.; Ji, L.; Kelly, G.; Yamaguchi, M. To Do List for Research and Development and International Standardization to Achieve the Goal of Running a Majority of Electric Vehicles on Solar Energy. *Coatings*, 8, 251, 2018.
- [2] IEC 60904:2020, Photovoltaic devices - ALL PARTS, International Standard (IEC), Published on 2020-01-06, <https://webstore.iec.ch/publication/3881>
- [3] Araki, K.; Ota, Y.; Yamaguchi, M. Measurement and Modeling of 3D Solar Irradiance for Vehicle-Integrated Photovoltaic. *Appl. Sci.*, 10, 872, 2020.
- [4] Ota, Y.; Masuda, T.; Araki, K.; Yamaguchi, M. Curve-Correction Factor for Characterization of the Output of a Three-Dimensional Curved Photovoltaic Module on a Car Roof. *Coatings*, 8, 432, 2018.
- [5] Tayagaki, T.; Araki, K.; Yamaguchi, M.; Sugaya, T. Impact of Nonplanar Panels on Photovoltaic Power Generation in the Case of Vehicles. *IEEE J. Photovolt.* 9, 1721–1726, 2019.
- [6] Araki, K.; Ota, Y.; Lee, K.H.; Nishioka, K.; Yamaguchi, M. Optimization of the Partially Radiative-coupling Multi-junction Solar Cells Considering Fluctuation of Atmospheric Conditions. In Proceedings of the IEEE 7th World Conference on Photovoltaic Energy Conversion (WCPEC) (A Joint Conference of 45th IEEE PVSC, 28th PVSEC & 34th EU PVSEC), Waikoloa Village, HI, USA, 10–15 June 2018; pp. 1661–1666.
- [7] Sato, D.; Lee, K.H.; Araki, K.; Masuda, T.; Yamaguchi, M.; Yamada, N. Design of low-concentration static III-V/Si partial CPV module with 27.3% annual efficiency for car-roof application. *Prog. Photovolt. Res. Appl.* 27, 501–510. 2019.
- [8] Araki, K.; Lee, K.-H.; Masuda, T.; Hayakawa, Y.; Yamada, N.; Ota, Y.; Yamaguchi, M. Rough and Straightforward Estimation of the Mismatching Loss by Partial Shading of the PV Modules Installed on an Urban Area or Car-Roof. In Proceedings of the 46th IEEE PVSC, Chicago, IL, USA, 16–21 June 2019.
- [9] Araki, K.; Ota, Y.; Yamaguchi, M. Performance Modeling of the Car-roof PV – Overview. In 13th PV Performance Modeling Workshop (PVPWC), Kushan, China, December 10, 2019. Presentation material can be downloaded from <https://www.solarbe.com/special/2019pvpmc/EN/index.html>
- [10] Araki K, Sato D, Masuda T, Lee KH, Yamada N, Yamaguchi M. Why and how does car-roof PV create 50 GW/year of new installations? Also, why is a static CPV suitable to this application?. In AIP Conference Proceedings 2019 Aug 26 (Vol. 2149, No. 1, p. 050003). AIP Publishing LLC.
- [11] Araki K, Ji L, Kelly G, Agudo E, Anton I, Baudrit M, Carr A, Herrero R, Kurtz S, Liu Z, Limpinsel M. Modeling and Standardization Researches and Discussions of the Car-roof PV through International Web Meetings. In 2019 IEEE 46th Photovoltaic Specialists Conference (PVSC) 2019 Jun 16 (pp. 2722-2729). IEEE.
- [12] Araki K, Algora C, Siefer G, Nishioka K, Leutz R, Carter S, Wang S, Askins S, Ji L, Kelly G. Standardization of the CPV technology in 2019–The path to new CPV technologies. In AIP Conference Proceedings 2019 Aug 26 (Vol. 2149, No. 1, p. 090001). AIP Publishing LLC.
- [13] Araki K, Algora C, Siefer G, Nishioka K, Leutz R, Carter S, Wang S, Askins S, Ji L, Kelly G. Standardization of the CPV and car-roof PV technology in 2018–Where are we going to go?. In AIP Conference Proceedings 2018 Sep 13 (Vol. 2012, No. 1, p. 070001). AIP Publishing LLC.



### 4.3 PV-powered vehicles in stationary mode and combination with possible infrastructures

Considering driver profiles and travel characteristics, PV-powered vehicles may increase vehicle autonomy by an extended drive range thanks to solar power. Use cases, study cases, as well as learning from experience show the positive impact on the vehicle driving range. However, also PV-powered vehicles, like all electric vehicles, need to be sometimes additionally recharged by electricity from the grid. Hence, the combination of PV-powered vehicles and charging infrastructures involve three other types of study to take advantage of PV integration into vehicles: PV production impact in stationary mode, requirements regarding the charging infrastructures, and PV benefits while services such as vehicle-to-grid/home/vehicle are associated with the charging terminals. In this section, the term of stationary mode covers aspects of the vehicle when it is parked for a while. Additionally, a PV-powered vehicle in stationary mode will be outlined.

#### 4.3.1 PV electricity production of PV-powered vehicles in stationary mode

On-board PV modules in Vehicle Integrated PV (VIPV) may encounter energy losses in the actual use situation that have to be appraised to evaluate the potential of PV energy production and its cost. Therefore, below a concise overview is given of these losses in order to give an insight into their scope.

Compared to a PV power plant, on-board PV modules produce less energy due to horizontally and vertically oriented body parts of a vehicle. Roof-integrated PV and door-integrated PV have non-optimal orientations or resp.  $\sim 0^\circ$  and  $\sim 90^\circ$  compared to an optimally tilted PV power plant with flat PV panels (Fig. 4.3-1).



**Fig. 4.3-1 Illustration of a PV roof orientation and PV door orientation (on the left) compared to a flat PV panel inclination in a power plant (on the right)**

The projected area of the PV modules is then reduced and induces losses that will depend on the latitude (Fig. 4.3-2). The figure shows that at locations close to the equator, hardly a difference exists between annually received solar irradiation on a horizontal plane and an optimally tilted surface. For instance, this is the case in Accra, with an optimal tilt angle of  $8^\circ$  and annual horizontal solar irradiation of  $2\,113\text{ kWh/m}^2$  and Dakar, with an optimal tilt of  $16^\circ$  and  $2\,253\text{ kWh/m}^2$ . However, the higher the latitude the less irradiation and the bigger the difference between annual horizontal irradiation and that received by optimally tilted planes. For instance, in Perpignan at a latitude of  $42,692^\circ$  the annual horizontal solar irradiation is  $1\,552\text{ kWh/m}^2$ , but the difference with irradiation on surface with an optimal tilt angle of  $39^\circ$  is  $-17\%$ . In Tromso, at a latitude of  $69,656^\circ$  and a horizontal solar irradiation of  $718\text{ kWh/m}^2$  this difference becomes even  $23\%$  as compared to  $923\text{ kWh/m}^2$  at an optimized tilt angle of  $50^\circ$ .

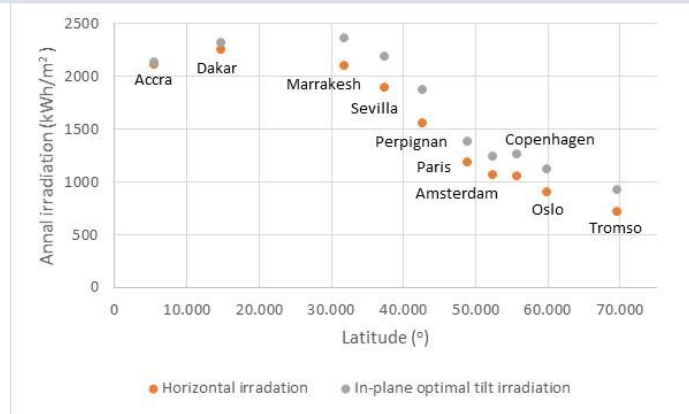


**Fig. 4.3-2 Annual horizontal and in-plane optimally tilted irradiation for locations on increasing latitude, source: PVGIS-SARAH**

Furthermore, slightly curved surfaces of integrated PV induce cosine and self-shading losses [1] (Fig. 4.3-3). Indeed, the panel will receive less irradiance per square meter (reduced projected area, Fig. 4.3-4) and the irradiance uniformity will be degraded compared to flat panels (mismatch losses), causing a lower energy production which depends on the amount of irradiance and the number of integrated bypass diodes in the PV panel.

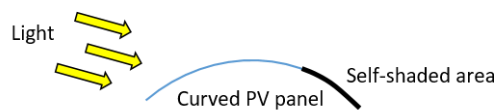


**Fig. 4.3-3 Illustration of self-shading in a curved PV panel that could be integrated in a vehicle's body parts.**

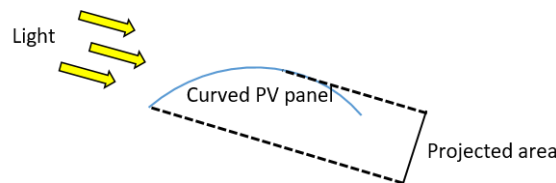


**Fig. 4.3-4 Illustration of the lower projected area due to a PV panel curvature**

Also, surrounding fixed objects such as street furnishings, buildings, vegetation, etc., can add shading and cause mismatch losses and hence cause a lower energy production of on-board PV modules [2], see Fig. 4.3-5.

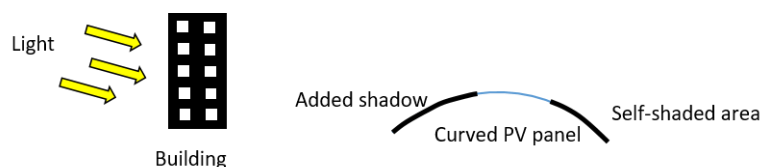


**Fig. 4.3-5 Illustration of shading by fixed objects of a curved PV panel**

The PV cell temperature of on-board PV will increase as compared to a PV power plant with, for instance, rack-mounted PV modules (Fig. 4.3-6), due to the lack of backside convection caused by the closed vehicle space underneath the PV modules. A higher PV cell temperature will lead to a reduced energy production according to



the temperature coefficient for power for silicon cells of 0,4 to 0,5%/°C with respect to the standard test temperature of 25 °C [3]. The temperature difference between a built-in VIPV application and a rack-mounted PV system can be estimated with the Ross model, which states that  $T_m = T_a + k G$ , where  $T_m$  is the module temperature,  $T_a$  the ambient temperature,  $k$  the Ross coefficient and  $G$  irradiance (Fig. 4.3-7). In addition, non-uniform variations of the PV cell temperature over the PV roof or PV doors will add to the already existing mismatch losses.



Fig. 4.3-6 Illustration of the convention situations for a built-in VIPV application and a solar PV panel in a rack-mounted system configuration

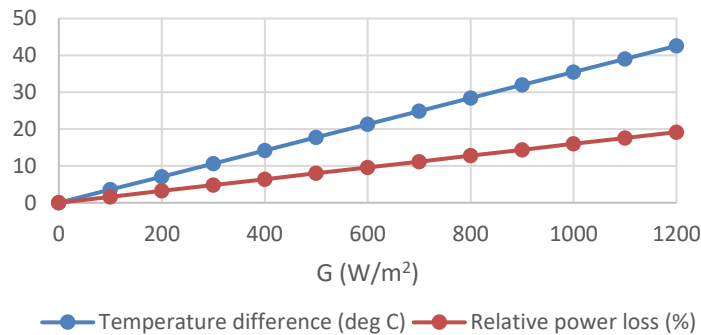


Fig. 4.3-7 Temperature difference between a built-in VIPV application ( $k= 0,0563 \text{ }^\circ\text{C}\cdot\text{m}^2/\text{W}$ ) and rack-mounted PV system ( $k= 0,0208 \text{ }^\circ\text{C}\cdot\text{m}^2/\text{W}$ ) as a function of irradiance and relative power loss of the built-in application vs rack-mounted, using a temperature coefficient for silicon PV cells of 0,45%/°C

Maximum power point tracking (MPPT) and power electronic converter DC/DC performance may be less effective and efficient due to the different energy loss mechanisms described before (Fig. 4.3-8). Indeed, non-uniformities of irradiance due to (self-)shading and of temperature of PV cells, will lead to non-ideal I-V curves that may add losses by a mis-tracking of the MPPT or due to a delayed tracking.

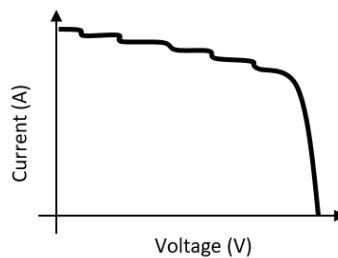


Fig. 4.3-8 Illustration of a non-ideal I-V curve of a PV panel due to non-uniform irradiance (Notice: the effect of bypass diodes over each cell by the small steps down in current.)

Finally, temporary storage of the PV energy in a battery will lead to losses during the battery charge/discharge cycle. Because of these losses, it would be interesting and required to add charging infrastructures to VIPV applications.



### 4.3.2 PV-powered vehicles connected to charging infrastructures

Charging infrastructures for electric vehicles are mainly classified in three types [4]: distributed normal charging, fast charging, and battery swapping infrastructures. They are powered by the grid, whatever is the infrastructure location: indoor / outdoor, residential charging, workplaces, fleets, public terminals, or dedicated electrical networks for other electrified means of transport. On the other hand, on-site PV supply solutions are also proposed, called PV-powered charging stations. PV modules are deployed on many types of available surfaces such as roofs of carports, parking lots, buildings, or simply on-site on the ground. Regarding the PV-powered vehicles connected to charging stations, the topology of the charging infrastructure must be adequately constructed to continue to increase the PV benefits.

#### 4.3.2.1 PV-powered vehicles connected to traditional grid-powered charging infrastructures

Charging infrastructures powered by the grid are generally installed in outdoor parking, but also in indoor parking. There are ground-based or wall-mounted charging terminals, as shown in Fig. 4.3-9.



Fig. 4.3-9 Charging infrastructures powered by the grid: outdoor and indoor

For outdoor charging infrastructures, the PV-powered vehicle can charge its battery from the power grid and from its own PV production. However, the PV energy can occur if the vehicle is exposed to the sunlight (depending on place to park) for a while. In this case, the PV integrated into the vehicle has advantages due to the generated production.

*Therefore, for outdoor charging infrastructures, the requirements and feasibility conditions are related to the characteristic of the vehicle spot, i.e. situated in clear area, or partially shady area, or full shaded area, and to vehicle's parking time duration. It should be noted that in outdoor charging infrastructures, well sunlit exposed vehicle spots should be indicated or even marked out for PV-powered vehicles. Consequently, this requirement must be mentioned from the design and construction of the charging infrastructure.*

For indoor charging infrastructures, the PV integrated into the vehicle may present a benefit provided that the indoor lighting is higher than the minimum irradiation for PV production. However, specific legislation and regulatory developments regarding the indoor lighting for public parking set energy efficiency requirements so that it is difficult to reach the minimum irradiation. The lighting of mostly of private indoor parking is automatically "on" while human presence is detected so that it is not possible to obtain any PV energy.

*Therefore, for indoor charging infrastructures, the PV-powered vehicle can charge its battery only from the power grid and, thus, there are no special requirements regarding the indoor charging infrastructures.*

Nevertheless, it always remains the advantage due to the PV production generated during the drive and outdoor stationary mode.



#### 4.3.2.2 PV-powered charging stations

PV-powered charging stations for EVs usually consist of the following components: PV modules, balance of system and EV supply equipment [5].

**PV Modules:** These are the station's main source of renewable electricity. Fixed arrays with silicon PV modules are usually the chosen technology because they offer the best trade-off between cost and efficiency. Tracking systems or concentrator PV modules have been used in some instances, however their feasibility depends on the share of direct beam irradiance and hence the local climate.

**Balance of system** such as power electronics, batteries, energy management systems and other:

- **Power Electronics:** these converters can be either DC-DC (MPPT) or AC-DC (inverter).
- **Battery Energy Storage System (BESS):** a BESS can be used to overcome the mismatch between the time when energy is produced and when it is used. Most PV charging stations rely on batteries for storing energy; lithium-ion technology is frequently chosen for this purpose but lead acid batteries could also be used in principle.
- **Energy Management System (EMS):** an EMS can use different charging algorithms to monitor and control the power flows of the PV charging station (particularly if the station has energy storage) in order to fulfil a specific objective such as ensuring the EV is always fully charged or minimizing the system's operating cost.
- **Other hardware:** wiring, switches, and mounting structure for the PV array.

**EV Supply Equipment:** this refers to the components necessary to connect the EV to the charging station such as the connector plug, power supply cable, charging stand and protection components, as well as the charging station's user interface.

A grid-connected PV charging station with BESS for EVs can hence have the following operating modes, see Fig. 4.3-10:

- 1) PV Charging Mode – Energy produced by the PV array is used to directly charge the EV
- 2) Grid Charging Mode – Energy from the local grid is used to charge the EV
- 3) PV Storage Mode – PV energy production is stored in the BESS
- 4) BESS Charging Mode – Energy stored in the BESS is used to charge the EV
- 5) Grid Supply Mode – Surplus energy from the PV array is sold back to the grid
- 6) Vehicle-to-Grid (V2G) Mode – Energy stored in the EV battery is used as a power source by the grid or a local load such as a household or office building.

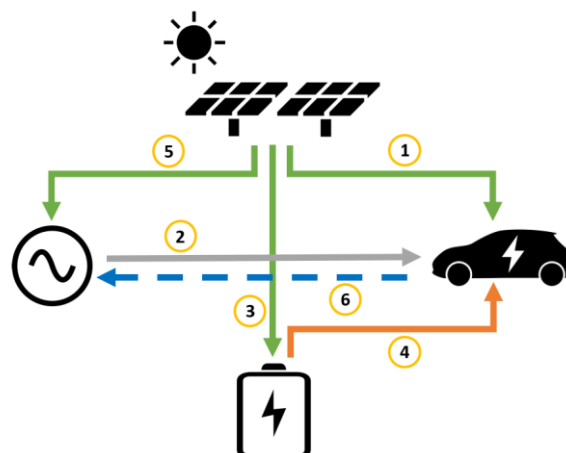


Fig. 4.3-10 Modes of operation in a grid-connected PV charging system with energy storage: PV charging (1), grid charging (2), PV storage (3), BESS charging (4), grid sale (5) and V2G (6)



A preliminary analysis of PV-powered charging stations assessing Strengths, Weaknesses, Opportunities, and Threats (SWOT) aspects is presented in Fig. 4.3-11 [5].

PV-powered charging stations can provide a source of renewable electricity at the point of consumption and reduce overloading in the local grid. However, potential barriers to its implementation include a higher initial cost and low charging speeds if power is flowing directly from the off-grid PV system to the EV. In addition, a key challenge is the difficulty of placing PV arrays in densely populated locations where there might be significant shading from surrounding objects.

Strengths	Weaknesses
<ul style="list-style-type: none"> <li>• Energy is produced locally, avoiding grid transmission losses</li> <li>• Reduced local grid overloading thanks to BESS if several EVs charge at the same time</li> <li>• Identical operation as regular charging points from user perspective</li> </ul>	<ul style="list-style-type: none"> <li>• Increased initial cost, particularly if local storage is considered</li> <li>• Requires upgrading existing electrical infrastructure with a bidirectional grid connection (V2G)</li> <li>• Insufficient PV power for EV fast charging</li> </ul>
Opportunities	Threats
<ul style="list-style-type: none"> <li>• Ability to use surplus PV production to meet energy demand from other local loads</li> <li>• Possibility to install grid-independent charging points if coupled with energy storage</li> </ul>	<ul style="list-style-type: none"> <li>• Lack of space for new charging stations from existing ones</li> <li>• Difficulty to place PV panels in an urban environment</li> </ul>

Fig. 4.3-11 SWOT Analysis for PV charging stations for EVs

#### 4.3.2.3 PV-powered vehicles connected to PV-powered charging station

PV-powered charging stations are often installed on parking lots, using a PV canopy covering the vehicles, on-site PV ground-mounted closely to the parking, or building-integrated PV charging solutions.

If the PV modules are deployed on on-site ground-mounted closely to the parking lot, or on the roof / walls of a building close to the parking lot, then the PV-powered vehicles are parked in outdoor or indoor parking lots. In such cases, the requirements and feasibility conditions to obtain benefits from PV integrated into the vehicles are the same as those presented in subsection, 4.3.2.1.

Regarding the PV-powered charging stations using PV canopy as illustrated in Fig. 4.3-12, the topology of the PV-powered charging infrastructure must be adequately designed to continue to increase the benefits from PV integrated into the vehicles.



Fig. 4.3-12 PV-powered charging infrastructure with PV vehicle parking shade



Aiming at PV benefits, when PV-powered vehicles are connected to a PV-powered charging station with PV vehicle parking shade, e.g. canopy, it is appropriate that the vehicles do not park under the vehicle parking shade. Being outside the shade of the PV-powered charging station, the PV-powered vehicles will charge simultaneously PV energy by two ways/paths: PV integrated into the vehicle to battery and PV-powered charging station to battery (Fig. 4.3-13). In this case, the PV advantage is increased at maximum.



Fig. 4.3-13 PV canopy infrastructure enhanced for PV-powered vehicle

However, in order to go on towards this goal, an additional necessary study is related to the suitable design of PV-powered charging stations including non-covered spots.

*Therefore, for PV-powered charging infrastructure with PV shade vehicle, the PV-powered vehicles may present maximum PV benefits while parked outside the shade of the station. Consequently, the requirements regarding this case are related to the adequately design of the station as well as the marking out of the vehicle spots dedicated to PV-powered vehicles.*

### 4.3.3 Possible impacts of V2X: PV-powered vehicles to grid/home/vehicle

Generally charging an electric vehicle means that the electricity flows from the power grid to vehicle and the vehicle is then considered an electricity consumer. Conversely, when the electric vehicle feeds an electric network or another vehicle and therefore offers a service of flexibility, the applications are commonly named V2X, i.e. vehicles to grid/home/vehicle.

These services associated with the charging infrastructures are classified as follow:

Vehicle-to-Grid (V2G) - The V2G characterizes the action of reinjecting the electricity contained in the batteries of electric vehicles into the public grid during parking periods as illustrated in Fig. 4.3-14 [6]. Hence, the batteries of electric vehicle fleets became energy storage units allowing ancillary services for the power grid, e.g. frequency regulation and voltage support [7].



Fig. 4.3-14 Principle scheme for V2G service [illustration based on [6]]



Vehicle-to-Home (V2H) - The V2H characterizes the action of reinjecting the electricity to supply a house for self-consumption and, in the case of a building, a cluster of electric vehicles supplies a residential or business building, as shown in Fig. 4.3-15 [6].



Fig. 4.3-15 Principle scheme for V2H service [illustration based on [6]]

Vehicle-to-Vehicle (V2V) - The V2V characterizes the action of reinjecting the electricity to another vehicle as presented in Fig. 4.3-16 (illustration based on [6]).

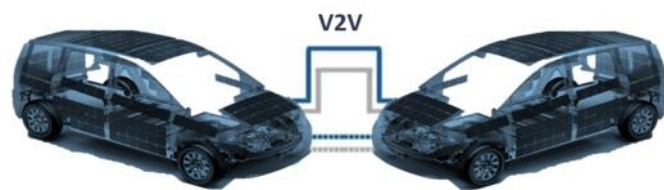


Fig. 4.3-16 Principle scheme for V2V service [illustration based on [6]]

PV-powered vehicles can produce and store PV electricity in their batteries. This PV electricity can be used as additional flow of electricity during all the V2X services. The PV electricity real-time production during the dwell time, on public parking or at home, represents the real “additional value” earned from vehicles powered by PV. In addition, regarding V2H, if at home the vehicle owner does not have a PV installation, the PV benefits provided by the vehicle are increased in this case.

#### 4.3.4 Summary and perspectives

This section focused on PV-powered vehicle in stationary mode and related to charging infrastructures. To take advantage of PV integration into vehicles, three types of study are required: PV production impact in stationary mode, requirements regarding the charging infrastructures, and PV benefits when services such as vehicle-to-grid/home/vehicle are associated with the charging terminals.

This study highlights that for outdoor charging infrastructures, sunny vehicle spots should be indicated or even marked out for PV-powered vehicles. Regarding the PV-powered charging infrastructure with a PV vehicle parking shade, the PV-powered vehicles may present maximum PV benefits while park outside the shade of the station; therefore, an additional study related to the station design is required. Although it will not change the V2X design and technology, the PV electricity produced and stored by PV-powered vehicles can be used an additional flow of electricity during all the V2X services. However, the real “additional value” earned from vehicles powered by PV is the PV electricity real-time production during the dwell time, on public parking or at home. In addition, regarding V2H, if at home the vehicle owner does not have PV installation, the PV benefits provided by the vehicle are increased in this case.



These issues will be analyzed within Task 17's next steps, which include the following objectives: requirements, barriers, and solutions for PV-powered infrastructure charging stations; feasibility conditions; and new services V2X associated with the PV-powered charging stations.

## [References]

- [1] Araki, K., Ota, Y., Yamaguchi, M., Measurement and modeling of 3D solar irradiance for vehicle-integrated photovoltaic, Applied Sciences (Switzerland), vol. 10, n°3, pp 872 (2020). DOI: 10.3390/app10030872
- [2] Brito, M.C., Assessing the impact of photovoltaics on rooftops and facades in the urban micro-climate, Energies, 13 (11), art. no. 2717 (2020). DOI: 10.3390/en13112717
- [3] Reinders, A.H.M.E., Verlinden, P.J., Van Sark, W.G.J.H.M. and Freundlich, A., Photovoltaic Solar Energy From Fundamentals to Applications, Hard-cover book, 718 pages, ISBN: 978-1-118-92746-5, Wiley & Sons, London, 2017
- [4] S. Sachan, S. Deb, S. N. Singh, Different charging infrastructures along with smart charging strategies for electric vehicles, Sustainable Cities and Society vol. 60 (2020), 102238, DOI: [10.1016/j.scs.2020.102238](https://doi.org/10.1016/j.scs.2020.102238)
- [5] Sierra, A., Gercek, C. and Reinders, A.H.M.E., Report 2.1 – Identification of Solutions for EV charging by PV, Report University of Twente, TKI Project number TEUE518019, 2020
- [6] [V2G-V2V-V2B, 2019. Available: https://www.automobile-propre.com/dossiers/v2g-v2h-v2b-les-voitures-electriques-et-les-reseaux-intelligents/](https://www.automobile-propre.com/dossiers/v2g-v2h-v2b-les-voitures-electriques-et-les-reseaux-intelligents/)
- [7] Wang, D., Sechilariu, M., Locment, F., PV-powered charging station for electric vehicles: power management with integrated V2G, Applied Sciences (Switzerland), vol. 10, n°6, pp 6500 (2020), DOI:10.3390/app10186500



## 4.4 Conclusions and the way forward

Battery and plug-in hybrid electric vehicles are being adopted globally as a solution to mitigate CO<sub>2</sub> emissions in the transport sector. In line with this, vehicle emission targets have been proposed and adopted by many countries and policy bodies around the world with goals on the adoption and use of electric vehicles in the near future. With widespread electrification of transportation, PV generated electricity and other renewable energy sources are needed to leverage EV adoption into even more significant CO<sub>2</sub> emission reductions. Exploitation of the distributed nature of PV products in parallel to battery electric vehicles offers a new opportunity in terms of mobile energy generation.

Options for low-carbon charging of electric vehicles include charging from the existing grid network with PV or other sustainable electricity sources, charging from a dedicated charge point with local PV electricity generation, or directly and independently with on-board PV (PV-powered vehicle). Among these options, this report has focused on PV-powered vehicles that can run anywhere without or with less fossil energy. These vehicles offer more than just low emission transport but also options of convenience and autonomy. Market introduction of PV-powered vehicles can be important for uptake of electric transport and create opportunities for other PV applications in the transport sector, as well.

In recent years, multiple projects, consortia and companies (both existing and start-ups) have been aimed at delivering PV-powered vehicles, especially on passenger vehicle based PV integration. All types of solar cells and encapsulation technology are being explored. For PV cell technologies for PV-powered vehicles, silicon-based cells are most common. III-V multijunction solar cells have also been applied to PV-powered vehicles due to higher power conversion efficiency. The disadvantages are higher price and spectrum mismatching loss compared with crystalline Si solar cells. For reducing such disadvantages, a four-terminal III-V on Si multijunction solar cells has also been demonstrated. Other thin-film solar cells, such as amorphous silicon and chalcogenide compare unfavourably in efficiency to other photovoltaic technologies. However, they represent the most efficient of the thin-film materials that can be deposited onto glass or metal foil providing the potential to fabricate curved PV active vehicle body parts directly and perhaps more cheaply. Perovskite cells have the potential of combining high efficiency, low-cost and flexibility, but this technology is not currently manufactured at large scale due to a lack of reliability/durability and, at present, lower efficiency than c-Si based PV at large scale. From the viewpoint of PV module assembly, there are additional module costs associated with reliable encapsulation of photovoltaic solar cells in the curved vehicle body part. Compared to conventional flat-plate PV modules, these vehicle parts will be manufactured in relatively small volumes for each vehicle design. Curved, flexible and light weight module technologies with low cost and high reliability are required. The modules will also be subject to vibrational environments that will be alien to any standard terrestrial module. The aesthetic appeal of a vehicle will be an important factor in any consumer purchase, so the modules must not only be efficient but also coloured. With well-engineered optical coatings, it is possible to deliver colour with relatively little efficiency loss.

PV-powered vehicles substitute, to a certain extent, grid or charging station electricity with on-board PV generated electricity. This offers benefits for users in terms of reduction of CO<sub>2</sub> emissions during driving, cost savings, and reduction in the frequency of charging. In order to foresee the expected benefits, some case studies are included in this report. Modelling and case studies confirm that all PV-powered vehicles will realise the benefits listed above to various levels. The degree of benefits is dependent upon variables such as driving patterns, solar irradiance available on the vehicle, vehicle efficiency, battery size, the amount of PV installed and the utilization of the PV resource. In all cases, CO<sub>2</sub> emissions are reduced during the operation of the vehicle by the on-board PV. However, in some cases, e.g. in countries with very clean grid energy, the embedded CO<sub>2</sub> based on the manufacturing of PV modules might lead to slightly higher lifetime emissions. In order to increase the CO<sub>2</sub> reduction achieved for all PV-powered vehicles, modules with lower embedded emissions are needed, in addition to higher efficiencies and/or longer PV component lifetimes. Well-integrated PV technologies such as curved, flexible and light weight PV modules, in addition to higher efficiency PV technologies, will contribute to increasing PV electricity generation.

These studies also find that maximizing PV utilisation is also very important to realise the maximum benefits of the PV. Driving patterns and solar irradiance vary by region, country, and driver. In order to increase utilised PV electricity, optimised design of PV-powered vehicles with respect to PV capacity considering effective solar irradiation and vehicle efficiency, battery capacity and efficiency and the operating condition is required. On the other hand, increasing the utilisation ratio of PV electricity also avoids surplus PV electricity. One of the most



promising approaches will be to provide PV electricity to surroundings when the PV-powered vehicle is parked, e.g. V2X. Another approach to maximizing PV utilisation is managing the battery state-of-charge (SOC) to ensure room for on-board PV electricity. When reserved capacity for PV electricity is well-managed, demand for grid electricity is reduced and PV electricity generated on-board can be more effectively used.

To promote development and adoption of PV-powered vehicles, it is also necessary to understand the effects of the dynamic environment of the vehicle for optimal design of on-board PV energy generation systems. The amount of PV electricity generated on-board depends on factors such as available solar irradiance and temperature. The solar irradiance falling on a PV-powered vehicle depends on the specific location and direction during parking and driving. Additionally, the solar irradiance during use is always changing; due to the surrounding environment of the route, such as whether buildings, structures or foliage are shading or even reflecting light on the vehicle. In response to this situation, several different methodologies have been developed for measuring the real irradiance falling on vehicles. At this time, there is not enough data collected to make generalizations on the characteristics of the solar irradiance experienced by a vehicle in all cases, both the impact of environmental shading and the impact of the inherent curvature of on-board PV increases with the decrease of the sun height, namely, increasing the latitude. However, both the curve-correction factor and effective solar resource to the vehicle's roof, normalized to GHI, do not show a strong correlation to latitude, and unlike other typical solar resource parameters, is affected by local meteorological conditions. Also, both the curve-correction factor and the effective solar resource relative to GHI, are strongly influenced by the specific distribution of shading objects. More irradiance measurements are needed in order to more accurately quantify the possible energy yields and driving distances on solar power throughout the year in specific locations and driving routes. Additionally, once a large data set is acquired, the measured values need to be normalized to standard irradiance levels measured in the past decades in order to eliminate statistical deviances. Data on solar irradiance acquired by a vehicle is a first step or gateway toward the use of PV in automobiles and is vital information for evaluating the significance and effect, as well as optimal design, of an on-board PV system.

PV-powered vehicles may offer significant benefits to drivers and may offer an important contribution to the energy transition. Their market introduction will require technical optimisation of the PV but also of vehicles and vehicle use. Short driving range commuter vehicles, ultra-light weight vehicles, and high efficiency electric vehicles are the most realistic concepts to apply PV power for smaller passenger vehicles. As a concept of bridge technology to PV-powered vehicles, it will be possible to consider PV-equipped vehicles for auxiliary components such as air conditioning systems, refrigerators and heating systems. This can already be seen in some passenger vehicles. For heavier commercial vehicles such as truck trailers, other goods delivery vehicles, and buses, on-board PV can make significant contributions to these auxiliary systems and the electric conversion of these systems. Taking into account the area available for PV and the possible use of PV electricity for auxiliary demand, PV-powered refrigerated truck trailers and buses are close to market introduction.

The questions of how to directly use and manage PV electricity for different types of vehicles, driving profiles, and locations with different solar irradiance, and how to integrate PV components on-board with keeping mechanical and physical reliability and safety including standardisation will be important for all kinds of PV-powered vehicles.

In order to effectively use the PV electricity generated on-board, an integral approach with PV applications for electric systems and infrastructures will be important. This may also contribute to reducing the impact of widespread PV generation and EV charging on the stability of the grid.

Currently, the PV market in the transport sector is still small. However, the potential impact is large and the electrified transport market will be a key driving force for the further development of PV in the coming years. PV-powered vehicles have the potential to further decrease the CO<sub>2</sub> emissions impact of electrified transport (particularly in the short term) and accelerate the adoption of electric vehicles overall due to decreased dependence on the grid. In order to utilise the potential and to realise PV-powered vehicles, expected benefits should be further validated and evaluated from viewpoints of not only energy, the environment, and from the perspective of users, but also the related industries, and shared with stakeholders such as automotive companies and relevant policy organisations.



ISBN 978-3-907281-15-4



9 783907 281154 >